UNIVERSIDAD AUTONOMA
DE MADRID

Facultad de Ciencias
Departamento de Biología Molecular

Interactions of P1b, the silencing suppressor protein from *Cucumber Vein Yellowing Virus*, with plant factors that contribute to its biological functions

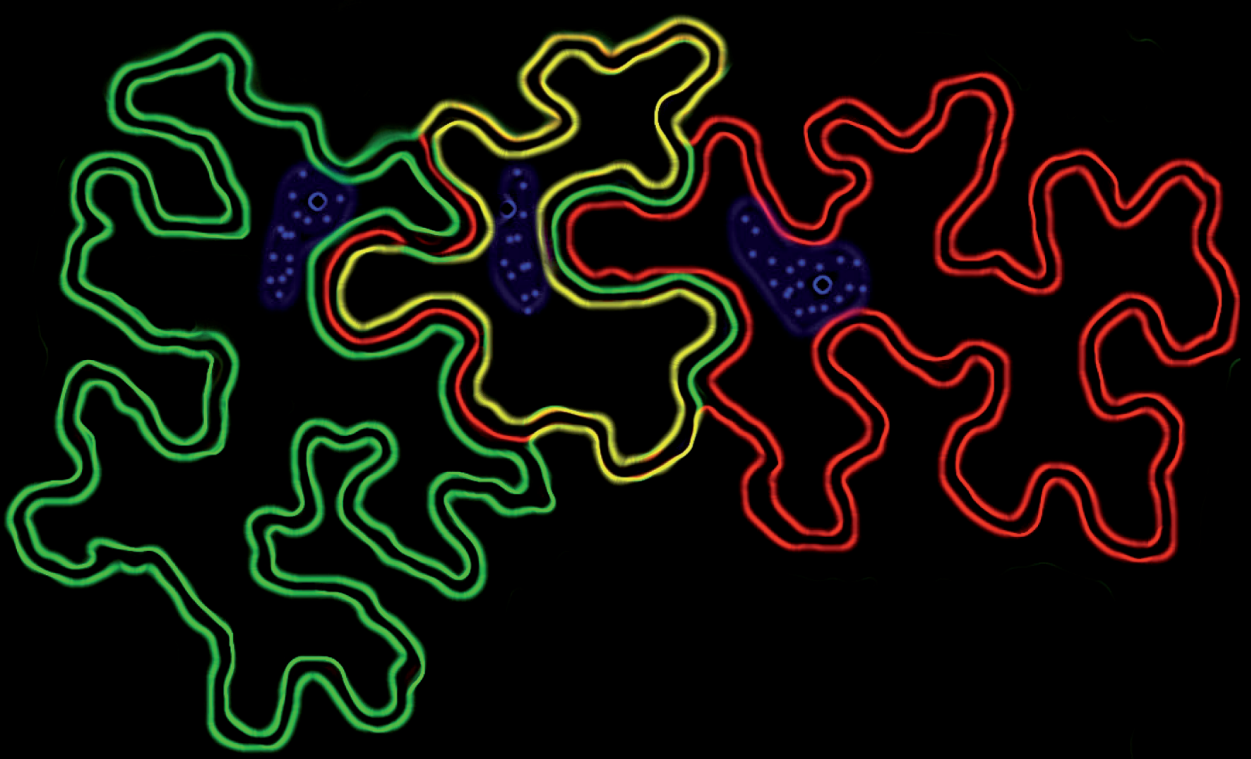

Jon A. Ochoa de Eribe Casas

Madrid, 2015

Jon Ander Ochoa de Eribe Casas
Laboratory 313
Dept. Plant Molecular Genetics
Centro Nacional de Biotecnología (CNB - CSIC)
C/ Darwin, 3, 28049 Cantoblanco
Madrid, Spain
Tel.: +34 91 585 45 27
FAX: +34 91 585 45 06
jochoa(at)cnb.csic.es
jon.ochoa(at)hotmail.com

Cover: **P1b, the silent passenger.** Artistic representation of *N. benthamiana* epithelial cells expressing different fluorescent proteins. Nucleoplasm is deformed to read P-1-b.

I hereby declare that my thesis or dissertation and abstract are my original work. Proper attribution has been given to all outside sources. I have obtained and attached hereto needed written permission statements(s) from the owner(s) of each third-party copyrighted matter to be included in my work, allowing electronic distribution (if such use is not permitted by the fair use doctrine).

I hereby grant to Universidad Autónoma de Madrid and its agents the non-exclusive license to archive and make accessible my work in whole or in part in all forms of media, now or hereafter known. I agree that the document mentioned above may be made available immediately for worldwide access unless a preapproved embargo applies.

I retain all other ownership rights to the copyright of my work. I also retain the right to use in future works (such as articles or books) all or part of my work. I understand that I am free to register the copyright to my work.

UNIVERSIDAD AUTÓNOMA DE MADRID
Facultad de Ciencias
Departamento de Biología Molecular

Interactions of **P1b**, the silencing suppressor protein from *Cucumber Vein Yellowing Virus*, with plant factors that contribute to its biological functions.

A DISSERTATION SUBMITTED IN PARTIAL FULLFILMENTS OF
THE REQUIREMENTS FOR THE DEGREE OF DOCTOR OF PHILOSOPHY
BY

Jon Ander Ochoa de Eribe Casas
M. Sc. Biology
M. Sc. Biotechnology

This PhD thesis has been executed in the Department of Plant Molecular Genetics of the National Centre for Biotechnology (CNB-CSIC) in the laboratory of Prof. Dr. Juan Antonio García under the co-supervision of Dr. Carmen Simón-Mateo, and Dr. Bernardo Rodamilans.

Madrid, October 2015

UNIVERSIDAD AUTÓNOMA DE MADRID
Facultad de Ciencias
Departamento de Biología Molecular

Interactions of **P1b**, the silencing suppressor protein from *Cucumber Vein Yellowing Virus*, with plant factors that contribute to its biological functions.

Memoria presentada por

Jon Ander Ochoa de Eribe Casas

Licenciado en Biología
Máster en Biotecnología

para optar al Título de Doctor

Esta tesis se ha realizado en el Departamento de Genética Molecular de Plantas del Centro Nacional de Biotecnología (CNB-CSIC) en el laboratorio del Dr. Juan Antonio García bajo la co-dirección de la Dra. Carmen Simón-Mateo y del Dr. Bernardo Rodamilans.

Madrid, Octubre 2015

AGRADECIMIENTOS

A quienes me han ayudado,
por enseñarme compasión,

A quienes no me han ayudado,
por enseñarme fortaleza.

日本や。
美しい日の出を、
ありがとう。

a mi madre,

a Bogavant,

SPANISH SUMMARY / RESUMEN EN ESPAÑOL

En los últimos años, se han realizado grandes avances en biología molecular que han permitido destramar antiguos aunque desconocidos procesos biológicos de gran importancia en las interacciones virus-hospedador. Uno de estos procesos es el denominado *Silenciamiento por RNA* o *Interferencia por RNA* (RNAi) que tiene como objeto, el control en la expresión génica, y en último termino, regular la producción de proteínas de la célula. Este proceso queda integrado en un complejo entramado de mecanismos de regulación que controlan una gran variedad de tareas fisiológicas relacionadas con el desarrollo ontogénico, la adaptación al entorno, la integridad y mantenimiento de la estabilidad genética, así como con la defensa frente a ácidos nucleicos invasores, entre los cuales se encuentran los genomas virales.

El sistema de silenciamiento por RNA cumple pues una función antiviral ancestral, posiblemente muy anterior a otros diferentes mecanismos de defensa descritos con anterioridad, detectando la presencia de formas replicativas invasoras, eliminando las moléculas de ácidos nucleicos foráneos mediante su degradación dependiente de secuencia e inmunizando el tejido adyacente y distal por medio de la amplificación y translocación de pequeñas moléculas de ácido ribonucléico (siRNA) portadoras de la información digital para el reconocimiento de su diana. Como consecuencia se dice que los virus, son pues, inductores y dianas del sistema del silenciamiento. Sin embargo, la lucha por la supervivencia ha favorecido una carrera bio-armamentística en la que los virus han desarrollado estrategias para permitir su evasión de los sistemas de defensa. Una de esas estrategias fue la evolutivamente reciente incorporación de funciones para suprimir el silenciamiento por RNA (RSS) por parte de las proteínas virales. Estos supresores del silenciamiento (RSS) buscan boicotear la maquinaria del silenciamiento celular inhibiendo así la defensa antiviral. Sin embargo, al ser esta función una adquisición evolutiva reciente, las proteínas RSS virales han de desarrollar funciones adicionales tanto fundamentales como accesorias durante el ciclo viral imprimidas con anterioridad. Las restricciones de tamaño en los genomas virales, imponen

una obligada dependencia de los procesos celulares del huésped en reclutar las funciones moleculares necesarias para el conjunto de procesos virales. Por este motivo, las proteínas virales poseen capacidades multifuncionales que emplean en los diversos requerimientos del ciclo viral en asociación con factores del huésped. Las diversas interacciones entre los RSS virales y factores del huésped vinculan a estas proteínas en numerosos procesos celulares y moleculares. El estudio de las interacciones de los RSS virales con factores celulares del huésped puede ayudar a entender no sólo los mecanismos de acción de la supresión del silenciamiento, sino además otras funciones todavía desconocidas asociadas a estas proteínas y relacionadas con el ciclo viral.

En esta tesis se realiza una búsqueda por doble híbrido en levaduras y purificación de proteínas mediante resina de afinidad a calmodulina de proteínas del huésped que interaccionan con el supresor del silenciamiento P1b codificado en el virus del amarillamiento de las venas del pepino (CVYV). Además, de manera paralela se realiza un estudio en plantas de Arabidopsis infectadas con un vector de expresión viral basado en el virus de la Sharka que expresa la proteína P1b funcional en un contexto viral con objeto de identificar tanto proteínas diferencialmente acumuladas en la firma proteómica del huésped infectado, como factores de trascripción que pudieran estar afectando a la infección del virus.

Como resultado de estos escrutinios se seleccionaron un grupo de factores del huésped para analizar su capacidad de interacción con la proteína P1b utilizando diversas técnicas moleculares y de microscopía óptica con objeto de caracterizar factores celulares necesarios para sus funciones virales. Las proteínas del huésped identificadas, una helicasa nuclear (PRH75), una esterol C-8-isomerasa (HYDR1) y la isoforma del factor de iniciación de la traducción de pepino (eIF(iso)4E), pudieran estar relacionadas con funciones de traducción y de RSS viral. Además mediante un estudio de inmunomarcaje por microscopia electrónica y ensayos de co-localización con microscopía confocal se localiza a la proteína P1b en el citosol de células infectadas de pepino, pudiendo estar formando parte de los cuerpos de producción de siRNAs en asociación con la proteína de la cápside viral.

TABLE OF CONTENTS

ABBREVIATIONS USED

ø	Empty
-P	Carboxy terminal tag consisting of Carboxy-terminal residues of the YFP protein
-YF	Carboxy terminal tag consisting of Amino-terminal residues of the YFP protein
20S	20 Svedberg
3-AT	3-Amino-1,2,4-triazole
40S	40 Svedberg
60S	60 Svedberg
ABA	Abscisic acid
ACN	Acetonitrile
AD	Activating domain
AGI	Arabidospis genome initiative
AGO(1-10)	Argonaute (1-10)
Amp	Ampicillin
AP/MS	Affinity purification tandem mass spectroscopy
APS	Ammonium persulfate
ATP	Adenosine triphosphate
BD	Binding domain
BiFC	Bi-molecular fluorescent complementation
bp	Base pair
BSA	Bovine serum albumin
C-terminus	Carboxy terminus
Carb	Carbenicillin
cDNA	Codifying deoxyribonucleic acid
CDS	Codifying sequence
CFU	Colony-forming unit
ChloroP 34kDA	34 Kilo Dalton Chloroplast Protein
CI	Cylindrical inclusion
CML38	Calcium Binding Protein 38
Co-IP	Co-immunoprecipitation
Col-0	Columbia ecotype
cPGK2	Chloroplast phosphoglycerate kinase
CRT	Calreticulin
D-bodies	Dicing bodies
DAPI	4',6-diamidino-2-phenylindole
DCL(1-4)	Dicer-like(1-4)
DCP(1-2)	Decapping protein (1-2)
DMSO	Dimethyl sulfoxide
DNA	Deoxyribonucleic acid
DNase	Deoxyribonucleic acid nuclease
dNTP	Deoxynucleoside triphosphate
dpi	Days post inoculation
dpx	Days post induction
dsRNA	Double stranded ribonucleic acid
DTT	Dithiothreitol
EDTA	Ethylenediaminetetraacetic acid
eEF1A	Eukaryotic translation elongation factor 1A
eIF(iso)4E	Eukaryotic translation initiation factor isoform 4E
eIF4E	Eukaryotic translation initiation factor 4E
eIFs	Eukariotic translation factors
ELISA	Enzyme-linked immuno sorbent assay
ER	Endoplasmic reticulum
Fam.	Family
FDR	False discovery rate
FdV	Ferredoxin V
Fib(2a-2b)	Fibrillarin (2a-2b)
Fig.	Figure
FRY1	Fiery1
GAPDH	Glyceraldehyde 3-phosphate dehydrogenase
GAL4	Galactose-responsive transcription factor 4
GAPC	Glyceraldehyde-3-phosphate dehydrogenase subunit C
GAPC(1-2)	Glyceraldehyde-3-phosphate dehydrogenase subunit C(1-2)
Gent	Gentamicin
GFP	Green fluorescent protein
gRNA	Genomic ribonucleic acid
GUS	β-glucuronidase
GW	Gateway
HA	Human influenza hemagglutinin epitope
HCPro	Helper component protease
HEN1	Hua enhancer 1
HEPES	4-(2-hydroxyethyl)-1-piperazineethanesulfonic acid
HIP(1-2)	Ring-finger protein (1-2)
HR	Hypersensitive response
HRP	Horseradish peroxidase
HSP70	Heat shock protein 70
HVR	Highly variable region
HYD1	Hydra1
Hygro	Hygromycin
ICTV	International committee on taxonomy of viruses
IgG	Immunoglobulin G
iTRAQ	Isobaric tag for relative and absolute quantitation

JA	Jasmonic acid
Kan	Kanamycin
Kbp	Kilobase pair
kDA	Kilo dalton
LB	Luria Bertani buffer
LC-MS/MS	Liquid chromatography coupled to tandem mass spectrometry
LC-Q-TOF	A liquid chromatography coupled quadrupole time-of-flight mass spectroscopy
LTP	Lipid transfer protein
MCS	Multiple cloning site
Met	Methionine
MinD	Minicell chloroplast division
miRNA	micro ribonucleic acid
MS	Mass spectroscopy
MSL	Master species lists
MsRB1	Methionine sulfoxide Rreductase B1
mut	Mutant
myc	c-myc avian myelocytomatosis viral oncogene homolog epitope
N-terminus	Amino terminus
Nal	Nalixidic acid
nat-siRNA	Natural antisense short interfering ribonucleic acid
NIa	Nuclear inclusion protein A
NIb	Nuclear inclusion protein B
NLS	Nuclear localisation signal
NO	Nitric oxide
NPC	Nuclear pore complex
ns	No statistically significant difference
NS1	Non-structural protein 1
NTAP	Amino-terminal tandem affinity purification
OD	Optical density
ORF	Open reading frame
P	Carboxy-terminal residues of the YFP protein
P-	Amino terminal tag consisting of Carboxy-terminal residues of the YFP protein
P-body	Processing body
P1bm1	P1b mutant 1 (RK68,69AA)
P1bm6	P1b mutant 6 (C103A)
P58^{IPK}	58 kilo dalton protein inhibitor of the interferon-induced double-stranded RNA-activated protein kinase
PABP(1-10)	Poly(A) binding protein (1-10)
PBS	Phosphate buffer saline
PCaP1	Plasma-membrane associated cation-binding protein 1
PCR	Polymerase chain reaction
PEG	Polyethylene glycol
PIPO	Pretty interesting potyviral ORF
ppp	dots per inch
PR(1-5)	Pathogenesis related proteins (1-5)
PRH75	Plant ribonucleic acid helicase 75
PSI	Pound-force per square inch
PSI-K	Chloroplastic photosystem I kappa subunit
PSM	Peptide spectrum match
PTGS	Posttranscriptional gene silencing
PVIP(1-2)	Potyviral interacting protein (1-2)
R-gene(s)	Resistance gene(s)
RAV2	Regulator of the ATPase of the vacuolar membranes 2
RdDM	Ribonucleic acid-directed deoxyribonucleic acid methylation
RDR(1-6)	Ribonucleic acid-dependent ribonucleic acid polymerase (1-6)
RdRp	Viral ribonucleic acid-dependent ribonucleic acid polymerase
RFP	Red fluorescent protein
rgs-CaM	Regulator of gene silencing-calmodulin-like protein
RH(1-53)	Ribonucleic acid helicase (1-53)
Rif	Rifampicin
RISC	Ribonucleic acid induced silencing complex
RITS	RNA induced transcriptional silencing
RLI	Relative labelling index
RNA	Ribonucleic acid
RNase	Ribonucleic acid nuclease
ROS	Reactive oxigen species
rpm	Revolutions per minute
rRNA	Ribosomal ribonucleic acid
RSS	RNA silencing suppresor
RT-PCR	Reverse trascriptase coupled polymerase chain reaction
Rubisco	Ribulose-1,5-bisphosphate carboxylase oxygenase
SA	Salicylic acid
SAR	Systemic acquired resistance
SCE1	SUMO-conjugating Enzyme 1
SD	Minimal synthetic dropout medium
SDS	Sodium dodecyl sulfate
SDS-PAGE	Sodium dodecyl sulfate polyacrylamide gel electrophoresis
SEL	Size exclusion limit
sGFP	Super green fluorescent protein
SGS(1-3)	Suppressor of gene silencing (1-3)
siRNA	small interfering ribonucleic acid
smRNA	small ribonucleic acid
SN	Signal to noise ratio
SOB	Super optimal broth
Spec	Spectinomycin
ssRNA	single stranded RNA

Strep	Streptomycin
T-DNA	Transfer deoxyribonucleic acid
Ta	Annealing Temperature
ta-siRNA	trans-acting small interfering ribonucleic acids
TBE	Tris borate EDTA
TBS	Tris buffer saline
TE	Tris EDTA
TEAB	Tetraethylammonium bromide
TEMED	Tetramethylethylenediamine
TF	Transcription factor
TGBp1	Trible gene block protein 1
TGS	Transcriptional genes silencing
Tm	Melting temperature
tRNA	Transfer ribonucleic acid
Ura	Uridine
UTR	Untranslated region
VIGS	Viral induced gene silencing
Vp3	Viral capsid protein 3
VPg	Viral protein genome-linked
VRC	Viral replication complexes
Y-2H	Yeast two hybrid
YF	Amino-terminal residues of the YFP protein
YF-	Amino terminal tag consisting of Amino-terminal residues of the YFP protein
YFP	Yellow fluorescent protein
YPGA	Yeast peptone glucose agar
Φ29	Bacteriophage Phi29

VIRUS CITED

Acronym	Name	Family	Genus
AMV	Alfalfa mosaic virus	*Bromoviridae*	*Alfamovirus*
BaYMV	Barley yellow mosaic virus	*Potyviridae*	*Bymovirus*
BMV	Brome mosaic virus	*Bromoviridae*	*Bromovirus*
BStMV	Brome streak mosaic virus	*Potyviridae*	*Tritimovirus*
BYDV-GPV	Barley yellow dwarf virus-GPV	*Luteoviridae*	*Unassigned*
BVY	Blackberry virus Y	*Potyviridae*	*Brambyvirus*
CaMV	Cauliflower mosaic virus	*Caulimoviridae*	*Caulimovirus*
CBSV	Cassava brown streak virus	*Potyviridae*	*Ipomovirus*
ChiVMV	Chilli veinal mottle virus	*Potyviridae*	*Potyvirus*
ClYVV	Clover yellow vein virus	*Potyviridae*	*Potyvirus*
CMV	Cucumber mosaic virus	*Bromoviridae*	*Cucumovirus*
CVB	Chrysanthemum virus B	*Betaflexiviridae*	*Carlavirus*
CVYV	Cucumber vein yellowing virus	*Potyviridae*	*Ipomovirus*
IVA	Influenza virus A	*Orthomyxoviridae*	*Influenza virus A*
LMV	Lettuce mosaic virus	*Potyviridae*	*Potyvirus*
MacMV	Maclura mosaic virus	*Potyviridae*	*Macluravirus*
PlAMV	Plantago asiatica mosaic virus	*Alphaflexiviridae*	*Potexvirus*
PoLV	Pothos latent virus	*Tombusviridae*	*Aureusvirus*
PPV	Plum pox virus	*Potyviridae*	*Potyvirus*
PVA	Potato virus A	*Potyviridae*	*Potyvirus*
PVY	Potato virus Y	*Potyviridae*	*Potyvirus*
RCNMV	Red clover necrotic virus	*Tombusviridae*	*Dianthovirus*
RSV	Rice stripe virus	*Unassigned*	*Tenuivirus*
SCMV	Sugarcane mosaic virus	*Potyviridae*	*Potyvirus*
SPMMV	Sweet potato mild mottle virus	*Potyviridae*	*Ipomovirus*
TBSV	Tomato Bushy Stunt Virus	*Tombusviridae*	*Tombusvirus*
TCV	Turnip crinkle virus	*Tombusviridae*	*Carmovirus*
TEV	Tobacco etch virus	*Potyviridae*	*Potyvirus*
TGMV	Tomato golden mosaic virus	*Geminiviridae*	*Begomovirus*
TMV	Tobacco mosaic virus	*Virgaviridae*	*Tobamovirus*
TuMV	Turnip mosaic virus	*Potyviridae*	*Potyvirus*
TVMV	Tobacco vein mottling virus	*Potyviridae*	*Potyvirus*
TYLCV	Tomato yellow leaf curl virus	*Geminiviridae*	*Begomovirus*
WSMV	Wheat streak mosaic virus	*Potyviridae*	*Tritimovirus*
ZYMV	Zucchini yellow mosaic virus	*Potyviridae*	*Potyvirus*

"There are things known and there are things unknown,
and in between are the doors of perception."

Aldous Huxley, *The Doors of Perception*

.

INTRODUCTION

In the beginning

Viruses have become increasingly popular in our daily news feeds. From Ebola outbreaks in Western Africa (Carroll et al., 2015), to new antibiotic therapy (Nobrega et al., 2015), viruses are gaining widespread attention in our modern society. Our increasingly interconnected and globalized societies and the unstoppable climate change are influencing changes in the natural distributions of viruses world wide, raising concerns on human, livestock and crop health policies (Gale et al., 2010). The emergence of new and recurring viral diseases represent a serious risk in the healthcare of human population worldwide (Pugliese et al., 2007; Howard & Fletcher, 2012; Marston et al., 2014). The spread of important agronomical loss-causing plant viruses from Europe into America and Asia (Cambra et al., 2006), or increasing prevalence of viruses causing disease in insects, ravaging natural plant pollinators, like Honeybees, disturbing natural pollination cycles, are protruding threats on the natural diversity of ecosystems (Enquist, 2009; Manley et al., 2015). Virology has played a major role in the biological revolution of the past century (Enquist, 2009). New advances in genome sequencing have expanded our vision on the distribution of remote viral communities (Lopez-Bueno et al., 2009), and new discoveries in molecular and cellular biology increase our understanding in the molecular adaptations between host and viruses (Getts et al., 2013; Csorba et al., 2015). Modern advances in genome sequencing, proteomics and synthetic biology among other scientific disciplines, are not only aiding in the understanding of functions and relationships of viruses and their biology but also providing new perspectives in old evolutionary discussions (Forterre, 2006; Raoult & Forterre, 2008; Forterre, 2011; Forterre, 2013; Nasir et al., 2015). Although distant from this PhD dissertation, these discussions evidence the excitement in the recent achievements in virology, and new discoveries from the exploration of the virosphere yet to come. Regardless of whichever theory of the origin of viruses the reader advocates for, he or she is likely to acknowledge that viruses are outstanding collaborators in genetic innovation involved in the evolutionary radiation of many modern genomes (Brosius, 2003; Ryna, 2006; Forterre & Prangishvili, 2009) and, until present, all reported viruses are obligated intracellular parasites, which as such, all

depend on successful interactions with their host cell to recruit the cellular machinery, to fulfil primary and accessory viral processes.

Viruses have long been accompanying human history, responsible for plagues affecting humans, livestocks and crops. The progression of humans into densely populated agricultural societies has facilitated the emergence of viral outbreaks and epidemics with important consequences to human societies throughout human history (Geddes, 2006). Likewise, radiation of Potyviruses, one of the largest plant viral families (Riechmann et al., 1992), seems to coincide with the development of irrigation and intensive crop production in the dawn of agriculture (Gibbs et al., 2008). Although viruses did not have their formal presentation to society until the late nineteenth century, early encounters were documented many centuries before. Symptoms caused by plant viruses have also been documented long before the discovery of viruses as disease agents. Ancient Japanese poems dating to 752 A.D. describing symptoms in Geminivirus-infected Eupatorium plants (Saunders et al., 2003) and Dutch paintings dating from the 17th Century describing the flower-breaking appearance of potyvirus-infected tulips (Dekker et al., 1993) are the oldest documents reporting early encounters with plant-infecting viruses. To date 1240 different plant viral species have been reported infecting plants and algae (ICTV, MSL 2014), classified in 108 recognized genera, and organized into 27 different viral families, with 35 genera yet unassigned to any family in particular. Three viral families are responsible for almost 50% of the total reported viral species, with Fam. *Geminiviridae* being the largest, accounting for 26.2% of the viral species, and closely followed by Fam. *Potyviridae* (15.3%) and more distantly, Fam. *Tombusviridae* (5.7%).

Family Potyviridae

The Potyviridae family is responsible for significant socio-economic impacts (Cambra et al., 2006). Appearing as flexuous filamentous rod-shaped particles ranging on average from 650 to 950 nm long and producing characteristic cytoplamic cylindrical inclusions or pinwheel structures (Riedel et al., 1998), the 8 recognized genera, grouping (to this date) 190 species (ICTV, MSL 2014) are

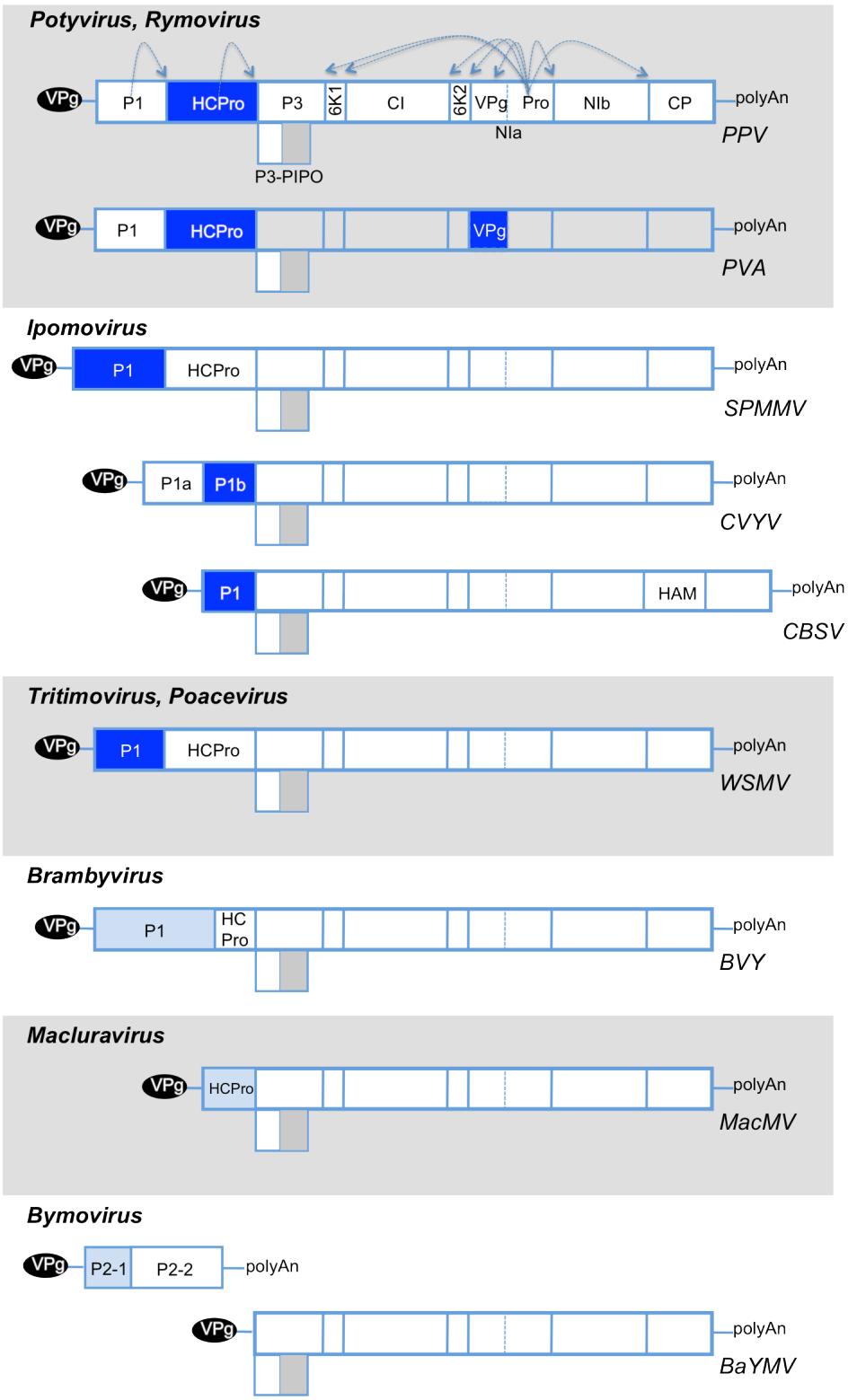

Figure 1. Genome organization in the *Potyviridae* Family. Open Reading Frames of the 8 genus grouped in the family are represented by long box divided into each individual cistron that gives rise to the corresponding mature protein product. The additional protein product PIPO originating from an alternative ORF is shown in a shaded box below each genome. The viral protein genome-linked (VPg) is shown as black ellipse at the beginning of the viral genome. For simplicity only PPV protease sites are indicated by blue arrow heads. The RSS protein reported in each virus is shown in dark blue. Viral proteins suspected to behave as RSS proteins are shown in light blue. Figure from (Revers & García, 2015) with modifications.

commonly classified under group IV of the Baltimore Classification relating to Picorna-like viruses. Genus Potyvirus is divided into two distinct paraphyletic groups: the monopartite group, with genome organisation consisting of one single positive sense VPg-linked polyadenylated RNA strand (+ssRNA) of approximately 9700 base pairs on average; and the bipartite group, with two single positive sense VPg-linked polyadenylated RNA strands of approximately 7600 and 3600 base pairs, both flanked by two UTRs at their 5' and 3' terminal ends (Fig. 1).

Genome organization and expression

Potyviral genomes belonging to the monopartite group encode for at least 11 genetic products in one single ORF (Fig. 1), flanked by two UTR at their 5' and 3' terminal ends, and translated as one single viral polyprotein of approximately 350 kDa. The viral polyprotein is proteolitically processed by viral encoded endopeptidases releasing at least 10 functional protein subunits (Adams et al., 2005; Revers & García, 2015) with one extra genetic product resulting from a transcriptional slippage of the viral RNA polymerase giving rise to a +2 frame shifted product named P3N-PIPO upon translation (Chung et al., 2008; Olspert et al., 2015). The processing kinetics of the polyprotein can generate cleavage intermediates that together with the multifunctional final cleavage products regulate all the necessary processes involved during the infection.

The viral process: Infection and multiplication

Due to size restrictions, viruses count on limited space to encode for proteins needed for infection. By coordinating interactions with host factors and developing multifunctional capacities, viruses can surrender host defences and recruit the necessary complexes to fulfil the biochemical requirements needed for viral replication and movement (Fig. 2).

Gene expression and genome multiplication are essential steps in viral cycles. All viruses must multiply, giving rise to a progeny of viruses termed quasispecies (Eigen & Schuster, 1977) to ensure propagation and adaptation (Domingo, 1997), but the replication machinery needed for viral multiplication is not present alone in either the virion particle or its host (Buck, 1996), instead it has to be

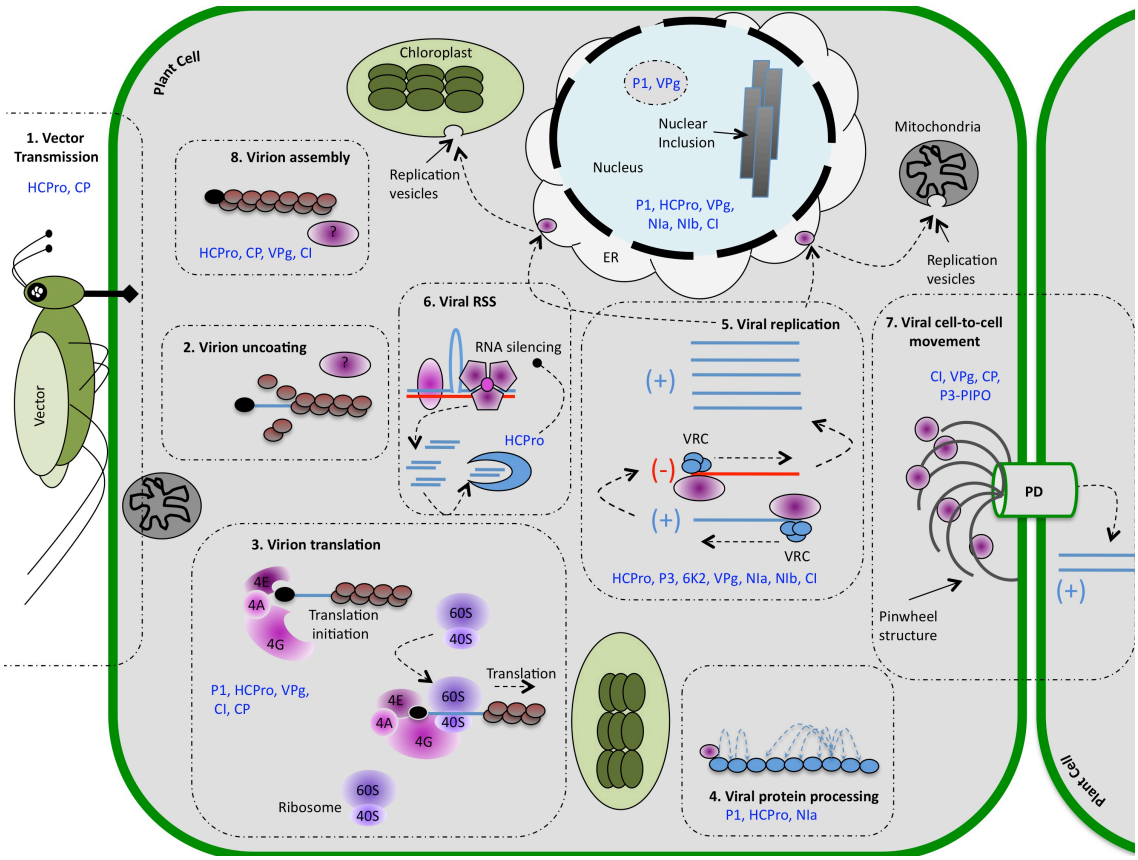

Figure 2. Diagram representing a simplified model of the potyvirus infection process. (1) Virus inoculation is mediated by arthropod vectors carrying virions, entering the cell during feeding. (2) Uncoating of the 5' end of the viral genome likely mediated by protein interactions with host proteins among other determinants. (3) The uncoated 5' end of the viral genome together with the VPg protein recruit the host factors to initiate translation and uncoating in finished co-translationally. (4) Viral polyprotein is proteolytically processed with the assistance of host factors. (5) Viral replicase recruits the cleaved viral products together with host factors into viral replicating complexes (VRC) to initiate viral replication. Additional host factors assist viral replication in membrane recruitment and movement into replication sites associated with cellular organelles. (6) The RNA silencing mechanisms triggered by the viral genome is suppressed by viral RNA silencing suppressor (RSS) proteins by interactions with RNA molecules and/or host proteins involved in the silencing machinery. (7) Viral cell-to cell movement results from membrane-bound replication vesicles and/or virions assisted by host factors associated with actin-myosin system and plasmodesmata. (8) Viral proteins together with the viral RNA genome associate to assemble virions likely assisted by host factors which will be sucked by feeding arthropod vectors providing a new non-persistant inoculation of healthy cells. Viral associated structures are shown in grey. Plant factors are shown in shades of pink-purple, viral VPg protein is represented as a black ellipse at the start of the viral genome which is represented in light blue. Viral subgenomic RNA is represented in red. Viral proteins are represented as light blue ellipses with the exception of the viral coat protein (CP) which is represented in brown. Diagram depicts a simplified representation of the processes and factors involved. Figure based on (Ivanov et al., 2014).

co-expressed and assisted by viral and host factors in a very specific and precise manner, determined in particular by each viral specie. The size constraints imposed in space prevent viruses from encapsidating ribosomal proteins, making viral protein translation dependent on the recruitment of functional translational machinery provided by the host (Walsh & Mohr, 2011).

To understand the different steps and requirements needed for the viral multiplication process a brief overview of the process relevant to plant viruses will be detailed further.

Viral Translation

An important viral event has to take place preceding viral translation. The RNA genome, tightly packed in the virion particles by repeated Coat Protein (CP) helix is to be uncoated. The exact mechanism by which potyviruses uncoat is still largely unknown. It is believed that the uncoating is favoured by two conditions: physical "sensing" of the cellular environment, and possible interactions with host factors. In TEV, for example, uncoating seems to start at the N-terminal region where the CP oligomers are destabilised and the genome is exposed to recruit the translation factors for its translation (Caspar & Namba, 1990; Mundry et al., 1991; Culver et al., 1995; Shaw, 1999; Culver, 2002). The exposure of the 5' region of the genome would be sufficient to recruit the host translational machinery and translation occurs co-translationally to disassembly (Shaw et al., 1986). Recruitment of the translation factors involved is achieved in some potyviruses by interactions with the viral VPg protein covalently linked to the 5' of the viral genome (Grzela et al. 2006; Robaglia & Caranta 2006; Beauchemin et al. 2007; Khan et al. 2008), although other potyviruses seem to employ a VPg-independent strategy (Riechmann et al., 1989; Simon-Buela et al., 1997; Gallie, 2001; Zeenko & Gallie, 2005). Translation has been proposed to be modulated by further interactions with other viral factors, like P1, HCPro or CP, assisting in different manners (Hafrén et al., 2010; Ala-Poikela et al., 2011; Martínez & Daròs, 2014). Cleavage of the endopeptidase P1 and HCPro would occur before the synthesis of the whole viral polyprotein is complete by co-translational processing (Carrington et al., 1989), and it is likely that these firstly released protein subunits have important roles in the early events of the infection other than proteolysis regulation (Pasin et al., 2014); RSS activity (Lakatos et al., 2006) or helper roles in aphid transmission (Atreya et al., 1992; Atreya & Pirone, 1993) which would be required in later stages of the infection. Because viral replicases are not encapsidated, viral replication cannot begin before translation has finished and the NIb replicase and other assisting viral factors are liberated from the viral polyprotein by the NIa

protease. Uncoating by the initial complete successful translation exposing the 3' end of the viral genome to interactions with the newly produced viral replicase, stimulate recruitment of the viral replicase complexes (VRC) and initiate the transcription of the viral negative sense subgenomic RNA concluding uncoating in a 3' to 5' direction (Wu et al., 1994; Wu & Shaw, 1997). Translation is thus a meaningful process that must be securely favoured both by co-opted host factors and intrinsic viral factors.

Viral Replication

At least one RNA dependent RNA polymerase protein (RdRp), functioning as the primary viral replicase, is required and encoded for in the viral genome (Bruenn, 1991). Since viral replicases are not encapsidated, RNA replication must be preceded by protein translation (Mundry et al., 1991; Walsh & Mohr, 2011), and for most (+) ssRNA viruses assisted by additional replication factors involved in membrane targeting, complex recruitment, and RNA unwinding among other functions (Ahlquist et al., 2003; Heinlein, 2015). The numerous host factors implicated in replication and recombination provide an overwhelming view of the complexity of the viral replication process (Barajas et al., 2014). Viral replication is performed in two steps. A first step involves the synthesis of the negative strand RNA by the VRC stimulated by the exposure of the 3' region of the genome which is then used as template in a, second coordinated RNA replication step, producing a newly synthesized viral genome (gRNA). Despite viral replication involves a wide variety of factors which are different for each virus, all (+) ssRNA viruses demand host membrane modification and recruitment (Ahlquist, 2002; Miller & Krijnse-Locker, 2008; den Boon et al., 2010; Sasvari & Nagy, 2010; Heinlein, 2015). Almost all cellular membranes types are co-opted in (+) ssRNA viral replications. Replication has been reported associated with chloroplast membranes (Hatta et al., 1973), tonoplast membranes (Falk et al., 1979; Hatta & Francki, 1981; Van Der Heijden et al., 2001; Cillo et al., 2002), mitochondrial membranes (Harrison & Roberts, 1968; Hatta et al., 1971; Erhardt et al., 2001; Mochizuki et al., 2009; Martínez-Turiño & Hernández, 2012), peroxisome membranes (McCartney et al., 2005; Panavas et al., 2005; Rubino et al., 2007), and endoplasmic reticulum (ER) derived membranes (Restrepo-Hartwig & Carrington, 1994; Martin et al., 1995;

Restrepo-Hartwig & Ahlquist, 1996; Heinlein et al., 1998; Carette et al., 2000; Dunoyer et al., 2002; Ritzenthaler et al., 2002) and assisted by numerous host factors participating in membrane organization and lipid metabolism (Lee et al., 2001; Lee & Ahlquist, 2003; Sharma et al., 2010; Sharma et al., 2011; Wang et al., 2011a; Zhang et al., 2012a), membrane sorting pathways (Barajas et al., 2009; Wang et al., 2011a; Hyodo et al., 2013; Wei et al., 2013) among other additional host membrane related factors (Yamanaka et al., 2002; Nicaise et al., 2007; Li et al., 2008; Pathak et al., 2008; Diaz et al., 2010; Nishikiori et al., 2011). It has been proposed that the replication vesicles derive from physical remodelling of cellular membranes is to provide shelter protecting viral replication from cellular defence responses (Paul & Bartenschlager, 2013). These replication vesicles have been observed to be mobile (Carette et al., 2002; Cotton et al., 2009; Grangeon et al., 2012) associated with actinmyosin motility system and involved in cell-to-cell movement in different viruses (Kawakami et al., 2004; Liu, 2005; Wei et al., 2010; Ibrahim et al., 2012; Amari et al., 2014; Heinlein, 2015). A number of viral factors have been implicated in potyvirus replication (Urcuqui-Inchima et al., 2001). Most potyviral mature proteins participate in some stage of the viral replication (Klein et al., 1994; Verchot & Carrington, 1995; Revers & García, 2015) and a precisely controlled regulation of the polyprotein processing can generate cleaved intermediate products with important biological roles in regulating different viral processes, including replication (Wellink & van Kammen, 1988; Merits et al., 2002; Revers & García, 2015). NIb composes the core VRC (Hong & Hunt, 1996) and its function is assisted by essential viral factors like 6K2-VPg-Pro (Beauchemin et al., 2007), CI (Lain et al., 1990; Eagles et al., 1994), P3 and 6K1 (Klein et al., 1994; Kekarainen, 2002; Merits et al., 2002; Zilian & Maiss, 2011; Revers & García, 2015) and likely non-essential factors like HCPro, P1 or CP (Verchot & Carrington, 1995; Hafrén et al., 2010; Ala-Poikela et al., 2011; Zilian & Maiss, 2011; Valli et al., 2014) as well. Moreover, viral replication can be regulated by posttranslational modifications of any of the viral proteins involved (Puustinen et al. 2002; Jakubiec & Jupin 2007; Hafrén & Mäkinen 2008; Xiong & Wang 2013) or by interactions with host factors. A series of host factors such as molecular chaperones (Tomita et al. 2003; Nishikiori et al. 2006; Serva & Nagy 2006; Dufresne et al. 2008a; Pogany et al. 2008; Wang et al. 2009; Hafrén et al. 2010; Huang et al. 2010; Mendu et al.

2010; Huang et al. 2012; Lin et al. 2012; Mine et al. 2012), RNA helicases (Thivierge et al., 2008; Huang et al., 2010; Kovalev et al., 2012a; Kovalev et al., 2012b) various components of the host translation machinery (Quadt et al., 1993; Wang et al., 2000; Leonard, 2004; Matsuda et al., 2004; Nishikiori et al., 2006; Yamaji et al., 2006; Beauchemin et al., 2007; Beauchemin & Laliberte, 2007; Nicaise et al., 2007; Dufresne et al., 2008; Thivierge et al., 2008; Li et al., 2009; Li et al., 2010; Sasvari et al., 2011) and cytosolic proteins with diverse functions (Diez et al., 2000; Mas et al., 2006; Beckham et al., 2007; Wang & Nagy, 2008; Kovalev et al., 2012b; Kaido et al., 2014) have all been reported to play important roles during potyviral multiplication.

Viral replication is a fundamental process in viral multiplication requiring not only the recruitment of large number of host and viral factors, but also a coordinated control with the translation machinery involved in viral expression. As a result, viral protein interactions tend to be extremely dynamic, highlighting their multifunctional abilities required for the correct function and coordination of all the viral processes. At the same time, recruitment and employment of all these cellular factors results in metabolic consequences for the infected plant. The rapid accumulation of viral RNA and the cellular stress caused by the viral-induced molecular re-programming of the cell are determinants in the induction of host defence systems against the virus (Soosaar et al., 2005).

RNA silencing as a defence mechanism against plant viruses

Viral infections are to be conceived as a set of complex and dynamic interactions between viruses and hosts. On one side, the host's efforts are directed in maintaining a cellular homeostasis to fulfil the metabolic requirements determined by its genetic programme, on the other side, the virus exerts all its efforts into manipulating the cellular components and machineries to employ in its own requirements to successfully complete its viral cycle (Walsh & Mohr, 2011).

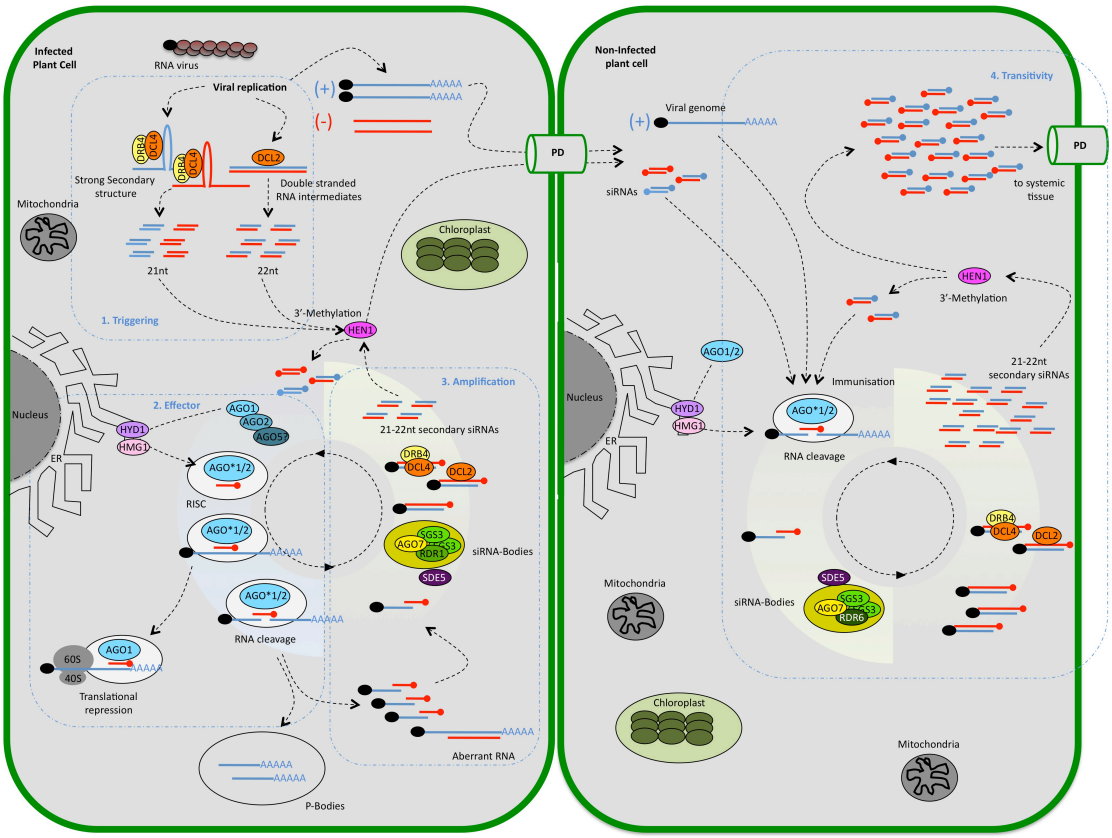

Figure 3. Antiviral RNA silencing against RNA viruses in *Arabidopsis thaliana*. (1) Triggering of the RNA silencing system by strong secondary RNA structures and/or subgenomic double stranded replicative intermediates induce the production of small interfering RNA (siRNA) molecules. 3'-methylation of the siRNA molecules is performed by HEN1 prior entering the effector phase. (2) Methylated siRNAs are loaded into the RNA Induced Silencing Complex (RISC) assembled with an AGO protein previously activated by a yet undetermined process involving isoprenoid biosynthesis enzymes HMG1 and HYD1. RNA cleavage or translational repression of target RNA is guided by the siRNA-loaded activated RISC complexes. (3) Secondary siRNA molecules are produced by capped RNA fragments generated in the effector phase entering siRNA-bodies where RDR1 in association with AGO7, SGS3 and SDE5 among other host factors mediates synthesis of complementary RNA, which will subsequently be processed by DCL2/4 nucleases. Secondary siRNA molecules are stabilised by HEN1 and move in association with host silencing movement factors to immunise neighbouring cells. (4) Secondary siRNA molecules in neighbouring cells result from capped RNA fragments derived from cleaved target RNA entering siRNA-bodies where RDR6 in association with AGO7, SGS3 and SDE5 among other host factors mediates synthesis of complementary RNA, and subsequently processed by DCL2/4 nucleases. Secondary siRNA molecules are stabilised by HEN1 prior to their spread throughout the systemic tissue conferring resistance and impeding the viral spread towards distant plant tissues and organs. Diagram represents a simplified representation of the silencing mechanisms and factors involved. Sizes are not to scale. Figure base on (Ding & Voinnet, 2007).

Consequences of this molecular-dependent relationship results in metabolic stress, which is sensed by different host defence sensing mechanisms, resulting into an adaptive response that initiates a selection of sophisticated antiviral defence mechanisms to defeat infection in the local tissue and confer resistance in the systemic, yet uninfected, tissue (Dangl & Jones, 2001; Soosaar et al., 2005; Jones & Dangl, 2006). A number of innate immune responses against viral attacks have been described in plants, involving dominantly and recessively inherited

resistance (R) genes (Martin et al., 2003). Defence mechanisms include activation of the proteosome system (Dielen et al., 2010), plant R-gene mediated hypersensitive (HR) (Loebenstein, 2009; Mandadi & Scholthof, 2013) and systemic acquired resistance (SAR) (Kachroo & Robin, 2013) responses, RNA silencing (Voinnet, 2001; Pumplin & Voinnet, 2013) and protein translation suppression recently reported as a plant antiviral immune pathway (Nicaise, 2014). Whereas suppression of protein translation and R-gene mediated immune responses trigger an array of physiological and biochemical defence processes broadly targeting pathogens (Nicaise, 2014), RNA silencing is a specific sequence-dependent molecular mechanism that selectively targets RNA sequences. Viral dsRNA replicative intermediates produced by viral (Waterhouse et al., 1998; Voinnet, 2001) or host (Dalmay et al., 2000; Ahlquist, 2002) RNA-dependent-RNA-polymerases and/or strong RNA secondary structures (Baulcombe, 2004) have been shown to be strong inducers and targets of the antiviral RNA silencing response (Covey et al., 1997; Ratcliff, 1997; Voinnet, 2001; Baulcombe, 2004).

The mechanism

RNA silencing is a controlled and precise genetic regulatory mechanism (Fire et al., 1998) conserved in most living organisms (Tijsterman et al., 2002; Aravin & Tuschl, 2005; Grishok, 2005; Kavi et al., 2005; Nakayashiki, 2005) originated from a common modern eukaryotic ancestor (Shabalina & Koonin, 2008) and involved in many fundamental physiological (Jones-Rhoades et al., 2006; Wilson & Doudna, 2013), developmental (Rhoades et al., 2002; Meins et al., 2005; Jones-Rhoades et al., 2006) and pathological (Esquela-Kerscher & Slack, 2006; Lu et al., 2008) processes. It has also been accepted as an ancestral genetic innate immune system preserving the integrity of the genome against invading nucleic acids like transposons and viruses (Plasterk, 2002; Martínez de Alba et al., 2013). Foreign genetic elements, like viruses, have been shown to trigger and induce the RNA silencing response (Ratcliff, 1997; Hamilton & Baulcombe, 1999) in the infected tissues, with spreading of effector molecules produced to adjacent and systemic tissues conferring protection against the invasion, in a process termed *transitivity* (Vance, 2001; Sijen & Plasterk, 2003; Bartel, 2004; Baulcombe, 2004; Bayne et al., 2005; Dunoyer & Voinnet, 2005; Schwach et al., 2005; Pyott & Molnar, 2015). The

discovery that viruses encode for RNA silencing suppressor (RSS) proteins was a definite finding in support of RNA silencing as an innate defence mechanism (Anandalakshmi et al., 1998; Beclin et al., 1998; Brigneti, 1998; Kasschau & Carrington, 1998). Co-evolution in virus-host interactions has steered a cellular arms-race proliferation where both defending and invading organisms have acquired, via selective pressure, state-of-the-art molecular mechanisms to surrender their opponent (Obbard et al., 2009; Murray et al., 2013). Viral RSS aims to arrest the silencing machinery to protect the viral genome from degradation, and as a consequence, also inhibiting the production and movement of the silencing signals to adjacent cells and systemic tissue (Csorba et al., 2015).

Today much is known about the RNA silencing pathways present in many organisms, shown to encode and function in a very diverse and complex set of molecular machinery, tightly regulated and coordinated to control many and important cellular processes. Although each specific pathway may have distinct biogenesis and cellular factors involved, the fundamental process shares common features with the antiviral RNA silencing pathway, which will be described briefly considering plant RNA viruses as the main focus of interest (Fig. 3).

Viral RNA silencing can mainly be divided into two distinct functional categories: *Posttranscriptional Gene Silencing* (PTGS), and *Transcriptional Gene Silencing* (TGS), although other functions have newly been discovered, involving DNA elimination or DNA repair (Duharcourt et al., 2009; Lee et al., 2009; Francia et al., 2012; Michalik et al., 2012; Wei et al., 2012). Whereas PTGS mediates control of protein expression through cleavage of cognate RNAs, guided by sequence complementarity (Hannon, 2002; Tijsterman et al., 2002), or by inhibition of translation in a process called *translational repression* (Chen, 2004; Brodersen et al., 2008), TGS is the result of RNA-directed DNA methylation (RdDM) events directed to transcribed regions of target genes with sequence homology (Matzke & Birchler, 2005) or promoter regions controlling expression (Matzke et al., 2004), resulting in a blockage of RNA transcription and downregulation of target gene expression. PTGS is the main mechanisms in antiviral RNA silencing against RNA

plant viruses and a brief description focusing into the antiviral mechanisms will follow.

PTGS is induced by viral RNA during replication. It has been demonstrated that both dsRNAs and highly structured ssRNAs can trigger RNA silencing with the production of *small interfering RNA* (siRNA) molecules (Carrington et al., 2001; Voinnet, 2001; MacDiarmid, 2005; Ding & Voinnet, 2007; Mlotshwa et al., 2008). Triggering starts by the processing of the viral RNA precursors by Dicer type RNAse III-like enzymes (DCL) producing short siRNA duplexes of variable sizes (21-22bp), depending on the DCL activity employed (Wang et al., 2011b), bearing 2 nucleotide 3'-terminal overhangs. DICER function has been seen to be assisted by numerous partner proteins (Han et al., 2004; Vazquez, 2004; Hiraguri et al., 2005; Lobbes et al., 2006; Yang et al., 2006; Gregory et al., 2008; Kim et al., 2008; Laubinger et al., 2008; Yu et al., 2008; Ren et al., 2012; Zhang et al., 2012b; Wu et al., 2013) in a number of tasks and functions.

Four DCL proteins have been reported to be encoded in *A. thaliana*. While all four DCL proteins mediate in the defence response against DNA viruses (Blevins et al., 2006; Moissiard & Voinnet, 2006), only DCL2, DCL3 and DCL4 have been associated with antiviral RNA silencing in response to ssRNA viruses. Both DCL2 and DCL4 are predominantly associated with antiviral siRNA production, yet some functional redundancy has been observed for DCL3 especially when DCL4 function is lost (Blevins et al., 2006; Bouché et al., 2006; Deleris et al., 2006; Fusaro et al., 2006; Du et al., 2007; Donaire et al., 2008; Qu et al., 2008; Garcia-Ruiz et al., 2010). On the other hand, DCL1 is proposed to function in a negative-feed back mechanism, negatively regulating DCL2 and DCL4, and as a consequence antiviral RNA silencing (Qu et al., 2008).

The siRNA molecules encode for the digital information of the *RNA Induced Silencing Complex* (RISC) (Wilson & Doudna, 2013), guiding RISC to their effector targets by means of sequence complementarity, producing the cleavage of the complementary RNA to the siRNA loaded in RISC. RISC is the main effector of the silencing pathway and its precise action in silencing depends on the argonaute

(AGO) protein associated in its assembly, which will determine its ribonuclease activity, interacting partners and subcellular localisation (Poulsen et al., 2013).

A total of 10 different AGO proteins have been reported to be encoded in the genome of *A. thaliana* although only certain members have been involved in different silencing pathways. Filogenetically, AGO proteins are proposed to group into three distinct clades (Vaucheret, 2008), of which AGO1 and AGO5 from one clade, AGO2, and AGO7 from different clades have been described involved in stages of the antiviral RNA silencing pathway (Morel et al., 2002; Zhang et al., 2006; Qu et al., 2008; Takeda et al., 2008; Vaucheret, 2008; Voinnet, 2009; Harvey et al., 2011; Brosseau & Moffett, 2015), among other RNA silencing functions (Brodersen et al., 2008; Kumakura et al., 2009; Voinnet, 2009; Jouannet et al., 2012; Wei et al., 2012; Martinez de Alba et al., 2015). AGO1 has been reported to localise in nuclear "dicing-bodies" (D-bodies) (Fang & Spector, 2007; Liu et al., 2012), and in cytosolic and microsomal fractions (Brodersen et al., 2012). Membrane association to the endoplasmic reticulum (ER) has been reported to be required for AGO1 function and dependent on various proteins involved in isoprenoid biosynthesis (Brodersen et al., 2012), among other interactions with host partner proteins (Iki et al., 2010). AGO2 has been reported to localise in the cytosol and nucleus (Takeda et al., 2008) playing a role in antiviral silencing (Harvey et al., 2011) and in DNA repair processes (Wei et al., 2012), whilst AGO7 has been seen accumulating in the cytosol co-localising with *RNA-Dependent-RNA-Polymerase 6* (RDR6) and *Suppressor of Gene Silencing 3* (SGS3) in cytosolic structures, termed *siRNA-bodies*, with distinct, but inter-related, functions from P-bodies (Kumakura et al., 2009; Jouannet et al., 2012; Martinez de Alba et al., 2015).

Following the RISC-mediated cleavage of the target RNA, secondary siRNA mediators are produced in an amplification process dependent on various cell factors in a process known as *Transitivity* (Gasciolli et al., 2005). Upon cleavage of the RNA target by RISC, RDR6 in

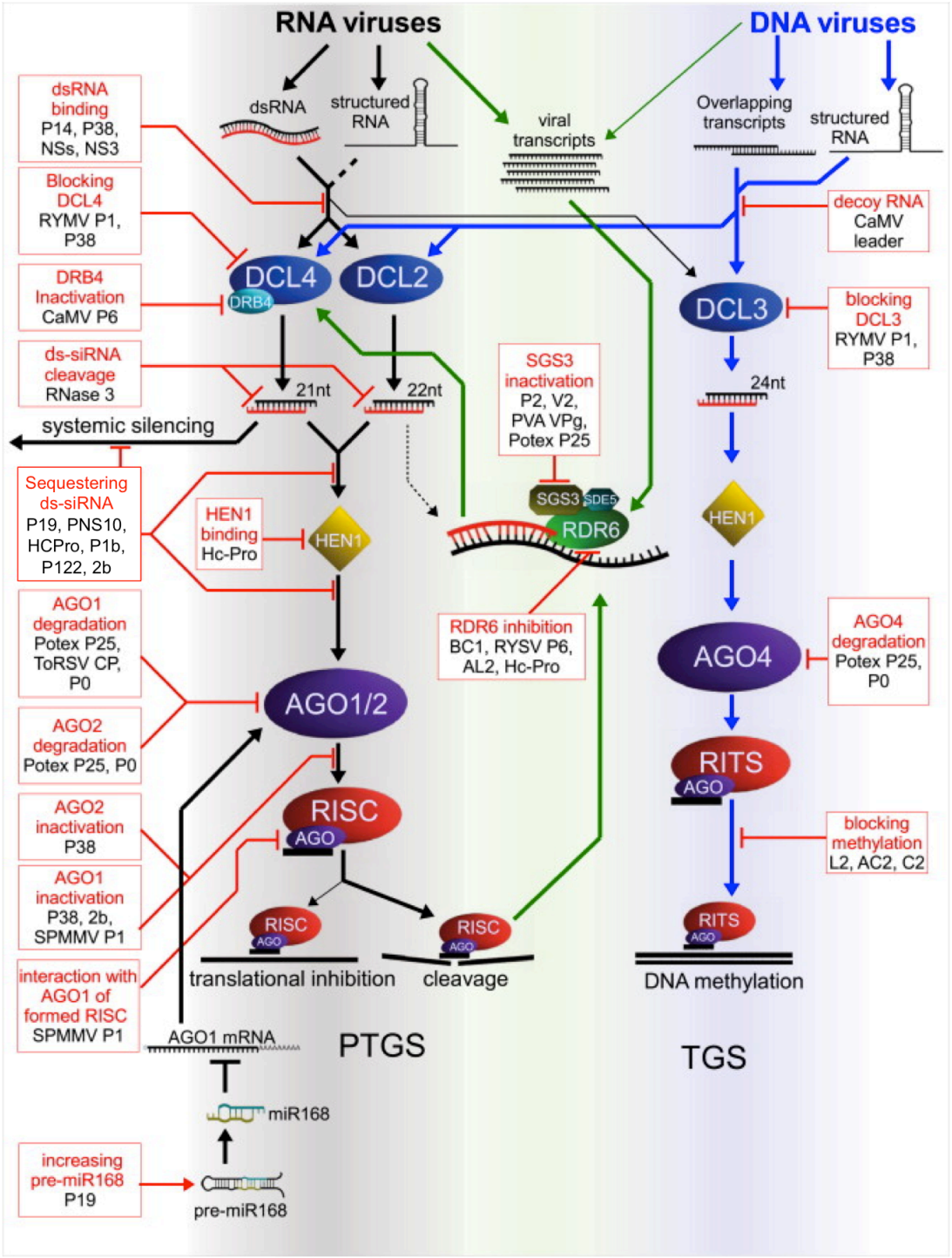

Figure 4. Inhibition of the RNA silencing pathway by different viral RSS proteins. RNA silencing response against RNA viruses is initiated by DCL4 and DCL2 through production of 21–22 nt viral siRNAs. Viral siRNAs are methylated by HEN1 and loaded into AGOs. AGO1 and AGO2 are the two main effectors of the assembled RISC complex mediating in the cleavage or translational repression of the target RNA. Cleaved-AGO products, aberrant RNAs serve as templates for RDR1/6 complexes to amplify the antiviral response in association with various partners. RNA amplification may be primed by DCL2-derived 22 nt vsiRNAs (middle). In DNA virus infections DCL4 and DCL3-derived viral siRNA initiate PTGS or transcriptional gene silencing (TGS) respectively. DCL3-generated 24 nt viral siRNA following the HEN1 stabilisation are loaded into AGO4. AGO4-RITS causes the methylation of viral genome to complete TGS (right side). The diverse viral suppressors inhibiting PTGS and/ or TGS are shown in black boxes along the sides of the figure. The dashed lines point to the interference place where the viral RSSs impairs the antiviral RNA silencing pathway. Figure from (Csorba et al., 2015) with modifications.

association with SGS3, among other factors, subsequently converts the 5' and 3' RISC-cleaved RNA fragments into long dsRNAs in siRNA-bodies that will then be processed into 21nt long secondary siRNA molecules, by a DICER-like nuclease (DCL4) in association to other cellular factors (Han et al., 2004; Vazquez, 2004; Hiraguri et al., 2005; Hernandez-Pinzon et al., 2007; Jauvion et al., 2010). Whilst RDR1 has been reported to be required for local silencing, RDR6 is an indispensable factor in the systemic silencing response (Garcia-Ruiz et al., 2010; Wang et al., 2010; Pyott & Molnar, 2015). Cleaved products are protected from degradation by SGS3 which is recruited by AGO1 or AGO7 associated RISC (Yoshikawa et al., 2013) in siRNA-bodies, involved in secondary siRNA production (Jouannet et al., 2012). Whilst RDR1, RDR2 and RDR6 have been associated to specific biological functions, other RDR members have not been yet assigned to any biological role (Willmann et al., 2011).

Viral counterattack. Viral suppression of RNA silencing

Viruses are triggers and targets of RNA silencing (Hamilton & Baulcombe, 1999) and the mere nature that drives their multiplication can count against them. Viral multiplication has to be performed stealthily, avoiding detection of host defence systems programmed to neutralise emerging infections. Viral survival is achieved through different strategies, among which are, inhibiting the RNA silencing pathway in any of its three phases (initiation, effector or amplification), escaping recognition by replicating in protected subcellular structures (Schwartz et al., 2002), introducing changes in the viral genome to elude sequence specificity powered by rapid evolution of highly mutating genomes (Simón-Mateo & García, 2006), rapidly moving into systemic tissue assisted by viral movement proteins complexes (Beck et al., 1994) or a combination of any of these mentioned. Production of viral RNA silencing suppressors is probably the most widespread strategy to escape host RNA silencing defence system (Lakatos et al., 2006). Most, if not all, viruses encode for a protein with RSS functions (Pumplin & Voinnet, 2013), and in some cases, RSS function can be complemented by various viral proteins simultaneously (Rajamäki et al., 2014), targeting one or multiple steps in

the RNA silencing pathway (Fig. 4). All steps in the silencing pathway are vulnerable to inhibition by viral RSS proteins causing an arrest in the silencing mechanism. As a result, silencing pathways need to be plastic enough to bypass viral hijacking, for example by surrogating functions like in the case of DCL4 and DCL2 (Ding & Voinnet, 2007; Moissiard et al., 2007; Azevedo et al., 2010) or AGO1 and AGO2 (Poulsen et al., 2013). On the other hand, to efficiently inhibit silencing, viruses must block different steps in the silencing pathway to compensate for this molecular plasticity. One example is HCPro, which sequesters smRNAs (Lakatos et al., 2006), but also inhibits HEN1 (Jamous et al., 2011) and downregulates RDR6 (Zhang et al., 2008) to affect smRNA stability and attenuate secondary smRNA production respectively. As a result, many viral RSS proteins are forced to interact with various host factors, both for processes needed during the viral cycle, and in inhibiting RNA silencing. In a general sense, viral RSS can be classified according to their general mechanisms of action: i. binding to long dsRNA conferring protection from DCL-like nucleases, as has been reported for PolV P14 (Merai et al., 2006), ii. binding, sequestering and destabilising smRNAs preventing loading of the smRNA into RISC, as observed for P19 (Vargason et al., 2003), HCPro (Maia & Bernardi, 1996; Sahana et al., 2014), and P1b (Valli et al., 2008), and iii. targeting effector proteins or factors involved in the silencing pathway causing their malfunction, inhibition or degradation (Giner et al., 2010). To date at least 70 different viral RSS proteins targeting different steps in the silencing pathway have been reported (Csorba et al., 2015).

Host partners in PPV infection

Recruitment of host partners is essential for all viruses, let alone potyviruses. The small size of RNA viral genome due to size constraints, has favoured the emergence of multifunctional viral proteins which are involved in numerous viral processes, requiring a coordinated recruitment of host partners to assist in their primary tasks and functions, whilst deactivating and surrendering host defence responses. The screening and study of host viral partners can provide useful information on functions of viral proteins to increase our understanding in their relevance during the host-virus crosstalk. To date, numerous potyviral host partners have been

reported by using different genetic and proteomic approaches (Fig. 5). The benefits in finding host partners essential for viral infections encompasses the potential for developing antiviral strategies targeting host-viral interactions, with important economical benefits in agricultural exploitations. Among the most studied viral proteins is HCPro, having been associated with numerous host partners involved in distinct processes, demonstrating the multifunctional requirements of viral proteins to support viral infection.

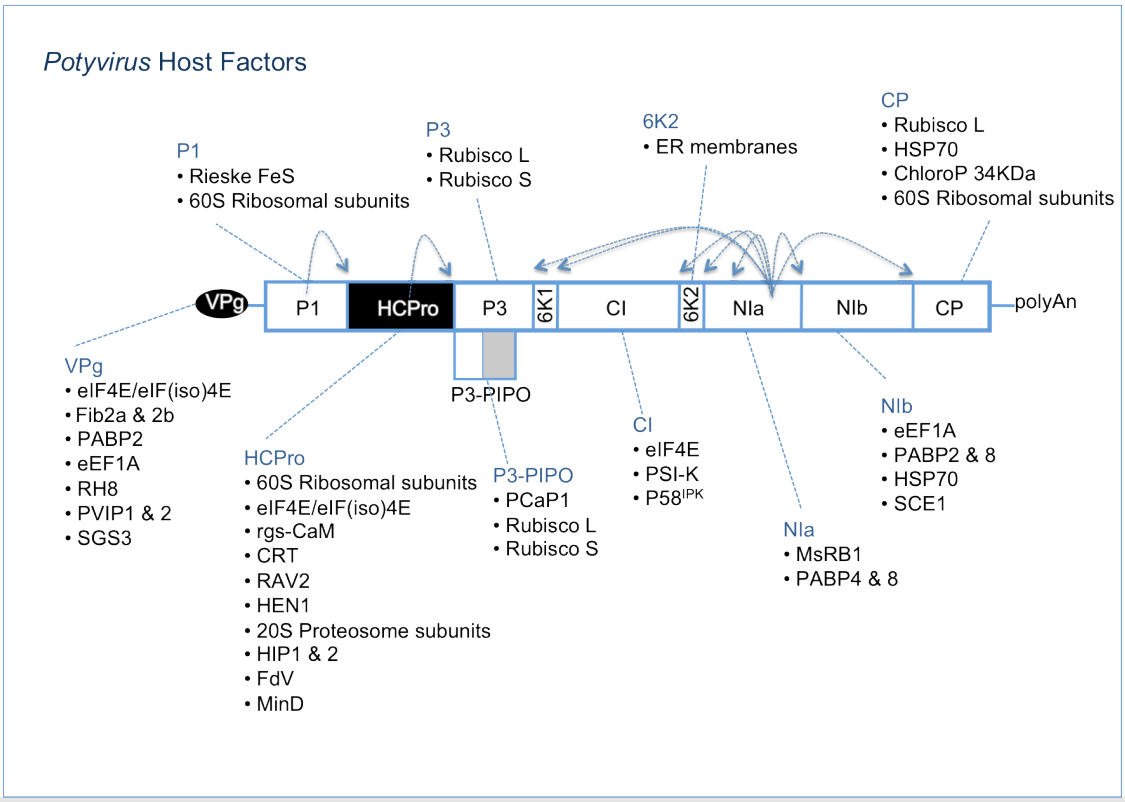

Figure 5. Host factors interacting with potyviral proteins. A general potyvirus genome ORF belonging from Genus *Potyvirus* is represented by long box divided into each individual cistrons that gives rise to the corresponding mature protein product. The additional protein product P3N-PIPO originating from an alternate ORF is shown in a shaded box below. The viral protein genome-linked (VPg) is shown as black ellipse at the beginning of the viral genome and a polyadenylated tail at the end. Arrows point at protease sites for each viral protease. For each mature viral protein product, known host interacting proteins are shown. The viral RSS protein, HCPro, is shown in a black box.

Host partners involved in HCPro functions

Host translation related proteins have been reported to interact with many of potyviral proteins evidencing the tremendous efforts of the virus to gain control over translational processes (Fig. 5). One important group of HCPro host partners are those related to translation. Subunits of the 60S structural constituent of the

ribosome have been co-purified with TEV P1 together with TEV HCPro and CP. TEV P1 interaction with the 60S subunit was shown to be independent of its nuclear localization (Martínez & Daròs, 2014) suggesting that nuclear trafficking of P1 is not a requirement for its association to the ribosomes, meaning that P1, HCPro and CP could be associating to the same cytosolic ribosomal complexes, involving these three viral proteins in translation processes. The translation initiation factors, eIF4E and its isoform, eIF(iso)4E are widely recruited during potyviral infections. VPg, CI and HCPro have been reported to interact in different virus-host combinations with either of the two isoforms or both (Wittmann et al., 1997; Ala-Poikela et al., 2011; Tavert-Roudet et al., 2012). Viral efforts in recruiting eIF4E factors are substantial judging from the high number of proteins interacting with these host factors, although the precise role of this interaction has not yet been described. Interaction with any of the two eIF4E isoforms has been shown to be a fundamental requirement for potyvirus infection in many crop species (Sato et al., 2005; Robaglia & Caranta, 2006; Hwang et al., 2009; Wang et al., 2013). Natural variations in eIF4E loci have been attributed to viral resistance breaking. Demonstrating that viral interactions with eukaryotic Translation Initiation Factors (eIFs) are critical for potyviral multiplication (Nicaise, 2003).

Another important group of HCPro interactors are those required for the RSS functions. *Regulator of the ATPase of the Vacuolar Membranes 2* (RAV2), one of the six reported members of the ethylen-inducible transcription factors was identified as an interacting partner of HCPro from different potyviruses and found to be required for RSS activity (Anandalakshmi, 2000; Endres et al., 2010). Zucchini Yellow Mosaic Virus (ZYMV) HCPro was also seen to interact with the methytransferase protein, *Hua Enhancer 1* (HEN1) (Jamous et al., 2011) to inhibit the methyltransferase catalytic activity (Yu et al., 2005) involved in protecting smRNAs from degradation resulting in the developmental abnormalities observed in transgenic HCPro expressing *A. thaliana* plants as a consequence of impairing host miRNA pathway (Mlotshwa, 2005). These finding are particularly interesting as it suggests that at least this viral RSS suppressor proteins require host factors for one of its RSS activity, and additional RSS activities different from sequestering smRNAs could be functioning synergistically in protecting the viral genome.

However, certain HCPro interactions seem to constrain RSS functions resulting in a favourable outcome towards the host. This is the case of *Regulator of gene silencing-Calmodulin-like protein* (rgs-CaM) identified as an interactor protein of HCPro from various potyviruses (Anandalakshmi, 2000; Nakahara et al., 2012) resulting in a strong inhibition of the RSS activity mediated by autophagosome induction. Direct interaction with at least four different members of the host proteosome core complex has also been described for various HCPro proteins (Dielen et al., 2011). Although HCPro interaction with the proteosome subunits was suggested to modify the proteosome activity (Ballut, 2005; Sahana et al., 2012), other reports claim the effect observed on the infection are rather due to inhibition of the RNAase activity of the proteosome (Ballut et al., 2003; Ballut, 2005; Dielen et al., 2011). Whether the 20S proteosome system is part of the host antiviral response system is yet to be determined.

On the other hand, other host proteins like, *Calreticulin* (CRT), *Ferredoxin V* (FdV), *Minicell Chloroplast Division Protein* (MinD), SPIRAL2/TORTIFOLIA1 (SPR2/TOR1), SPIRAL2-like (SP2L) and an unknown Ring-finger protein (HIP1) were all found to interact with HCPro from different potyviruses, with yet undetermined functions (Jin et al., 2007; Cheng et al., 2008; Haikonen et al., 2013).

Viral RSS proteins are multifunctional proteins

Because of their extraordinary differences in sequence and structures, RSS activity seems to be a recently acquired function by viral proteins in addition to their original primary functions, thus it is speculated that viral RSS is a recent converging evolutionary adaptation to the RNA silencing defence response (Ding & Voinnet, 2007; Incarbone & Dunoyer, 2013; Csorba et al., 2015). As a result, many viral RSS proteins retain primordial interactions with host factors, both for processes established prior to acquiring the RSS activity needed during the viral cycle, along interactions in impairing RNA silencing.

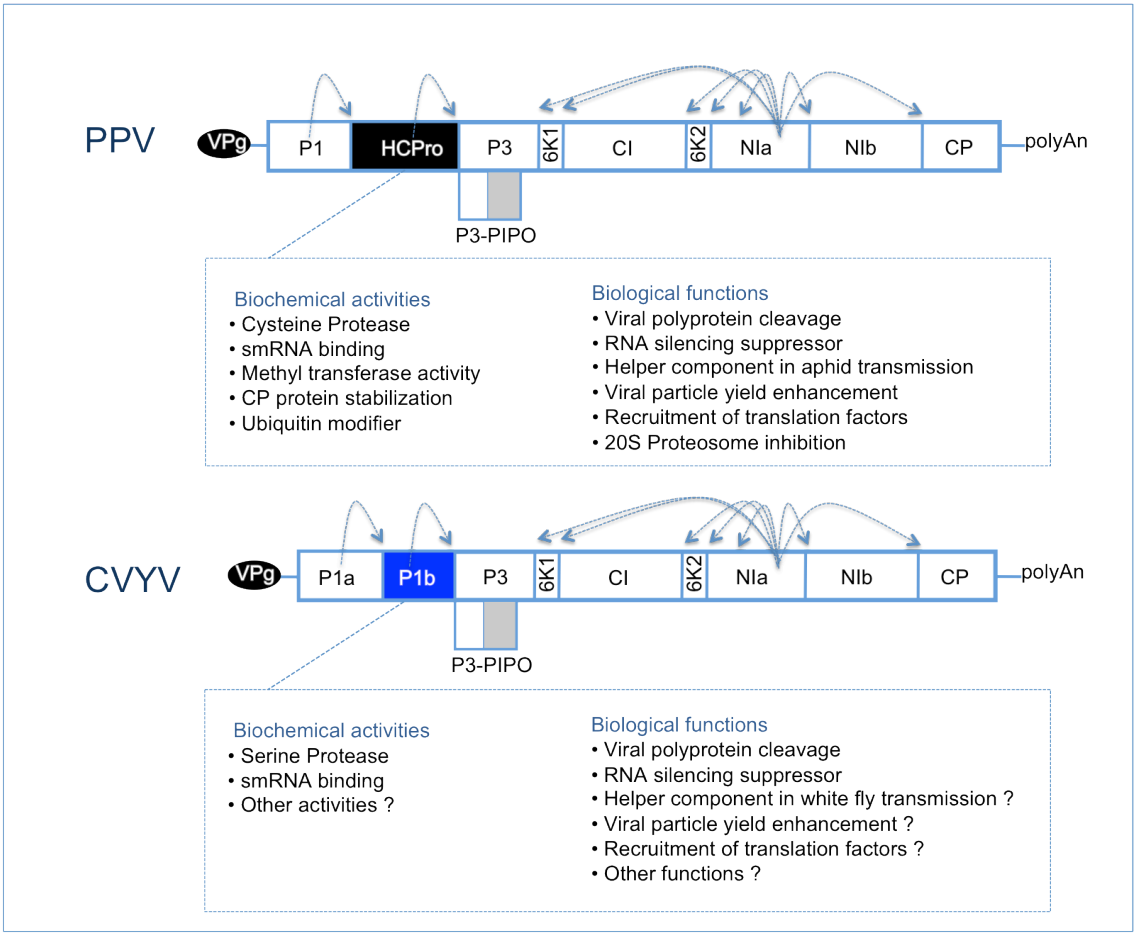

Figure 6. Biochemical activities and functions reported for two different RSS proteins belonging to Fam. Potyviridae. PPV (*Potyvirus*) and CVYV (*Ipomovirus*) genome ORFs are represented by long box divided into each individual cistrons that gives rise to the corresponding mature protein product. The additional protein product PIPO originating from an alternate ORF is shown in a shaded box below. The viral protein genome-linked (VPg) is shown as black ellipse at the beginning of the viral genome and a polyadenylated tail at the end. Arrows point at protease sites for each viral protease. For each RSS protein, known or suspected biochemical activities and biological functions are shown. The viral RSS proteins, HCPro, and P1b are shown in a black or blue box respectively.

Either independently or through numerous interactions with host factors, HCPro has been reported to be involved in a wide variety of viral functions (Fig. 6), including viral protein cleavage, helper component in aphid transmission, viral protein translation, virion yield and stability, and proteosome inhibition. However, recent reports show HCPro to be dispensable for PPV infection if substituted by a protein with RSS activity (Carbonell et al., 2012). Interestingly, not all RSS strategies can be functional when challenged in a viral context. A particular RSS activity might be preferred by certain viruses if to replace their canonical viral RSS. This seems to be the case for PPV, as only RSS proteins with smRNA binding activity can efficiently replace HCPro, causing systemic spread and accumulation

levels similar to wild type PPV (Maliogka et al., 2012). Other RSS operating with different silencing strategies like Influenza virus A (IVA) NS1 or Sweet potato mild mottle virus (SPMMV) P1 can only partially replace HCPro in a viral context, as infection is highly challenged, resulting in low viral accumulation independently of the RSS strength (Maliogka et al., 2012). This suggests that not all RSS strategies are equally favourable, and the efficiency of the infection depends on other viral determinants amidst RSS activity. This can clearly be seen by the fact that even RSS with similar RSS strategies, like HCPro and P1b, the RSS protein encoded in *Cucumber Vein Yellowing Virus* (CVYV), an Ipomovirus member of the *Potyviridae* family, display distinct infection phenotypes, resulting in a partial recovery of systemic tissue in plants infected with the chimeric virus harbouring P1b (Carbonell et al., 2012). This seems especially noteworthy as has been mentioned earlier; since RSS is a recent evolutionary acquisition other functions imprinted before acquiring RSS activity will be affected in the substitution between both RSS proteins. In this sense, although P1b can substitute HCPro RSS activity in PPV, functions affecting virion stability have been observed to be highly challenged (Valli et al., 2014), suggesting that other important HCPro functions cannot be supplied by P1b.

The occurrence that certain potyviruses did not encode for any HCPro cistron, but a large P1 sequence instead led the motivation to further research this exceptional P1, encoded in viruses belonging to the Ipomovirus genus (Janssen et al., 2005). Taking CVYV P1 as a model, the long P1 cistron was observed to encode for two serine endopeptidases (Valli et al., 2006), thought to originate from an ancestral genetic duplication (Valli et al., 2007). Cleavage by the endopeptidase activity would produce two mature protein products, P1a and P1b, of 525 and 318 amino acids (aa), respectively. The P1a sequence was observed to cluster predominantly with the potyviral and rymoviral P1s, whereas the P1b domain was more related to the tritimoviral P1s (Valli et al., 2007). P1b was demostrated to posses smRNA binding activity and function as a RSS protein (Valli et al., 2008), likely by sequestering smRNAs, a common RSS strategy employed by similar viral proteins like HCPro (Anandalakshmi et al., 1998; Brigneti, 1998; Kasschau & Carrington, 1998). Apart from P1b, no other CVYV protein products have been characterized

further, and are thought to function similarly to other potyviral proteins. P1b interactions with host partners could be required to perform important functions assisting its RSS activity, and any other functions imprinted beforehand, similarly as reported for HCPro. Regretfully, at present no CVYV cDNA infectious clone is available to use in the study of P1b functions and the only hosts susceptible to CVYV infection are restricted to few plant species, including cucurbits. PPV has been reported to be an advantageous tool as a biofactory in the expression of heterologous proteins (García et al., 2014). The availability of PPV based cDNA expression systems to use in the expression and study of P1b functions is an exceptional tool with clear advantages despite the minor flaws observed. To continue in the study and understanding of RSS proteins from the *Potyviridae* family, P1b is a yet unexplored RSS protein which can furnish new information in the understanding of viral and host processes. This PhD thesis is focused in the discovery of host interactors that could contribute to important or accessory P1b functions.

"My dreams were at once more fantastic
and agreeable than my writings."

Mary Shelley, *Frankenstein*.

OBJECTIVES

OBJECTIVES

Understanding the molecular functions required for a viral genome to sustain a functional infection is important to address new ways of protecting crops and organisms from viral infections and furthermore, in understanding functional implications to enable us develop new technological tools to control gene expressions and translation of industrially attractive products. In this work the following objectives were determined:

1. To find physical interacting cellular factors of P1b using different heterologous expression systems and validate interactions functionally.

2. To screen for new transcriptional regulators affecting potyviral accumulation in plants.

3. To analyze the deregulation caused by Plum pox virus on the proteome signature of plant cells.

4. To insight on new uncharacterized functions of CVYV silencing suppressor protein P1b in the context of a viral infection.

"We learn from failure, not from success!"

Bram Stoker, *Dracula*.

MATERIAL & METHODS

BIOLOGICAL MATERIAL

Plants

The following plant species were used in this study:

Table 1. List of the plant species used during the course of this study.

Family	Genus	Species	subspecie
Brassicaceae	Arabidopsis	*A. thaliana*	Col-0
Solanaceae	Nicotiana	*N. benthamiana*	
Cucurbitaceae	Cucumis	*C. sativus*	SMR
		C. sativus	Albatroz
		C. sativus	Cádiz

The following transgenic plant lines were used in this study:

Table 2. *A. thaliana* T-DNA insertion plant lines used in this work. Locus affected, line accession, T-DNA insertion site, seed stock, and antibiotic selection is as indicated.

Gene Affected	AGI code	Line ID	T-DNA insertion site	Seed Stock	Selection	Source
WRKY47	AT4G01720	GK-193B03	Exon 1	N418447	Sul^r	(Robatzek & Somssich, 2002)
UBQ2-RPL40A	AT2G36170	SALK_040108	Promoter	N670598	Kan^r	NASC
MYB75	AT1G56650	pap1-D	Exon 1	N3884	$BASTA^r$	NASC
MYB90	AT1G66390	SALK_041562	Intron 1	N679574	Kan^r	NASC
PRH75	AT5G62190	SAIL_302_D12	Exon 1	N81988	$BASTA^r$	NASC
		SALK_016729	Exon 4	N678155	Kan^r	NASC
HP2	AT1G47860	SALK_044041	Exon	N654169	Kan^r	NASC
DNAJ	AT1G72070	SALK_020586	Exon 3	N657168	Kan^r	NASC
NTH2	AT1G05900	SALK_013055	Exon 6	N667805	Kan^r	NASC
WRKY6-2	AT1G62300	N/A	Exon 4	N/A	Kan^r	(Robatzek & Somssich, 2002)
SIGF6	AT2G36990	SALK_099845	5'-UTR	N684337	Kan^r	NASC
RPL31A	AT2G19740	SALK_107543	Promoter	N684393	Kan^r	NASC
ATPP2-B14	AT1G56250	SALK_024254	Promoter	N524254	Kan^r	NASC
eIF4E1	At4G18040	SALK_067430	Exon 1	N655590	Kan^r	(Yoshii et al., 2004)
eIF4E2	At1G29550	SALK_101805	5'-UTR	N663501	Kan^r	(Gallois et al., 2010)
eIF4E3	At1G29590	SALK_103888	Exon 3	N603888	Kan^r	(Gallois et al., 2010)
eIF(iso)4E	At5G35620	dSpm	Exon 2	N/A	$BASTA^r$	(Duprat et al., 2002)
SGS3	AT5G23570	SALK_039005	Exon 2	N539005	Kan^r	(Kumakura et al., 2009)

Sul^r, sulfadiazine resistance; Kan^r, Kanamycin resistance; BASTA^r, Phosphinothricin resistance; N/A, not available.

The following *A. thaliana* over-expressing transgenic plant lines were used or generated during the course of this work:

Table 3. Over-expressing transgenic *A. thaliana* plants employed and/or generated. Expression vector employed, construct expression and the selection agent employed are shown.

Plant Line	Vector	Expression	Selection Agent	Source
WRKY6-9	pBT8	35S::WRKY6	Kan^r	(Robatzek & Somssich, 2002)
NTAP-HCPro$_{PPV}$	pNTAPi-HCPro$_{PPV}$	35S::TAP-HCPro$_{PPV}$	Hygro^r	(Valli et al., 2009)
NTAP-P1b	pNTAPi-P1b	35S::TAP-P1b	Hygro^r	(Valli et al., 2009)
NTAP-P1b$_{mut1}$	pNTAPi- P1b$_{mut1}$	35S::TAP-P1bm1 (RK68,69AA)	Hygro^r	This work
NTAP-P1b$_{mut6}$	pNTAPi- P1b$_{mut6}$	35S::TAP-P1bm6 (C103A)	Hygro^r	This work
NTAP-P1b$_{mut10}$	pNTAPi- P1b$_{mut10}$	35S::TAP-P1b10 (S264A)	Hygro^r	This work
NTAP-NS1	pNTAPi- NS1	35S::TAP-NS1	Hygro^r	This work
NTAP-Vp3	pNTAPi- Vp3	35S::TAP-Vp3	Hygro^r	This work
NTAP-GFP	pNTAPi-GFP	35S::TAP-GFP	Hygro^r	This work
NTAP	pNTAPi-ø	35S::TAP	Hygro^r	This work
P1bwt	pGWB2-P1b	35S::P1b	Kan^r	This work
sGFP	pGWB5-ø	35S::sGFP	Kan^r	This work
TF1-TF515	pER8	ß-estradiol inducible expression of different transcription factors	Hygro^r	Transplanta collection

Kan^r., Kanamycin resistant; Hygro^r., Hygromycin resistant.

Other A. thaliana mutants used in the course of this work can be seen in the table below:

Table 4. Other *A. thaliana* mutant plants employed. Allele name and ATI accession is shown together with the mutation and the restriction enzyme used to genotype the plants.

Allele	AGI	Mutation	Genotype	Source
E508	AT1G20050	GAT(D)102AAT(N)	CAPS (MluCI)	(Schrick et al., 2002)

Bacteria and Yeast stains

The following bacterial and yeast strains were employed in this study:

Table 5. List of bacteria and yeast strains employed. Strain, selection agents, genotype and source are indicated.

Species	Strain	Genotype	Selection	Source
Escherichia coli	DH5α	F- endA1 glnV44 thi-1 recA1 relA1 gyrA96 deoR nupG Φ80d*lacZ*ΔM15 Δ(*lacZYA-argF*)U169, hsdR17(r_K^- m_K^+), λ–	Nal^r	(Meselson & Yuan, 1968)
	DH10B	F- endA1 recA1 galE15 galK16 nupG rpsL ΔlacX74 Φ80lacZΔM15 araD139 Δ(ara,leu)7697 mcrA Δ(mrr-hsdRMS-mcrBC) λ-	Strep^r	(Casadaban & Cohen, 1980; Durfee et al., 2008)
	TOP10	F- mcrA Δ(mrr-hsdRMS-mcrBC) φ80lacZΔM15 ΔlacX74 nupG recA1 araD139 Δ(ara-leu)7697 galE15 galK16 rpsL(Str^R) endA1 λ-	Strep^r	Invitrogen
	DB3.1	F- gyrA462 endA1 glnV44 Δ(sr1-recA) mcrB mrr hsdS20(r_B^-, m_B^-) ara14 galK2 lacY1 proA2 rpsL20(Sm^r) xyl5 Δleu mtl1	Strep^r, ccdB^r	(Bernard & Couturier, 1992; Miki et al., 1992)
Agrobacterium tumefaciens	GV2260	C58	Rif^r, Carb^s	(Deblaere et al., 1985)
Saccharomyces cerevisiae	AH109	*MATa, trp1-901, leu2-3, 112, ura3-52, his3-200, gal4Δ, gal80Δ, LYS2∷GAL1$_{UAS}$-GAL1$_{TATA}$-HIS3, GAL2$_{UAS}$-GAL2$_{TATA}$-ADE2, URA3∷MEL1$_{UAS}$-MEL1$_{TATA}$-lacZ*	Met$^+$, Ura$^+$.	(James et al., 1996)

Nal^r., Nalixidic acid resistant; Strep^r., Streptomycin resistant; ccdB^r., ccdB toxin resistant; Rif^r., Rifampicin resistant; Carb^s., Carbenicillin sensitive; Met$^+$, SD/-Met positive selection; Ura$^+$, SD/-Ura positive selection.

Virus

Virus constructs

The following DNA viral constructs were used in this study:

Table 6. Viral cDNA constructs employed. Construct name, isolate of origin and plasmid backbone is indicated. Genotype of each virus and selection of the viral constructs are shown.

Virus	Isolate	Plasmid backbone	Genotype	Bacterial Selection	Source
PPVwt	PPV-R	pBIN61	*P3::st_LS1-IVS1*	Kan^r	(López-Moya & García, 2000)
PPV-nk-sGFP	PPV-R	pBin19	*P3:: st_LS1-IVS1, CI::sGFP*	Kan^r	(Fernández-Fernández et al., 2001)
PPV-P1b-nk-sGFP	PPV-R	pBin19	*P1::P1b, ΔHCPro, P3:: st_LS1-IVS1, CI::sGFP*	Kan^r	(Valli et al., 2011)
PPV-P19-nk-sGFP	PPV-R	pBin19	*P1::P19, ΔHCPro P3:: st_LS1-IVS1, CI::sGFP*	Kan^r	(Maliogka et al., 2012)

st_LS1-IVS1, *S. tuberosum* LS1-intervening sequence *1;* Kan^r, Kanamycin resisitance.

Virus strains

C. sativus subsp Albatroz leaves infected with CVYV were obtained from Dr. Juan José López-Moya. Tissue was ground with a mortar in liquid nitrogen and the ground tissue was kept at -80°C in eppendorf tubes to be used in future inoculations.

MATERIALS

Antibiotics and selective agents employed

The following antibiotics and selective agents were employed during the course of this study:

Table 7. Selective agents and stock concentrations. Solvent, storage temperature and working dilutions used is indicated.

Agent	Stock Concentration	Solvent	Storage	Working Dilution	Selection in organism
Ampicilin	100 mg/ml	MiliQ H_2O	-20°C	X1000	Bacteria
Carbenicilin	100 mg/ml	MiliQ H_2O	-20°C	X1000	Bacteria
Kanamycin	50 mg/ml	MiliQ H_2O	-20°C	X1000	Bacteria, Plants
Gentamicin	10 mg/ml	MiliQ H_2O	-20°C	X1000	Bacteria
Chloramphenicol	34 mg/ml	Ethanol	-20°C	X1000	Bacteria
Streptomycin	50 mg/ml	MiliQ H_2O	-20°C	X1000	Bacteria
Spectinomycin	50 mg/ml	MiliQ H_2O	-20°C	X1000	Bacteria
Rifampicin	50 mg/ml	DMSO	-20°C	X1000	Bacteria
Tetracycline	5 mg/ml	Ethanol	-20°C	X1000	Bacteria
Hygromycin B	40mg/ml	MiliQ H_2O	-20°C	X1000	Plants
Phosphinothricin (BASTA)	10mg/ml	MiliQ H_2O	-20°C	X1000	Plants
Tunicamycin	10mg/ml	DMSO	-20°C	X66 666	Plants

Antibodies employed

Table below shows the anti-sera employed during the course of this work, working dilutions used, organism were it was raised in and the source of origin.

Table 8. Anti-sera employed. Epitope recognition, dilutions employed in TBS buffer and source of each anti-sera is indicated.

Serum	Organism	Dilution x1000 (K)	Source
anti-GFP	Mouse	1:1K-5K	Roche(#11814460001)
anti-GUS	Rabbit	1:1K	5'-3' (#5307-246448)
anti-tagRFP	Rabbit	1:5K	Evrogen (#AB233)
anti-myc	Mouse	1:5K	AbMART (#M20002)
anti-flag	Mouse	1:2K	Sigma Aldrich (#F9291)
anti-HA	Mouse	1:1K	Casasnovas et al., CNB
anti-P1b	Rabbit	1:5K	(Valli et al., 2008)
anti-CP_{PPV-R3}	Rabbit	1:100K	(Garcia et al., 1989)
anti-CP_{CVYV}	Rabbit	1:1K	(Martínez-García et al., 2004)
anti-$HCPro_{PPV}$	Rabbit	1:1K	(Ravelonandro et al., 1993)
anti-rabbit-HRP	Goat	1:10K	Jackson's (#111-035-003)
anti-mouse-HRP	Sheep	1:10K	Amersham (#NA931-1ML)
anti-$P19_{TBSV}$	Rabbit	1:3K	(Omarov et al., 2006)

Oligonucleotides

Desalted oligonuclotides in synthesis scale of 0.025 - 0.05µmol were purchased from Sigma-Aldrich in 100µM liquid suspensions from which 10µM working dilutions were made and stored at 4°C until used. Oligonucleotide sequence was designed according to specific purposes and attaining sequence specificity. Design was validated for primer dimers and hairpin formations using the on-line oligo analysis tool Oligocal

http://www.basic.northwestern.edu/biotools/oligocalc.html

The following oligonucleotides were used in cloning the Yeast two Hybrid candidate full length cDNA sequences into pUC18:

Table 9. Oligonucleotides used in cloning Yeast Two Hybrid full length cDNA sequences into pUC18.
Melting temperature (Tm) in degrees °C and locus amplified is indicated.

Number	Name	Sequence 5'----->3'	Tm	Accession	Purpose
J-1	1_WRKY47_L	TCTCTATCTATCTCTCTTTGTCTGC	63	AT4G01720	pUC18 Cloning
J-2	1_WRKY47_R	GCCAAAATCGTGTAAACCTG	56	AT4G01720	pUC18 Cloning
J-3	2_MYB90_L	GAAGCCACAATAACCCCC	56	AT1G66390	pUC18 Cloning
J-4	2_MYB90_R	GAAAGAAAAGCCACCCAC	54	AT1G66390	pUC18 Cloning
J-5	4y35_RPL40A_L	CGAAGAAGACGAACGCAAAG	58	AT2G36170	pUC18 Cloning
J-6	4y35_RPL40A_R	CAAAATTCACTGAAACAAGGTTTG	58	AT2G36170	pUC18 Cloning
J-7	5_MYB75_L	TTTGTTCCATGGAGGGTTCG	58	AT1G56650	pUC18 Cloning
J-8	5_MYB75_R	AAAGCAAACCTATACACAAACGC	59	AT1G56650	pUC18 Cloning
J-9	8_PB1_L	TTGAGCAAAGAAGAGGACG	55	AT5G09620	pUC18 Cloning
J-10	8_PB1_R	CCTCAATGTTAACTCAATCTCAC	59	AT5G09620	pUC18 Cloning
J-11	11_PRH75_L	GTCGTCTCTCCCTGCTTTCG	63	AT5G62190	pUC18 Cloning
J-12	11_PRH75_R	CGACAACCTGAAAGATGGATTG	60	AT5G62190	pUC18 Cloning
J-13	20_ATPP2-B13_L	CGGCAAACAAAAGGAAGAAG	54	AT1G56240	pUC18 Cloning
J-14	20_ATPP2-B13_R	TTATATATTATCATACACGTGACACAGAC	63	AT1G56240	pUC18 Cloning
J-15	22_WRKY6_L	CTCTCTTTCAACCAAACCCC	58	AT1G62300	pUC18 Cloning
J-16	22_WRKY6_R	CTGTTTCCTATAACCCAGTTGG	60	AT1G62300	pUC18 Cloning
J-17	25_TGA3_L	TCTTCTCTCTTGTGGTCACC	58	AT1G22070	pUC18 Cloning
J-18	25_TGA3_R	CTGAGAGATAAGCAAGTCCC	58	AT1G22070	pUC18 Cloning
J-19	30_bHLH-32_L	GGGATGTTTGTGACCTTTTG	56	AT3G25710	pUC18 Cloning
J-20	30_bHLH-32_R	TCAAATCCCATTTTGCAAGTC	55	AT3G25710	pUC18 Cloning
J-21	31y32_SIGF6_L	TCTTCTTCCTTAGCCATTCG	56	AT2G36990	pUC18 Cloning
J-22	31y32_SIGF6_R	GAAACCAATATCTCCATGAGC	58	AT2G36990	pUC18 Cloning
J-23	41_LBD41_L	CGATCAAAGTTGTTGGTACTTG	58	AT3G02550	pUC18 Cloning
J-24	41_LBD41_R	GGGGGCAAAACTTCTGAG	56	AT3G02550	pUC18 Cloning
#1445	2_MYB90_L2	TAACCCCCTATTCCTCGGCC	63	AT1G66390	pUC18 Cloning
#1446	2_MYB90_R2	GAAAGAAAAGCCACCCACAA	56	AT1G66390	pUC18 Cloning
#1447	11_PRH75_L2	TGCTTTCGCACTTCATAGCC	58	AT5G62190	pUC18 Cloning
#1448	11_PRH75_R2	AAGAGGGTACAAGAGAGCCTCC	64	AT5G62190	pUC18 Cloning
#1449	20_ATPP2-B13_L2	CTCGATCGGCAAACAAAAGG	58	AT1G56240	pUC18 Cloning
#1450	20_ATPP2-B13_R2	CATCTTGATCCCTATTTCAGAGG	61	AT1G56240	pUC18 Cloning
#1451	41_LBD41_L2	CAGAGTCAAAGAGTTCCAAATCG	61	AT3G02550	pUC18 Cloning
#1452	41_LBD41_R2	GAGCCGAATAGAGCTGATGG	60	AT3G02550	pUC18 Cloning
#1461	18_DEN3_L	TGATGAAACACAAAAATTGATTGG	57	AT1G05900	pUC18 Cloning
#1462	18_DEN3_R	GGAGAATCCAGAGCCAAAGC	60	AT1G05900	pUC18 Cloning

The following oligonucleotides were used in cloning the Yeast two Hybrid candidate CDS sequences into pDONR207 either maintaining the original AUG start codon and eliminating the final stop codon to generate Carboxi-terminal tagged fusion proteins or removing the original AUG and maintaining the final stop codon to generate Amino-terminal tagged fusion proteins:

Table 10. Oligonucleotides employed in Gateway cloning for Carboxi-terminal tagging. Melting temperature (Tm) in degrees °C and locus amplified is indicated.

Oligos used in cloning into pDONR207 for C-terminal tagging				
Number	Name	Sequence 5'----->3' [a]	Tm[1]	Accession
#1463	1_WRKY47_Fa	GGGGACAAGTTTGTACAAAAAAGCAGGCTY YATGGAAGAACATATTCAAGATCGC	60	AT4G01720
#1466	1_WRKY47_R	GGGGACCACTTTGTACAAGAAAGCTGGGTY GTTTGTAGAGAAAGTGGTGCAAGAC	64	
#1467	4_RPL40A_Fa	GGGGACAAGTTTGTACAAAAAAGCAGGCTY YATGCAGATTTTCGTGAAAACG	55	AT2G36170
#1470	4_RPL40A_R	GGGGACCACTTTGTACAAGAAAGCTGGGTY CTTGATCTTCTTCTTTGGCCTC	60	
#1471	5_MYB75_Fa	GGGGACAAGTTTGTACAAAAAAGCAGGCTY YATGGAGGGTTCGTCCAAAG	58	AT1G56650
#1474	5_MYB75_R	GGGGACCACTTTGTACAAGAAAGCTGGGTY ATCAAATTTCACAGTCTCTCCATC	60	
#1475	11_PRH75_Fa	GGGGACAAGTTTGTACAAAAAAGCAGGCTY YATGCCTTCCCTAATGTTATCTGAT	60	AT5G62190
#1478	11_PRH75_R	GGGGACCACTTTGTACAAGAAAGCTGGGTY ATATCTCTGGCCTCTACCACCA	62	
#1479	14_HEXK_Fa	GGGGACAAGTTTGTACAAAAAAGCAGGCTY YATGGCTCCTCTCCCTTTCAT	58	AT1G47860
#1482	14_HEXK_R	GGGGACCACTTTGTACAAGAAAGCTGGGTY AGGCTCGGAGACTTTGTAGATAACT	64	
#1483	17_DNAJ_Fa	GGGGACAAGTTTGTACAAAAAAGCAGGCTY YATGATACGAAATTTCCGGTTCA	56	AT1G72070
#1486	17_DNAJ_R	GGGGACCACTTTGTACAAGAAAGCTGGGTY GTAAGAAATACCTGATGGTATCCCTC	65	
#1487	18_DEN3_Fa	GGGGACAAGTTTGTACAAAAAAGCAGGCTY YATGATTCTCACCGGAGCC	56	AT1G05900
#1490	18_DEN3_R	GGGGACCACTTTGTACAAGAAAGCTGGGTY AAGCTTCTTGCTTTTGATAGATTTCT	60	
#1491	20_ATPP2-B13_Fa	GGGGACAAGTTTGTACAAAAAAGCAGGCTY YATGATGATGTTACCTGAAGCATG	59	AT1G56240
#1494	20_ATPP2-B13_R	GGGGACCACTTTGTACAAGAAAGCTGGGTY TTTCAGAGGTATAGGCCTCACTTC	64	
#1495	22_WRKY6_Fa	GGGGACAAGTTTGTACAAAAAAGCAGGCTY YATGGACAGAGGATGGTCTGG	61	AT1G62300
#1498	22_WRKY6_R	GGGGACCACTTTGTACAAGAAAGCTGGGTY TTGATTTTTGTTGTTTCCTTCG	55	
#1499	31_SIGF6_Fa	GGGGACAAGTTTGTACAAAAAAGCAGGCTY YATGGAAGCTACGAGGAACTTG	60	AT2G36990
#1502	31_SIGF6_R	GGGGACCACTTTGTACAAGAAAGCTGGGTY GACAAGCAAATCAGCATAAGCA	58	
#1503	43_RPL31A_Fa	GGGGACAAGTTTGTACAAAAAAGCAGGCTY YATGGAGAAAGGAAAGGGAAGAA	58	AT2G19740
#1506	43_RPL31A_R	GGGGACCACTTTGTACAAGAAAGCTGGGTY CTCCTCTTCTTCAATGACCTTAGTACC	67	
#2041	39_HYD1 Fa	GGGGACAAGTTTGTACAAAAAAGCAGGCTT CATGGAGGAGTTGGCGCATC	60	AT1G20050
#2042	39_HYD1 R	GGGGACCACTTTGTACAAGAAAGCTGGGTC ACGGGTTTTCTTCTTCGTCTTTG	61	
#2533	at_DCP1_Fa	GGGGACAAGTTTGTACAAAAAAGCAGGCTT CATGTCTCAAAACGGGAAGATAATC	60	AT1G08370
#2534	at_DCP1_R	GGGGACCACTTTGTACAAGAAAGCTGGGTT TTGTTGAAGTGCATTTTGTAAAGTT	59	

[a], Sequence complementary to CDS is underlined.

[1], Tm temperature was calculated considering only the sequence complementary to de CDS sequence to be amplified.

Table 11. Oligonucleotides and sequences used in Gateway cloning for Amino-terminal tagging. Melting temperature (Tm) in degrees °C and locus amplified is indicated.

Oligos used in cloning into pDONR207 for N-terminal tagging				
Number	Name	Sequence 5'----->3' [a]	Tm[1]	Accession
#1464	1_WRKY47_F	GGGGACAAGTTTGTACAAAAAAGCAGGCTY YGAAGAACATATTCAAGATCGCCG	61	AT4G01720
#1465	1_WRKY47_Rs	GGGGACCACTTTGTACAAGAAAGCTGGGTY TTAGTTTGTAGAGAAAGTGGTGCAAG	63	
#1468	4_RPL40A_F	GGGGACAAGTTTGTACAAAAAAGCAGGCTY YCAGATTTTCGTGAAAACGCTAAC	59	AT2G36170
#1469	4_RPL40A_Rs	GGGGACCACTTTGTACAAGAAAGCTGGGTY TCACTTGATCTTCTTCTTTGGC	58	
#1472	5_MYB75_F	GGGGACAAGTTTGTACAAAAAAGCAGGCTY YGAGGGTTCGTCCAAAGGG	58	AT1G56650
#1473	5_MYB75_Rs	GGGGACCACTTTGTACAAGAAAGCTGGGTY CTAATCAAATTTCACAGTCTCTCCATC	64	
#1476	11_PRH75_F	GGGGACAAGTTTGTACAAAAAAGCAGGCTY YCCTTCCCTAATGTTATCTGATAAGAAA	62	AT5G62190
#1477	11_PRH75_Rs	GGGGACCACTTTGTACAAGAAAGCTGGGTY TCAATATCTCTGGCCTCTACCAC	63	
#1480	14_HEXK_F	GGGGACAAGTTTGTACAAAAAAGCAGGCTY YGCTCCTCTCCCTTTCATACC	61	AT1G47860
#1481	14_HEXK_Rs	GGGGACCACTTTGTACAAGAAAGCTGGGTY TTAAGGCTCGGAGACTTTGTAGAT	62	
#1484	17_DNAJ_F	GGGGACAAGTTTGTACAAAAAAGCAGGCTY YATACGAAATTTCCGGTTCAAAG	56	AT1G72070
#1485	17_DNAJ_Rs	GGGGACCACTTTGTACAAGAAAGCTGGGTY CTAGTAAGAAATACCTGATGGTATCCC	65	
#1488	18_DEN3_F	GGGGACAAGTTTGTACAAAAAAGCAGGCTY YATTCTCACCGGAGCCG	54	AT1G05900
#1489	18_DEN3_Rs	GGGGACCACTTTGTACAAGAAAGCTGGGTY CTAAAGCTTCTTGCTTTTGATAGATTT	61	
#1492	20_ATPP2-B13_F	GGGGACAAGTTTGTACAAAAAAGCAGGCTY YATGATGTTACCTGAAGCATG	54	AT1G56240
#1493	20_ATPP2-B13_Rs	GGGGACCACTTTGTACAAGAAAGCTGGGTY CTATTTCAGAGGTATAGGCCTCACTT	65	
#1496	22_WRKY6_F	GGGGACAAGTTTGTACAAAAAAGCAGGCTY YGACAGAGGATGGTCTGGTCTC	63	AT1G62300
#1497	22_WRKY6_Rs	GGGGACCACTTTGTACAAGAAAGCTGGGTY CTATTGATTTTTGTTGTTTCCTTCG	59	
#1500	31_SIGF6_F	GGGGACAAGTTTGTACAAAAAAGCAGGCTY YGAAGCTACGAGGAACTTGGTTTC	63	AT2G36990
#1501	31_SIGF6_Rs	GGGGACCACTTTGTACAAGAAAGCTGGGTY CTAGACAAGCAAATCAGCATAAGC	62	
#1504	43_RPL31A_F	GGGGACAAGTTTGTACAAAAAAGCAGGCTY YATGGAGAAAGGAAAGGGAAGAA	58	AT2G19740
#1505	43_RPL31A_Rs	GGGGACCACTTTGTACAAGAAAGCTGGGTY TCACTCCTCTTCTTCAATGACCT	61	

Table 11. Continued.

#2043	39_HYD1_F	GGGGACAAGTTTGTACAAAAAAGCAGGCTT CGAGGAGTTGGCGCATCC	57	AT1G20050
#2044	39_HYD1_Rs	GGGGACCACTTTGTACAAGAAAGCTGGGTC TCAACGGGTTTTCTTCTTCG	56	
#2474	at_AGO1_F	GGGGACAAGTTTGTACAAAAAAGCAGGCTT CGTGAGAAAGAGAAGAACGGATGC	56	AT1G48410
#2475	at_AGO1_Rs	GGGGACCACTTTGTACAAGAAAGCTGGGTT TCAGCAGTAGAACATGACACGCTT	59	
#2476	at_AGO10_F	GGGGACAAGTTTGTACAAAAAAGCAGGCTT CCCGATTAGGCAAATGAAAGA	51	AT5G43810
#2477	at_AGO10_Rs	GGGGACCACTTTGTACAAGAAAGCTGGGTT TTAGCAGTAGAACATTACTCTCTTCAC	54	
#2478	cs_AGO1_F	GGGGACAAGTTTGTACAAAAAAGCAGGCTT CGGGAGGAAGAAGAGAACCGA	56	XM_004137339
#2479	cs_AGO1_Rs	GGGGACCACTTTGTACAAGAAAGCTGGGTT TCAACAATAGAACATAACCCTCTTGA	54	
#2480	cs_AGO10_F	GGGGACAAGTTTGTACAAAAAAGCAGGCTT CCCAGTACGGCAAATGAAA	50	XM_004134066
#2481	cs_AGO10_Rs	GGGGACCACTTTGTACAAGAAAGCTGGGTT CTAACAGTAAAACATTACTCTCTTCAC	52	
#2482	at_AGO7_F	GGGGACAAGTTTGTACAAAAAAGCAGGCTT CGAAGAAAAAACTCATCATCATCATCA	61	AT1G69440
#2483	at_AGO7_Rs	GGGGACCACTTTGTACAAGAAAGCTGGGTT TCAGCAGTAAAACATGAGATTCTTG	60	
#2484	cs_AGO7_F	GGGGACAAGTTTGTACAAAAAAGCAGGCTT CGAAGAGTCAGATGAGCCTAAG	60	XM_004135112
#2485	cs_AGO7_Rs	GGGGACCACTTTGTACAAGAAAGCTGGGTT TCAACAGTAGAACATTAGTTTCCTAAC	62	
#2529	at_SGS3_F	GGGGACAAGTTTGTACAAAAAAGCAGGCTT CAGTTCTAGGGCTGGTCCAATG	61	AT5G23570
#2530	at_SGS3_Rs	GGGGACCACTTTGTACAAGAAAGCTGGGTT TCAATCATCTTCATTGTGAAGGC	61	
#2531	at_RDR6_F	GGGGACAAGTTTGTACAAAAAAGCAGGCTT CGGGTCAGAGGGAAATATGAAGA	59	AT3G49500
#2532	at_RDR6_Rs	GGGGACCACTTTGTACAAGAAAGCTGGGTT TTAGAGACGCTGAGCAAGAAACT	60	

[a], Sequence complementary to CDS is underlined.
[1], Tm temperature was calculated considering only the sequence complementary to de CDS sequence to be amplified.

The following oligonucleotides were used in sequencing reactions in different occasions during the course of this work:

Table 12. Oligonucleotides employed during sequencing analysis. Melting temperature (Tm) in degrees °C. and annealing site on the DNA sequence is indicated.

Oligos used in sequencing reactions					
Number	Name	Sequence 5'----->3'	Tm	Annealing site	Direction
#2519	at_AGO1_Fseq2	GAACTGCCTGATAAGGATTTGC	60	at_AGO1	Forward
#2520	at_AGO1_Fseq3	GATATTTCTTCTCGACCTTTATCTGAT	59	at_AGO1	Forward

Table 12. Continued.

#2521	at_AGO1_Fseq4	GGAACGGTGAATAATTGGATCT	59	at_AGO1	Forward
#2522	at_AGO1_Fseq5	CAGGAGCTCATTCAGGATCTG	60	at_AGO1	Forward
#2426	at_AGO4_Rseq2	ACATGAGCGAAACCCTATAAG	58	at_AGO4	Reverse
#2523	at_AGO7_Fseq2	AACAGAAGCTTGTTGAGACAGATC	59	at_AGO7	Forward
#2524	at_AGO7_Fseq3	AGAAAGCACTTAAGAACATAAGAGTCT	57	at_AGO7	Forward
#2525	at_AGO7_Fseq4	AAAAGTGTGAGCATTTGGGAGT	60	at_AGO7	Forward
#2526	at_AGO10_Fseq2	AGTCTTTACACTGCTGGAGAACTTC	60	at_AGO10	Forward
#2527	at_AGO10_Fseq3	GTAGATGAGAACTGTACTATGAAGTCAGTT	58	at_AGO10	Forward
#2528	at_AGO10_Fseq4	CAAGTCGAGAAAGCTCTAAAGCA	60	at_AGO10	Forward
#2450	HYD1_seq2_F	GGTGGACATTCACTGGTCTCACTC	62	at_HYD1	Forward
#1453	22_WRKY6_LSeq	AGAGCAGTAGGTGAGGCCG	62	at_WRKY6	Reverse
#2422	pGWB700-R1-rev	TAATGCGGCCCCTCGAGG	61	attR1	Reverse
#2423	ccdB-For-seq	CGCCATTAACCTGATGTTCTG	60	ccdB	Forward
#2698	cs_AGO1_seq2	GGAGATCGGCTTCCTGCT	61	cs_AGO1	Forward
#2700	cs_AGO1_seq3	ATAATGATCCATATGCCAAGGAGT	60	cs_AGO1	Forward
#2699	cs_AGO7_seq2	AGCAAGCCTTTAAACTCTTCAGG	60	cs_AGO7	Forward
#2701	cs_AGO7_seq3	AAGAATGCTTAAGATGGGTTGC	60	cs_AGO7	Forward
#2702	P1a_seq2F	GAGGATGACAACGGTTGAATC	60	cvyv_P1a	Forward
#2703	P1a_seq2R	GATTCAACCGTTGTCATCCTC	60	cvyv_P1a	Reverse
#1444	P1bMid-R	GACTGCAGGGTGCACATC	58	cvyv_P1b	Reverse
#2558	P1_3R	TGACTGTTTTGCTAAACTCACGC	61	ppv_P1	Reverse
#2451	sGFP_5'_R_Seq	CTCGCCCTTGCTCACCAT	59	sGFP	Reverse
#2491	sGFP_midseq	CTACCTGAGCACCCAGTCC	62	sGFP	Forward
#2452	C-ter_YFP_R_Seq	GGCGGATCTTGAAGTTCACC	61	YFP	Reverse

The following oligonucleotides have been used in genotyping *Arabidopsis thaliana* mutants:

Table 13. Oligonucleotides employed in genotyping *Arabidopsis thaliana* mutant plants. Melting temperature (Tm) in degrees °C and annealing site on the DNA locus is indicated.

Oligos used in genotyping T-DNA and SNP *A. thaliana* lines				
Number	Name	Sequence 5'----->3'	Tm[1]	Annealing loci
#1765	SALK_LB_rev	GGTTCACGTAGTaGGCCATCG[1]	60	T-DNA LB[2]
#1787	GABI_LB_rev	CGCTGCGGACATCTACATTTTTG	65	T-DNA LB[2]
#1792	SAIL_LB_rev	GCATCTGtATTTCATAACCAATCTCG[1]	62	T-DNA LB[2]
#1799	Wisconsin_RB_rev	CAgACTATTCGGGCCTAACTTTTG[1]	62	T-DNA RB[3]
#1945	wrky47_LP	ATTCTCCTCGTGAAGCCTCTC	61	WRKY47
#1946	wrky47_RP	ATGCAACGCTGTAAATTTTCG	55	
#1947	ubq2a_LP	ATCCAAAATGTTCAATGCTGC	55	UBQ2-RPL40A
#1948	ubq2a_RP	GCCTCAGAACAAGATGCAAAG	60	
#1949	myb90_LP	ATGCACGTCATTTTCCTATGC	58	MYB90
#1950	myb90_RP	TTTTGACATCATTAGCGGTCC	58	
#1953	prh75a_LP	ATGTTTTACCCTGCACCACAC	60	PRH75
#1954	prh75a_RP	TAAATGTGTACCGTTTTGGGG	58	
#1955	prh75b_LP	TCGGTATTGTGAATCTCCTGC	60	
#1956	prh75b_RP	ATATCAGGAATCAACCGAGCC	60	
#1957	hp2_LP	CTCTTGACTAGGCCACACCAC	63	AT1G47860
#1958	hp2_RP	AGCTTGGAAAGAAAAACAGCC	58	

Table13. Continued.

#1959	dnaj_LP	TCACCAAAGTCCCACAAAAAG	58	DNAJ
#1960	dnaj_RP	AACCCAGGAGAAGCAGAAATC	60	
#1961	den3_LP	ACATCATTCCAGGCTACATGC	60	DEN3
#1962	den3_RP	GAAAACTGGGAAAAGGTGCTC	60	
#1963	sigf6_LP	ATGACTGTAACCATTCACCGG	60	SIGF6
#1964	sigf6_RP	GCATGTGACAGAGGCCTAGAC	63	
#1965	rpl31a_LP	GCTCCTTTTTGTGGCATATTG	58	RPL31A
#1966	rpl31a_RP	GCCAAGGTGATCAACAACAAC	60	
#1967	atpp2-b14_LP	TGAGGCTTTTGTAATCCGATG	58	ATPP2-B14
#1968	atpp2-b14_RP	CTTGGCCAATAGGACTCAATG	60	
#2444	HYD1_E508_F	TCTAGTAGTTCCACAAACTCACATT	55	HYD1
#2445	HYD1_E508_R	AGACTCATGTTCATTTGCTATAACAGC	61	
#2446	HYD1-Intron2*_F	TATCTTCTTCTTAGTGTTGTCATTGTTGTTC gATTAGACCgATTCGTAAG[4]	80	
#2447	HYD1-Intron2*_R	TGGCATAACTGAATcTCCATCAACAACAACA AACTTCAATcACTTTTTAG[4]	82	
#2448	HYD1_CDS_F	GAGGAGTTGGCGCATCCG	62	
#2449	HYD1_CDS_R	ACGGGTTTTCTTCTTCGTCTT	58	

[1], Small caps bases refer base changes introduced to improve stability.
[2], Annealing site on T-DNA Left Border sequence.
[3], Annealing site on T-DNA Right Border sequence..
[4], Small caps bases refers to base changes introduced to eliminate MluCI restriction sites.

The following oligonucleotides were used in amplifying or cloning viral ORFs during the course of this work:

Table 14. . Oligonucleotides employed in amplifying viral cistrons. Melting temperature (Tm) in degrees °C, cistron amplified is indicated.

Oligos used in amplifying viral cistrons						
Purpose	Number	Name	Sequence 5'----->3'[a]	Tm	ORF	Virus
pDONR207 cloning	#2468	cvyv_P1a_F	GGGGACAAGTTTGTACAAAAAAGCAGGCTTC GCCGAAGTTTACAGTTTCGTTC	55	P1a	CVYV
	#2469	cvyv_P1a_Rs	GGGGACCACTTTGTACAAGAAAGCTGGGTTT TAGTAATTGCGAATCCTTCTTAATTG	52		
Fusion PCRs	#2694	cvyv_P1a_F2	CAAAGTGTGCGATGGCGCCTGCTAC	63		
	#2695	cvyv_P1a_R2	GTAGCAGGCGCCATCGCACACTTTG	63		
	#2696	cvyv_P1a_F3	GACAATTCCAGGGTGGCCATGGAAGAG	63		
	#2697	cvyv_P1a_R3	CTCTTCCATGGCCACCCTGGAATTGTC	63		
pDONR207 cloning	#2692	cvyv_P3_F2	GGCCAATTCAAGTTCGTCTTCGACCATTTCG	63	P3	
	#2693	cvyv_P3_R2	CGAAATGGTCGAAGACGAACTTGAATTGGCC	63		
pDONR207 cloning	#2472	cvyv_Vpg_F	GGGGACAAGTTTGTACAAAAAAGCAGGCTTC GGAAAGGTTGGTTACAGACGC	56	Vpg	
	#2473	cvyv_Vpg_Rs	GGGGACCACTTTGTACAAGAAAGCTGGGTTT TATTGAACTTCCACTTCCTCTTCT	54		

Table14. Continued.

pDONR207 cloning	#2314	bstmv-P1_F	GGGGACAAGTTTGTACAAAAAAGCAGGCTTC ATGCAGCAGACGCACGTTAAGC	57	P1	BSTMV
	#2315	bstmv-P1_R	GGGGACCACTTTGTACAAGAAAGCTGGGTTA ATAATACTCAATCCGCTCACC	52		
	#2316	bstmv-HCPro_F	GGGGACAAGTTTGTACAAAAAAGCAGGCTTC ATGAGTAGCAAGAGGCGCATGGC	59	HCPro	
	#2317	bstmv-HCPro_R	GGGGACCACTTTGTACAAGAAAGCTGGGTTA ACCAATCTCGTATTCCTTAAGTTC	54		
	#2360	bstmv-CP_ F	GGGGACAAGTTTGTACAAAAAAGCAGGCTTC ATGAGTGCAGCATCAGGAAC	52	CP	
	#2361	bstmv-CP_ R	GGGGACCACTTTGTACAAGAAAGCTGGGTTA GAAAGCCCGCGCTCCACCTAG	61		

[a], Sequence complementary to CDS is underlined.

Other ologonucleotides used with various uses used during the course of this work can be seen in the table below:

Table 15. Other oligonucleotides employed during this work for various uses. Melting temperature (Tm) in degrees °C and annealing site is indicated.

Oligos used for various needs					
Purpose	Number	Name	Sequence 5'----->3'	Tm	Annealing site
PCR	#1867	pER8-5F	GGATCCACCTGAGGATCACA	65	pER8 plasmid backbone
	#1868	pER8-5R	AACGGAGGATCACCACTTTG	64	
PCR Probe	#1973	TF178_F	CAACATAGAGAGTAGTGTTTCTCAAG	63	AT3G04030
	#1974	TF178_R	CTCACTCCTCTATACGTCGGATG	65	
PCR	#332	N-GFP-5´	ATGGTGAGCAAGGGCGAG	58	sGFP
	#333	N-GFP-3´	CAGGTACCCTTGTACAGCTCGTC	59	
PCR	#2490	attR1-rev2	GGCCGCCATAGTGACTGG	61	attR1 site
RT-PCR	#2132	NVdT18	TTTTTTTTTTTTTTTTTTVN	58	polyA tail
A. thumefaciens genotyping	#2050	A.tu._pTi_repB_for	GCcATTGTCCGAAATCTCACG[1]	61	repB
	#2051	A.tu._pTi_repB_rev	CTGGAAATGCGATTCTCTTAGC	60	
PCR	#18	oligo80/CP1	TTGGGTTCTTGAACAAGC	52	CP_{PPV}
Probe	#2398	U6	GGCCATGCTAATCTTCTCTGTATCGTT	67	U6 snRNA

[1], Small caps bases refers to base changes introduced to improve stability.

Plasmids

The following plasmids were used and/or generated during the course of this work:

Table 16. Plasmids generated and/or employed during this work. Description of the plasmid, selection encoded in bacteria or plants and reference were it was first reported is indicated.

Plasmid	Description	Selection		Reference
		Bacteria	Plants	
Yeast-2 Hybrid				
pGBKT7-ø	BD empty vector with MCS	Kan^r	-	Clonetech
pGBKT7-P1b	BD vector expressing $P1b_{wt}$	Kan^r	-	This work
pGBKT7-GW	BD vector with Gateway attB cassette to use in recombination with pDONR	Kan^r	-	Boter et al., unpublished
pGBKT7-GW- $P1b_{mut6}$	BD Gateway vector expressing $P1b_{mut6}$	Kan^r	-	This work
pGBKT7-GW- $P1b_{mut10}$	BD Gateway vector expressing $P1b_{mut10}$	Kan^r	-	This work
pGBKT7-GW-$P1b_{wt}$	BD Gateway vector expressing $P1b_{wt}$	Kan^r	-	This work
pGADT7-ø	AD empty vector with MCS	Amp^r	-	Clonetech
pGADT7-1	AD vector containing 5'UTR + $WRKY47_{1\text{-}216aa}$ peptide codifying sequence in a +2 Frame.	Amp^r	-	This work
pGADT7-2	AD vector containing $MYB90_{10\text{-}211aa}$ peptide codifying sequence	Amp^r	-	This work
pGADT7-3	AD vector containing $RPL17A_{4\text{-}176aa}$+3'UTR peptide codifying sequence	Amp^r	-	This work
pGADT7-4	AD vector containing UBQ2-$RPL40A_{5\text{-}118aa}$ peptide codifying sequence	Amp^r	-	This work
pGADT7-5	AD vector containing $MYB75_{4\text{-}248aa}$ +3'UTR peptide codifying sequence	Amp^r	-	This work
pGADT7-6	AD vector containing $PDF1B_{6\text{-}192aa}$ peptide codifying sequence	Amp^r	-	This work
pGADT7-7	AD vector containing $RPL17B_{6\text{-}175aa}$ +3'UTR peptide codifying sequence	Amp^r	-	This work
pGADT7-8	AD vector containing 5'UTR + $PB1_{1\text{-}183aa}$ peptide codifying sequence in a +2 Frame.	Amp^r	-	This work
pGADT7-9	AD vector containing $AT3G59680_{85\text{-}229aa}$ +3'UTR peptide codifying sequence	Amp^r	-	This work
pGADT7-10	AD vector containing 5'UTR + $LHCB3_{1\text{-}218aa}$ peptide codifying sequence in a +2 Frame.	Amp^r	-	This work
pGADT7-11	AD vector containing $PRH75_{405\text{-}614aa}$ peptide codifying sequence	Amp^r	-	This work
pGADT7-12	AD vector containing 5'UTR + $HSR2_{1\text{-}150aa}$ peptide codifying sequence in a +2 Frame.	Amp^r	-	This work
pGADT7-13	AD vector containing $LBD41_{58\text{-}263aa}$ peptide codifying sequence	Amp^r	-	This work
pGADT7-14	AD vector containing $AT1G47860_{12\text{-}260}$ peptide codifying sequence	Amp^r	-	This work
pGADT7-15	AD vector containing $NRX2_{272\text{-}392aa}$ peptide codifying sequence	Amp^r	-	This work
pGADT7-16	AD vector containing $ARGAH2_{228\text{-}334aa}$ peptide codifying sequence	Amp^r	-	This work
pGADT7-17	AD vector containing 5'UTR + $DNAJ_{1\text{-}126aa}$ full codifying sequence	Amp^r	-	This work
pGADT7-18	AD vector containing $NTH2_{89\text{-}237aa}$ peptide codifying sequence	Amp^r	-	This work
pGADT7-19	AD vector containing $PHR1_{1\text{-}496aa}$ full codifying sequence	Amp^r	-	This work
pGADT7-20	AD vector containing $PP2\text{-}B13_{124\text{-}284aa}$ peptide codifying sequence	Amp^r	-	This work
pGADT7-21	AD vector containing $NFD3_{63\text{-}280aa}$ peptide codifying sequence	Amp^r	-	This work
pGADT7-22	AD vector containing $WRKY6_{49\text{-}271aa}$ peptide codifying sequence	Amp^r	-	This work

Table16. Continued.

pGADT7-23	AD vector containing $DR4_{6\text{-}209aa}$ + 3'UTR peptide codifying sequence	Amp^r	-	This work
pGADT7-24	AD vector containing $GFA2_{148\text{-}267aa}$ peptide codifying sequence	Amp^r	-	This work
pGADT7-25	AD vector containing $TGA3_{300\text{-}384aa}$ + 3'UTR peptide codifying sequence	Amp^r	-	This work
pGADT7-26	AD vector containing $MGD1_{114\text{-}300aa}$ peptide codifying sequence	Amp^r	-	This work
pGADT7-27	AD vector containing 5'UTR + $ARA4_{1\text{-}182aa}$ full codifying sequence in a +2 Frame	Amp^r	-	This work
pGADT7-28	AD vector containing $LON_{13\text{-}256aa}$ peptide codifying sequence	Amp^r	-	This work
pGADT7-29	AD vector containing 5'UTR + $RAB11_{1\text{-}217aa}$ full codifying sequence in a +2 Frame.	Amp^r	-	This work
pGADT7-30	AD vector containing 5'UTR + $BHLH32_{1\text{-}219aa}$ peptide codifying sequence in a +2 Frame.	Amp^r	-	This work
pGADT7-31	AD vector containing $SIG6_{142\text{-}392aa}$ peptide codifying sequence	Amp^r	-	This work
pGADT7-32	AD vector containing $SIG6_{142\text{-}392aa}$ peptide codifying sequence	Amp^r	-	This work
pGADT7-33	AD vector containing 5'UTR + $AP2C1_{1\text{-}150aa}$ peptide codifying sequence in a +2 Frame.	Amp^r	-	This work
pGADT7-34	AD vector containing $QPT_{203\text{-}348aa}$ +3'UTR peptide codifying sequence	Amp^r	-	This work
pGADT7-35	AD vector containing $UBQ2\text{-}RPL40A_{18\text{-}118aa}$ peptide codifying sequence	Amp^r	-	This work
pGADT7-36	AD vector containing 5'UTR + $MAT3_{1\text{-}190aa}$ peptide codifying sequence in a +2 Frame.	Amp^r	-	This work
pGADT7-37	AD vector containing 5'UTR + $AT3G22210_{1\text{-}69aa}$ peptide codifying sequence in a +2 Frame.	Amp^r	-	This work
pGADT7-38	AD vector containing $AT1G47860_{12\text{-}200aa}$ peptide codifying sequence	Amp^r	-	This work
pGADT7-39	AD vector containing 5'UTR + $HYD1_{1\text{-}223aa}$ full codifying sequence in a +2 Frame.	Amp^r	-	This work
pGADT7-40	AD vector containing $DNAJ_{280\text{-}442aa}$ peptide codifying sequence	Amp^r	-	This work
pGADT7-41	AD vector containing 5'UTR + $LBD41_{58\text{-}263aa}$ peptide codifying sequence in a +2 Frame.	Amp^r	-	This work
pGADT7-42	AD vector containing 5'UTR + $SYN23_{1\text{-}165aa}$ peptide codifying sequence in a +2 Frame.	Amp^r	-	This work
pGADT7-43	AD vector containing 5'UTR + $RPL31A_{1\text{-}119aa}$ full codifying sequence	Amp^r	-	This work
pGADT7-GW	AD vector with Gateway attB cassette to use in recombination with pDONR	Amp^r	-	Boter et al. unpublished
pGADT7-GW-$P1b_{wt}$	AD Gateway vector expressing $P1b_{wt}$	Amp^r	-	This work
pGADT7-GW-HYDRA1c	AD Gateway vector expressing at_HYD1 full CDS sequence.	Amp^r	-	This work
pGADT7-GW-PRH75c	AD Gateway vector expressing at_PRH75 full CDS sequence.	Amp^r	-	This work
pUC18				
pUC18-ø	pUC18 empty vector	Amp^r	-	
pUC18-WRKY47	pUC18 carrying the complete cDNA sequence of at_WRKY47 (AT4G01720)	Amp^r	-	This work
pUC18-MYB90	pUC18 carrying the complete cDNA sequence of at_MYB90 (AT1G66390)	Amp^r	-	This work

Table16. Continued.

pUC18-UBQ2-RPL40A	pUC18 carrying the complete cDNA sequence of at_UBQ2-RPL40A (AT2G36170)	Amp^r	-	This work
pUC18-MYB75	pUC18 carrying the complete cDNA sequence of at_MYB75 (AT1G56650)	Amp^r	-	This work
pUC18-PB1	pUC18 carrying the complete cDNA sequence of at_PB1 (AT5G09620)	Amp^r	-	This work
pUC18-PRH75	pUC18 carrying the complete cDNA sequence of at_PRH75 (AT5G62190)	Amp^r	-	This work
pUC18-ATPP2-B13	pUC18 carrying the complete cDNA sequence of at_PP2-B13 (AT1G56240)	Amp^r	-	This work
pUC18-WRKY6	pUC18 carrying the complete cDNA sequence of at_WRKY6 (AT1G62300)	Amp^r	-	This work
pUC18-TGA3	pUC18 carrying the complete cDNA sequence of at_TGA3 (AT1G22070)	Amp^r	-	This work
pUC18-bHLH-32	pUC18 carrying the complete cDNA sequence of at_bHLH32 (AT3G25710)	Amp^r	-	This work
pUC18-SIG6	pUC18 carrying the complete cDNA sequence of at_SIG6 (AT2G36990)	Amp^r	-	This work
pUC18-LBD41	pUC18 carrying the complete cDNA sequence of at_LBD41 (AT3G02550)	Amp^r	-	This work
pUC18-DEN3	pUC18 carrying the complete cDNA sequence of at_NTH2 (AT1G05900)	Amp^r	-	This work
pDONR207				
pDONR207-ø	Empty pDONR plasmid to perform the attB recombination with the PCR products	Gent^r	-	
pDONR207-WRKY47a	pDONR207 plasmid harbouring WRKY47 (AT4G01720) CDS with AUG for C-terminus tagging.	Gent^r	-	This work
pDONR207-WRKY47s	pDONR207 plasmid harbouring WRKY47 (AT4G01720) CDS with stop codon for N-terminus tagging.	Gent^r	-	This work
pDONR207-RPL40Aa	pDONR207 plasmid harbouring UBQ2-RPL40A (AT2G36170) CDS with AUG for C-terminus tagging.	Gent^r	-	This work
pDONR207-RPL40As	pDONR207 plasmid harbouring UBQ2-RPL40A (AT2G36170) CDS with stop codon for N-terminus tagging.	Gent^r	-	This work
pDONR207-MYB75a	pDONR207 plasmid harbouring MYB75 (AT1G56650) CDS with AUG for C-terminus tagging.	Gent^r	-	This work
pDONR207-MYB75s	pDONR207 plasmid harbouring MYB75 (AT1G56650) CDS with stop codon for N-terminus tagging.	Gent^r	-	This work
pDONR207-PRH75a	pDONR207 plasmid harbouring PRH75 (AT5G62190) CDS with AUG for C-terminus tagging.	Gent^r	-	This work
pDONR207-PRH75s	pDONR207 plasmid harbouring PRH75 (AT5G62190) CDS with stop codon for N-terminus tagging.	Gent^r	-	This work
pDONR207-HEXKa	pDONR207 plasmid harbouring HEXK (AT1G47860) CDS with AUG for C-terminus tagging.	Gent^r	-	This work
pDONR207-HEXKs	pDONR207 plasmid harbouring HEXK (AT1G47860) CDS with stop codon for N-terminus tagging.	Gent^r	-	This work

Table16. Continued.

pDONR207-DNAJa	pDONR207 plasmid harbouring DNAJ (AT1G72070) CDS with AUG for C-terminus tagging.	Gent^r	-	This work
pDONR207-DNAJs	pDONR207 plasmid harbouring DNAJ (AT1G72070) CDS with stop codon for N-terminus tagging.	Gent^r	-	This work
pDONR207-DEN3a	pDONR207 plasmid harbouring NTH2 (AT1G05900) CDS with AUG for C-terminus tagging.	Gent^r	-	This work
pDONR207-DEN3s	pDONR207 plasmid harbouring NTH2 (AT1G05900) CDS with stop codon for N-terminus tagging.	Gent^r	-	This work
pDONR207-ATPP2-B13a	pDONR207 plasmid harbouring PP2-B13 (AT1G56240) CDS with AUG for C-terminus tagging.	Gent^r	-	This work
pDONR207-ATPP2-B13s	pDONR207 plasmid harbouring PP2-B13 (AT1G56240) CDS with stop codon for N-terminus tagging.	Gent^r	-	This work
pDONR207-WRKY6a	pDONR207 plasmid harbouring WRKY6 (AT1G62300) CDS with AUG for C-terminus tagging.	Gent^r	-	This work
pDONR207-WRKY6s	pDONR207 plasmid harbouring WRKY6 (AT1G62300) CDS with stop codon for N-terminus tagging.	Gent^r	-	This work
pDONR207-SIGF6a	pDONR207 plasmid harbouring SIG6 (AT2G36990) CDS with AUG for C-terminus tagging.	Gent^r	-	This work
pDONR207-SIGF6s	pDONR207 plasmid harbouring SIG6 (AT2G36990) CDS with stop codon for N-terminus tagging.	Gent^r	-	This work
pDONR207-RPL31Aa	pDONR207 plasmid harbouring RPL31A (AT2G19740) CDS with AUG for C-terminus tagging.	Gent^r	-	This work
pDONR207-RPL31As	pDONR207 plasmid harbouring RPL31A (AT2G19740) CDS with stop codon for N-terminus tagging.	Gent^r	-	This work
pDONR207-HYD1a	pDONR207 plasmid harbouring HYD1 (AT1G20050) CDS with AUG for C-terminus tagging.	Gent^r	-	This work
pDONR207-HYD1s	pDONR207 plasmid harbouring HYD1 (AT1G20050) CDS with stop codon for N-terminus tagging.	Gent^r	-	This work
pDONR207-DCP1a	pDONR207 plasmid harbouring DCP1 (AT1G08370) CDS with AUG for C-terminus tagging.	Gent^r	-	This work
pDONR207-at_AGO1s	pDONR207 plasmid harbouring AGO1 (AT1G48410) CDS with AUG for C-terminus tagging.	Gent^r	-	This work
pDONR207-cs_AGO1s	pDONR207 plasmid harbouring cs_AGO1 (XM_004137339) CDS stop codon for N-terminus tagging.	Gent^r	-	This work
pDONR207-at_AGO7s	pDONR207 plasmid harbouring AGO7 (AT1G69440) CDS with stop codon for N-terminus tagging.	Gent^r	-	This work

Table16. Continued.

pDONR207-cs_AGO7s	pDONR207 plasmid harbouring cs_ AGO7 (XM_004135112) CDS stop codon for N-terminus tagging.	Gent^r	-	This work
pDONR207-at_AGO10s	pDONR207 plasmid harbouring AGO10 (AT5G43810) CDS stop codon for N-terminus tagging.	Gent^r	-	This work
pDONR207-cs_AGO10s	pDONR207 plasmid harbouring cs_ AGO10 (XM_004134066) CDS stop codon for N-terminus tagging.	Gent^r	-	This work
pDONR207-at_SGS3s	pDONR207 plasmid harbouring SGS3 (AT5G23570) CDS with stop codon for N-terminus tagging.	Gent^r	-	This work
pDONR207-at_RDR6s	pDONR207 plasmid harbouring RDR6 (AT3G49500) CDS with stop codon for N-terminus tagging.	Gent^r	-	This work
pDONR207-cvyv_P1as	pDONR207 plasmid harbouring P1a CDS from CVYV infected *C. sativus* with stop codon for N-terminus tagging.	Gent^r	-	This work
pDONR207-cvyv_P3s	pDONR207 plasmid harbouring P3 CDS from CVYV infected *C. sativus* with stop codon for N-terminus tagging.	Gent^r	-	This work
pDONR207-cvyv_Vpgs	pDONR207 plasmid harbouring Vpg (NIa) from CVYV infected *C. sativus* CDS with stop codon for N-terminus tagging.	Gent^r	-	This work
pDONR207-bstmv_P1	pDONR207 plasmid harbouring P1 CDS from BSTMV infected plant tissue with stop codon for N-terminus tagging.	Gent^r	-	This work
pDONR207-bstmv_HCPro	pDONR207 plasmid harbouring HCPro CDS from BSTMV infected plant tissue with stop codon for N-terminus tagging.	Gent^r	-	This work
pDONR207-bstmv_CP	pDONR207 plasmid harbouring CP CDS from BSTMV infected plant tissue with stop codon for N-terminus tagging.	Gent^r	-	This work
pDONR207-cm_eIF4E	pDONR207 plasmid harbouring eIF4E CDS from *C. melo* with stop codon for N-terminus tagging.	Gent^r	-	Aranda et al. unpublished
pDONR207-cm_eIF(iso)4E	pDONR207 plasmid harbouring eIF(iso)4E CDS from *C. melo* with stop codon for N-terminus tagging.	Gent^r	-	Aranda et al. unpublished
pBiFP				
pBiFP1-ø	Empty BiFC plasmid to fuse the N-terminal residues of YFP on the C-terminus.	Spec^r, Strep^r	BASTA	(Desprez et al., 2007)
pBiFP2-ø	Empty BiFC plasmid to fuse the N-terminal residues of YFP on the N-terminus.	Spec^r, Strep^r	BASTA	(Desprez et al., 2007)
pBiFP3-ø	Empty BiFC plasmid to fuse the C-terminal residues of YFP on the N-terminus.	Spec^r, Strep^r	BASTA	(Desprez et al., 2007)
pBiFP4-ø	Empty BiFC plasmid to fuse the C-terminal residues of YFP on the N-terminus.	Spec^r, Strep^r	BASTA	(Desprez et al., 2007)
pBiFP1-WRKY47	BiFC plasmid to fuse the N-terminal residues of YFP on the C-terminus of WRKY47 (Expresses WRKY47::"YF").	Spec^r, Strep^r	BASTA	This work
pBiFP2-WRKY47	BiFC plasmid to fuse the N-terminal residues of YFP on the N-terminus of WRKY47 (Expresses "YF"::WRKY47).	Spec^r, Strep^r	BASTA	This work

Table16. Continued.

pBiFP3-WRKY47	BiFC plasmid to fuse the C-terminal residues of YFP on the N-terminus of WRKY47 (Expresses "P"::WRKY47).	$Spec^r$, $Strep^r$	BASTA	This work
pBiFP4-WRKY47	BiFC plasmid to fuse the C-terminal residues of YFP on the N-terminus of WRKY47 (Expresses WRKY47::"P").	$Spec^r$, $Strep^r$	BASTA	This work
pBiFP1-UBQ2-RPL40A	BiFC plasmid to fuse the N-terminal residues of YFP on the C-terminus of UBQ2-RPL40A (Expresses UBQ2-RPL40A::"YF").	$Spec^r$, $Strep^r$	BASTA	This work
pBiFP2-UBQ2-RPL40A	BiFC plasmid to fuse the N-terminal residues of YFP on the N-terminus of UBQ2-RPL40A (Expresses "YF"::UBQ2-RPL40A).	$Spec^r$, $Strep^r$	BASTA	This work
pBiFP3-UBQ2-RPL40A	BiFC plasmid to fuse the C-terminal residues of YFP on the N-terminus of UBQ2-RPL40A (Expresses "P"::UBQ2-RPL40A).	$Spec^r$, $Strep^r$	BASTA	This work
pBiFP4-UBQ2-RPL40A	BiFC plasmid to fuse the C-terminal residues of YFP on the N-terminus of UBQ2-RPL40A (Expresses UBQ2-RPL40A::"P").	$Spec^r$, $Strep^r$	BASTA	This work
pBiFP1-MYB75	BiFC plasmid to fuse the N-terminal residues of YFP on the C-terminus of MYB75 (Expresses MYB75::"YF").	$Spec^r$, $Strep^r$	BASTA	This work
pBiFP2-MYB75	BiFC plasmid to fuse the N-terminal residues of YFP on the N-terminus of MYB75 (Expresses "YF"::MYB75).	$Spec^r$, $Strep^r$	BASTA	This work
pBiFP3-MYB75	BiFC plasmid to fuse the C-terminal residues of YFP on the N-terminus of MYB75 (Expresses "P"::MYB75).	$Spec^r$, $Strep^r$	BASTA	This work
pBiFP4-MYB75	BiFC plasmid to fuse the C-terminal residues of YFP on the N-terminus of MYB75 (Expresses MYB75::"P").	$Spec^r$, $Strep^r$	BASTA	This work
pBiFP1-PRH75	BiFC plasmid to fuse the N-terminal residues of YFP on the C-terminus of PRH75 (Expresses PRH75::"YF").	$Spec^r$, $Strep^r$	BASTA	This work
pBiFP2-PRH75	BiFC plasmid to fuse the N-terminal residues of YFP on the N-terminus of PRH75 (Expresses "YF"::PRH75).	$Spec^r$, $Strep^r$	BASTA	This work
pBiFP3-PRH75	BiFC plasmid to fuse the C-terminal residues of YFP on the N-terminus of PRH75 (Expresses "P"::PRH75).	$Spec^r$, $Strep^r$	BASTA	This work
pBiFP4-PRH75	BiFC plasmid to fuse the C-terminal residues of YFP on the N-terminus of PRH75 (Expresses PRH75::"P").	$Spec^r$, $Strep^r$	BASTA	This work
pBiFP1-HEXK	BiFC plasmid to fuse the N-terminal residues of YFP on the C-terminus of HEXK (Expresses HEXK::"YF").	$Spec^r$, $Strep^r$	BASTA	This work
pBiFP2-HEXK	BiFC plasmid to fuse the N-terminal residues of YFP on the N-terminus of HEXK (Expresses "YF"::HEXK).	$Spec^r$, $Strep^r$	BASTA	This work
pBiFP3-HEXK	BiFC plasmid to fuse the C-terminal residues of YFP on the N-terminus of HEXK (Expresses "P"::HEXK).	$Spec^r$, $Strep^r$	BASTA	This work
pBiFP4-HEXK	BiFC plasmid to fuse the C-terminal residues of YFP on the N-terminus of HEXK (Expresses HEXK::"P").	$Spec^r$, $Strep^r$	BASTA	This work
pBiFP1-DNAJ	BiFC plasmid to fuse the N-terminal residues of YFP on the C-terminus of DNAJ (Expresses DNAJ::"YF").	$Spec^r$, $Strep^r$	BASTA	This work

Table16. Continued.

pBiFP2-DNAJ	BiFC plasmid to fuse the N-terminal residues of YFP on the N-terminus of DNAJ (Expresses "YF"::DNAJ).	$Spec^r$, $Strep^r$	BASTA	This work
pBiFP3-DNAJ	BiFC plasmid to fuse the C-terminal residues of YFP on the N-terminus of DNAJ (Expresses "P"::DNAJ).	$Spec^r$, $Strep^r$	BASTA	This work
pBiFP4-DNAJ	BiFC plasmid to fuse the C-terminal residues of YFP on the N-terminus of DNAJ (Expresses DNAJ::"P").	$Spec^r$, $Strep^r$	BASTA	This work
pBiFP1-DEN3	BiFC plasmid to fuse the N-terminal residues of YFP on the C-terminus of NTH2 (Expresses NTH2::"YF").	$Spec^r$, $Strep^r$	BASTA	This work
pBiFP2-DEN3	BiFC plasmid to fuse the N-terminal residues of YFP on the N-terminus of NTH2 (Expresses "YF"::NTH2).	$Spec^r$, $Strep^r$	BASTA	This work
pBiFP3-DEN3	BiFC plasmid to fuse the C-terminal residues of YFP on the N-terminus of NTH2 (Expresses "P"::NTH2).	$Spec^r$, $Strep^r$	BASTA	This work
pBiFP4-DEN3	BiFC plasmid to fuse the C-terminal residues of YFP on the N-terminus of NTH2 (Expresses NTH2::"P").	$Spec^r$, $Strep^r$	BASTA	This work
pBiFP1-ATPP2-B13	BiFC plasmid to fuse the N-terminal residues of YFP on the C-terminus of PP2-B13 (Expresses PP2-B13::"YF").	$Spec^r$, $Strep^r$	BASTA	This work
pBiFP2-ATPP2-B13	BiFC plasmid to fuse the N-terminal residues of YFP on the N-terminus of PP2-B13 (Expresses "YF":: PP2-B13).	$Spec^r$, $Strep^r$	BASTA	This work
pBiFP3-ATPP2-B13	BiFC plasmid to fuse the C-terminal residues of YFP on the N-terminus of PP2-B13 (Expresses "P"::PP2-B13).	$Spec^r$, $Strep^r$	BASTA	This work
pBiFP4-ATPP2-B13	BiFC plasmid to fuse the C-terminal residues of YFP on the N-terminus of PP2-B13 (Expresses PP2-B13::"P").	$Spec^r$, $Strep^r$	BASTA	This work
pBiFP1-WRKY6	BiFC plasmid to fuse the N-terminal residues of YFP on the C-terminus of WRKY6 (Expresses WRKY6::"YF").	$Spec^r$, $Strep^r$	BASTA	This work
pBiFP2-WRKY6	BiFC plasmid to fuse the N-terminal residues of YFP on the N-terminus of WRKY6 (Expresses "YF"::WRKY6).	$Spec^r$, $Strep^r$	BASTA	This work
pBiFP3-WRKY6	BiFC plasmid to fuse the C-terminal residues of YFP on the N-terminus of WRKY6 (Expresses "P"::WRKY6).	$Spec^r$, $Strep^r$	BASTA	This work
pBiFP4-WRKY6	BiFC plasmid to fuse the C-terminal residues of YFP on the N-terminus of WRKY6 (Expresses WRKY6::"P").	$Spec^r$, $Strep^r$	BASTA	This work
pBiFP1-SIG6	BiFC plasmid to fuse the N-terminal residues of YFP on the C-terminus of SIG6 (Expresses SIG6::"YF").	$Spec^r$, $Strep^r$	BASTA	This work
pBiFP2-SIG6	BiFC plasmid to fuse the N-terminal residues of YFP on the N-terminus of SIG6 (Expresses "YF"::SIG6).	$Spec^r$, $Strep^r$	BASTA	This work
pBiFP3-SIG6	BiFC plasmid to fuse the C-terminal residues of YFP on the N-terminus of SIG6 (Expresses "P"::SIG6).	$Spec^r$, $Strep^r$	BASTA	This work
pBiFP4-SIG6	BiFC plasmid to fuse the C-terminal residues of YFP on the N-terminus of SIG6 (Expresses SIG6::"P").	$Spec^r$, $Strep^r$	BASTA	This work

Table 16. Continued.

pBiFP1-RPL31A	BiFC plasmid to fuse the N-terminal residues of YFP on the C-terminus of RPL31A (Expresses RPL31A::"YF").	$Spec^r$, $Strep^r$	BASTA	This work
pBiFP2-RPL31A	BiFC plasmid to fuse the N-terminal residues of YFP on the N-terminus of RPL31A (Expresses "YF"::RPL31A).	$Spec^r$, $Strep^r$	BASTA	This work
pBiFP3-RPL31A	BiFC plasmid to fuse the C-terminal residues of YFP on the N-terminus of RPL31A (Expresses "P"::RPL31A).	$Spec^r$, $Strep^r$	BASTA	This work
pBiFP4-RPL31A	BiFC plasmid to fuse the C-terminal residues of YFP on the N-terminus of RPL31A (Expresses RPL31A::"P").	$Spec^r$, $Strep^r$	BASTA	This work
pBiFP1-HYD1	BiFC plasmid to fuse the N-terminal residues of YFP on the C-terminus of HYD1 (Expresses HYD1::"YF").	$Spec^r$, $Strep^r$	BASTA	This work
pBiFP2-HYD1	BiFC plasmid to fuse the N-terminal residues of YFP on the N-terminus of HYD1 (Expresses "YF"::HYD1).	$Spec^r$, $Strep^r$	BASTA	This work
pBiFP3-HYD1	BiFC plasmid to fuse the C-terminal residues of YFP on the N-terminus of HYD1 (Expresses "P"::HYD1).	$Spec^r$, $Strep^r$	BASTA	This work
pBiFP4-HYD1	BiFC plasmid to fuse the C-terminal residues of YFP on the N-terminus of HYD1 (Expresses HYD1::"P").	$Spec^r$, $Strep^r$	BASTA	This work
pBiFP4-E508	BiFC plasmid to fuse the C-terminal residues of YFP on the N-terminus of the E508 mutant allele of HYD1(Expresses E508::"P").	$Spec^r$, $Strep^r$	BASTA	This work
pBiFP1-DCP1	BiFC plasmid to fuse the N-terminal residues of YFP on the C-terminus of DCP1 (Expresses DCP1::"YF").	$Spec^r$, $Strep^r$	BASTA	This work
pBiFP4-DCP1	BiFC plasmid to fuse the C-terminal residues of YFP on the N-terminus of DCP1 (Expresses DCP1::"P").	$Spec^r$, $Strep^r$	BASTA	This work
pBiFP2-AGO1	BiFC plasmid to fuse the N-terminal residues of YFP on the N-terminus of AGO1 (Expresses "YF"::AGO1).	$Spec^r$, $Strep^r$	BASTA	This work
pBiFP3-AGO1	BiFC plasmid to fuse the C-terminal residues of YFP on the N-terminus of AGO1 (Expresses "P"::AGO1).	$Spec^r$, $Strep^r$	BASTA	This work
pBiFP2-cs_ AGO1	BiFC plasmid to fuse the N-terminal residues of YFP on the N-terminus of cs_ AGO1 (Expresses "YF"::cs_ AGO1).	$Spec^r$, $Strep^r$	BASTA	This work
pBiFP3-cs_ AGO1	BiFC plasmid to fuse the C-terminal residues of YFP on the N-terminus of cs_ AGO1 (Expresses "P"::cs_ AGO1).	$Spec^r$, $Strep^r$	BASTA	This work
pBiFP2-AGO7	BiFC plasmid to fuse the N-terminal residues of YFP on the N-terminus of AGO7 (Expresses "YF"::AGO7).	$Spec^r$, $Strep^r$	BASTA	This work
pBiFP3-AGO7	BiFC plasmid to fuse the C-terminal residues of YFP on the N-terminus of AGO7 (Expresses "P"::AGO7).	$Spec^r$, $Strep^r$	BASTA	This work
pBiFP2-cs_ AGO7	BiFC plasmid to fuse the N-terminal residues of YFP on the N-terminus of cs_ AGO7 (Expresses "YF"::cs_ AGO7).	$Spec^r$, $Strep^r$	BASTA	This work
pBiFP3-cs_ AGO7	BiFC plasmid to fuse the C-terminal residues of YFP on the N-terminus of cs_ AGO7 (Expresses "P"::cs_ AGO7).	$Spec^r$, $Strep^r$	BASTA	This work

Table 16. Continued.

pBiFP2-AGO10	BiFC plasmid to fuse the N-terminal residues of YFP on the N-terminus of AGO10 (Expresses "YF"::AGO10).	Spec^r, Strep^r	BASTA	This work
pBiFP3-AGO10	BiFC plasmid to fuse the C-terminal residues of YFP on the N-terminus of AGO10 (Expresses "P"::AGO10).	Spec^r, Strep^r	BASTA	This work
pBiFP2-cs_ AGO10	BiFC plasmid to fuse the N-terminal residues of YFP on the N-terminus of cs_ AGO10 (Expresses "YF"::cs_ AGO10).	Spec^r, Strep^r	BASTA	This work
pBiFP3-cs_ AGO10	BiFC plasmid to fuse the C-terminal residues of YFP on the N-terminus of cs_ AGO10 (Expresses "P"::cs_ AGO10).	Spec^r, Strep^r	BASTA	This work
pBiFP2-SGS3	BiFC plasmid to fuse the N-terminal residues of YFP on the N-terminus of SGS3 (Expresses "YF"::SGS3).	Spec^r, Strep^r	BASTA	This work
pBiFP3-SGS3	BiFC plasmid to fuse the C-terminal residues of YFP on the N-terminus of SGS3 (Expresses "P"::SGS3).	Spec^r, Strep^r	BASTA	This work
pBiFP2-RDR6	BiFC plasmid to fuse the N-terminal residues of YFP on the N-terminus of RDR6 (Expresses "YF"::RDR6).	Spec^r, Strep^r	BASTA	This work
pBiFP3-RDR6	BiFC plasmid to fuse the C-terminal residues of YFP on the N-terminus of RDR6 (Expresses "P"::RDR6).	Spec^r, Strep^r	BASTA	This work
pBiFP2-cvyv_P1a	BiFC plasmid to fuse the N-terminal residues of YFP on the N-terminus of P1a from CVYV (Expresses "YF"::P1a).	Spec^r, Strep^r	BASTA	This work
pBiFP3-cvyv_P1a	BiFC plasmid to fuse the C-terminal residues of YFP on the N-terminus of P1a from CVYV (Expresses "P"::P1a).	Spec^r, Strep^r	BASTA	This work
pBiFP2-cvyv_P3	BiFC plasmid to fuse the N-terminal residues of YFP on the N-terminus of P3 from CVYV (Expresses "YF"::P3).	Spec^r, Strep^r	BASTA	This work
pBiFP3-cvyv_P3	BiFC plasmid to fuse the C-terminal residues of YFP on the N-terminus of P3 from CVYV (Expresses "P"::P3).	Spec^r, Strep^r	BASTA	This work
pBiFP2-cvyv_Vpg	BiFC plasmid to fuse the N-terminal residues of YFP on the N-terminus of Vpg (NIa) from CVYV (Expresses "YF"::Vpg).	Spec^r, Strep^r	BASTA	This work
pBiFP3-cvyv_Vpg	BiFC plasmid to fuse the C-terminal residues of YFP on the N-terminus of Vpg (NIa) from CVYV (Expresses "P"::Vpg).	Spec^r, Strep^r	BASTA	This work
pBiFP2-bstmvP1	BiFC plasmid to fuse the N-terminal residues of YFP on the N-terminus of P1 from BSTMV (Expresses "YF"::P1).	Spec^r, Strep^r	BASTA	This work
pBiFP2-bstmvP1*	BiFC plasmid to fuse the N-terminal residues of YFP on the N-terminus of P1 protease mutant from BSTMV (Expresses "YF"::P1*).	Spec^r, Strep^r	BASTA	This work
pBiFP3-bstmvCP	BiFC plasmid to fuse the C-terminal residues of YFP on the N-terminus of CP from BSTMV (Expresses "P"::CP).	Spec^r, Strep^r	BASTA	This work
pBiFP2-bstmvHCPro	BiFC plasmid to fuse the C-terminal residues of YFP on the N-terminus of HCPro from BSTMV (Expresses "YF"::HCPro).	Spec^r, Strep^r	BASTA	This work
pBiFP2-ppvHCPro	BiFC plasmid to fuse the C-terminal residues of YFP on the N-terminus of HCPro from PPV (Expresses "YF"::HCPro).	Spec^r, Strep^r	BASTA	This work

Table16. Continued.

pBiFP3-ppvCP	BiFC plasmid to fuse the C-terminal residues of YFP on the N-terminus of CP from PPV (Expresses "P"::CP).	Spec^r, Strep^r	BASTA	This work
pBiFP2-cm_4E	BiFC plasmid to fuse the N-terminal residues of YFP on the N-terminus of cm_eIF4E (Expresses "YF"::eIF4E).	Spec^r, Strep^r	BASTA	This work
pBiFP3- cm_4E	BiFC plasmid to fuse the C-terminal residues of YFP on the N-terminus of eIF4E from C. melo(Expresses "P"::eIF4E).	Spec^r, Strep^r	BASTA	This work
pBiFP2-cm_iso4E	BiFC plasmid to fuse the N-terminal residues of YFP on the N-terminus of eIF(iso)4E (Expresses "YF"::eIF(iso)4E).	Spec^r, Strep^r	BASTA	This work
pBiFP3- cm_iso4E	BiFC plasmid to fuse the C-terminal residues of YFP on the N-terminus of cm_eIF(iso)4E (Expresses "P"::eIF(iso)4E).	Spec^r, Strep^r	BASTA	This work
pMDC				
pMDC43-ø	Empty gateways expression vector to fuse gateway cassettes with GFP6 in the N-terminus.	Kan^r	Hyg^r	(Curtis & Grossniklaus , 2003)
pMDC43-PP2-B13	Gateway expression vector expressing PP2-B13 CDS tagged with GFP6 in the N-terminus. (35S::GFP6::PP2-B13)	Kan^r	Hyg^r	This work
pMDC43-UBQ2-PRL40A	Gateway expression vector expressing UBQ2-RPL40A CDS tagged with GFP6 in the N-terminus (35S::GFP6::UBQ2-RPL40A).	Kan^r	Hyg^r	This work
pMDC43-DNAJ	Gateway expression vector expressing DNAJ CDS tagged with GFP6 in the N-terminus (35S::GFP6::DNAJ).	Kan^r	Hyg^r	This work
pMDC43-MYB75	Gateway expression vector expressing MYB75 CDS tagged with GFP6 in the N-terminus (35S::GFP6::MYB75).	Kan^r	Hyg^r	This work
pMDC43-DEN3	Gateway expression vector expressing NTH2 CDS tagged with GFP6 in the N-terminus (35S::GFP6::NTH2).	Kan^r	Hyg^r	This work
pMDC43-PRH75	Gateway expression vector expressing PRH75 CDS tagged with GFP6 in the N-terminus (35S::GFP6::PRH75).	Kan^r	Hyg^r	This work
pMDC43-SIG6	Gateway expression vector expressing SIG6 CDS tagged with GFP6 in the N-terminus (35S::GFP6::SIG6).	Kan^r	Hyg^r	This work
pGWB				
pGWB-ø	Empty gateways expression vectors to fuse gateway cassettes with different tags both in the C-terminus and N-terminus.	Kan^r	Hyg^r, Kan^r	(Nakagawa et al., 2007)
impGWB7XX-ø	Improved gateways expression vectors to fuse gateway cassettes with different tags both in the C-terminus and N-terminus.	Kan^r	Tun^r	(Tanaka et al., 2011)
pGWB2-P1bwt	Gateway expression clone expressing P1b wt sequence from CVYV with no tags (35S::P1bwt)	Kan^r	Hyg^r, Kan^r	Valli et al.
pGWB6-P1bwt	Gateway expression clone expressing P1b wt sequence from CVYV tagged with sGFP in the N-terminus (35S::sGFP::P1bwt)	Kan^r	Hyg^r, Kan^r	Valli et al. unpublished

Table16. Continued.

pGWB5-P1bwt	Gateway expression clone expressing P1b wt sequence from CVYV tagged with sGFP in the C-terminus (35S::P1b::sGFP)	Kan^r	Hyg^r, Kan^r	Valli et al. unpublished
pGWB5-WRKY6	Gateway expression clone expressing WRKY6 sequence tagged with sGFP in the C-terminus (35S::WRKY6::sGFP)	Kan^r	Hyg^r, Kan^r	This work
pGWB5-WRKY47	Gateway expression clone expressing WRKY47 sequence tagged with sGFP in the C-terminus (35S::WRKY47::sGFP)	Kan^r	Hyg^r, Kan^r	This work
pGWB5-MYB75	Gateway expression clone expressing MYB75 sequence tagged with sGFP in the C-terminus (35S::MYB75::sGFP)	Kan^r	Hyg^r, Kan^r	This work
pGWB5-PRH75	Gateway expression clone expressing PRH75 sequence tagged with sGFP in the C-terminus (35S::PRH75::sGFP)	Kan^r	Hyg^r, Kan^r	This work
pGWB5-HYD1	Gateway expression clone expressing HYD1 sequence tagged with sGFP in the C-terminus (35S::HYD1::sGFP)	Kan^r	Hyg^r, Kan^r	This work
impGWB702-HYD1	Gateway expression clone expressing HYD1 sequence with no tags (35S::HYD1)	Spec^r, Strep^r	Tun^r	This work
impGWB702Ω-HYD1	Gateway expression clone expressing HYD1 sequence with no tags under the translational enhancer Ω from TMV (35S Ω::HYD1)	Spec^r, Strep^r	Tun^r	This work
impGWB708-HYD1	Gateway expression clone expressing HYD1 sequence tagged with 6xHis on the C-terminus (35S::HYD1::6xHis)	Spec^r, Strep^r	Tun^r	This work
impGWB711-HYD1	Gateway expression clone expressing HYD1 sequence tagged with Flag on the C-terminus (35S::HYD1::Flag)	Spec^r, Strep^r	Tun^r	This work
impGWB714-HYD1	Gateway expression clone expressing HYD1 sequence tagged with 3xHA on the C-terminus (35S::HYD1::3xHA)	Spec^r, Strep^r	Tun^r	This work
impGWB717-HYD1	Gateway expression clone expressing HYD1 sequence tagged with 4xMyc on the C-terminus (35S::HYD1::4xMyc)	Spec^r, Strep^r	Tun^r	This work
impGWB720-HYD1	Gateway expression clone expressing HYD1 sequence tagged with 10xMyc on the C-terminus (35S::HYD1::10xMyc)	Spec^r, Strep^r	Tun^r	This work
impGWB760-HYD1	Gateway expression clone expressing HYD1 sequence tagged with TagRFP on the C-terminus (35S::HYD1::TagRFP)	Spec^r, Strep^r	Tun^r	This work
impGWB718-cm_4E	Gateway expression clone expressing eIF4E sequence from *C. melo* tagged with 4xMyc on the N-terminus (35S::4xMyc::eIF4E)	Spec^r, Strep^r	Tun^r	This work
impGWB718-cm_iso4E	Gateway expression clone expressing eIF(iso)4E sequence from *C. melo* tagged with 4xMyc on the N-terminus (35S::4xMyc::eIF(iso)4E)	Spec^r, Strep^r	Tun^r	This work
pBIN				
pBIN19-P19	Binary plasmid expressing the silencing suppressor protein P19 from TBSV (35S::P19).	Kan^r	Kan^r	(Voinnet et al., 2003)
pBIN61-GFPwt	Binary plasmid expressing GFP wt (35S::GFP5).	Kan^r	Kan^r	(Voinnet et al., 2000)

Table 16. Continued.

pBIN61-GUS	Binary plasmid expressing GUS (35S::GUS).	Kan^r	Kan^r	(Voinnet et al., 2003)
pNTAPi				
pNTAPi-ø	Gateway expression clone used to TAP tag on the N-terminus (35S::2xProtA::CBP)	$Spec^r$, $Strep^r$	Hyg^r	(Rohila et al., 2004)
pNTAPi-P1b	Gateway expression clone expressing P1b sequence from CVYV tagged with TAP tag on the N-terminus (35S::TAP::P1b)	$Spec^r$, $Strep^r$	Hyg^r	(Valli et al., 2008)
pNTAPi-P1bm1	Gateway expression clone expressing P1b mutant RK68,69AA sequence from CVYV tagged with TAP tag on the N-terminus (35S::TAP::P1bm1)	$Spec^r$, $Strep^r$	Hyg^r	(Valli et al., 2008)
pNTAPi-P1bm6	Gateway expression clone expressing P1b mutant C103A sequence from CVYV tagged with TAP tag on the N-terminus (35S::TAP::P1bm6)	$Spec^r$, $Strep^r$	Hyg^r	(Valli et al., 2008)
pNTAPi-VP3	Gateway expression clone expressing VP3 sequence from IBDV tagged with TAP tag on the N-terminus (35S::TAP::VP3)	$Spec^r$, $Strep^r$	Hyg^r	This work
pNTAPi-NS1	Gateway expression clone expressing NS1 sequence from IFV tagged with TAP tag on the N-terminus (35S::TAP::NS1)	$Spec^r$, $Strep^r$	Hyg^r	This work

METHODS

CULTURE CONDITIONS

Plants

Greenhouse practice

Seed germination

Seeds were germinated by sprinkling them on most soil pots and vernalising them for 4 days at 4°C covered with Saran wrap to maintain moisture before passing them to the greenhouse. When seeds were scarce, seeds were resuspended in Miliq water and the desired amounts of seeds were planted on moist soil before vernalising as described above. The remaining seeds were centrifuged to collect them and remove the remaining water, dried for 7 days and stored again.

Growth conditions

N. benthamiana, *A. thaliana* and *C. sativus* plants were cultured in the greenhouse at a temperature cycle of 18°C when dark and 24°C when lit, and under long-day light conditions of 16h light and 8h darkness cycles using mercury and neon fluorescent lamps to supplement illumination when needed. Light intensity when lit ranged from 4500 to 7000 lux depending on the bench used.

In vitro practice

Seed germination

Seeds were epi-sterilised in successive incubations of 70% ethanol for 2 minutes, 50% commercial bleach for 8 minutes and 5 washes in miliq sterile water. Seeds were vernalised by incubating them in the last water wash for 6 days at 4°C before planting them on 0.5X MS agar using sterile glass Pasteur pipettes.

Growth conditions

A. thaliana seeds were cultured in *in vitro* conditions growing on 0.5X MS agar (with selection agents when needed) in light chambers with temperature set to 22-25°C and long-day light conditions of 16h light and 8h darkness cycles using neon fluorescent lamps rendering a light intensity of 3000 to 9000 lux depending on the shelf used. If transfer to the greenhouse was needed, as to harvest seeds, plantulas grown *in vitro* were removed from the agar using tweezers and transplanted to moist soil alveoli, covered with plastic Saran wrap before passing them into the greenhouse and culturing them for 4 days before slowly removing the plastic wrapping.

Selection of transgenic plants

T_0 transformants were selected for after floral dip transformation by plating 2000 seeds in MS medium plates carbenicillin and the appropriate selective agent according to the plasmid's resistance gene. Carbenicillin was used to avoid *Agrobacterium thumefaciens* growing on the agar plates. Transformants were then passed to soil and grown and seeds sawed. The T_1 seeds were then plated on MS

agar with the appropriate selective agent as for the T_0 seeds and the segregation of the transgene was observed for each transformant. Transformants that showed a 3:1 segregation are believed to have a single copy of the transgene inserted in the genome. A representative number of the growing T_1 plant lines were selected and passed to soil to saw seeds. The resultant T_2 plants were checked for segregation and gene expression by western blotting. Plants from the T_2 populations that did not show segregation and had good expression levels of the transgenes were selected and seeds sawn. Plants resulting from these seeds are homozygous T_3 plants.

Yeast

Yeast cells were grown on SD/-Met agar and liquid SD/-Met to select for the strain, frozen in 20% Glycerol SD/-Met and kept at -80°C. Cells were grown on liquid or solid YPG media supplemented with 0.003% Adenine hemisulfate (YPGA), liquid or solid SD/-2 media and solid SD/-3, SD/-4 or SD/-4 supplemented with 10mM 3-AT agar medium when needed and incubated in a dark growth chamber at 28°C until colonies become sufficiently visible to work with.

Bacteria

E. coli and *A. tumefaciens* were grown on LB agar plates or liquid LB using the appropriate selection agent when needed and incubated in a dark growth chamber at 37°C or 28°C respectively ,until colonies become sufficiently visible to work with.

PREPARATION OF COMPETENT CELLS

Chemically competent cells

Escherichia coli

E. coli heat shock competent cells were prepared according to the method described in http://openwetware.org/wiki/TOP10_chemically_competent_cells using CCMB80 buffer (10mM KOAc pH7.0, 80mM $CaCl_2$, 20mM $MnCl_2$, 10mM $MgCl_2$, 10% Glycerol, pH 6.4 wiht HCl, filter sterilize and keep at 4°C) 250ml of SOB medium was inoculated with 1ml vial of seed stock and grown at 20°C 250rpm

until OD_{600} of 0.3. Culture was centrifuged at 3000g 4°C for 10 minutes and gently resuspended in 80ml ice cold CCMB80 buffer and incubated on ice for 20 minutes. Cells were centrifuged again at 3000g 4°C for 10 minutes and resuspended in 10ml ice cold CCMB80 buffer. Cell suspension was adjusted to obtain a final OD_{600} of 1.0-1.5. Cells were incubated for a further 20 minutes before making aliquots in dry ice pre-chilled eppendorf tubes and stored at -80°C till needed.

Saccharomyces cerevisiae

S. cerevisiae heat shock competent cells were prepared as described in Matchmaker GAL4 Two-Hybid System 3 & libraries User Manual (Clonetech). Several good looking AH109 colonies growing on YPGA agar were resuspended in 1ml liquid YPGA by vortexing vigorously for 5 minutes and used to inoculate a 50ml YPGA pre-culture. Culture was incubated for 16-18 hours at 30°C shaking at 250rpm till stationary phase (OD_{600}>1.5). Pre-culture was used to inoculate a 300ml YPG culture to a final OD_{600} of 0.2-0.3. Culture is incubated at 30°C for 3 hours shaking at 250rpm until a final OD_{600} of 0.4 to 0.6 is reached. Culture is divided into 6 50ml phalcon tubes and centrifuged at 1000g (2200rpm in a F10-6X500Y Sorvall RC5C rotor) for 5 minutes at room temperature. Cells are washed twice with sterile water and pooled in one final tube. Pellet is resuspended in 1.5ml of freshly prepared and steril 1X TE/LiAc solution. Cell suspension is kept on ice and must be used immediately for heat shock transformation.

Electrocompetent cells

Escherichia coli

E. coli electrocompetent cells were prepared using the protocol described by A. Untergasser in http://www.untergasser.de/lab/protocols/competent_cells_electro_v1_0.htm. A 3ml salt free LB (10g/L Tryptone, 5g/L Yeast extract) pre-culture with the appropriate selective agent depending on the stain was inoculated with 1 colony growing on LB agar and incubated at 37°C for 16-18 hours. Pre-culture is used to inoculate 2 litres salt free LB before dividing it into 4 2L Erlenmeyer flasks and incubating them at 37°C shaking at 200rpm until OD_{600} reaches 0.9. Flask are

chilled on ice-water bath for 15 minutes and centrifuged at 4°C, 3500g for 20 minutes. Pellets are washed twice with 150ml ice-cold sterile water and pooled in two 150ml ice-cold sterile water suspension. Cells are centrifuged at 4°C, 5000g for 20 minutes and resuspended in 100ml ice cold sterile 8.7% Glycerol and centrifuged again. Pellets are resuspended in 2.5ml ice cold sterile 8.7% Glycerol and pooled in one tube before making aliquots and storing them in -80°C until needed. Transformation efficiencies of up to $7.0x10^9$ CFU/µg were achieved using this method.

Agrobacterium tumefaciens

Colony PCR screening for the Ti plasmid with oligos #2050 and #2051 was performed on the repB gene of the pTi plasmid to select for a pTi positive clone as sequencing of the stain in use revealed Carbenicillin resistance gene lost by plasmid re-organization and can thus not be selected on the appropriate selective agent. A PCR pTi positive colony that showed a band size of 730bp was used to inoculate a 5ml LB rifampicin pre-culture which was incubated at 28°C for 2 days. The pre-culture was used to inoculate a 200ml LB culture to a final OD_{600} of 0.02 and culture was incubated at 28°C with agitation of 250rpm until an OD_{600} of 1 is reached (approximately 18 hour if duplication rate is 3 hours). Culture is centrifuged at 4°C 4000rpm for 15 minutes, resuspended in 100ml ice cold sterile water and washed 4 times resuspending pellet in 50ml ice cold sterile water, 25ml ice cold sterile water, 5ml ice cold sterile 10% glycerol and 1ml ice cold sterile glycerol pooling cells into 1 tube when finished. Aliquots were made in cold eppendorf tubes and, frozen in liquid nitrogen and kept in -80°C until needed.

BACTERIA AND YEAST TRANSFORMATION

Heat shock transformation

Escherichia coli

E. coli cells were transformed by incubating 50µl of thawn cells with 1µl plasmid DNA at variable concentrations on ice for 15 minutes, heat shocking cells for 45

seconds and incubating them back on ice for 3 minutes. 950µl sterile LB was added to each transformation reaction and incubated at 37°C for 1 hour prior plating 100µl on the appropriate LB selective plates. Plates were incubated at 37°C for 16-18 hours before analyzing clones.

Saccharomyces cerevisiae

S. cerevisiae heat shock transformations were performed as described in Matchmaker GAL4 Two-Hybid System 3 & libraries User Manual (Clonetech). To transform cells 100µl fresh yeast chemical competent cells were vortexed with 1µl 100ng/µl of each plasmid to be transformed and 0.1mg of herring testes carrier DNA. 600µl of sterile PEG/LiAc solution was added to each reaction and mixed vigorously by vortexing for 10 seconds, followed by an incubation at 30°C with shaking at 200rpm for 30 minutes. Following this incubation 70µl DMSO was added and tubes mixed by gentle inversion. Cells were then heat shocked for 15 minutes at 42°C and chilled on ice-water for 2 minutes. Cell were centrifuged for 5 seconds at 14000rpm at room temperature and the supernatant removed to resuspend the cells in 500µl sterile TE buffer. 100µl were used to spread on selective plates and grown at 30°C until colonies became visible (approximately 2 to 3 days)

Electrotransformation

Escherichia coli

Electrotransformation of *E. coli* cells was performed in 0.1mm electroporation cuvettes using a BTX electroporation system by adding 1µl 10ng/µl plasmid DNA to 50µl electrocompetent cell suspension, incubating them on ice for 10 minutes and electroshocking cells at 1.75Kv with parameters set to 2.5Kv resistance, 129Ω resistance timing, 800µF Capacitance timing. Cell suspension is recovered from the cuvettes by adding 950µl of sterile LB and incubating cells at 37°C for 1 hour before plating them on the appropriate selective LB plates.

Agrobacterium tumefaciens

Electrotransformation of *A. tumefaciens* cells was performed as described for E. *coli* cells but electroshocking cells at 1.40Kv using the same parameter settings. Cell suspension is recovered from the cuvettes by adding 950µl of sterile LB and incubating cells at 28°C for 3 hour before plating them on the appropriate selective LB rifampicin plates.

PLANT AGROBACTERIA MEDIATED TRANSFORMATION

Transient expression

Transient expression in *N. benthamiana* leaves was performed by inoculating a LB liquid preculture with the *A. thumefaciens* stock culture of interest kept at -80°C using a pipette tip and incubating the preculture at 28°C for 2 days after which 100µl of the culture is used to inoculate a 20ml liquid media (1:200 dilution) and cultured for 16h at 28°C. The culture is pelleted by centrifugation at 4000rpm in 2 10ml tubes of which one is induced with Induction Buffer (10 mM MES pH 5.6, 10 mM $MgCl_2$ and 0.15 mM Acetosyringone) for 3 hours at room temperature and the other pellet is stored at -20°C for future analysis if needed. Passed 3h induction culture is diluted to a final OD_{600} of 0.5 and infiltrated through the reverse side of 4th and 5th leaves of 4 week-old plants. Leaves were harvested according to the experimental needs.

Stable transgenic expression

Stable transgenic A. thaliana plants were produced by transforming flowers using the floral dip procedure described previously (Zhang et al., 2006). Pots containing 15 A. thaliana flowering plants were dipped in 400ml agrobacteria cell suspension of interest and infiltrated under vacuum for 10 minutes. Flowers were rinsed with plenty of water and fitted in plastic bags to grow resting sideways for 3 days in the greenhouse before removing the plastic and putting them upright. Growth was maintained until sufficient inflorescences develop and seeds harvested. Harvested seed were dried at 37°C for 7 days. Transformants were screened for by growing 2000 seeds on 0.5X MS agar containing the appropriate selective agent with

Carbenicillin and passing each transformant T_0 lines to soil as described previously in the *in vitro* practice.

VIRAL INOCULATION

Agro Inoculation

Arabidopsis thaliana

For the inoculation of *in vitro* grown *A. thaliana* plants, autoclaved and sterile toothpicks were dipped in the appropriate culture at a final OD_{600} of 0.5 before pricking three leaves per plant supported by a sterile spatula to avoid contaminating the agar beneath.

Nicothiana benthamiana

Agro-bacterial inoculation of the viral constructs was performed by inducing *A. thumefaciens* cultures harbouring the viral construct of interest as in the transient expression described above and diluting the culture to a final OD_{600} of 0.5, 0.1 or 0.01 depending on the needs of each experiment before infiltrating the reverse side of *N. benthamiana* leaves as described for the transient expression.

Manual Viral Inoculation

Cucumis sativus

Approximately 100mg of liquid nitrogen ground leave tissue infected with CVYV was homogenized in 100µl of 0.5M PBS buffer using a plastic hand held pestle. The inoculum is centrifuged briefly at 13000rpm in a microfuge for 2 minutes and 10µl supernatant was caressed on the leaves to be infected being previously dusted with carborundum powder.

NUCLEIC ACID PURIFICATION AND ANALYSIS

DNA plasmid purification

Escherichia coli

Small-scale DNA plasmid purification was performed from 5ml *E. coli* cultures using the alkaline lysis protocol described (Sambrook et al., 1989). Purified samples could be subjected to a clean up using phenol by resuspending the pellet in 200µl of miliQ water, and vortexing each sample with 200µl Phenol-Chloroform-Isoamyl Alcohol (39:39:1), separating both phases by a quick spin and precipitating with 2.5 volumes of absolute ethanol after adding 1/10 volume of 3M Sodium Acetate and 1µl Glycan Blue (Ambion) to the recovered aqueous phase. Samples are left at -20°C over-night to precipitated and pellet is washed with 1ml 70% Ethanol once, before resuspending it in the desired volume of MiliQ water upon dried. Alternatively to avoid the long and tedious clean up using phenol Favorprep mini extraction kit columns (Favor Biotech) were used according to the manufacture's instructions. Miniprep purifications were stored momentaneously at 4°C for short-term storage until analyzed or at -20°C for long-term storage.

Large-scale plasmid purification was performed using the PEG maxiprep protocol from 200ml bacterial cultures and the final DNA pellet was resuspended in 100µl MiliQ water and stored at -20°C until needed.

Agrobacterium thumefaciens

Small-scale DNA plasmid purification was performed from 5ml *E. coli* cultures using the lysoprep protocol. Final pellets were resuspended in 30µl MiliQ water. Alternatively, purified DNA was subjected to clean up using phenol as described for the E. coli small-scale purifications above if DNA was to be sequenced.

Saccharomyces cerevisiae

Plasmid isolation from *Saccharomyces cerevisiae* was performed by resuspending 2ml of an over-night grown culture in yeast resuspension buffer (2.5M LiCl, 50mM Tris-Cl pH 8.0, 20mM EDTA, 4% Triton X-100). Cells were disrupted by vortexing the cell suspension with 200mg of glass beads for 2 minutes followed by a two 3

minute consecutive vortexes adding a mixture of phenol/Chloroform/Iso-amyl-alcohol (25:24:1) both times, the later with TE. Aqueous phase was recovered and plasmid DNA was precipitated as a normal phenol/chloroform DNA precipitation. Pellet was resuspended in 50µl MiliQ water and stored at -20°C until needed.

Pheno/chloroform plasmid precipitation

To further purify plasmid DNA when downstream applications required higher purity DNA or when resuspension buffer was to be changed, plasmid DNA samples were extracted with equal volumes of phenol/chloroform/Iso-Amyl Alcohol (25:24:1) once. Aqueous phase was recovered, 1/10 volume 3M Sodium Acetate and 2 volumes of 96% Ethanol was added before precipitating samples at -20°C. Pellet was washed twice with 70% Ethanol before resuspending it in MiliQ water when dry.

Plant genomic Purification

Plant genomic DNA for PCR analysis was purified using the Plant Genomic DNA prep protocol with modifications available at:

http://www.dartmouth.edu/~tjack/TAILDNAprep.html

Plant total RNA Purification

Arabidopsis thaliana

Total RNA was extracted from 100-200mg of liquid nitrogen ground whole plant tissue using the Z6 RNA extraction protocol. Pellets were air dried at room temperature and resuspended in 100µl MiliQ water, incubated at 50°C for 10 minutes and stored at -20°C until needed.

For RT-PCR amplifications, total RNA was extracted using Favorprep plant total RNA purification kit following the steps through the DNase I digestion as described in the manufacture's instructions.

Nicothiana benthamiana

Total RNA was extracted from 100-200mg of liquid nitrogen ground plant leaf tissue samples from *N. benthamiana* using the Z6 RNA extraction protocol

described for *A. thaliana*, but adding 5µl 14.7M ß-mercaptoethanol per 1ml of Z6 buffer to be used.

Cucumis sativus

Total RNA was extracted from 100-200mg of liquid nitrogen ground inflorescence tissue samples from *C. sativus* subsp. cádiz using Favorprep plant total RNA purification kit following the steps through the DNase I digestion as described in the manufacture's instructions.

Plant small RNA Purification

Nicothiana benthamiana

smRNAs were extracted from 100-200mg of liquid nitrogen ground agroinfiltrated plant leaf tissue samples from *N. benthamiana* using either the small RNA purification protocol described previously (Lagrimini et al., 1987) with modifications. After LiCl precipitation, the pellet fraction containing large RNAs, was resuspended in water. The supernatant fraction containing small RNAs was precipitated with ethanol and resuspended in water.On other occasions smRNAs were purified by simply extracting total RNA using the Z6 protocol described above and separating smRNAs on a 15% poly acryl amide gel.

Alternatively when in time-crisis, fractional separation of the smRNAs was performed by separating large RNAs using Favorprep plant total RNA purification kit and recovering the smRNAs from the column eluate and subjecting it to a second selective purification step by adding 1 volume of isopopanol and 1/10 volume of 3M Sodium Acetate and precipitating the mixture over-night at -20°C. smRNAs are pelleted by centrifugation at 13000 rpm in a microfuge for 30 minutes and washed with twice with 1ml 80% Ethanol, dried at room temperature, resuspended in 50µl MiliQ water and stored at -20°C until needed.

Nucleic Acid quantification

Nucleic acids were quantified using a nanodrop ND-1000 spectrophotometer and software ND-1000 v3.3.0 from Coleman technologies Inc.

Alternatively to double check nanodrop quantifications when quantifying linear DNA used for cloning or probes 1µl of DNA was run on a 1% agarose gel by electrophoresis along side 100ng of HindIII digested Φ29 genomic DNA and the band was quantified as relative densitometry with respect to the most similar band density from the digested Φ29 genomic DNA using the formula:

(Band size/19460) x 100ng Φ29 = ng DNA loaded on gel.

PCR amplification of DNA products

During the course of this study various DNA polymerases have been used each with different properties and cycle constraints. PCR amplifications were performed in an electronic PTC-100 Thermo-Cycler Machine (MJ Research Inc, Waltham, MA), using Expand High Fidelity (Roche) Pwo (Roche) Amplitaq (Pelkin Elmer) Phusion Hot Start Flex (New Enlgand BioLabs) or Phusion Green Hot Start II (Thermo Fisher Scientific) using the specific cycle conditions detailed.

Table 17. PCR cycle conditions employed. Depending on the DNA polymerases used, Temperature in degrees °C and time in seconds for each step is as indicated.

PCR Cycle	Amplitaq			Expand High Fidelity, Pwo			Phusion Hot Start Flex, Phusion Green Hot Start II		
Step	Temp. °C	Time sec.	Cycles	Temp. °C	Time sec.	Cycles	Temp. °C	Time sec.	Cycles
1	95	300	x1	94	240	x1	98	30	x1
2	95	25		94	30		98	10	
3	Ta	30	x30	Ta	60	x30	Ta	30	x40
4	72	60/Kbp		72	45/Kbp		72	30/Kbp	
5	72	300	x1	95	420	x1	72	600	x1
6	4	∞	x1	4	∞	x1	4	∞	x1

Ta, Annealing temperature; Kbp, Kilo base pairs.

Annealing temperature was calculated by using the lowest of the temperatures obtained for each primer pair using the formula: Tm-5°C, being Tm the melting temperature of the oligonucloetide provided by the manufacturer (Sigma Aldrich).

PCR amplifications using individual colonies instead of purified template DNA were performed with modified PCR cycle conditions as shown in the table below.

In the case of *E.coli*, individual colonies were resuspended in the PCR reaction mix and cycle started after toothpicks used were streaked on LB agar. For *S. cerevisiae* and *A. thumefaciens*, individual colonies were resuspended in 10µl sterile MiliQ water with sterile toothpicks and the same toothpick was used to streak an agar plate with the appropriate growth medium. The cell suspension was subjected to 3 freeze-boil cycles by freezing in liquid nitrogen for 5 minute and boiling at 95°C for 5 minutes with a final boil at 95°C for 20 minutes in order to lyse the cells. Cell suspension was centrifuged at 12000rpm for 10 minutes and the supernatant was used as template DNA in subsequent PCRs using amplitaq DNA polymerase (Pelkin Elmer)

Table 18. Colony PCR cycle conditions employed. Depending on the microorganism used, Temperature in degrees °C and time in seconds for each step is as indicated.

Colony PCR Cycle	*E. coli*			*A. thumefaciens*			*S. cerevisiae*		
Step	Temp. °C	Time sec.	Cycles	Temp. °C	Time sec.	Cycles	Temp. °C	Time sec.	Cycles
1	98	600	x1	95	900	x1	95	600	x1
2	95	30		94	30		95	30	
3	Ta	40	x40	Ta	30	x35	Ta	30	x40
4	72	90/Kbp		72	150/Kbp		72	90/Kbp	
5	72	360	x1	95	300	x1	72	300	x1
6	4	∞	x1	4	∞	x1	4	∞	x1

PCR confirmation of homozygous T-DNA lines

Asymmetric PCR amplification was used to confirm homocigosity of T-DNA insertion lines. PCR mixes were assembled using the genomic DNA extraction for each individual plant line and a mix of two oligonucleotides, one pair annealing on the loci to be analysed and the third on the T-DNA border. Sequence of the T-DNA oligonucleotide depended on the origin of the seed stock, and can be seen on Table 14. Amplitaq polymerase was used and the cycling conditions described in Table 17.

DNA agarose gel electrophoresis

DNA fragments were mixed with 6X DNA Loading buffer (10mM Tris HCl pH 7.6, 60mM EDTA, 60% Glycerol, 0.15% Orange G) and subjected to 0.8% to 1.4% agarose gel electrophoresis depending on their size in 0.5X TBE (45mM Tris-

borate, 1mM EDTA) buffer with 0.1mg/ml of Ethidium Bromide. Visualization of the stained DNA was performed using a Gel Doc 2000 image system (BioRad).

DNA agarose gel purification

QIAEX II gel purification kit (QIAGEN), QIAEX minelute gel purification kit (QIAGEN), Favorprep PCR/gel purification mini kit (Favorgen Biotech), or Favorprep microelute PCR/gel purification mini kit (Favorgen Biotech), was used to extract DNA fragment from agarose gels depending on individual needs.

DNA cloning

cDNA synthesis

cDNA was synthesized using Superscript III (invitrogen) as described by the manufacturer. Table below summarizes a 20µl reaction:

Table 19. cDNA synthesis reaction set up using Superscript III. Components, concentrations and volumes are as indicated. Temperature in degrees °C and time in minutes.

Step	Action	Set up
1	Mix	1µl 10µM NVdT18 (#2131) 1µl 10mM dNTP mix 100ng total RNA up to 12 µl MIliQ water
2	Incubate	65°C for 15 minutes
3	Incubate	on ice for 1 minute
4	Mix	4µl 5X FS Buffer 1µl 0.1M DTT 1µl RNase out 2µl Superscript III
5	Incubate	25°C for 5 minutes
6	Incubate	50°C for 60 minutes
7	Incubate	70°C for 15 minutes
8	Add	1µl RNase H
9	Incubate	37°C for 20 minutes

cDNA was kept at -20°C until needed for PCR amplification using gene specific primers. 1µl of the cDNA mix was used as template in PCR reactions that follwed.

Alternately cDNA was synthesized coupled to PCR amplification using Titan One tube RT-PCR kit (Roche, Cat. No. 11 939 823 001) with gene specific primers as

described by the manufacturer but optimized for a final reaction volume of 20µl. Reaction components and volumes can been seen in the table below:

Table 20. One tube RT-PCR reaction set up using Titan. Components, concentrations and volumes for each step as indicated. Temperature in degrees °C and time in minutes.

Step	Action	Set up
1	Mix R1	5.8µl MiliQ water 0.2µl 10mM dNTPs Mix 1µl 10µM Forward Oligo 1µl 10µM Reverse Oligo 1µl 100mM DTT 1µl 100ng/µl total RNA
2	Incubate	95°C for 2 minutes
3	Incubate	on ice for 5 minute
4	Mix R2	In laminar flux hood mix: 5.8µl MiliQ water 4µl 5X Titan Buffer 0.2µl Titan Enzyme
5	Mix	10µl R1 with 10µl R2
6	Incubate	in thermocycler using Titan RT-PCR cycle

After mixing the reactions, samples were incubated in the thermocycler using the cycling conditions described below:

Table 21. One tube RT-PCR cycling conditions using Titan. Temperature in °C, time in second and number of cycles for each step as indicated.

PCR Cycle	Titan RT-PCR		
Step	Temp. °C	Time sec.	Cycles
1	50	3000	x1
2	94	120	x1
3	94	30	
4	Ta	30	x40
5	68	60/Kbp	
6	68	300	x1
7	4	∞	x1

RT-PCR products were gel or column purified as described in this work and used in either BP recombinations or sequencing reactions depending on needs.

pUC18 constructs

RT-PCR products amplified using oligos in Table. 9 were gel purified as described above and ligated using T4 DNA ligase (Thermo Fisher Scientific) as described by the

manufacturer into pUC18 proviosuly linearized with SmaI and gel purified as described above.

pDONR207

Gel purified PCR products were recombined using the BP recombinase enzyme mix (invitrogen) with PvuII linearized or non-linearized pDONR207 plasmid DNA in reactions set up as follows:

Table 22. BP Reaction. Components of the BP recombinase reaction and volumes.

Compound	Volume in µl
BP enzyme mix	1
TE pH 8.0	1
Purified PCR product 100ng/µl	1
pDONR207 100ng/µl	1
MiliQ water	1
Total Reaction volume	5

Reactions were incubated thin-wall PCR tubes at 25°C for 2 hours. Following this incubation time 1µl Protease K supplied with the kit was added to stop the reaction with a further incubation at 37°C for 20 minutes. 2.5µl of the BP reaction mix was used to transform *E. coli* DB3.1 cells, plated on LB gentamicin agar plates, and incubated at 37°C until transformants became visible.

Gateway destination vectors

Gateway destination and expression vectors were achieved by recombination between the pDONR207 harbouring the ORF of interest and the gateway vector by means of recombination catalysed by the LR recombinase enzyme mix (invitrogen). Reaction set up was as follows:

Table 23. LR Reaction. Components of the recombinase reaction and volumes.

Compound	Volume in µl
LR enzyme mix	1
TE pH 8.0	1
pDONR207-ORF 100ng/µl	1
pDEST 100ng/µl	1
MiliQ water	1
Total Reaction volume	5

Reactions were incubated thin-wall PCR tubes at 25°C for 2 hours. Following this incubation time 1µl Protease K supplied with the kit was added to stop the reaction with a further incubation at 37°C for 20 minutes. 2.5µl of the BP reaction mix was used to transform *E. coli* DH5α, DBH10 or TOP10 cells, plated on selective LB agar plates determined by the specific resistances harboured in the plasmid, and incubated at 37°C until transformants became visible.

Northern Blot analysis

Radio labelled probe production

PCR Probes

Radio labelled probes were produced using Amersham Rediprime II random prime labelling system kit (GE Healthcare, RPN1633) following the manufacture's instructions using PCR gel purified products which were gel quantified.10-20ng of DNA used per reaction together with 5µl ^{32}P-α-dCTP 3000Ci/mmol (Perkin Elmer, NEG513H). Reaction was taken to a final volume of 100µl with MiliQ water and filtered through Microspin Sephacryl-G200HR columns (GE Healthcare, 27-5120-01) recovering 10-12 fractions. Radio-emissions from recovered fractions were quantified in a Liquid Scintillator Counter (Wallag 1410) and the appropriate fraction was used for hybridization.

Oligo Probes

DNA oligo probes were produced by phosphorilation of a DNA oligo complementary to the sequence to detect using a T4 polynucleotide kinase and ^{32}P-α-ATP 3000Ci/mmol (Perkin Elmer, NEG502A) as substrate in a 25µl reaction as follows:

Table 24. Radio labelling DNA oligo Probes. Components of the labelling reaction and volumes.

Compound	Volume in µl
10µM Oligo DNA	2
10X T4 Kinase Forward Buffer	2.5
7.5u T4 Polynucleotide Kinase	0.5
3000Ci/mmol ^{32}P-α-ATP	4
MiliQ water	16
Total Reaction volume	25

Reaction mixture was incubated at 37°C for 1 hour and reaction was stopped by adding 1.5µl 0.5M EDTA pH 8.0. Reaction was taken to a final volume of 100µl with MiliQ water and filtered through Microspin Sephacryl-G200HR columns (GE Healthcare, 27-5120-01) recovering 10-12 fractions. Radio-emissions from recovered fractions were quantified using a Liquid Scintillator Counter (Wallag 1410) and the appropriate fraction was used for hybridization.

RNA gel electrophoresis

Denaturing RNA gel electrophoresis

Total RNA gel electrophoresis was performed on 2.5% agarose under denaturing conditions (X1 MEN, 5% Formaldehyde, 2.5% Agarose). Samples were loaded "dry" and gel was covered with Saran wrap to prevent formaldehyde evaporation before running at constant amperage of 250mΩ at room temperature until tRNA is completely resolved. 1X MEN (20mM MOPS, 50mM Sodium Acetate, 20mM EDTA, pH 7.0) running buffer was used for running the gel

Poly-Acrilamyde Urea Gel electrophoresis

Poly-acrylamide gel electrophoresis of small RNAs was performed as described (Blevins, 2010). RNA samples were resolved in 15% poly-acrylamide 7M Urea denaturing gels by pre-running the gels for two hours before loading either 20µg of total Z6 purified RNA, or 5µg of purified smRNAs in 2X smRNA loading buffer. Electrophoresis was performed at 80V until both the Bromophenol blue and the Xylene cyanol dyes have entered the gel, before cleaning the well with a syringe to wash the mRNAs and continuing at 400V until the Bromophenol blue dye had left through the bottom of the gel.

RNA blotting and UV-crosslinking

Total and small RNAs were blotted on Hybond-H^+ nylon membranes (GE Healthcare, RPN303B, 0.45µm) by capillary for 16-18 hours. Blotted membranes were crosslinked once on the side in contact with the gel using a UV-crosslinker oven (Amersham Life Science) set to 70000 microjoules/cm^2.

Methylene Blue RNA staining

Crosslinked membranes blotted with total RNAs were washed for 15 minutes with 5% Glacial acetic acid and incubated in MethBlue staining solution (0.5M Sodium Acetate pH 5.2, 0.04% Methylene Blue) for 20 minutes followed by three 5 minutes washes with distilled water. Stained membranes were sandwiched between two plastic covers and scanned as described below.

Probe Hybridization and radio detection

Methylene Blue stained membranes were pre-hybridized with 50ml pre-hybridization solution (200mM PBS pH 7.2, 7% SDS, 500µM EDTA pH 8.0) for at least 2 hours at 65°C for total RNA blots and 35°C for small RNA blots. The clean radio labbled probe was boiled at 95°C for 5 minutes and cooled on ice for a further 5 minutes to denature the probe before adding it to 20ml of the pre-hybdridization solution used in pre-hybridizing the membrane. Incubation of the membrane was done at 65°C for 16 hours following three consecutive 30 minute washes in 2X SSC, 0.2X SSC and 0.1X SSC supplemented with 0.1% SDS either at 65°C for total RNA blots or 35°C for small RNA blots. Hybridized membranes were sealed in plastic bags and expossed on phosphoimage screens for 1 to 3 hours depending on the signal and visualized using a Molecular Imager FX system (Bio-Rad).

YEAST TWO HYBRID ANALYSIS

Transformant colonies growing on SD/-2 agar plates were picked with at sterile tip and used to inoculate liquid SD/-2 media. Inoculated media was cultured at 28°C for 48-72 hours. Cultures were centrifuged and washed in sterile MiliQ water once before making dilutions in sterile MiliQ water to a final OD_{600} of 1. 5µl of each culture was used to spot on SD/-2, SD/-3, SD/-4 and SD/-4 + 5mM 3-AT agar plates and incubated at 28°C for 6 to 12 days.

BI-MOLECULAR FLUORESCENT COMPLEMENTATION ANALYSIS

N. benthamiana leaves were infiltrated making mixes with the corresponding *A. thumafaciens* transformed with the appropriate plasmids to a final OD_{600} of 0.5 per culture in Induction Buffer (10mM MES pH 5.6, 10mM $MgCl_2$ and 0.15mM Acetosyringone) as described above. Agro-infiltrated leaves were harvested at 6 days post-infiltration and fluorescent complementation was visualized under a MZ FLIII (Leica Microsystems) fluorescence binocular stereoscope and a DMR (Leica Microsystems) epifluorescence binocular microscope as described Imaging and Image Analysis.

PROTEIN AND PROTEOMIC PURIFICATIONS AND ANALYSIS

Total Denaturing protein extraction

Total protein was extracted by adding 6M Urea Cracking Buffer (200mM Tris HCl pH6.8, 10% SDS, 6M Urea, 20% Glycerol, 5% ß-mercaptoethanol, 0.05% Bromophenol Blue) in a mass:volume ratio of 1:2, boiled for 3 minutes at 96°C and kept on ice or at -20°C until needed.

Blue-native electrophoresis

Blue native gel electrophoresis was performed as described in Niepmann & Zheng 2006 by resuspending samples in 2X Loading buffer (200mM Tris-Cl pH 8.0, 80% Glycerol, 1.0% Serva Blue G) and loading a 5-15% gradient poly-acrylamide gel which was run with Cathode Buffer (100mM Histidine pH 8.0, 0.002% Serva Blue G) and Anode Buffer (100mM Tris-Cl pH 8.8) until the protein complexes are completely resolved. Gel was scanned and proteins were then blotted on nitrocellulose membranes using a Biorad semi-dry transfer system at 400mΩ for 3 hours at 4°C.

Crosslinking

In vivo protein crosslinking

Agrobacterium infiltrated *N. benthamiana* leaves or CVYV *C. sativus* infected leaves were harvested and cut into approximately $1cm^2$ pieces and vacuum infiltrated in ice-cold PBS buffer on ice supplemented with 1% Formaldehyde for 30 minutes

(Hall & Struhl, 2002). Reaction was quenched with a vacuum infiltration of 300mM Glycine for 5 minutes on ice followed by three washes using ice cold MiliQ water and dryed on a paper towel before grinding tissue in liquid nitrogen using a cold mortar and pestle. Samples were stored at -80°C until needed.

Dynabeads Protein A/G-Antibody crosslinking

Dynabeads were chemically crosslinked to antiserum as described previously (Miernyk & Thelen, 2008). 400µl magnetic Dynabeads Protein A/G (50% slurry) were mixed with 200µg of rabbit antiserum raised against P1b and incubated with 10 mM dimethyl pimelimidate and 10 mM dimethyl suberimidate in 20 ml PBS buffer pH 8.5, for 1 hour at 25°C. Reaction was stopped by adding 10 ml of 100 mM TRIS–HCl, pH 8.8. Beads are blocked overnight overnight at 4°C with 10 ml of 0.2% BSA in 100 mM TRIS–HCl pH 8.8, and washed three times with PBS buffer before use.

Co-immunoprecipitation

Nicotiana benthamiana

Co-immunoprecipitation of *N. benthamiana* agroinfiltrated crosslinked leave tissue was performed by extracting total proteins from 150mg of liquid nitrogen ground tissue in Co-IP extraction buffer softly with and eppendorf size hand held homogenizer and incubating them on a End-to-top wheel for 10 minutes at 4°C followed by a 10 minutes centrifugation at 4000rpm 4°C. Extracts were diluted 3 times in Co-IP wash buffer and 5µl mouse anti-myc serum was added incubating samples for 16 hours End-to-top wheel at 4°C. 50µl Dynabeads previously washed and blocked in Co-IP wash buffer supplemented with 0.5% BSA Fraction V for 16h at 4°C, were added to each reaction and incubated again on a End-to-top wheel for 4 hours at 4°C. Dynabeads were collected using a magnetic rack and washed 5 times with Co-IP washing buffer. Input, unbound and final elution samples were collected and mixed with the same volume Cracking Buffer, boiled for 3 minutes and stored at -20°C till needed. Buffer composition used for Co-IPs is detailed below:

Table 25. Co-IP buffer composition used with *N. benthamiana* samples. Concentration of each component is indicated.

Co-IP Buffers used with *N. benthamiana* tissue	
Co-IP Extraction Buffer	Co-IP Wash Buffer
Co-IP wash Buff +	25mM Tris-Cl pH 8,0
1mM PMSF	75mM NaCl
50µM MG132	0.5% Nonidet
5mM ß-Mercaptoetanol	0.05% Sodium Deoxycholate pH 8,0
2X Compete EDTA-free Protease inhibitor cocktail	10% Glicerol

Isobaric Tag for Relative and Absolute Quantification (iTRAQ)

The iTRAQ labelling and mass spectroscopy Triple-TOF analysis was supported at the proteomics facility of the CNB through the proteored (www.proteored.org) webpage.

Quantification and labelling

Whole 12dpi infected *A. thaliana* plants grown *in vitro* were ground in liquid nitrogen with a mortar and pestle. Approximately 20mg of tissue powder was resuspended in 1ml in two independent extractions using the native iTRAQ extraction Buffer (50mM Tris-HCl pH 8.0, 150mM NaCl, 0.05% Tween-20), pooled in one and passed through a Seppro RUBISCO spin depletion column (Sigma-Aldrich, SEP070) as described by the manufacturer. Total protein was precipitated using methanol/chloroform, resuspended and quantified. 30µg of total protein from each condition was precipitated by methanol/chloroform method. Protein pellets were resuspended and denatured in 20 µl 6 M guanidine hydrochloride/100mM HEPES, pH 7.5, (SERVA Electrophoresis GmbH), reduced with 1 µl of 50mM Tris(2-carboxyethyl) phosphine (TCEP, AB SCIEX), pH 8.0, at 60°C for 30 min and followed by 2 µl of 200mM cysteine-blocking reagent methyl methanethiosulfonate (MMTS, Pierce) for 10 min at room temperature. Samples were diluted up to 120 µl to reduce guanidine concentration with 50mM TEAB. Digestions were initiated by adding 1.5 µl (1 µg/µl) sequence grade-modified trypsin (Sigma-Aldrich) to each sample in a ratio 1/10 (w/w), which were then incubated at 37°C overnight on a shaker. Sample digestions were evaporated to dryness. Each peptide solution was labelled at room

temperature for 2 hours with a half unit of iTRAQ Reagent Multi-plex kit (AB SCIEX, Foster City, CA, USA) previously reconstituted with 80 µl of 70% ethanol/50mM TEAB. In the iTRAQ labelling, tags 115 and 116 were used for PPV-P1b-nk-sGFP biological replicates, 117 for PPV-nk-sGFP and 115 for non-infected *A. thaliana* samples. Afterwards, all labelled samples were combined and labelling reaction stopped by addition of 100 µL of 50% ACN and evaporation in a Speed Vac. The digested, labelled and pooled peptide mixture was desalted using a Sep-PAK C18 Cartridge (Waters), following manufacture indications before tryptic peptides were evaporated to dryness and stored at -20°C for downstream LC-MS analysis.

Liquid chromatography and mass spectrometry (LC-MC) analysis

A 2.5 µg aliquot of the desalted peptide mixture was subjected to 1D-nano LC ESI-MSMS analysis using a nano liquid chromatography system (Eksigent Technologies nanoLC Ultra 1D plus, AB SCIEX) coupled to high speed Triple TOF 5600 mass spectrometer (AB SCIEX) with a duo spray ionization source. A silica-based reversed phase column C18 ChromXP 75 µm × 15 cm, 3 µm particle size and 120 Å pore size (Eksigent Technologies, AB SCIEX) analytical column was employed together with a C18 ChromXP (Eksigent Technologies, AB SCIEX), 3 µm particle diameter, 120 Å pore size, switched on-line with the analytical column. A solution of 0.1% formic acid in water at 2 µl/min was delivered using a loading pump. A flow-rate of 300 nl/min operating under gradient elution conditions, using 0.1% formic acid in water as mobile phase A, and 0.1% formic acid in acetonitrile as mobile phase B was provided by a nano-pump. Gradient elution was performed according the following scheme: isocratic conditions of 98% A: 2% B for 1 minutes, a linear increase to 30% B in 210 minutes, a linear increase to 40% B in 10 minutes, a linear increase to 90% B in 5 minutes, isocratic conditions of 90% B for 5 minutes and return to initial conditions in 2 min. Injection volume was 5 µl. Data acquisition was performed in a TripleTOF 5600 System (AB SCIEX) and acquired using an ionspray voltage floating (ISVF) 2800 V, curtain gas (CUR) 20, interface heater temperature (IHT) 150, ion source gas 1 (GS1) 20, declustering potential (DP) 85 V. All data was acquired in information-dependent acquisition (IDA) mode with Analyst TF 1.5 software (AB SCIEX). For IDA parameters, 0.25 seconds MS survey scan in the mass range of 350–1250 Da were followed by 15 MS/MS scans of

0.250 seconds in the mass range of 100–1800 (total cycle time: 4.04 seconds). Switching criteria were set to ions greater than mass to charge ratio (m/z) 350 and smaller than m/z 1250 with charge state of 2–5 and an abundance threshold of more than 90 counts (cps). Former target ions were excluded for 20 seconds. IDA rolling collision energy (CE) parameters script was used for automatically controlling the CE.

Data analysis

MS and MS/MS data obtained for pooled samples were processed using Analyst® TF 1.5.1 Software (AB SCIEX). Raw data file conversion tools generated mgf files which were searched against a customized database asembled with *Arabidopsis thaliana* (taxonid:3702) and PPV (taxonid:12211) proteins, containing 76391 protein coding genes and their corresponding reversed entries using the Mascot Server v. 2.3.02 (Matrix Science). Search parameters were set as follows: enzyme, trypsin; allowed missed cleavages, 1; fixed modifications, iTRAQ4plex (N-term and K) and beta-methylthiolation of cysteine; variable modifications, oxidation of methionine. Peptide mass tolerance was set to ± 20 ppm for precursors and 0.05 Da for fragment masses. The confidence interval for protein identification was set to ≥ 95% ($p<0.05$) and only peptides with an individual ion score above the 1% False Discovery Rates (FDR) threshold were considered correctly identified. Only proteins having at least two quantitated peptides were considered in the quantitation.

SDS-polyacrylamide gel electrophoresis (SDS-PAGE)

SDS-Page gels were casted using the Biorad mini-protean III gel electrophoresis system. Gels were casted with different Acrilamide (1:29 bisacrylamide:acrilamide) concentrations depending on the needs of each individual gel used and target protein size to be resolved. The linear range of separation for different acrylamide gels can be seen in table below.

Table 26. Effective range of separation of SDS-PAGE gels. Gel percentage concentration and expected linear range separation for proteins of size range indicated. Modified from (Sambrook et al., 1989).

Range of separation SDS-PAGE gels	
Acrylamide Concentration	Linear Range of separation in kDA
5%	57 - 212
7.5%	36 - 94
10%	16 - 68
15%	12 - 43

SDS-PAGE gels were casted depending on the molecular sizes of the proteins to de resolved by mixing the components in the proportions described in the table below and polymerizing the gels between two glasses separated by either 0.75mm or 1.0mm depending on the combs to be used to prepare the loading wells on the stacking gel and bubbles removed by adding 0.5ml of Iso-propanol on the top of the solution.

Table 27. Solution volumes for casting different percentage SDS-PAGE gels. Component concentrations and volumes for gel mold volumes indicated. Modified from (Sambrook et al., 1989).

Gel Percentage	Solution Components	Component volumes in ml per gel mold volume of		
		10ml	15ml	20ml
8%	MiliQ H_2O	4.6	6.9	9.3
	30% Acrylamide mix	2.7	4.0	5.3
	4X Lower Tris pH 8.8	2.5	3.8	5.0
	10% APS	0.1	0.15	0.2
	TEMED	0.006	0.009	0.012
10%	MiliQ H_2O	4.0	5.9	7.9
	30% Acrylamide mix	3.3	5.0	6.7
	4X Lower Tris pH 8.8	2.5	3.8	5.0
	10% APS	0.1	0.15	0.2
	TEMED	0.004	0.006	0.008
12%	MiliQ H_2O	3.3	4.9	6.6
	30% Acrylamide mix	4.0	6.0	8.0
	4X Lower Tris pH 8.8	2.5	3.8	5.0
	10% APS	0.1	0.15	0.2
	TEMED	0.004	0.006	0.008

After polymerization of the resolving gel concluded (aprox. 30 miuntes), iso-propanol was removed by washing the gel with distilled water and polymerizing the stacking gel on top with the appropriate 10, 12 or 15 well-comb. Composition of the stacking gel is described in the table below.

Table 28. Solution volumes for casting 5% Stacking gel. Component concentrations and volumes for gel mold volumes of 5ml are indicated.

5% Stacking Gel Solution Composition	
Solution Components	Component volumes for 5ml gel mold volume
MiliQ H_2O	3.0
30% Acrylamide mix	0.650
4X Upper Tris pH 6.8	1.250
10% APS	0.050
TEMED	0.0075

Once gels were casted, combs are removed wells are washed with water, wrapped with humid paper towel, sealed in Saran wrap and kept at 4°C until needed with a maximum storage period of 14 days. Gels older than 14 days were discarded if not used. Gel electrophoresis was performed using the Biorad mini-protean III acrylamide gel electrophoresis system in Tris-glycine Running Buffer (25mM Tris, 250mM Glycine, 1% SDS) at 80-130V until proteins were completely resolved. To visualize protein sizes 3µl Blue Star Protein Marker (Nippon Genetics) was used in each gel.

SDS-PAGE gel staining

Coomasie blue protein gel staining

SDS-PAGE gels were stained in Coomasie blue when required by incubating the gels in Coomasie staining solution (0.05% Coomasie Briliant Blue-R (Sigma), 10% Acetic Acid, 25% Isopropanol) for 6 hours and distaining the gel over night in 10% Acetic Acid. Stained gels were scanned at 400ppp using an Epson Perfection 3200 Photo scanner and standard image acquiring software.

Non-fixing Silver salts protein gel staining

SDS-PAGE gels were silver stained as described previously (Ansorge, 1985) with modifications. Gels were incubated in successive solutions at room temperature: 5 minutes in Solution A (10% ethanol, 5% acetic acid), 5 minutes in 0.01% Potassium permanganate, 2 minutes in Solution A, 5 minutes in 10% ethanol, 5 minutes in distilled water, 5 minutes in silver nitrate, 5 minutes in 10% potassium

carbonate, variable time in 2% potassium carbonate with 0.01% Formaldehyde until bands become visible before stopping the reaction with distilled water.

Western blot analysis and immunodetection

Western blot

Proteins were transferred to Biotrace NT nitrocellulose membranes (Pal Life Sciences ø0.2µm, P/N 66485) using a Biorad wet electro-blot transfer apparatus in Transfer Buffer (25mM Tris, 250mM Glycine, 20% Methanol) for 60 minutes at room temperature and at constant amperage of 250mΩ. After transfer membranes were incubated for 10 minutes in Ponceau Red Buffer to stain transfered proteins and washed twice with distilled water before scanning them as described below.

Immunodetection

Immunodetection was performed by blocking the membrane with 6% skimmed milk powder in TBS250 or 5% BSA if the antibody against streptavidin was to be used. Primary antibody was incubated from 15 minutes to 16h depending on the expression levels of the protein to be detected in 1.5% Blocking buffer, followed by three 10 minute washes with Washing Buffer (0.2% Tween-20 in TBS250) before incubating the membrane with horse radish peroxidase conjugated secondary antibody for 1 hour and washing the membrane three times with Washing Buffer. Membranes were then visualized with the LiteABlot enhanced Chemioluminescence detection kit (Euroclone) and exposed to AGFA Curix RP2 Plus X-ray films in film cassettes at variable exposure times. X-ray films were developed using an SRX-101A automatic film developer machine (Konika Minolta) coupled to an Automixer II Plus unit (Kodak) and films were scanned as described below.

Stripping and re-probing membranes

Membranes were stripped using 50ml Re-blot Plus strong antibody stripping solution (millipore) incubating membranes maximum 15 minutes at room temperature on an oscillating shaker.

ß-ESTRADIOL INDUCTION EXPRESSION

In plate inductions of *Arabidopsis thaliana*

10 days-old *Arabidopsis thaliana* seedlings growing in vitro on MS agar were submerged in a 10µM ß-estradiol (Sigam-Aldrich, E8875-250MG) MS solution and infiltrated on the agar plate for 3 minutes at 0.9PSI. Seedlings were then transplanted onto MS agar plates containing 10µM ß-estradiol and grown as described for *in vitro* practice.

WHOLE-MOUNT GUS STAINING

Whole-mount GUS staining of whole *A. thaliana* plants was performed as described previously (Weigel & Glazebrook, 2002) with modifications. Whole plants were infiltrated 2 minutes under vacuum 24 hours after ß-estradiol induction in GUS Staining Buffer (50mM PBS, 0.2% Triton X-100, 0.5mg/ml X-Gluc weighed fresh) and incubated at 37°C for 8 hours, followed by successive 30 minutes ethanol washes (20%, 35% and 50%), one 30 minute incubation at room temperature in FAA (50% Ethanol, 10% Glacial Acetic acid, 5% Formaldehyde), and various washes in 70% Ethanol until all chlorophylls are removed.

IMAGING AND IMAGE ANALYSIS

Membrane and Film Imaging

Membranes and exposed X-ray films were placed between two plastic covers and scanned at 400ppp using an Epson Perfection 3200 Photo scanner and standard image acquiring software on an iMac OS X (10.6.8).

Plant UV macro fluorescent images

GFP fluorescence was visualized using a MZ FLIII (Leica Microsystems) fluorescence binocular stereoscope using a GFP2 filter (MZ FLIII, GFP2, Leica) with excitation and barrier filters of 480/40 nm and 510 nm, respectively. Images were acquired with an OLYMPUS DP 70 digital camera and processed using DP Controller and DP manager software (Olympus Optical).

Plant UV micro fluorescent images

Epi fluorescent UV microscope

GFP fluorescence was visualized using a DMR (Leica Microsystems) epifluorescence binocular microscope with excitation and barrier filters of 450/90 nm and 500/550 nm, respectively. Images were adquired with an OLYMPUS DP 70 digital camera and processed using DP Controller and DP manager software (Olympus Optical).

Confocal UV microscope

YFP, GFP and tagRFP fluorescence were visualized on a confocal multispectral Leica TCS-SP5 (Leica Microsystems) controlled with a LAS AF v.2.7.3 software (Leica Microsystems) and a 63x/1.20 NA water inmersion objective with excitation Argon laser at 488 nm and emission bandwidth of 501–568 nm for the GFP signal, excitation at 561 nm and emission bandwidth of 581–649 nm for the tagRFP signal, and excitation at 633 nm and emission bandwidth of 678–756 nm for the chloroplast autofluorescence. Transmitted white light images were also taken.

Plant electron micrography

N. benthamiana plants were agroinoculated with agrobacteria harbouring pBIN-PPV-P1b-sGFP at an OD_{600} of 0.01 and infiltrated on the reverse of two leaves per plant. Plants were cultured in the greenhouse as described. Young systemically infected leaves obtained at 18dpi were used. *C. sativus* plants were mechanically inoculated with fresh CVYV-infected plant extract, prepared by extracting 50mg of infected *C. sativus* liquid-nitrogen-ground tissue powder in 100µl PBS buffer with a quick vortex and 10µl per inocula were used to inoculate two young leaves per plant. Plants were cultured in the greenhouse as described. Young systemically infected leaves obtained at 18dpi were used. Infected systemic leaves were processed immediately.

Tissue Processing

1-2mm2 leave fragments were fixed under mild conditions using a 0.1M pH 7.2 PBS solution containing 4% paraformaldehyde, 0.1% glutaraldehyde. Samples

were cryoimmobilised by rapid immersion in super-cooled ethanol at -170°C, and stored in liquid nitrogen. Cryosubstitution was performed in a 0.5% Uranyl acetate/methanol solution for 54 hours before infiltration in lowicry HM20 at -40°C following ultraviolet-light polymerisation at -40°C. Ultra-thin sections of aprox. 60-70nm were excised using a Leica EM UC6 ultramicrotome and mounted on formvar-covered gold grids.

Sections were stained with uranyl acetate and lead citrate following the standard procedure described elsewhere.

Immunogold labelling of thin leaf sections

The ultra-thing-mounted sections were blocked with 1% BSA in TBS buffer and incubated in a 1:500 dilution rabbit polyclonal anti serum raised against P1b in TBS for 1h at room temperature, following 3 consecutive washes in TBS and an incubation in a secondary 10nm gold-coupled antibody raised against IgG antibody solution for 45 minutes at room temperature. Sections were washed in TBS and miliQ water and dried completely until visualized under the electron microscope.

Electron micrography images

Images were obtained in a Jeol JEM 1011 electron microscope operated at 100kV and captured using a Gatan Erlangshen ES1000W camera.

Densitometry and Image analysis

Scanned X-ray film bands density was analyzed using ImageJ software as described in (Schneider et al., 2012).

"One of the advantages of being disorganised
is that one is always having surprising discoveries."

A. A. Milne, *Winnie the Pooh*.

RESULTS

RESULTS

Screening for P1b interactors

In order to determine host proteins interacting with P1b a series of screening experiments were performed. Ideally the perfect search would have been performed in a CVYV infected plant. However, at the time when the screenings were started, the only known hosts susceptible to CVYV infections were all members of either cucurbit subclass crop plants or plant weeds from diverse plant families such as *Convolvulaceae*, *Malvaceae* or *Asteraceae*, none of which had their genomes sequenced and sequences available. Although there is one report claiming symptoms supposedly caused by CVYV infection on *Datura stramonium*, *Nicotiana benthamiana* and *Nicotiana tabacum* plants using *Bemisia tabaci* as transmission vectors, with infections only confirmed for *Datura stramonium* and *Nicotiana tabacum* (Morris et al., 2006), persistent attempts in infecting *Nicotiana benthamiana* and *Arabidopsis thaliana* were all unfruitful, rendering impossible the use of an annotated plant models for proteomic studies or genetic validations using infected CVYV plant material as inocula.

To bypass these technical flaws in the study of any possible P1b interactors with a relevant biological function in the context of a non-existing experimental viral infection, the search for proteins interacting with P1b was divided into two main and distinct groups of screenings. Those performed with an overexpression of a functional P1b bait protein in a heterologous expression system, and those performed using a functional (at least in part) P1b viral expression system. It had been published that N-terminal tagging of P1b did not compromise its RSS activity (Valli et al., 2008), and transgenic expression of N-terminal TAP tagged P1b in *A. thaliana* caused pathogenic symptoms and developmental defects diagnostic of interference with endogenous RNA silencing pathways (Valli et al., 2009). These symptoms and defects correlated in magnitude with P1b protein accumulation levels. In consequence, to detect protein interactions that might be involved in the

RSS activity of P1b two datasets of putative interactors were obtained using a Yeast Two Hybrid approach and TAP tag protein purification coupled with mass spectroscopy from trangenic Arabidopsis plants expressing N-TAP-P1b . Data sets were confronted hoping to find common interactors to be validated for biological relevance.

On the other hand, screenings involving P1b in a viral context were also performed to provide P1b with the most similar cellular and molecular conditions encountered during a CVYV infection. As attempts in infecting both *Nicotiana benthamiana* and *A. thaliana* all failed using CVYV infected cucumber plant extracts, a viral expression vector belonging to the same viral family as CVYV was used. Experiments in course at the time of this work revealed that P1b could replace HCPro in the potyvirus PPV and the genome of this chimeric virus to be stable enough to inhibit host RNA silencing and allow viral replication and movement through the plant tissues (Carbonell et al., 2012). This demonstrated that P1b could replace HCPro in all essential functions and raised the possibility that P1b and HCPro could share conserved activities important for the viral machinery although being structurally very different. Later reports showed that replacing HCPro with other unrelated RSS proteins, like P19, Vp3 or NS1 was feasible, although not all suppression strategies appear to be equally suitable for efficient PPV infection (Maliogka et al., 2012). Although P1b and HCPro can efficiently provide the RNA silencing suppression required for PPV infection, these two proteins can also have additional specific activities, apart from the role of HCPro in vector transmission. Thus, a recent report shows that HCPro contributes to enhance the yield of virions maintaining their correct architecture, and this HCPro function, whose biological significance is still obscure, could not be achieved by P1b (Valli et al., 2014).

To explore convergent or divergent novel functions of P1b and HCPro, a second group of screenings was performed using viral vectors expressing PPV-sGFP, a recombinant PPV expressing green fluorescent protein (GFP) and PPV-P1b-sGFP, in which HCPro has been replaced by CVYV P1b. On one hand, to determine what proteins would be more susceptible to be deregulated by PPV-sGFP or PPV-P1b-

sGFP infections, proteomes of infected *A. thaliana* plants were relatively quantified and compared using iTRAQ labelling mass spectroscopy, thus hoping that any significantly deregulated proteins detected would be biologically relevant in the host-virus interplay. On the other hand, to explore the possibility of finding new transcription factors involved in response to virus induced biotic stress, a series of screenings were performed using recently available *A. thaliana* ß-estradiol-inducible over expression transgenic plant lines. These plant lines have been developed by the TRANSPLANTA consortium and available under the NASC seed collection. This work has been involved in the productions and validation of part of the transgenic lines (Coego et al., 2014).

To complement the biochemical analysis performed, a visual screening for modifications in cellular distribution and morphology using gold inmunolabelling with antisera against P1b was performed. Using this physical method to localise P1b protein within the cell would ideally help to determine what cellular pools of proteins are potentially interesting in searching for P1b interactors and any cellular changes affecting morphology in response to PPV and the HCPro depleted PPV virus PPV-P1b-sGFP.

P1b localisation using Gold Immunolabelling electron microscopy

Previous reports analysing P1b self-interaction using heterologous BiFC expression in *N. benthamiana* leaves have reported P1b homo-complex interaction possibly localising in the cytosol (Valli et al., 2008). This together with the observed binding of mature small RNA population (Valli et al., 2011) and the easy extraction and solubilisation in native detergent-free buffers seems to suggest that P1b is mainly a cytosolic viral protein. However, tag-based heterologous over-expression systems can be biased as they often result in altered protein activities and mislocalisations, both because of sterical hindrances from the tags used or because of the non-physiological over accumulation of the expressed proteins. Further more, biological activities of P1b could be dependant on other viral factors that are not present in the healthy host being determinant in the biological

processes in which P1b could be involved. It is evident that to clearly understand the biological nature of P1b considering all possible biological vicissitudes, P1b localisation is to be studied under a physiological CVYV infection in its natural host.

To study the localisation of P1b under a physiological infection, an inmunogold labelling approach was chosen mainly because a good anti-serum against P1b was available, and secondly because the system involves minimal physiological disturbance, providing a visual snapshot of the cellular interior and discrete data to which statistical analysis can be implemented.

P1b localises in the cytosol of CVYV-infected cucumber.

Although the P1b anti-serum available has been previously used in biochemical analysis to detect P1b accumulation showing clear specificity against different P1b fusion proteins (Valli et al., 2008), it has not been tested for other antibody applications like immunocytochemical plant tissue analysis. To assess the specificity of P1b antiserum in ultra-thin leaf tissue sections and to determine the antiserum dilution with best Signal to Noise ratio (SN), a series of incubations with serial antibodies dilutions were performed and SN ratios compared. Of the 5 different antiserum dilutions evaluated on samples of CVYV-infected *C. sativus* (data not shown), the 1:500 dilution showed the best SN ratio and was chosen as the working antiserum dilution during the whole inmunogold labelling analysis.

Once the working dilution of the P1b antiserum was set, the specificity of the anti-serum was evaluated using non-infected healthy *C. sativus* and *N. benthamiana* plants. Antibodies, and proteins in general, have a tendency to adhere non-specifically to surfaces, mainly due to hydrophobic and/or electrostatic interactions (Griffiths, 1993). To determine whether reagents used for immuno gold labeling could be adhering non-specifically to particular subcellular compartments, the intracellular lumen was divided into 8 subcellular volume categories (Mayhew, 2011). Gold particles frequencies corresponding to each category were analysed by comparing them to random point lattices frequencies

with which a Relative Labelling Index (RLI) was calculated (Mayhew et al., 2002). Chi-χ2 hypothesis test (Sokal & Rohlf, 2012) analysis was used to determine whether differences in observed gold frequencies are due to random or non-random events.

Test incubations of mock-inoculated *C. sativus* leaf sections with P1b antiserum and CVYV infected *C. sativus* leaf sections with rabbit pre-inmune serum were performed and analysed (data not shown). For both cases results showed sufficient evidence to consider chloroplast compartment as being preferentially but non-specifically labelled. As a result, any preferential labelling of this compartment is to be disregarded. To avoid confusions, the chloroplast compartment will be considered as "residuum" through the entire analysis.

Having established which subcellular compartments show low non-specific adhesion of the immuno gold reagents, initial visual inspection of the gold-labelled electron micrographs revealed P1b antiserum to decorate predominantly the cytosol (Fig. 7 & Fig. 8). Although characteristic potyviral pinwheels structures (Lecoq et al., 2000) and crystalline inclusions (Riedel et al., 1998), can be observed in the cytosol, no gold particles could be seen specifically decorating these structures. Instead, amorphous inclusions generally of globular shape, evoking cytosolic amorphous inclusions formed by HCPro of different potyviruses, including PPV (Riedel et al., 1998), could occasionally be seen, heavily decorated with gold particles (Fig. 7. d & Fig. 8. d). These amourphous globular structures do not seem to have a membrane envelope and are slightly electro dense suggesting they could be some kind of macromolecular complex. Gold particles could also be seen in other oraganells, including nuclei. To determine whether the cytosol and other organells were being preferentially labelled, the number of gold particles detected in the 8 volume categories in which the cell lumen was divided was compared to expected distributions calculated using a random lattice of test points. Table 1 summarizes the results of the analysis. Using the accumulated data of two independant biological replicates of CVYV-infected leaves, only the cytosol presented a RLI greater than 1 suggesting that this compartment is being preferentially labelled. Furthermore, partial χ^2 value calculated for this

compartment supports that labelling is not due to random events. P1b preferentially labels cytosol with probability confidence level of $P < 0.001$.

Table 29. Observed and expected distributions of gold particles in organelle compartments of ultrathin sections of CVYV-infected *C. sativus* leaves immunolabelled with anti-P1b serum and calculation of Relative Labelling Index and chi-squared values. Asterisks (*) identify compartments that are preferentially labelled. Gold counts and lattice test points not satisfying compartment groups were grouped as Residuum.

Compartments	Observed Golds, Go	Observed Points, P	Expected Golds, Ge	RLI, Go/Ge	Partial χ^2 values
Nucleoplasm	296	908	886.29	0.33	393.14
Nucleolus	10	38	37.09	0.27	19.79
Cytosol	2801	1529	1492.43	1.88*	1147.35*
Mitochondria	78	119	116.15	0.67	12.53
Peroxisome	25	32	31.23	0.80	1.24
Vacuole	64	265	258.66	0.25	146.50
Residuum	1134	1625	1586.14	0.71	128.88
Totals	4408	4516	4408.00	1.00	1849.44

These results support that P1b is mainly localised in the cytosol compartment of spongy mesophyll cells of CVYV-infected cucumber plants. However, the cytosolic localisation of P1b in spongy mesophyll cells might not be representative of what is happening in other different cell types, and could differ at different infection stages. This may be especially relevant for multi functional viral proteins, requiring different subcellular localisations to fulfil different biological activities. Thus, it could be advisable to investigate further if P1b localisation suffers changes during the infection dynamics.

P1b localisation is significantly altered when expressed in *N. benthamiana*.

As mentioned above, it has been reported previously that HCPro can be functionally replaced by other RSS proteins, including CVYV P1b during a PPV infection (Carbonell et al., 2012). This raises the issue if the sole function of HCPro and P1b during the cellular cycle of the virus is exclusively related to silencing suppression. Thus, it is interesting to compare the behaviour of P1b during a natural CVYV infection and during an heterologous PPV P1b expression.

Ultrathin sections of *N. benthamiana* leaves infected with PPV-P1b-sGFP, a recombinant PPV expressing P1b in substitution for HCPro, were immunolabelled with anti-P1b serum (Fig. 9 & Fig. 10). Although P1b could only be seen to decorate

the cytosol compartment of CVYV infected *C. sativus* mesophyll cells, in mesophyll cells of PPV-P1b-sGFP-infected *N. benthamiana* the anti-P1b serum preferentially and specifically labelled cytosol, nucleoplasm and nucleoli in two independent biological replicates (Table 2). RLI was considerably higher than 1 for cytosol, nucleoplasm and nucleolus compartments, being highest for the nucleolus, suggesting that P1b strongly accumulates in the nucleolus during PPV-P1b-sGFP infection. Partial χ^2 values provide statistical support in rejecting the null hypothesis (compartments are labelled randomly) and accepting that the labelling is due to non-random events at a probability confidence level of $P < 0.001$. These results are surprising, as not only P1b exhibits a localisation pattern quite different from that of CVYV infected *C. sativus* samples, but also because P1b is heavily decorating an intra nuclear structure, which was not anticipated from previously published functional information.

Table 30. Observed and expected distributions of gold particles in organelle compartments of ultrathin section of PPV-P1b-sGFP-infected *N. benthamiana* leaves immunolabelled with anti-PPV serum and calculation of Relative Labelling Index and Chi-squared values. Asterisks (*) identify compartments that are preferentially and specifically labelled. Gold counts and lattice test points not satisfying compartment groups were grouped as Residuum.

Compartments	Observed Golds, Go	Observed Points, P	Expected Golds, Ge	RLI, Go/Ge	Partial χ^2 values
Nucleoplasm	6984	888	3402.19	2.05*	3770.90*
Nucleolus	411	48	183.90	2.23*	280.44*
Cytosol	11670	1657	6348.46	1.84*	4460.73*
Mitochondria	455	224	858.21	0.53	189.44
Peroxisome	15	14	53.64	0.28	27.83
Vacuole	260	900	3448.17	0.08	2947.77
Residuum	1235	1758	6735.42	0.18	4491.87
Totals	21030	5489	21030	1.00	16168.99

P1b was seen to accumulate in the cytosol of infected *N. benthamiana* mesophyll cells, similarly to what was seen in CVYV infected *C. sativus*. As in CVYV infected *C. sativus,* characteristic cytosolic pinwheel and amorphous crystalline structures, similar to those previously reported (Riedel et al., 1998), could be observed in PPV-P1b-GFP-infected *N. benthamiana* cells, which were not predominantly decorated by the anti-P1b serum. No heavily decorated amorphous globular structures similar to those detected in CVYV infected *C. sativus* cells could be observed in the cytosol of PPV-P1b-sGFP-infected *N. benthamiana* cells. NIa and NIb form crystalline inclusions (nuclear inclusions, NI) in the nucleus of cells

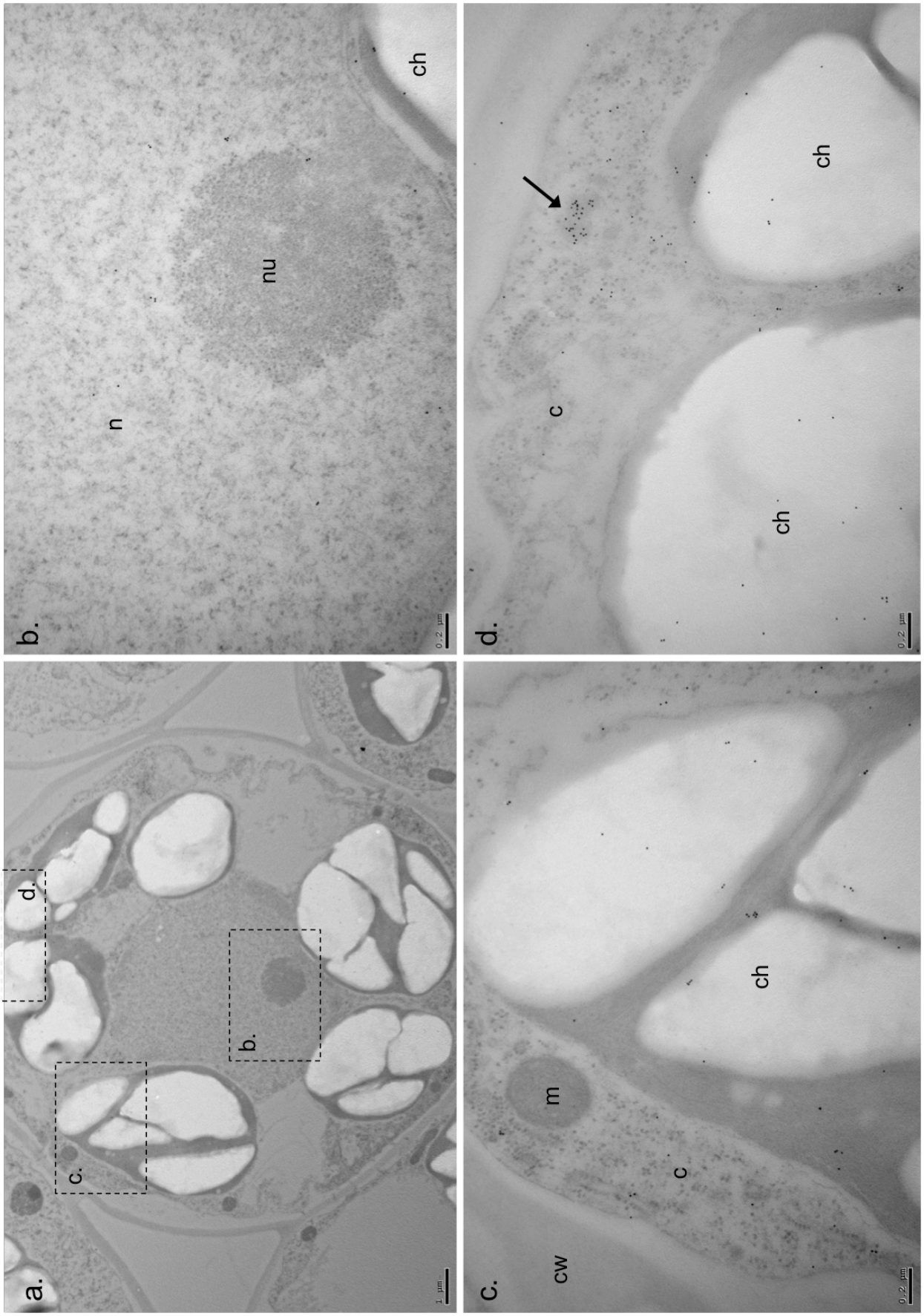

Figure 7. Electron micrograph of a representative spongy mesophyll cell from a CVYV-infected *C. sativus.* An ultrathin section was immunolabelled using P1b-specific anti-serum. Gold particles are seen as small electrodense dots. (a) General image of the cell. (c-d) Amplified details of the sectors boxed in panel (a). n, nucleus; nu, nucleolus; c, cytosol; ch, chloroplast; m, mitochondria; v, vacuole; cw, cell wall; Arrow points to a globular amorphous structure heavily decorated with gold particles. Scale bars represent 1 µm (a) and 0,2 µm (b-d).

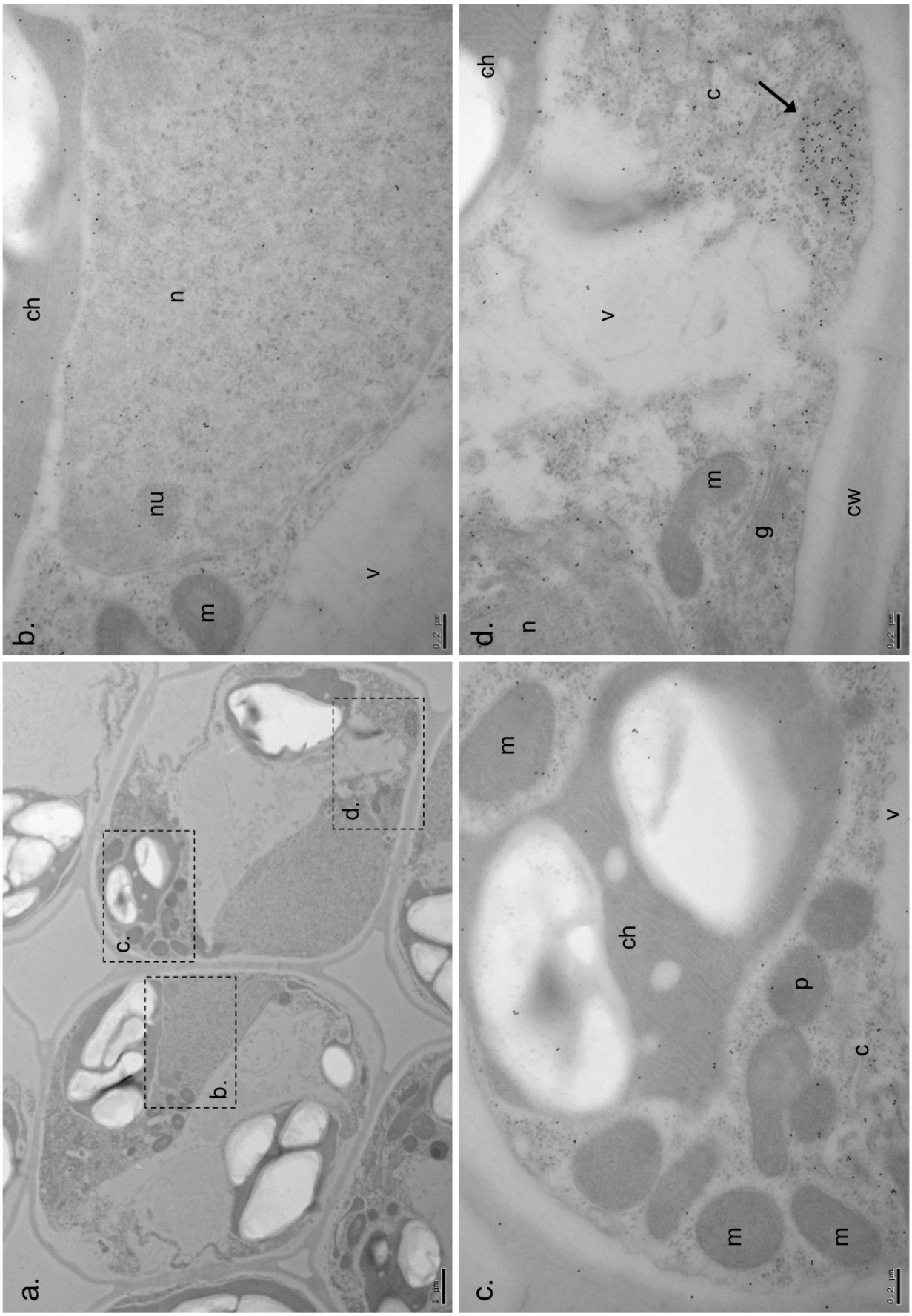

Figure 8. Electron micrograph of a representative spongy mesophyll cell from a *C. sativus* plant that was infected with a CVYV inoculum different from that used to infect the plant of Fig. 1. An ultrathin section was immunolabelled with P1b -specific anti-serum. Gold particles are seen as small electrodense dots. (a) General image of the cell. (c-d) Amplified details of the sector boxed in panel (a). n, nucleus; nu, nucleolus; c, cytosol; ch, chloroplast; m. mitochondria; g, Golgi apparatus; v, vacuole; cw, cell wall; pw, CI pinwheel structure. Arrow points to a globular amorphous structure heavily decorated with gold particles. Scale bars represent 1 µm (a) and 0,2 µm (b-d).

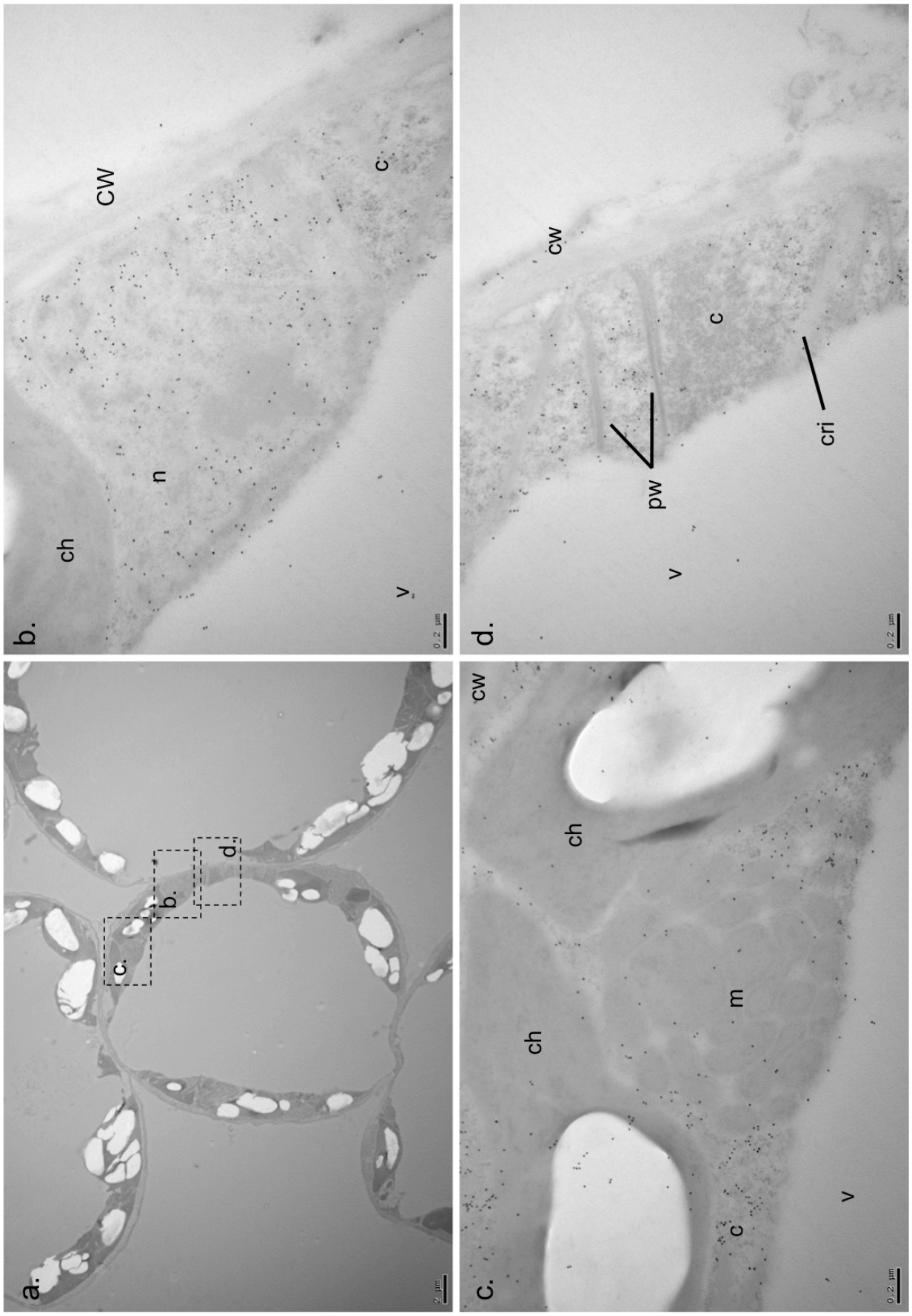

Figure 9. Electron micrograph of a representative spongy mesophyll cell from a *N. benthamiana* plant infect by agroinoculation with PPV-P1b-sGFP. An ultrathin section was immunolabelled with P1b-specific antiserum. Gold particles are seen as small electrodense dots. a., General image of the cell. (c.-d) Amplified details of the sectors boxed in panel (a). n, nucleus; nu, nucleolus; c, cytosol; ch, chloroplast; m. mitochondria; v, vacuole; cw, cell wall; pw, CI pinwheel structure; cri, cytosolic amorphous crystalline inclusion. Scale bars represent 2 µm (a) and 0,2 µm (b-d).

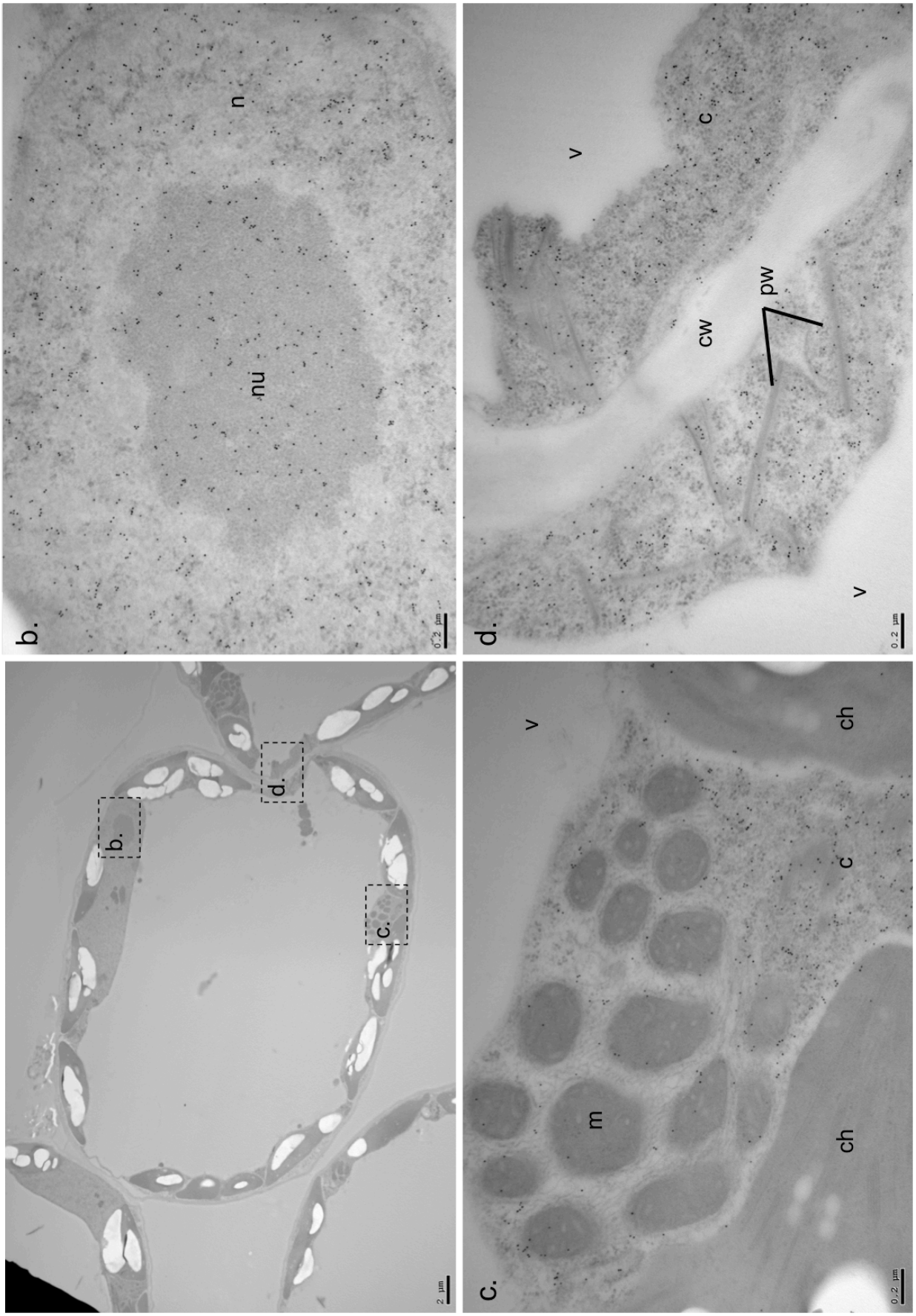

Figure 10. Electron micrograph of a representative spongy mesophyll cell from a *N. benthamiana* plant infect by agroinoculation with PPV-P1b-sGFP using a bacteria cultural different from that used to infect the plant of Fig. 3. An ultrathin section was immunolabelled with P1b-specific antiserum. Gold particles are seen as small electrodense dots. (a) General image of the cell. (c.-d) Amplified details of the sectors boxed in panel (a). n, nucleus; nu, nucleolus; c, cytosol; ch, chloroplast; m. mitochondria; v, vacuole; cw, cell wall; pw, CI pinwheel structure. Scale bars represent 2 µm (a) and 0,2 µm (b-d).

infected with different potyvirusese, including PPV (Martin & Gélie, 1997; Riedel et al., 1998). NI-like structures could be observed in the majority of the nucleus of PPV-P1b-sGFP infected *N. benthamiana* cells, which were not observed in CVYV infected *C. sativus*. The fact that no predominant gold labelling could be associated with these structures suggests that P1b does not associate with NIa and NIb in the nuclei.

Taken together these results, P1b appears to be a cytosolic viral protein that does not interact with CI pinwheel structures, preferentially accumulating in cytosolic amorphous inclusions, similar to those described for HCPro from different potyviruses, being occasionally of globular and highly electro dense nature. The fact that PPV-P1b-sGFP infects *N. benthamiana* efficiently, suggests that the delocalisation of P1b into the nucleus as a result of expression in an heterologous PPV expression system does not affect its RSS activity or self-protease processing from the viral polyprotein.

Interactors of CVYV P1b

Yeast mating using *A. thaliana* cDNA library

An *A. thaliana* cDNA library provided by Dr. Mabel Puga (CNB-CSIC) to retrieve coding sequences of putative P1b interactors was used in this screening. The cDNA library consisted of $2.6x10^6$ clones. The coding DNA sequences (CDS) of P1b, amplified by RT-PCR from CVYV infected tissue was cloned into vectors pGBKT7 and pADKT7, tagging the N-terminus of P1b with the Binding Domain (BD) and Activating Domain (AD), respectively, of the GAL4 transcription factor (Fields & Song, 1989; Chien et al., 1991).

To determine whether P1b could self-activate the reporter genes of the yeast two hybrid system, co-transformation of each plasmid alone expressing either P1b fused to the DNA binding domain (BD-P1b) or fused to the activating domain (AD-P1b) with its complementary empty plasmid was evaluated. None of the constructs activated the reporter genes in the transformed cells (Fig. 11). RSS activity of P1b

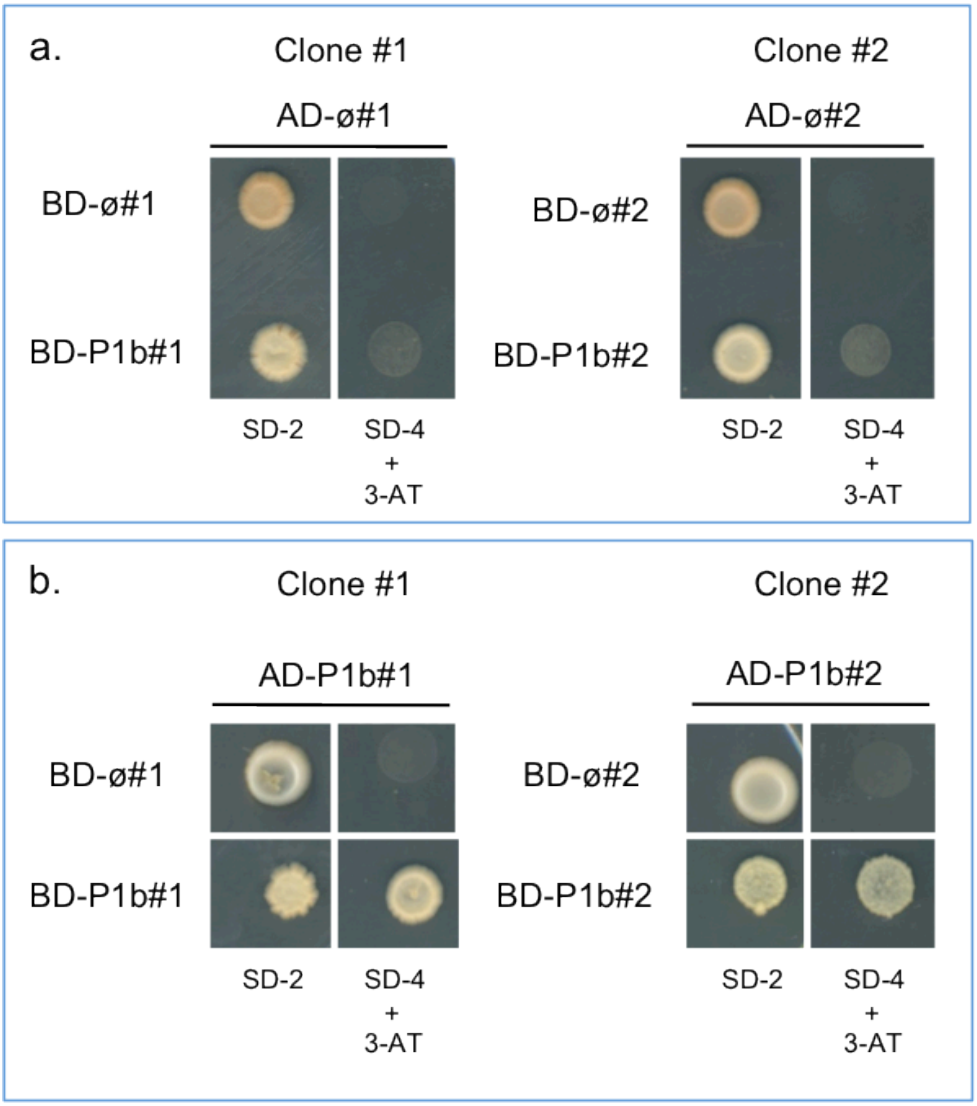

Figure 11. Validation of the GAL4 Y-2H reporter system using P1b. P1b fused to the GAL4 activator domain (AD) or binding domain (BD) was tested for autoactivation of the reporter system by co-transformation of yeast cells with their respective empty vector plasmids. (a) No yeast growth can be seen on restrictive selection media supplemented with 3-AT (SD-4 + 3-AT) indicating BD-P1b indicating P1b does not autoactivate the reporter system. (b) Yeast growth can be observed on SD-4 + 3-AT media when AD-P1b is co-transformed with BD-P1b but not with BD-ø indicating that AD-P1b does not autoactivate the reporter system and P1b self-interaction is functional in yeast cells. Pictures taken after 12 days incubation at 30°C.

has been shown to be dependent on self-interaction of the protein. To evaluate whether tagged P1b maintain the ability to self-interact in a yeast heterologous expression system, BD-P1b and AD-P1b were co-transformed into AH109 yeast cells and cultured in SD-4 restrictive medium. Yeast growth in SD-4 restrictive medium supplemented with up to 10mM 3-AT revealed that P1b self-interacts strongly, and thus suggests that it is most probably functional in its RSS activity as it would be in plant cells.

Table 31. *A. thaliana* sequences isolated from yeast colonies after yeast two hybrid mating. Length of the peptides expressed and the full proteins together with the corresponding TAIR or genbank accession code and biological process proposed for each putative P1b factor.

Accession	Peptides	Peptide(s) length (aa)	Full Protein length (aa)	Name	Biological function
AT1G56650	1	4-248	248	MYB75	Anthocyanin biosynthesis
AT4G08870	1	228-334	344	ARGINASE	Arginine metabolism
AT3G05935	1	12-95	95	Unknown protein	Biological process unknown
AT3G52920	1	1-180	180	Unknown protein	
AT3G59680	1	85-229	230	Unknown protein	
AT5G09620	1	1-83 (FS+1)	531	PB1 family	
AT3G22210	1	1-69 (FS+1)	69	Unknown protein	
AT5G61820	1	1-475	475	Unknown protein	
AT1G56240	1	124-284	284	PP2-B13	Carbohydrate binding
AT4G13930	1	1-471 (FS+1)	471	SHM4	Circadian rhythm
AT1G02920	1	1-209 (FS+1)	209	GSTF7	Defence response
AT1G22070	1	300-384	384	TGA3	
AT3G56400	1	1-294	294	WRKY70	
AT5G15090	1	1-150	274	HSR2	
AT1G05900	1	89-237	386	NTH2	DNA catabolic process
AT1G73330	1	6-209	209	DR4	Drought response
AT5G02380	1	1-77 (FS+1)	77	MT2B	Glucose catabolic process
AT4G31780	1	133-355	533	MGD1	Glycolipid biosynthesis
AT2G36880	1	1-190 (FS+1)	390	METK3	Lignin biosynthesis
AT1G72070	1	1-126	126	DNAJ	Molecular Chaperone
AT2G22360	1	280-442	442	DNAJ	
AT5G48030	1	148-267	456	GFA 2	
AT2G01350	1	203-348	348	QPT	NAD biosynthesis
AT1G62300	1	49-271	553	WRKY6	Phosphate starvation
AT4G31240	1	272-392	392	NRX2	
AT4G33520	1	11-949	949	HMAC6	Photosynthesis
AT5G38410	1	1-181 (FS+1)	181	RBCS3B	
AT5G54270	1	1-218 (FS+1)	265	LHCB3	
AT1G35340	1	13-256	311	LON	Proteolysis
AT2G36990	2	123-340, 142-392	547	SIGF6	Response to blue light
AT5G20230	1	1-196 (FS+1)	196	BCB	Response to oxidative stress
AT5G62190	1	405-614	671	PRH75	RNA methylation
AT1G69930	1	1-234 (FS+1)	234	GSTU11	Signalling pathway
AT2G30020	1	1-150 (FS+1)	396	PHOSPHATASE 2C	
AT1G20050	1	1-223 (FS+1)	223	HYD1	Sterol biosynthesis, RNA silencing
AT4G29840	1	1-30 (FS+1)	526	MTO2	Threonine biosynthesis
AT1G66390	1	10-211	249	MYB90	Transcription regulation
AT1G75710	1	11-462	462	C2H2-like Zn finger prot.	
AAF99784.1	2	12-260, 12-200	419	C2H2-like Zn finger prot.	
AT3G02550	2	5-263, 58-263	263	LBD41	
AT3G25710	1	1-119 (FS+1)	344	bHLH-32	
AT4G01720	1	1-216 (FS+1)	489	WRKY47	
AT1G27400	1	4-176	176	RPL17	Translation
AT1G31817	1	63-280	314	NFD3	
AT1G67430	1	6-175	175	RPL17	
AT2G19740	1	1-119	119	RPL31A	
AT2G36170	2	5-118, 18-118	128	UBQ2-RPL40A	
AT5G14660	1	6-192	273	PDF1B	
AT2G43130	1	7-182 (FS+1)	214	ARA4	Vesicle transport
AT3G46830	1	1-217 (FS+1)	217	RAB11	
AT4G17730	1	1-165 (FS+1)	255	SYN23	

FS+1, insertion causing a +1 Frame shift in the CDS of the peptide.

Once determined that P1b could be used in the yeast two hybrid system, mating of cells expressing BD-P1b with the *A. thaliana* library was performed. Only when a AD-fused factor from the library interact with the BD-P1b bait, the cells recover prototrophy and grow on SD-4 medium supplemented with 3-AT. Plasmids from clones selected in the restrictive medium were extracted and sequenced revealing a pool of 55 sequences from a total of 51 *A. thaliana* factors putatively interacting with P1b (Table. 3).

Once identified, library plasmids retrieved from the mating were co-transformed with plasmids expressing GAL4 BD alone, or fused to wild type P1b or to P1b with a C103A mutation in the zinc-binding region (P1bmut6) that has been reported to be required for P1b self interaction and RSS activity (Valli et al., 2008), to verify whether: i. the plant factor does not activate the reporter genes by itself, ii. the factor reproducibly interacts with the BD-P1b bait used in the mating and iii. the factor selectively interact with a functional P1b able to self-interact.

Two series of co-transformation experiments using in both experiments were performed with two independent clones from each candidate selected in the first screen. The results classified the potential *A. thaliana* P1b interactors in three different groups: I. factors activating the reporter genes by themselves when co-transformed with the control plasmid BD-ø, II. factors interacting with both BD-P1b and BD-P1bmut6, and III. factors interacting exclusively with BD-P1b (Fig. 12 & Fig. 13).

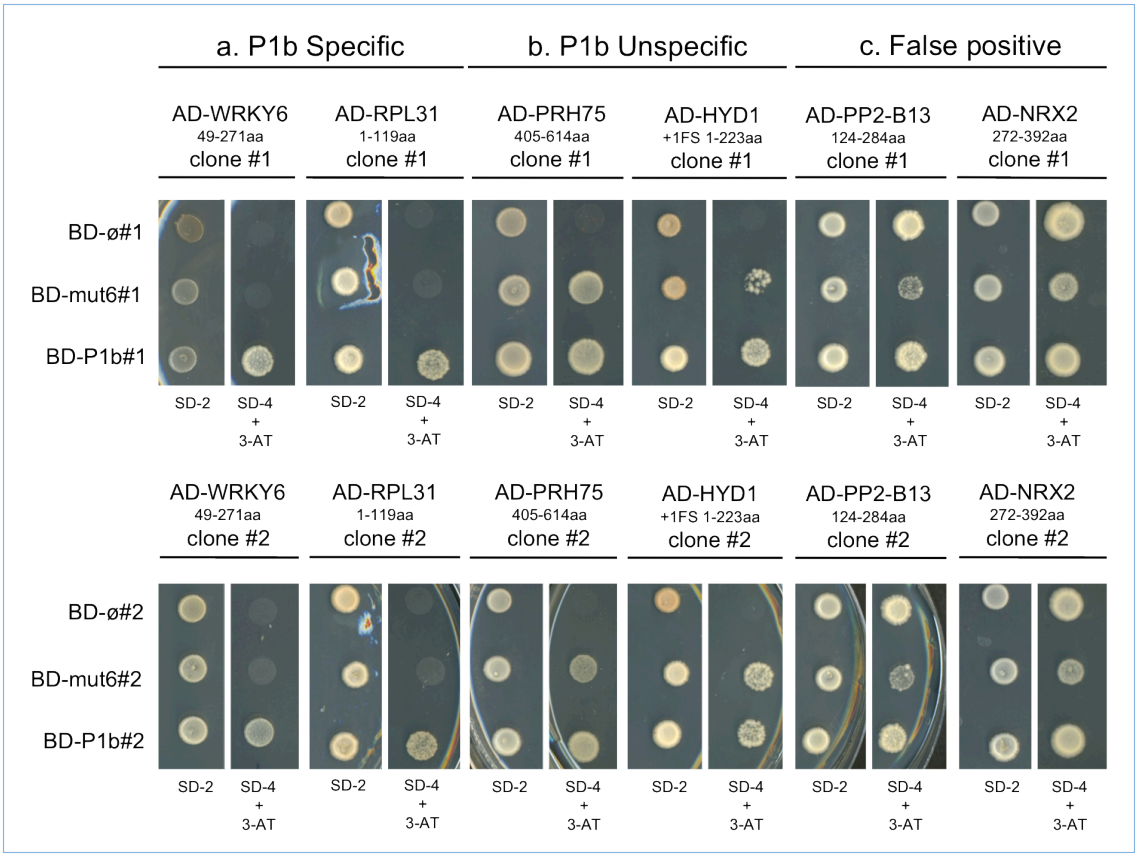

Figure 12. Validating specific P1b interactions using the GAL4 Y-2H reported system. Co-transformations of library plasmids with plasmids expressing GAL4 BD fused to *wild type* P1b (BD-P1b), conformational P1b mutant (C103A) affected in the zinc-finger domain (BD-P1bmut6) and the control BD-ø classified potential interactions of *A. thaliana* candidates in three distinct categories: (a) interactions depending on appropriate P1b conformation (P1b Specific); (b) interactions that require P1b, regardless of P1b structure (P1b Unspecific); (c) activation of the system without requirement of P1b (False positives). Colonies growing on either SD-2 or SD-4 restrictive media supplemented with 10mM 3-AT. Pictures taken after 12 days incubation at 30°C.

A group of plasmids encoding AD-fused protein fragments corresponding to 33 *A. thaliana* proteins were confirmed to activate the reporter genes when co-transformed with plasmids expressing GAL4 BD domain alone (BD-ø) or fused to P1b. For twenty of these candidates, the activation depended on P1b since they did not activate reporter genes when co-transformed with the plasmid expressing the BD domain alone. Reporter activation that specifically depended on a P1b allele with functional protein structure conformation (positive activation for P1b but not for P1b-mut6) was observed for a subset of 5 candidates (WRKY47, WRKY6, PB1, NFD3, RPL31A). Factors interacting with P1b are shown in Fig. 13.

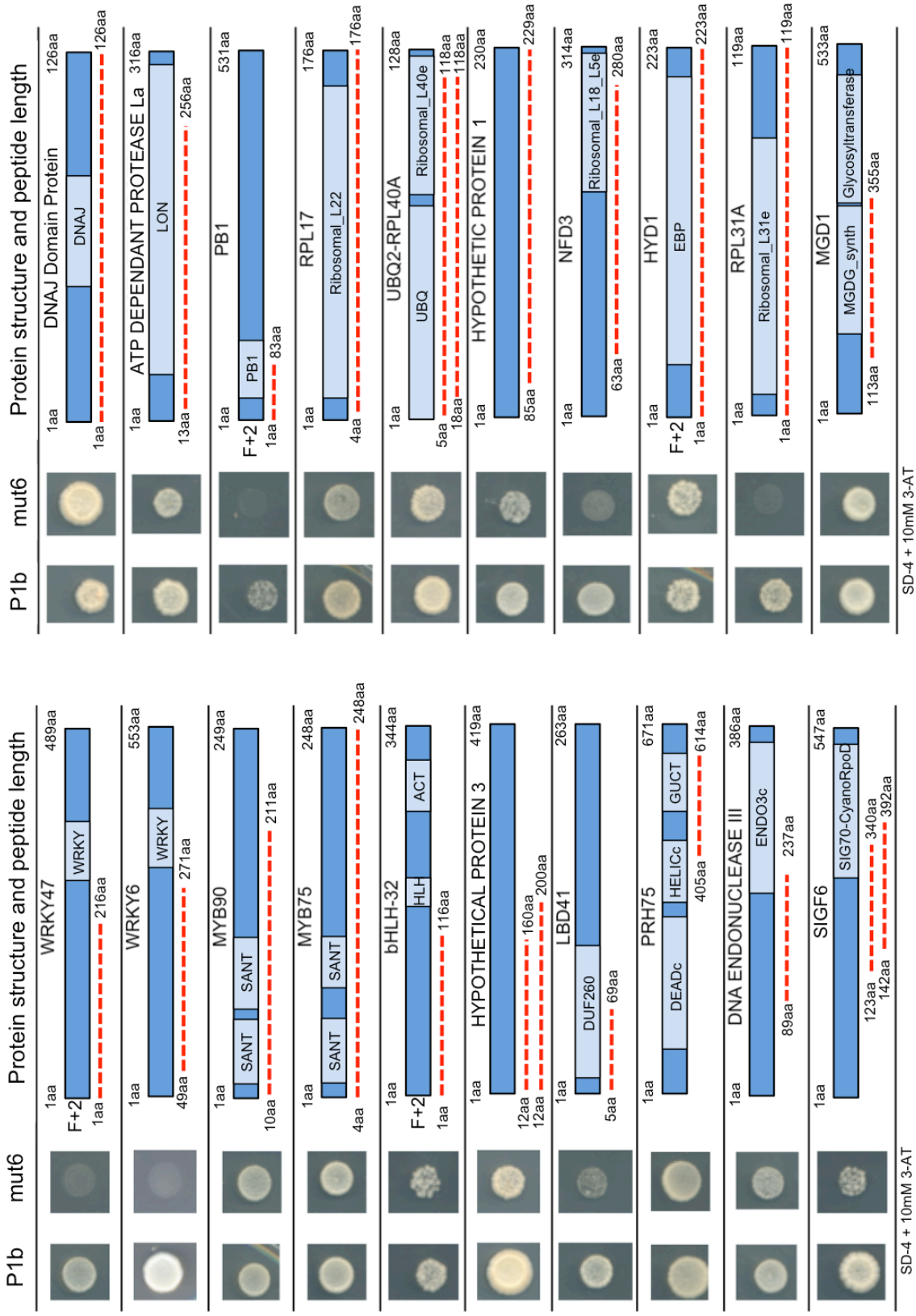

Figure 13. Factors confirmed to interact when co-transformed with P1b. Peptides encoded by the library plasmids are represented as red dashed lines in the protein map including annotated domains. Protein length, and number of amino acids for each peptide identified is indicated. P1b, BD-P1b; mut6, BD-P1b Zinc-finger mutant 6 (C103).

The Y-2H cDNA library used in the P1b screening had been used widely in our department for other screenings using different unrelated bait proteins. A comparison of the factors interacting with P1b with the sequences isolated in other screenings was made in order to identify sequences that are commonly promiscuous and can interact with bait proteins unspecifically (Fig. 14). Only AT1G32640, a MYC related transcription factor, was identified in two different mating screens, and none of the factors that interacted with P1b were isolated in screens using other unrelated baits, suggesting that the interactions detected might be specific to P1b.

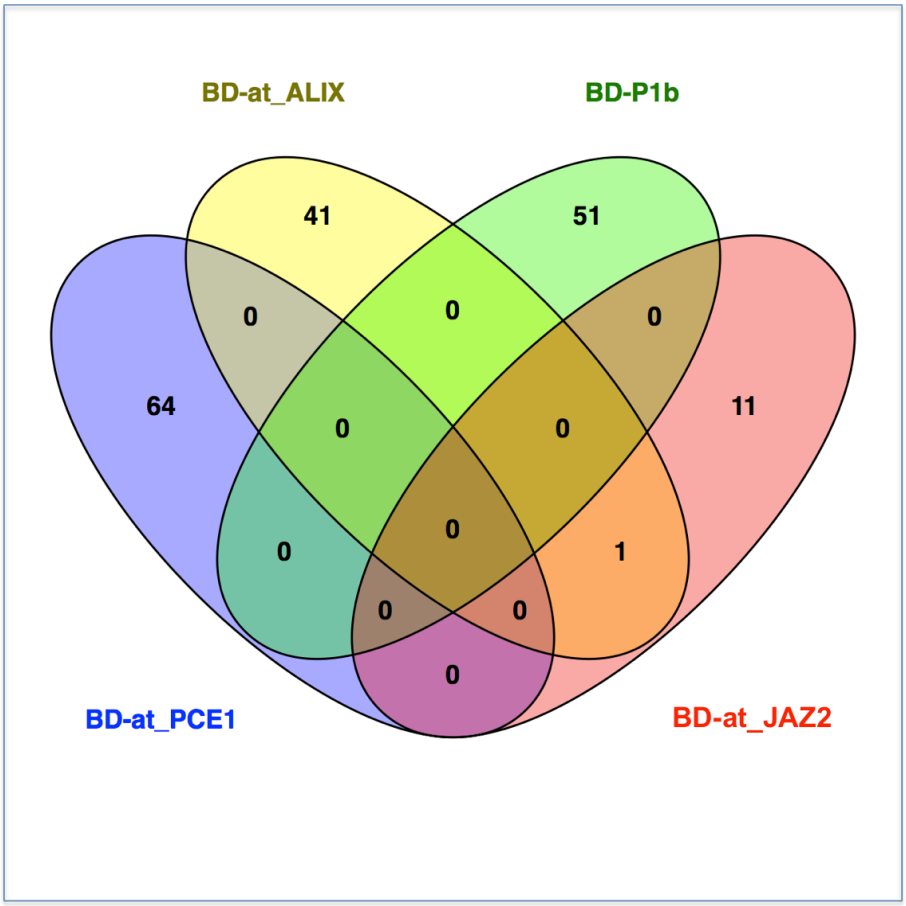

Figure 14. Venn diagram comparing the different protein sequences identified in different yeast two hybrid mating screens using the same cDNA library. Only one common element was identified in screens performed with ALIX and JAZ2 as baits. No common elements were observed with sequences identified using P1b as bait.

A gene ontology analysis for factors interacting with P1b, showed a variety of molecular functions involved in different biological processes, being translation, anthocyanine biosynthesis, and transcription regulation the predominant GO

terms associated with the interacting host factors obtained in the yeast two hybrid screen.

TAP Purification

Numerous interacting host partners of viral proteins have been identified by means of different protein-complex purifications systems. Among them, the Tandem Affinity Purifications (TAP) system has proven to be to be especially useful. The TAP system coupled to mass spectroscopy (MS) is an advanced system to characterize protein complexes using a bait protein fussed to two different affinity tags in tandem linked by a TEV protease target site.

Since the initial development of the TAP purification system, TAP purifications have evolved rapidly and new modifications and improvements have been introduced. Initially the TAP tag strategy was first tested in yeast (Rigaut et al., 1999). In the original TAP protocol, a bait protein was fused to a double tag consisting of two IgG-binding units of protein A from *Staphylococcus aureus* and a calmodulin-binding peptide separated by the TEV protease cleavage site site. The protein complexes partners trapped by the active bait protein were then isolated under native conditions and sequentially purified using chromatography affinity first against IgG and then, after protease treatment to remove the IgG-binding domain, to calmodulin to elute a high quality matrix of interacting proteins. The eluted proteins were analyzed by mass spectroscopy either directly or after separation by gel electrophoresis. The success of this strategy encouraged other researchers to adopt the TAP system in other model organisms including bacteria (Gully et al., 2003), insect cells (Forler et al., 2002), mamalian cells (Knuesel, 2003) and plants (Rohila et al., 2004). In order to express the TAP tag bait proteins in the different model systems, vectors were improved by optimizing codon usage and including intervening sequences for enhanced stability and expression (Rohila et al., 2004). Expression of bait proteins has been reported to be possible both by transient expression in plant leaves or by stable transformation in transgenic plant lines or cell cultures (Rohila et al., 2004; Rubio et al., 2005; Van Leene et al., 2007). It is evident that each expression system used has its flaws and advantages, whereas cell culture and transient expression in plant leaves can yield higher

amount of bait protein to purify, they may lack the correct ontogenic environment needed for its correct molecular functions if expressed only in specific tissues or at specific development stage in physiological conditions. In these cases, a stable transgenic expression, ideally with it endogenous promoter would be preferred.

To adapt the purification conditions to the requirements of the diverse nature of protein complexes, different tag strategies have been developed in combination with a number of protease cleavage sites (Fig. 15).

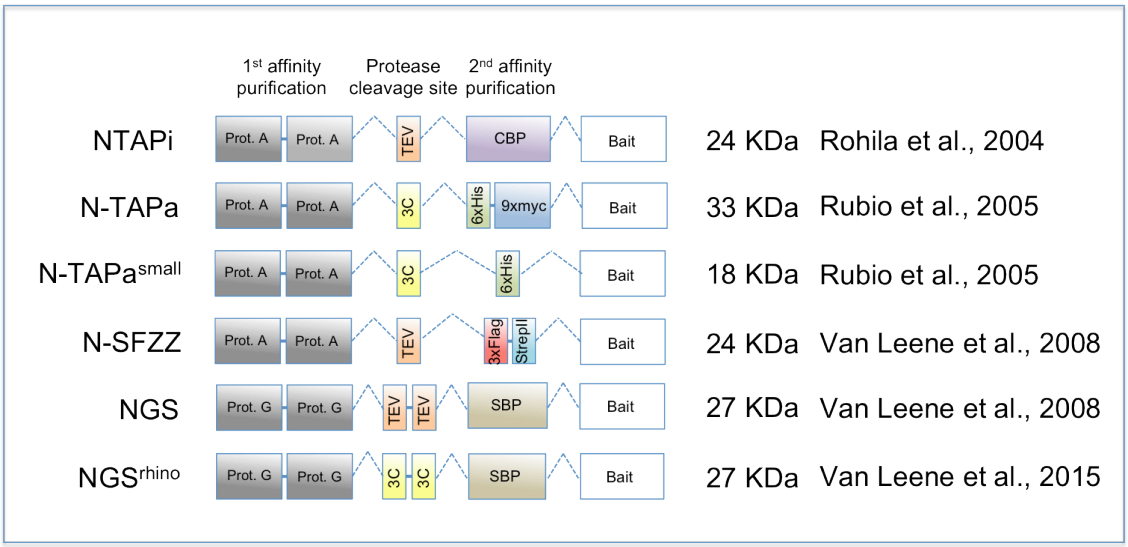

Figure 15. Different TAP strategies reported for tagging the bait protein at the N-terminus and the publication were it is described. Molecular size of the TAP tag is shown in Kilo Daltons (kDA). Prot. A, *Staphylococcus aureus* Protein A IgG-binding domains; CBP, Calmodulin-binding peptide; SBP, Streptavidin-binding peptide; TEV, TEV protease cleavage site; 3C, HRV 3C protease cleavage site; 6xHis, 6 tandem Histidine tag; 3xFlag, 3 tandem Flag tag; 9xmyc, 9 tandem myc tag; StrepII, Strepatavidin II tag.

It has been reported previously that P1b maintains its RSS activity when tagged in its N-terminus but not in its C-terminus (Valli et al., 2008). From possible options reported in the bibliography, the NTAPi strategy was chosen to tag the P1b bait as it was reported to surpass the rest in yielding the highest number of protein complexes by tandem purification (Van Leene et al., 2008), and thus expecting to purify the highest number of protein complexes possible in which an active P1b participates.

Expression of NTAP-tagged P1b in *A. thaliana* transgenic lines

Transgenic lines expressing P1b fused to the NTAPi tag, consisting of two copies of protein A IgG-binding domain and a calmodulin-binding peptide separated by a TEV cleavage site (NTAPi-P1b), were obtained by floral dip transformation of *A. thaliana* (Fig. 16). NTAPi-P1b had been shown previously to maintain its RNA silencing suppression activity in a *N. benthamiana* agroinfiltration assay (Valli et al., 2008). In addition transgenic lines expressing NTAPi-P1b showed severe developmental abnormalities of NTAPi-P1b similar to those previously described for plants expressing the potyvirus P1-HCPro, which have been attributed to its RNA silencing suppression activity (Kasschau et al., 2003; Dunoyer et al., 2004; Mlotshwa, 2005). NTAPi-P1b expressing lines grew much smaller than wild type plants, with long petioles, obtuse or elliptic leave folioles with serrate curled margins as opposed to the orbicular-ovate non-serrated leave folioles of the Col-0 wild type plants (Fig. 16. b & c).

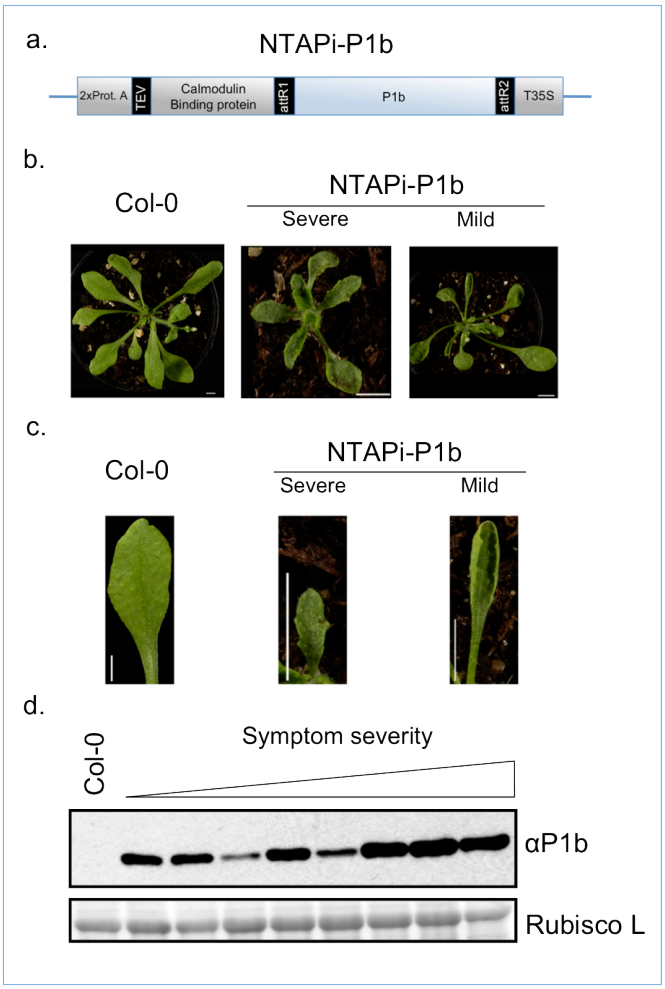

Figure 16. Phenotypic and morphological analysis of NTAPi-P1b transgenic lines. (a) NTAPi-P1b construct generated for stable expression in transgenic *A. thaliana* plants. P1b CDS was inserted upstream of the termination region of the CaMV 35S mRNA (T35S), tagged with 2 protein A domains in tandem and a Calmodulin binding protein domain separated by a TEV protease cleavage site. Expression is driven by a CaMV 35S promoter. (b) General view of the transgenic plants. NTAPi-P1b plants with sever symptoms grow smaller and present obtuse or elliptic folioles with serrate margins compared with Col-0 non-transformed plants. (c) Close up view of the leave folioles considerably smaller in size than those of Col-0 plants, with larger petioles and serrate margins. Scale bars represent 5mm. Adapted from (Valli et al., 2009) (d) Western blot analysis of the P1b accumulation in individual plants aligned phenotypically attending to possible symptom severity. P1b accumulation correlates on average with symptom severity. Col-0, negative control. Immunoblot was incubated with antiserum raised against P1b. Ponceau Red was used as loading control.

Differences in NTAPi-P1b protein accumulation positively correlated with symptom severity. Plants transformed with a mutated form of P1b defective in protease activity also caused developmental abnormalities (data not shown), suggesting that they are not related to ectopic proteolytic processing, but a consequence of the deregulation in the expression of gene targets of small RNA populations sequestered by P1b, similar to what has been previously reported for other RNA silencing suppressors (Kasschau et al., 2003; Dunoyer & Voinnet, 2005; Jay et al., 2011). Taken together these results, evidence obtained insinuates that NTAPi-P1b is a functional RSS protein when expressed in transgenic *A. thaliana* plants, with similar mechanistic features as those reported for HCPro.

Purification of protein complexes including NTAPi-P1b

The TAP purification method involves two column affinity purification steps in tandem separated by an incubation with the TEV NIa endopeptidase to release the protein complexes trapped by the Protein A IgG-binding domains under the mildest conditions possible. However, it has been noted in different reports (Rubio et al., 2005; Van Leene et al., 2008) that incubation with the TEV NIa protease at 16°C can affect the stability of complexes purified, risking being degraded or modified if incubation times are long. Although the final purity results of the tandem affinity purification is reported to be very high (Van Leene et al., 2008), control purifications using wild type plant extracts, or native bait proteins are used to further discriminate non-specific proteins contaminants which have remained. However, the popularity of this purification method has generated an immense amount of data concerning false positive interactions observed throughout a vast number of experiments all using the same column affinity purification conditions. With this large number of false positive data sets available it is possible to remove recurrent common contaminants with high statistical confidence from a purified pool of putative interacting proteins.

To protect purified complexes from degradation or modification during the first affinity purification step and the TEV protease digestion, NTAPi-P1b complexes

were purified from crude *A. thaliana* transgenic plant protein extracts directly by affinity to calmodulin using a calmodulin chromatographic column. Collected protein fractions were separated SDS-PAGE and silver stained (Fig. 17). Fraction 4 showed the largest amount of NTAPi-P1b and the highest protein complexity. Fractions 3 and 4, which accounted for approximately 64% of the total eluted NTAPi-P1b protein, were concentrated and subjected to LC-MS/MS analysis.

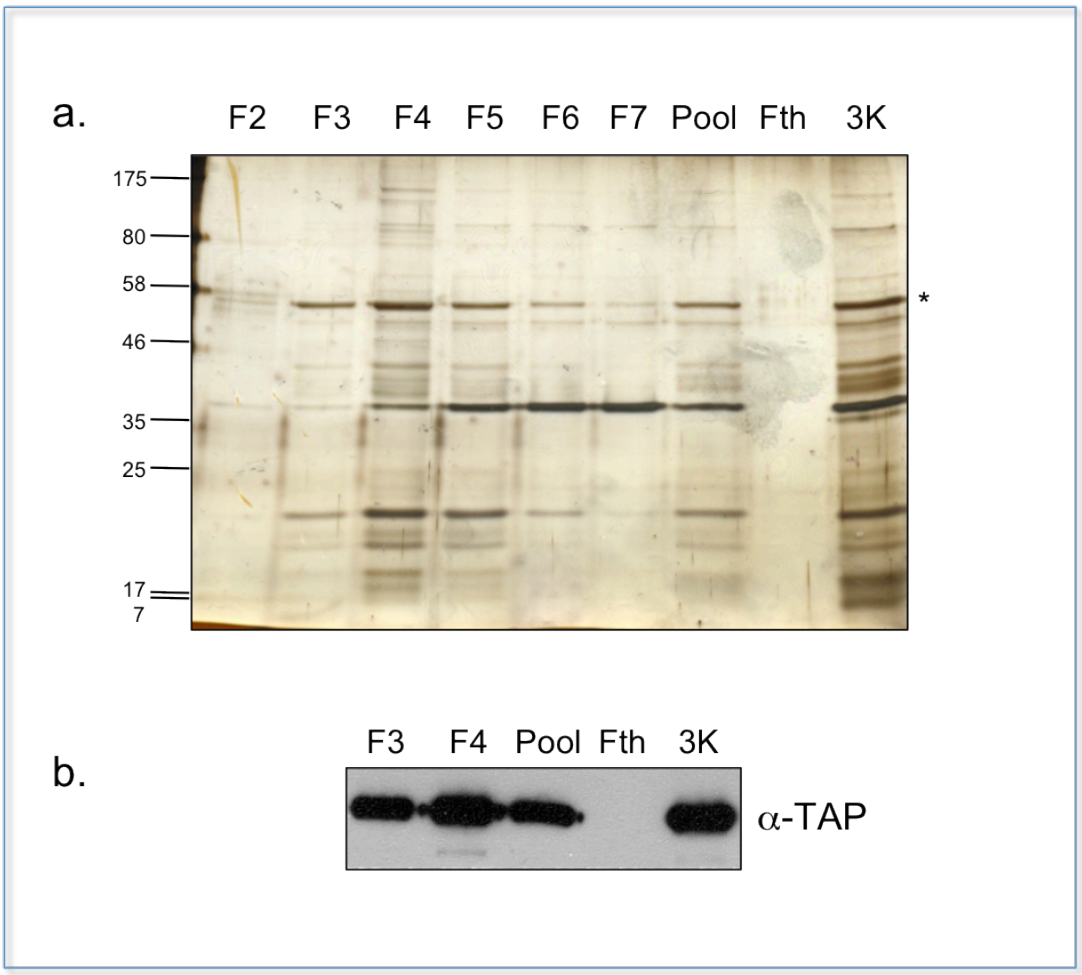

Figure 17. Visualisation of proteins co-purified with NTAPi-P1b by calmodulin affinity. (a) Silver stained 10% SDS-PAGE gel of the eluted samples, F2-F7; fractions eluted after calmodulin purification; Pool, pool of samples F3 and F4; Fth, flow through of the 3K centricon concentration; 3K, F3-F4 pool after concentration by centrifugation in a 3K Centricon device. Asterisk indicates NTAPi-P1b band (58 kDa); the positions of pre-stained molecular weight standards (in kDa) running on the same gel are indicated on the left of the gel. (b) Western blot confirming the presence of NTAPi-P1b in the indicated samples. Immunoblot detection was performed against the TAP tag by incubating membrane with PAP reagent.

A total of 33 proteins were identified from an *A. thaliana* database of 65587 sequences using MASCOT with a Peptide Spectrum Match (PSM) confidence greater than 99%. Known NTAPi contaminants from previous reported purifications using Mock, GFP and GUS baits protein extracts (Van Leene et al.,

2007), together with any of their annotated interacting partners and any annotated calmodulin binding proteins were removed from the list. The 29 resulting putative NTAPi-P1b interacting proteins are listed in Table 32.

Table 32. Proteins identified using NTAPi-P1b as bait by calmodulin affinity purification. Peptides corresponding to 33 different *A. thaliana* proteins were identified by MALDI-TOF/TOF mass spectroscopy. Protein name, locus TAIR accession code, protein size together with peptide matches, percentage coverage and mascot score is indicated.

Mascot Score	Peptide Matches	Percentage Coverage	Protein Size (kDA)	AGI	Name
538	16	21	95.6	AT4G11850	Phospholipase gamma1
496	16	57	24.6	AT4G20260	PCAP1
371	15	32	64.1	AT1G72150	Patellin-1
339	6	24	52.0	AT2G39730	Rubisco Activase
280	5	4	141.1	AT5G10470	Geminivirus Rep-interacting motor protein
259	13	24	56.1	AT1G65960	Glutamate Descarboxylase 2
106	3	6	60.8	AT5G16370	Acyl activating enzyme 5
102	2	4	53.0	ATCG00490	Rubisco L
101	2	2	121.1	AT2G42010	Phospholipase beta1
92	1	7	18.6	AT3G53020	Ribosomal Protein L24
70	3	3	124.5	AT5G06970	Munc13-like protein PATROL1
68	2	6	39.5	AT4G18060	SH3 domain-containing protein
62	2	4	55.3	ATCG00120	ATP Synthase Subunit Alpha
62	1	7	20.8	AT5G38410	Rubisco Small subunit 3B
60	3	7	53.7	AT2G36070	Translocase Inner membrane subunit 44-2
57	1	1	83.4	AT3G14590	Calcium-dependent Lipid binding protein
55	4	9	44.0	AT2G34560	Nucleoside triphosphatase
47	1	4	54.5	AT2G19860	Hexokinase 2
46	1	1	53.9	AT5G22610	Putative F-box
45	1	1	141.4	AT4G23160	Receptor like Protein Kinase 8
42	2	7	42.9	AT1G12900	GAPDH A subunit 2
42	1	3	46.9	AT4G15760	Monooxigenase 1
42	1	*1*	61.0	AT4G13990	Exostosin like
39	1	1	57.3	AT3G10410	Serine carboxypeptidase-like 49
38	2	12	34.4	AT4G13010	Oxidoreductase
38	1	4	53.4	AT4G13940	Homology dependant Gene Silencing 1
37	1	3	41.3	AT5G04890	Restricted TEV movement 2
36	1	4	40.7	AT1G27060	Regulator of chromosome condensation 1
34	1	2	63.4	AT2G41080	Tetratricopeptide repeat-like

With no clear GO term enrichment for any particular molecular function it could be worthwhile noting interesting proteins identified, as they show features that could be related with viral infections. Among them, Phospholipase D gamma1 (AT4G11850) and beta1 (AT2G4210), which belong to a family of proteins including host partners of *Red clover necrotic virus* replication complexes (Hyodo et al., 2015), the potyvirus movement host factor PCaP1 (AT4G20620) reported to associate with P3-PIPO from various potyviruses (Vijayapalani et al., 2012; Geng et

al., 2015), Patellin-1 (AT1G72150), which belongs to a protein family including members involved in the movement of *Alfalfa mosaic virus* (Peiro et al., 2014) and Geminivirus Rep-interacting motor protein (AT5G10470), which interacts with the replication protein of the *Tomato golden mosaic virus* (Kong & Hanley-Bowdoin, 2002), with high MASCOT scores and, in the case of PCAP1, Patellin-1 and Phospholipase gamma1, also with high protein coverage. Other virus-related candidates, although with lower score and coverage, are Restricted TEV Movement 2 (AT5G04890), involved in potyvirus movement (Whitham et al., 2000; Chisholm et al., 2001), Homology dependent Gene Silencing 1 (AT4G13940), involved in DNA-methylation gene silencing (Rocha, 2005), Glyceraldehyde 3-phosphate dehydrogenase A subunit 2 (AT1G12900) orthologs of which have been reported to be involved in the infection of different viruses (Schultz et al., 1996; Huang & Nagy, 2011; Prasanth et al., 2011; Kaido et al., 2014), and Serine carboxypeptidase-like 49 (AT3G10410) reported to be involved in plant defence and Pathogenesis Related gene family (PR-1, PR-2 and PR-5) induction in rice (Liu et al., 2008).

Production of transgenic lines expressing different NTAP-tagged RSS proteins

To further characterize and validate host factors specifically required for P1b activities and for activities shared with other RSS proteins, transgenic *A. thaliana* lines producing either NTAPi-P1b or other NTAPi-tagged RSS proteins, showing active RSS functions replacing HCPro during PPV infection (Maliogka et al., 2012) were produced by floral dip. Initially, vector constructs were tested for correct expression and activity using agroinfiltration transient expression in *N. benthamiana* leaves (Fig. 18).

All the NTAP-tagged RSS proteins tested suppressed silencing of plongGFP, providing evidence that they are being expressed correctly and are functional fusion proteins. Only P1b mutant variants P1bm1 and P1bm6 harbouring mutations that inhibit RSS activity of P1b either by affecting directly the RNA binding domain (RK68,69AA) or the Zinc finger domain needed for the correct conformational structure (C103A) of the suppressor protein (Valli et al., 2008), were unable to suppress silencing of plongGFP.

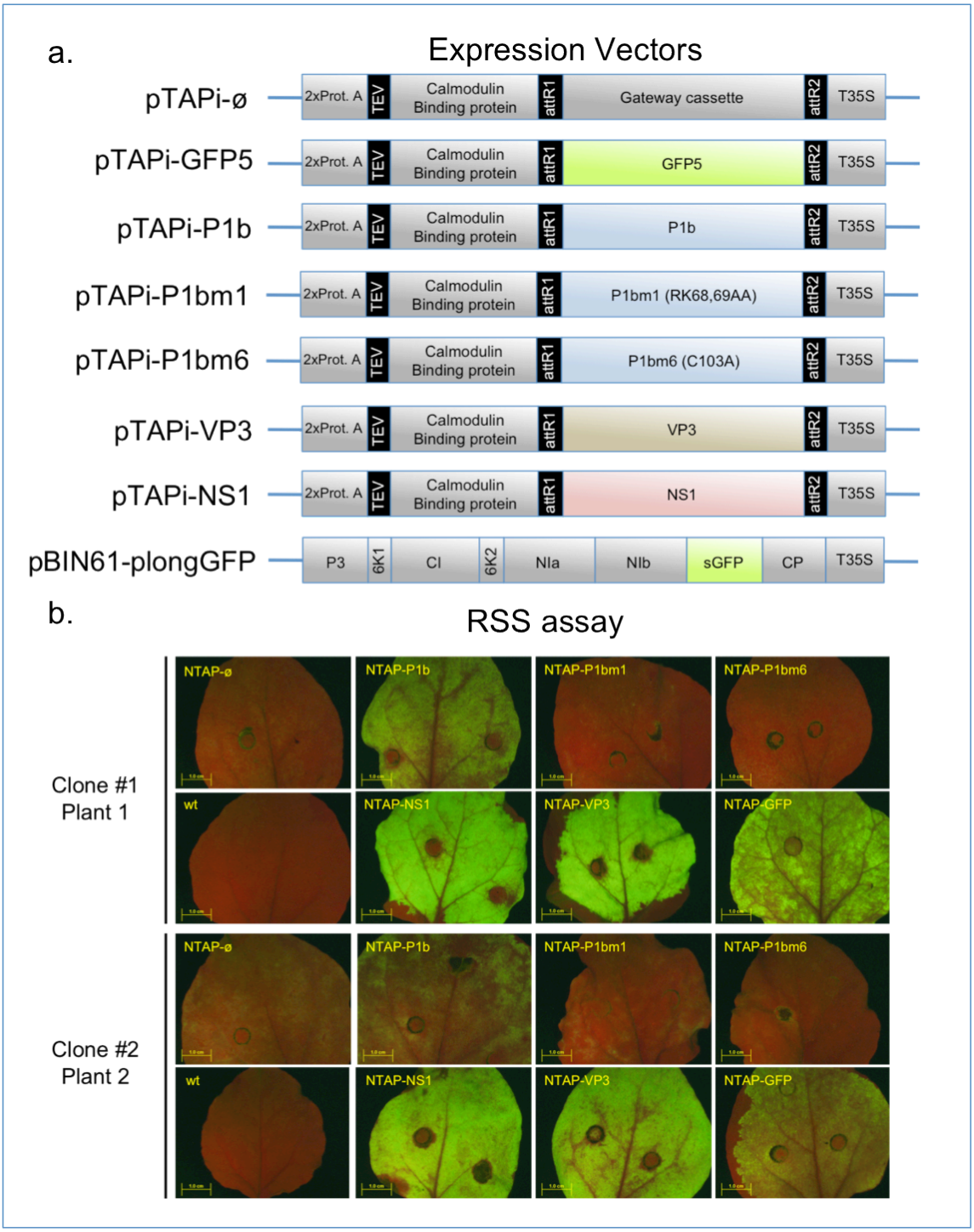

Figure 18. a. pNTAPi constructs for stable expression in transgenic *A. thaliana* plants. (a) CDS sequences corresponding to RSS proteins VP3 (IBDV), NS1 (IFV), P1b (CVYV), P1b mutant alleles P1bm1 and P1bm6, and the GFP control were recombined with the gateway cassette to produce the constructs shown. In all cases CDS sequences were inserted upstream of the termination region of the CaMV 35S mRNA (T35S), tagged with 2 protein A domains in tandem and a calmodulin binding protein domain separated by a TEV protease cleavage site. In all cases expression is driven by a CaMV 35S promoter. (b) The RSS activity of the constructs was assessed in an agroinfiltration assay. Constructs indicated were co-expressed together with pBIN61-plongGFP (a strong silencing-inducing GFP tagged construct) by agroinfiltration. Sustained green fluorescence is indicative of RSS activity. Pictures were taken under an epi-fluorescence stereoscope at 6 days post agroinfiltration.

The NTAPi constructs tested by agroinfiltration were used to transform *A. thaliana* by floral dip to produce stable transgenic lines expressing the different NTAPi-tagged RSS proteins and the NTAPi-GFP as control. At least two independent transgenic lines per construct were selected and propagated by self-fertilization to obtain homozygous plants. Ideally these plants would be used as comparison between the different protein complexes purified in the tandem purifications to further analyse interactions between host proteins, different P1b alleles harbouring different RSS activities and other non-related, but functionally active, RSS proteins. Since production and selection of stable homozygous transgenic lines is usually a long and arduous process, the P1b TAP protein purification was started before the different NTAPi expressing RSS proteins had been produced and fully validated. The widespread use of the NTAPi strategy enables false TAP contaminants to be detected from shares pools of false positive data sets published (Van Leene et al., 2007) which can be used to curate initial purifications in anticipation of the remaining *A. thaliana* NTAPi transgenic lines.

Assessing proteome signatures in PPV-based infections supported by two different RSS proteins using iTRAQ labelling

Recent advances in genomics and proteomics have enabled wide genome or proteome searches of differentially represented targets in different biological conditions hoping to understand the biological processes involved in the adaptation to the imposed physiological conditions. Gene expression arrays can provide a snapshot of the transcriptional activity of a certain biological sample. However, up-regulated gene do not necessarily correspond to subsequent over accumulation of their corresponding active proteins, as the gene products are susceptible to regulation and post-translational modifications that can activate or deactivate the protein despite having a transcriptionally active gene. Technical advances in mass spectroscopy and bioinformatics have enabled proteomic screenings to be useful in determining the precise proteomic profile of biological samples, permitting relative abundance quantifications to unveil directly differential protein accumulations. Despite transcriptome analysis having been

already reported for multiple potiviruses (Agudelo-Romero et al., 2008; Babu et al., 2008), few studies analyzing the proteome of potyvirus infected plants have been published (Diaz-Vivancos et al., 2008). To gain knowledge on how the host proteome is remodelled in response to different viral silencing suppressors, experiments using isobaric tag for relative and absolute quantitation (iTRAQ) technology were performed to detect shared and specific protein changes in plants infected with two PPV variants differing only in the silencing suppressors they express.

Protein extraction and optimisation for iTRAQ quantifications

One of the major challenges in quantitative proteomic of complex biological systems is the high dynamic range of proteins in samples. In human plasma, more than 10 orders of magnitude in concentration separate albumin (55% of the total protein content, 35-50 mg/ml) and the rarest protein, interleukin 6 (0-5 pg/ml,) and it has been estimated that detecting peptides from interleukin 6 to identify the protein in blood plasma would account to searching for a sole person in the entire planet (Anderson, 2002). Likewise in plants, the TAIR10 release contains 27,416 protein-coding genes and it is estimated that in leaf protein samples, the most abundant protein species, Rusbisco, represents at least 65% of soluble protein content (Ellis, 1979). Plant protein samples represent a large heterogeneous mix of different proteomes originating from different organs within the same tissue sample with very distinct proteome signatures. Detecting scarce proteins originating from organs with different proteome signatures in total protein leaf samples with large dynamic range entrains a tremendous challenge.

It becomes evident that to succeed in this challenge, removing Rubisco from protein samples provides an advantage for protein identification, and a differential protein analysis should not be performed without an optimised method of minimizing the Rubisco contents of the samples.

The first option tested, among the different options to minimise Rubisco content in the samples was to use protein extracts from different plant tissues. Considering

that the Rubisco content would be highest in active photosynthetic tissues, different types of tissues in infected plants were examined for Rubisco content and virus accumulation (Fig. 19. a). Rubisco content was very high both in whole plant and in inflorescence tissue. As expected, no Rubisco was observed in root samples, which showed high accumulation level of PPV-sGFP, however virus accumulation was very low in PPV-P1b-sGFP-infected root samples. The low PPV-P1b-sGFP virus accumulation in root samples and the high Rubisco accumulation in inflorescence tissue revealed no clear advantage of using selected plant tissues for the proteomic analysis.

A second strategy tested in reducing the Rubisco content of the samples was to culture the infected plants in the dark for different time periods (Fig. 19. b). With this strategy, Rubisco was greatly reduced by long incubation periods in the darkness; however, no or little virus accumulation could be detected in plants subjected to that treatment. Incubating plants for shorter time periods in the dark once a decent virus accumulation was achieved did not cause significant changes in the Rubisco content of the samples. Surprisingly, placing infected plants in the dark seemed to arrest the infection as no increase in viral accumulation could be observed in samples taken at later infection times. Not being able to find a condition with reduced Rubisco content by light deprivation but with sufficient viral accumulation this strategy was abandoned.

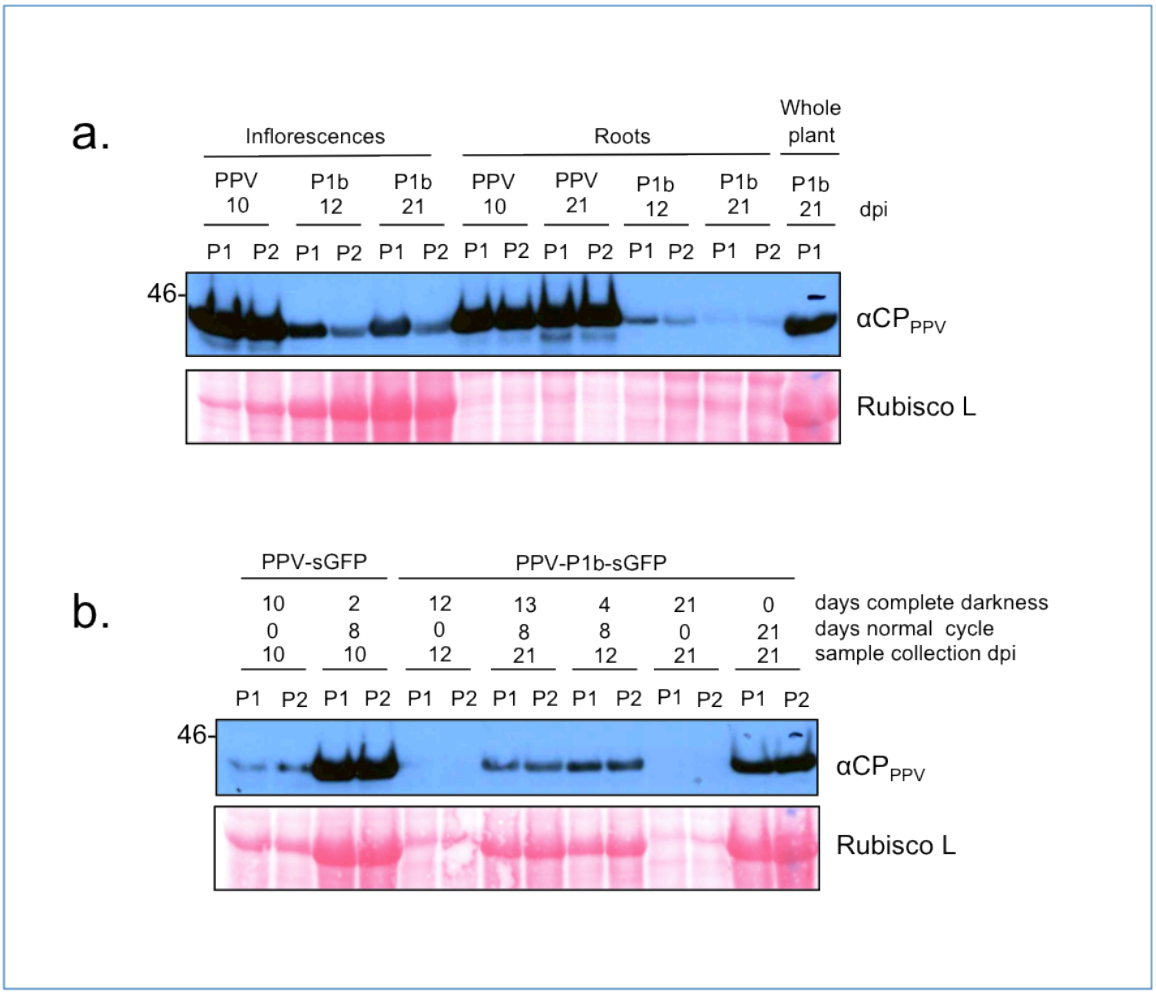

Figure 19. Western blot analysis of *A. thaliana* infected plants from different plant tissues (a) or under different growth cycles (b). (a) Viral accumulation in different tissue types and corresponding Rubisco accumulation. (b) Viral and Rubisco accumulation of inoculated plants after light deprivation. PPV-sGFP and PPV-P1b-sGFP infected samples collected at 10, 12 or 21 days post inoculation (dpi) as indicated. For all samples similar amounts of liquid nitrogen-ground tissue were extracted and equal volumes loaded. Ponceau Red is used to monitor Rubisco content of the samples. Blots were incubated with anti-serum raised against PPV CP. Positions of the corresponding pre-stained molecular weight standard (in kDa) running on the same gel are indicated on the left.

The third strategy tested was the use of a Rubisco depletion column (Fig. 21. a). This strategy proved to be the best strategy in efficiently removing Rubisco from whole plant protein extract. Removal of Rubisco was performed in a couple of quick centrifugation steps permitting samples to be quickly processed minimising any possible protein degradation. Due to the good efficiency, convenience and long life span of the depletion column, this strategy was chosen and Rubisco was depleted biochemically from all samples used.

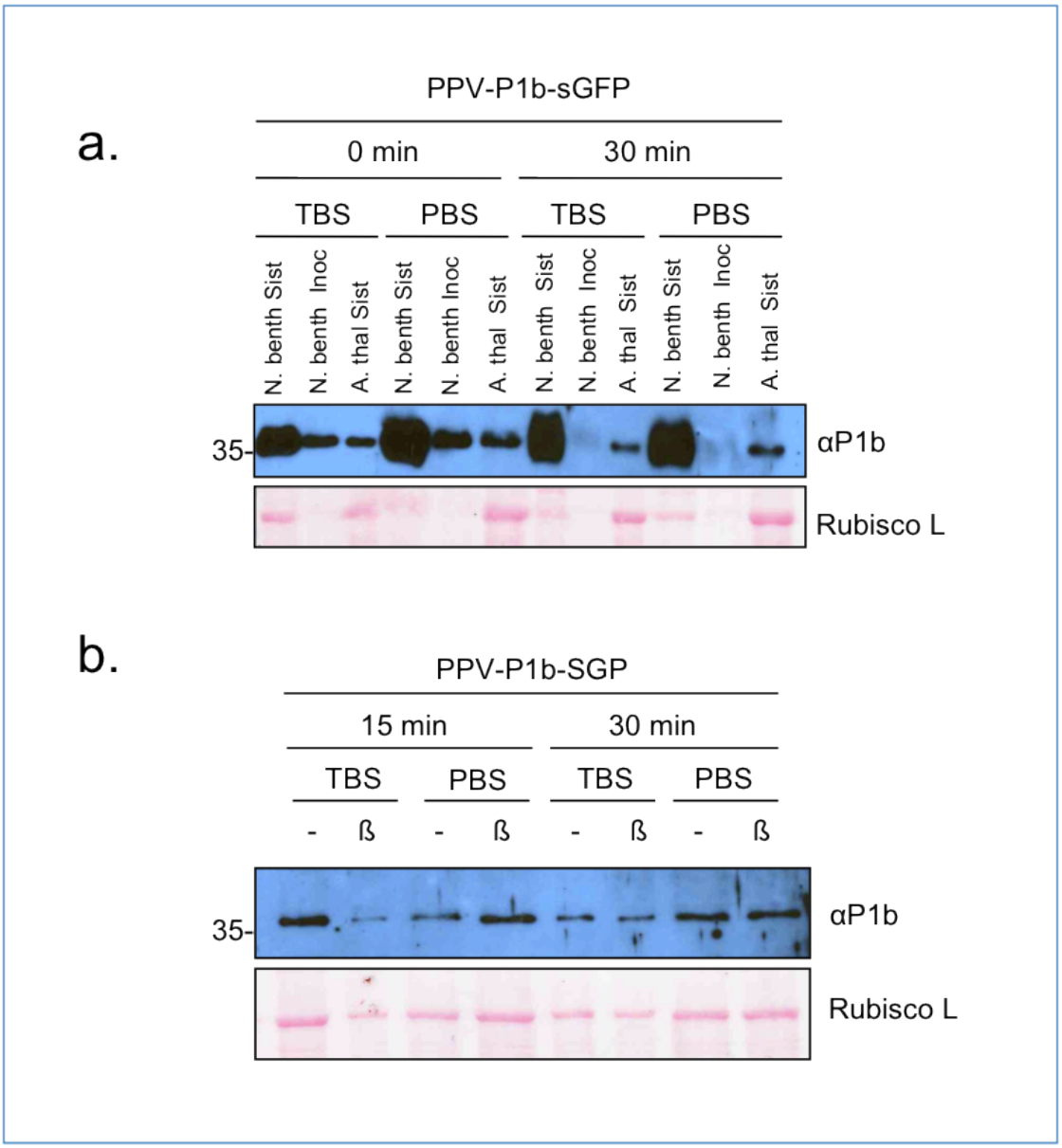

Figure 20. Biochemical analysis of different native protein extraction buffers used with PPV-P1b-sGFP infected tissue from different plant species. Samples were collected at 12dpi. Equal amounts of fine liquid nitrogen-ground tissue was used for every extraction. (a) Native protein extracts from *N. benthamiana* and *A. thaliana* infected plants extracted using Tris-Borate Buffer (TBS) or Phosphate Buffer (PBS) at different times after extraction. (d) Native protein extracts from *A. thaliana* infected plants extracted using Tris-Borate Buffer (TBS) or Phosphate Buffer (PBS) supplemented or not with ß-mercaptoethanol and at different times after extraction. ß-mercaptoethanol shows no effect on P1b protein extraction with the native buffers used. Blots were incubated with anti-serum raised against P1b. Positions of the corresponding pre-stained molecular weight standard (in kDa) running on the same gel is shown on the left. Ponceau red is used to monitor Rubisco extraction.

Having been reported viral instability in native extracts of PPV-P1b-sGFP-infected plants, a stability test was performed on the plant tissue to be analysed (Fig. 20. a). Decrease in P1b stability was only observed in agroinoculated leaf tissue, but not in systemically infected tissue. Thus, infected *A. thaliana* tissue other than

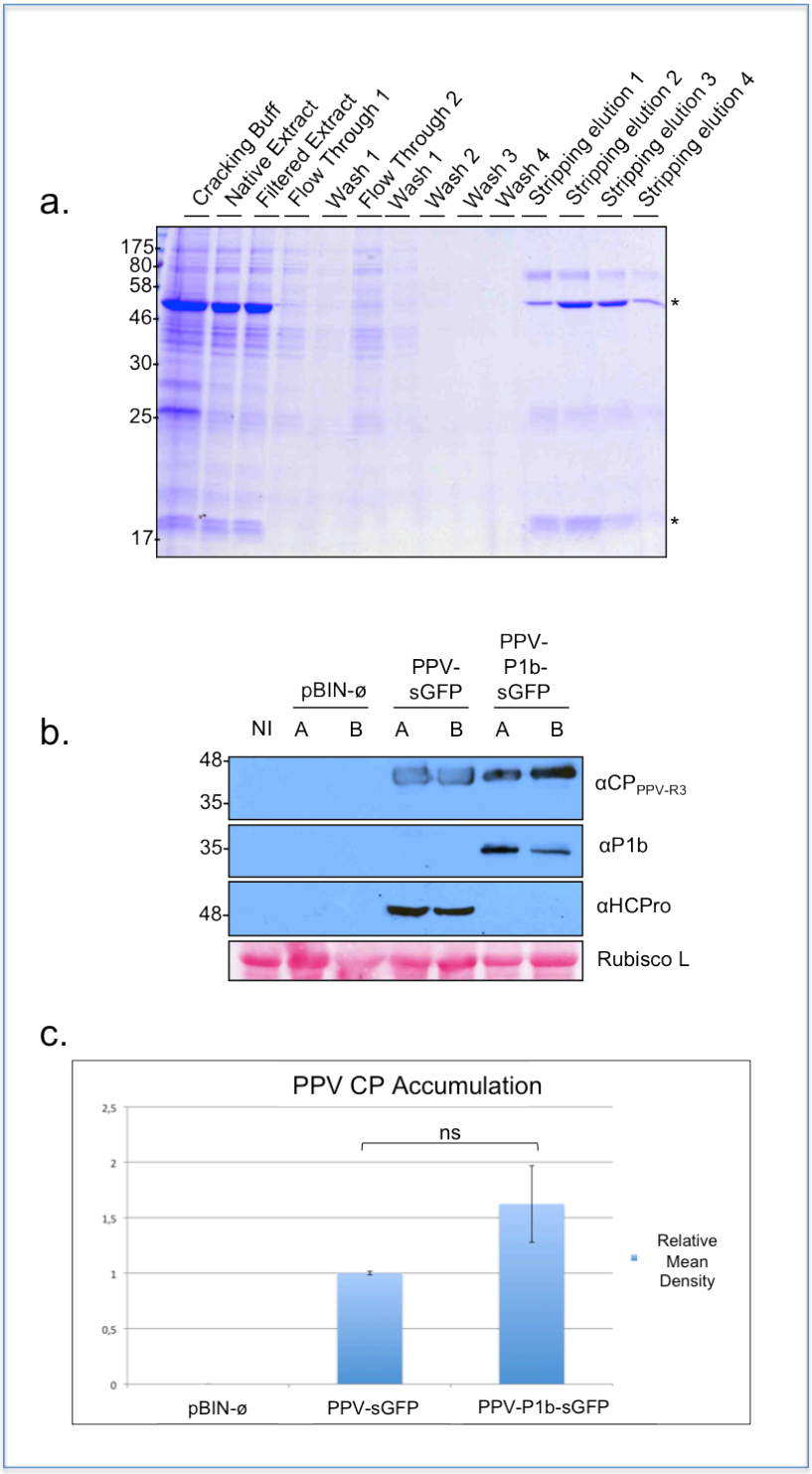

Figure 21. Rubisco depletion and viral CP accumulation of infected samples used in iTRAQ quantification. (a) 12% SDS-PAGE gel coomassie stain of native protein samples from *A. thaliana* during the Rubisco depletion using the SEPCRO depletion column. Asterisk indicates both Rubisco subunit bands. Positions of the corresponding Bluestar molecular weight standards (in kDa) running on the same gel are shown on the left. Approximately equal amounts of total protein extracted with Cracking buffer and Native buffer was loaded. Depletion was performed twice (flow through 1 and flow through 2) with the filtered extract without stripping the column to test whether saturation was reached after depletion of flow through 1. Rubisco specifically bound to the column during depletion and subsequent washes with buffer, but eluted when stripping buffer was used to regenerate the column. (b) Western blot analysis of the viral accumulation in the *A. thaliana* infected systemic plant tissue used for the native extractions. Plants inoculated with either agrobacteria carrying pBIN-PPV-sGFP, pBIN-PPV-P1b-sGFP or pBIN-ø (empty plasmid) were collected in pools of 4 infected plants samples. PPV-sGFP samples were collected at 8 dpi whilst PPV-P1b-sGFP and pBIN-ø samples were collected at 12dpi to achieve comparable CP accumulation levels between both viruses. Immunoblot analysis was performed with anti-serum raised against PPV CP protein, common for both viruses, and anti-serum raised against PPV HCPro or P1b to confirm expression of each viral RSS protein. Both PPV-sGFP and PPV-P1b-sGFP showed similar CP accumulation. Ponceau Red was used as loading control. (c) Densitometry analysis of PPV CP accumulation seen in (b). No statistical significant differences can be seen between PPV-sGFP and PPV-P1b-sGFP CP accumulation.

inoculated rossette leaves or roots was used for further analysis. It has also been reported that efficient P1b extraction depends on the use a reducing agent in the extraction buffer. Being the Rubisco depletion column unable to tolerate the presence of reducing agents in the samples, the effect of removing ß-mercaptoethanol from the extraction buffer was tested (Fig. 20. b). As no clear advantage was observed in using ß-mercaptoethanol, the protein extraction was performed in the absence of a reducing agent.

Plant samples were collected at times of infection when both PPV-sGFP and PPV-P1b-sGFP showed similar accumulation levels to mitigate differences on the host proteome alterations derived from differences in virus accumulation, which could obscure specific differences derived from the use of two different silencing suppressors (Fig. 21. a & c).

Protein quantification and differential display

Two biological replicates of pools of four *A. thaliana* plants infected with PPV-P1b-sGFP and pools of four plants infected with PPV-sGFP and four mock-inoculated plants were processed for isobaric tag labelling (iTRAQ) and liquid chromatography coupled mass spectroscopy triple TOF (LC-Q-TOF). From the total database available using MASCOT search engine a total of 988 non-redundant proteins with at least two peptide matches and common in at least two of the three technical replicates made for each clone were identified. A subset of these proteins were differentially accumulated with respect to the mock inoculated sample. Relative quantification of the protein abundance was performed using the mean value of peptides quantified in the three technical replicates. For each condition, a cut off threshold for *p*-value greater than 0.05 and a false discovery rate (FDR) of below 5% (meaning that maximum only 1 in every 20 proteins is expected to be falsely differentially quantified) was applied, calculated using a decoy version of the same database used for the identification.

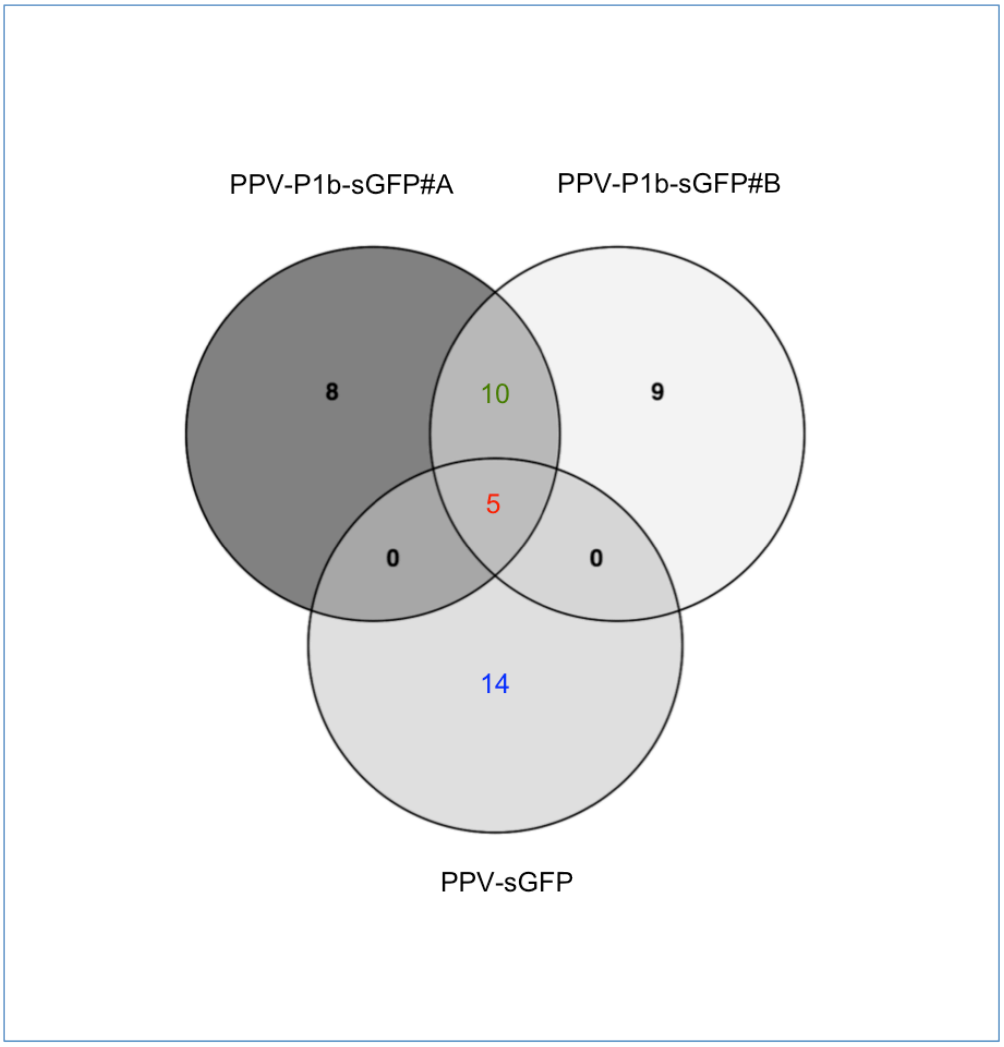

Figure 22. Summary of the differential protein accumulation in infected samples compared to non-infected samples that passed the statistical threshold criteria. For each condition systemic tissue from pools of 4 plants infected with either PPV-sGFP or PPV-P1b-sGFP were used for the native protein extraction and iTRAQ quantification. To be identified as significantly differentially expressed, proteins must be identified with at least two peptide matches common in two of the three technical replicates and follow the statistical threshold criteria of pval<0.05 and 5% FDR. Numbers inside each set correspond to total number of proteins identified and quantified for each condition. Number in green represents common elements between two PPV-P1b-sGFP-infected biological replicates, number in blue represents elements exclusive to the PPV-sGFP-infected sample, and number in red represents common elements between both PPV-P1b-sGFP-infected biological replicates and the PPV-sGFP infected sample.

Applying these cut off parameters, 46 host proteins in total passed the selection criteria being statistically significant differentially accumulated in the infected samples. Of this group of 46 proteins, 32 host proteins were differentially accumulated in PPV-P1b-sGFP-infected samples with respect to the mock-inoculated sample, of which 15 host proteins were in common to both PPV-P1b-sGFP-infected biological replicates. Ten of them appear to be specific of PPV-P1b-sGFP-infected tissue, and the remaining 5 proteins were over accumulated in all PPV-infected plant (Fig. 22). Relative abundance ratios of these 46 proteins

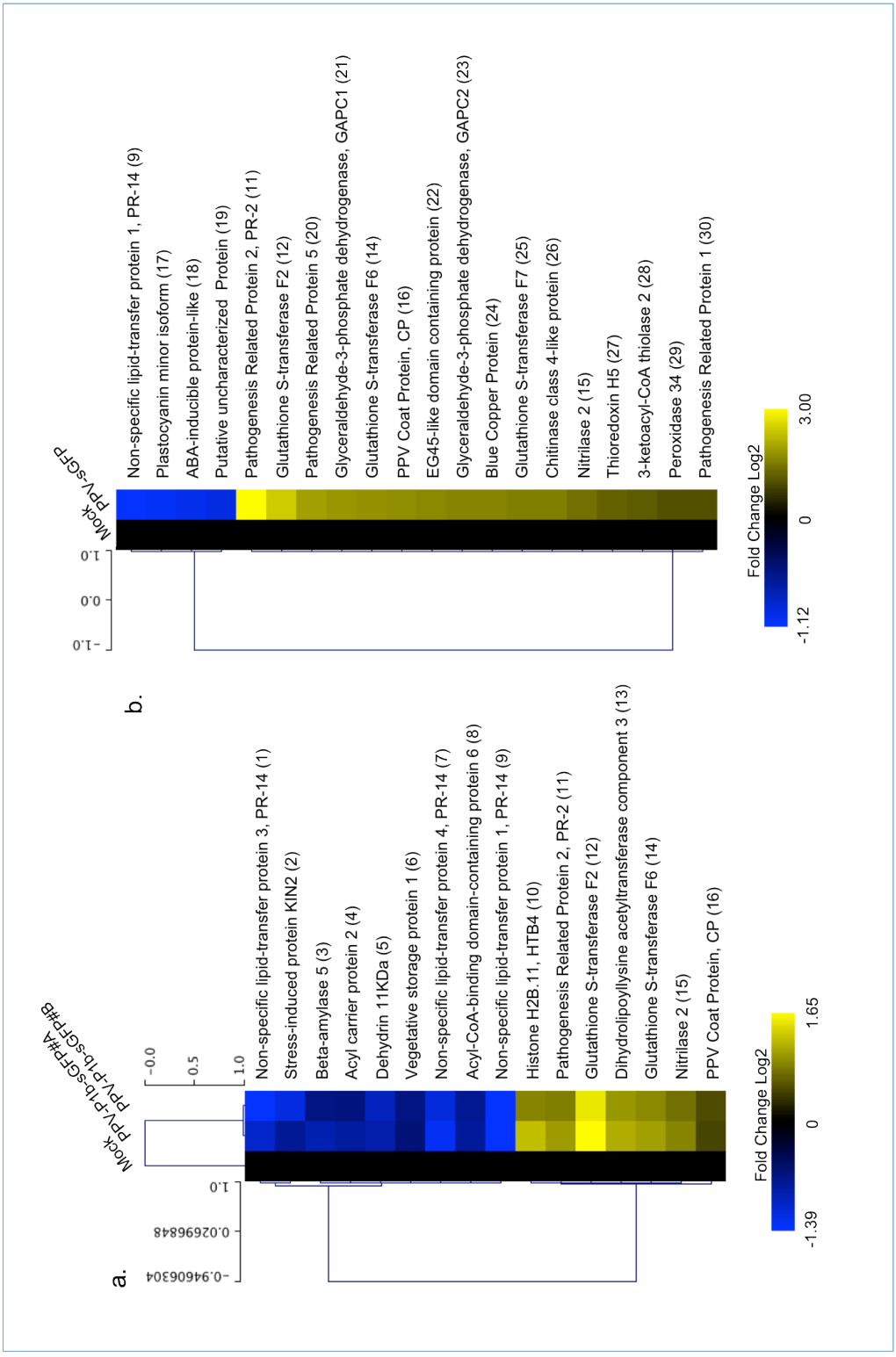

Figure 23. Heat map diagrams of the relative abundance ratios in Log2 of the statistically significant and differentially accumulated proteins in PPV-P1b-sGFP (a.) and PPV-sGFP (b.) infected samples and the hierarchical clustering using Pearson correlation. 1, LTP3 (AT5G59320); 2, KIN2 (AT5G15970); 3, BAM5 (AT4G15210); 4, ACP2 (AT1G54580); 5, HIRD11 (AT1G54410); 6, VSP1 (AT5G24780); 7, LTP4 (AT5G59310); 8, ACBP6 (AT1G31812); 9, LTP1 (AT2G38540); 10, H2B1.11 (AT5G59910); 11, PR-2 (AT3G57260); 12, GSTF2 (AT4G02520); 13, DHLAT (AT1G54220); 14, GSTF6 (AT1G02930), 15, NIT2 (AT3G44300), 16, PPV CP (P17767); 17, PETE (AT1G76100); 18, ABA-IPL (AT5G53820); 19, (AT3G47070); 20, PR-5 (AT1G75040); 21, GAPC1 (AT3G04120); 22, EGC2 (AT2G18660); 23, GAPC2 (AT1G13440); 24, BCB (AT5G20230); 25, GSTF7 (AT1G02920); 26, CHI (AT2G43570); 27, TRX5 (AT1G45145); 28, PED1 (AT2G33150); 29, PER34 (AT3G49120); 30, PR-1 (AT2G14610).

compared to proteins for the mock inoculated sample was represented on a heat map graph (Fig. 23 & 25) with their average iTRAQ ratios expressed in Log2 scale. Both PPV-P1b-sGFP biological replicates grouped in the same hierarchical cluster with Pearson correlation metric different from that of mock inoculated plants. From the group of 15 statistically significant differentially accumulated proteins in PPV-P1b-sGFP infected samples, 9 of them were under accumulated and 6 over accumulated relative to the mock inoculated (Fig. 23. a).

A Gene Onthology molecular function classification of the over and under differentially accumulated proteins is shown in Fig. 24. PPV-P1b-sGFP-infected samples differentially under accumulated proteins mainly belonging to three functional clusters: Binding (GO:0005488), Catalytic Activity (GO:0003824) and Enzyme Regulator Activity (GO:0030234). Among the under accumulated proteins three Non-specific Lipid Transfer Proteins, LTP1, LTP3 and LTP4, all of them members of the same Pathogenesis related protein 14 family, with two of them showing the lowest fold change ratio are to be noted. On the other hand, differentially over accumulated proteins were classified in four functional clusters, with two GO profiles shared with the under accumulated proteins: Binding (GO:0005488), Catalytic Activity (GO:0003824), Structural Molecule Activity (GO:0005198) and Translation Regulation Activity (GO:0045182).

Using the same cut off parameters as for the PPV-P1b-sGFP samples, a total of 19 proteins were selected, complying with the statistical and technical criteria to be statistically significant differentially accumulated in PPV-sGFP infected samples (Fig. 22). The relative abundance ratios of the PPV-sGFP and mock inoculated samples were compared and data was represented on a Heat map graph (Fig. 23. b & 25) with their average iTRAQ ratios expressed in Log2 scale. Of the 19 differentially accumulated proteins, 4 under accumulated and 15 over accumulated with respect to the mock inoculates samples.

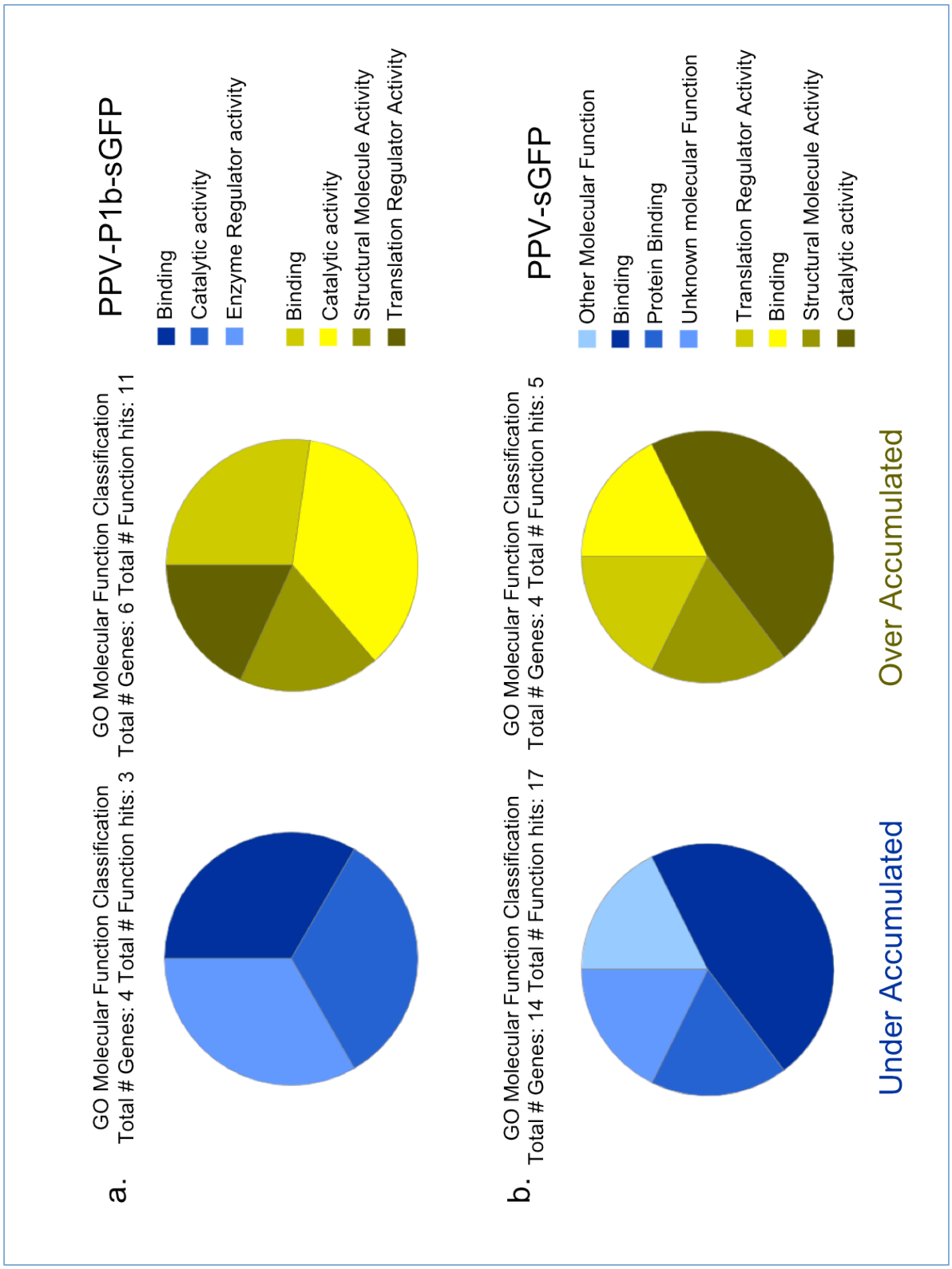

Figure 24. Gene Onthology classification of the under and over differentially accumulated proteins for PPV-P1b-sGFP (a) and PPV-sGFP (b) infected samples.

In PPV-sGFP infected samples, non-specific LTP1 was found under accumulated as in PPV-P1b-sGFP infected samples. Whereas Glutation S-transferase F2, Glutation S-transferase F7, Pathogenesis Related protein 2 and Nitrilase 2 were all over accumulated, like in PPV-P1b-sGFP infected samples. It is worthwhile noting a number of Pathogenesis related proteins, PR-1, PR-2, and PR-5 being over accumulated in the PPV-sGFP infected sample, consistent with previous reports (Pasin et al., 2014). PR-5 is described as a Thaumatin like protein induced in inflorescences by viral infection, although Thaumatin is described as 100 000 times sweeter than sucrose, the role of Thaumatin like proteins is yet unknown, it is stimulating to think that they could be involved in aphid signalling, attracting the propagation vector to the virus infected plants as has been previously reported for PR-1 and PR-2 (Moran & Thompson, 2001).

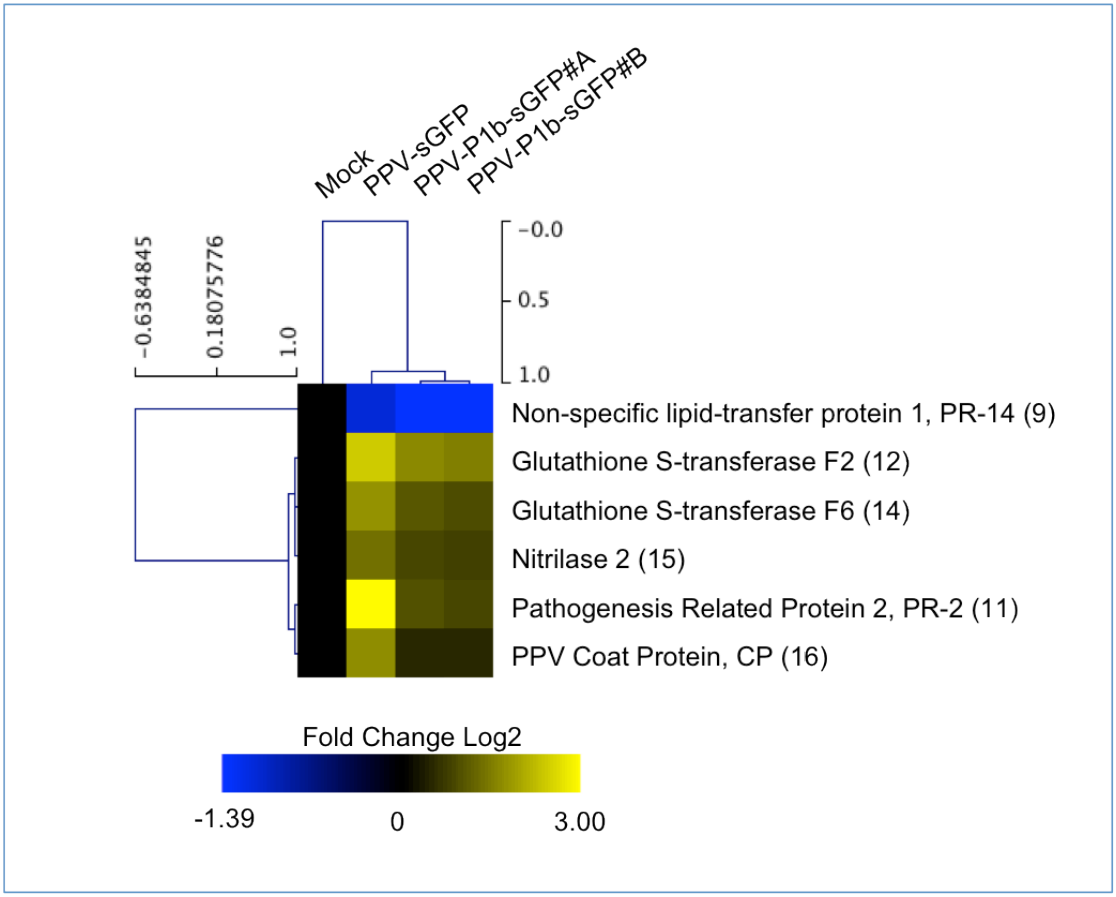

Figure 25. Heat map diagrams of the relative abundance ratios in Log2 of the 5 statistically significant and differentially accumulated proteins PPV-P1b-sGFP and PPV-sGFP. 9. LTP1 (AT2G38540); 11, PR-2 (AT3G57260); 12, GSTF2 (AT4G02520); 14, GSTF6 (AT1G02930), 15, NIT2 (AT3G44300), 16, PPV CP (P17767).

From a total of 46 identified proteins complying with the statistical and technical thresholds for PPV-P1b-sGFP and PPV-sGFP infected samples, only 5 proteins in common passed the statistical thresholds (Fig. 22). For comparative purposes, relative abundance ratios of the common 5 proteins are shown represented as a heat map graph (Fig. 25). Both PPV-P1b-sGFP biological replicates grouped in the same hierarchical cluster with Pearson correlation metric different from that of PPV-sGFP inoculated plants. Of these 5 proteins, 4 showed a differential over accumulation in both infections and only one was seen differentially under accumulated.

Differential protein accumulation between PPV-sGFP- and PPV-P1b-sGFP-infected plants

A direct comparison between protein accumulations in PPV-sGFP and PPV-P1b-sGFP infected samples was performed. A total of 16 host differentially accumulated proteins passed the statistical threshold criteria and abundance ratios relative to PPV-sGFP represented in heat map graph (Fig. 26). All 16 proteins were found to be under accumulated in PPV-P1b-sGFP with respect to PPV-sGFP, with 4 proteins (PR-2, PR-5, GAPC1 and GAPC2) showing at least a 2 fold lower accumulation in PPV-P1b-sGFP infected samples. GAPC1 and GAPC2 have been reported to be cytosolic and peroxisomic proteins (Quan et al., 2013), involved in energy metabolism, lipid metabolism (Guo et al., 2014) and hydrogen peroxide signal transduction by interacting with phospholipase D, activating plant stress responses (Guo et al., 2012), GAPC in mammals also performs non metabolic functions in processes such as apoptosis, vesicular transport, DNA repair and replication, transcription, and tRNA export (Sirover, 2011; Tristan et al., 2011). In addition, Glyceraldehyde 3-phosphate dehydrogenases have also been involved in the infection of different plant viruses (Schultz et al., 1996; Huang & Nagy, 2011; Prasanth et al., 2011; Kaido et al., 2014).

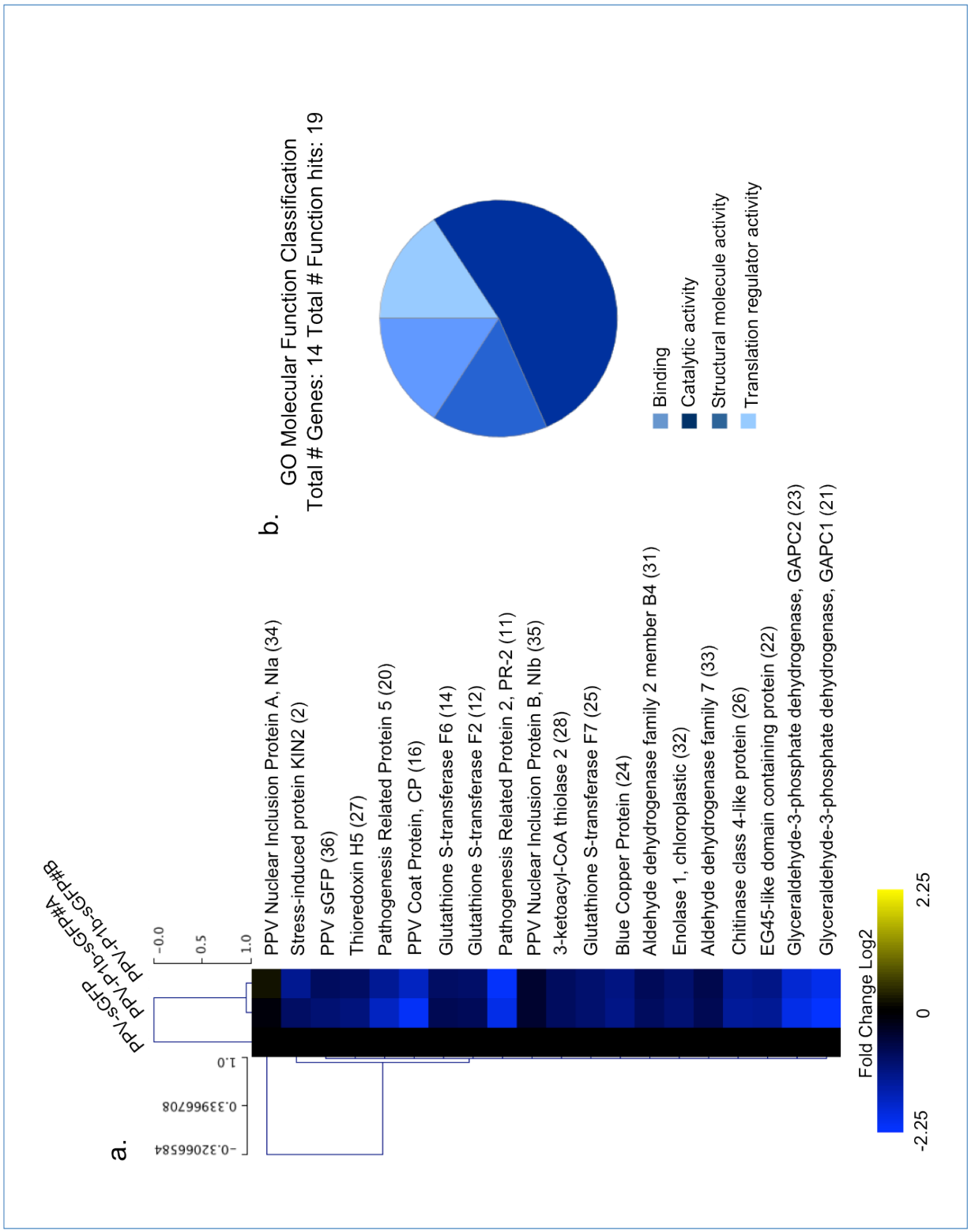

Figure 26. iTRAQ analysis of the PPV-P1b-sGFP samples with respect to the PPV-sGFP inoculated samples. a, Heat map diagrams of the relative abundance ratios in Log2 of the 5 statistically significant and differentially accumulated proteins PPV-P1b-sGFP. 2, KIN2 (AT5G15970); 11, PR-2 (AT3G57260); 12, GSTF2 (AT4G02520); 14, GSTF6 (AT1G02930), 16, PPV CP (P17767); 20, PR-5 (AT1G75040); 21, GAPC1 (AT3G04120); 22, EGC2 (AT2G18660); 23, GAPC2 (AT1G13440); 24, BCB (AT5G20230); 25, GSTF7 (AT1G02920); 26, CHI (AT2G43570); 27, TRX5 (AT1G45145); 28, PED1 (AT2G33150); 31, ALDH2 (AT3G48000); 32, ENO1 (AT1G74030); 33, ALBH7B4 (AT1G54100); 34, PPV NIa (P17767); 35, PPV NIb (P17767); 36, PPV sGFP (EF569215). b, Gene Onthology classification of the differentially accumulated proteins in PPV-P1b-sGFP infection.

Among the proteins identified in the iTRAQ analysis, 4 viral proteins were identified and relative protein abundance quantified. Only PPV CP showed a significant differential accumulation between PPV-sGFP and PPV-P1b-sGFP infected samples. However the fact that similar CP accumulation was observed by western blot analysis (Fig. 21. b), and no differential accumulation was detected in the iTRAQ analysis for other PPV viral proteins (NIa, NIb and PPV-expressed GFP) suggest that all samples were infected at similar levels. The fact that CP accumulation is considerably reduced in PPV-P1b-sGFP-infected samples is consistent with previously published data (Valli et al., 2014) and reinforces the hypothesis that HCPro could have a stabilising effect on the accumulation of PPV CP in which P1b is deficient. Although the differences in accumulation levels quantified do not look very dramatic, it is reported that current iTRAQ methods underestimates fold changes, implying small changes may indicate significant differences between samples (Bantscheff et al., 2007; DeSouza et al., 2009; Karp et al., 2010).

Taken together these iTRAQ experiments, results suggest that PPV-P1b-sGFP and PPV-sGFP similarly induce the over accumulation of host Glutation S-Transferases involved in redox metabolism, oxidative stress and translation regulation; Nitrilase involved in auxin metabolism, and Pathogenesis Related Proteins known to be biotic stress markers, and repress the accumulation of Lipid Transfer Proteins reported to be involved in different processes like cutin synthesis (Pyee et al., 1994), ß-oxidation (Tsuboi et al., 1992), plant defences (Molina & Garcia-Olmedo, 1993; Kristensen et al., 2000; Buhot et al., 2001; Maldonado et al., 2002; Girault et al., 2008) and non-vesicular lipid and sterol transport (Lev, 2012).

Differences in protein accumulation between both viruses mainly involved some Pathogenesis Related Proteins (PR-2 and PR-5) reported to be biotic stress markers with unknown functions, and Glyceraldehyde 3-phospate dehydrogenases (GADPC1 and GADPC1), reported to be related with energy, lipid metabolism and hydrogen peroxide signal transduction in biotic stress and the viral CP.

Screening for Transcription Factors with effects PPV infection

Transcription factors are key regulators of many biological processes in eukaryotes. Biological processes subjected to transcriptional regulation range from organogenesis and development, to light sensing, and adaptation to biotic and abiotic stresses, including defence responses against pathogens. At the time of writing this report, tair10 database describes a total of 2839 annotated transcription factors for *A. thaliana* from 2191 loci and grouped in 58 different families. Many Transcription factors are therefore, often members of large families with functional redundancy, which regulate gene expression by binding to *cis*-specific regulatory sequences present in the genome. This transcriptional control of the genes expressed does not only determine the cell fate and allocation to a determined tissue type, but also the ontogenetic processes it participates in, throughout their continuous development of plants as sessile organism. As a result plants must entrain a strict control of the gene expression in order to guarantee the correct response for every possible situation to encounter, yet having the sufficient plasticity to respond rapidly to constantly changing conditions. It is believed that this transcriptional control in by far more important in plants than in animals due to the higher percentage of Transcription factor coding genes (Franco-Zorrilla et al., 2014).

The study of transcription factors involved in specific biological processes can result challenging. Being transcription factors subjected to strict expression profiles, constitutive expression can cause severe developmental defects restricting growth and reproduction. To overcome these disorders, a collection of 1636 ß-estradiol-inducible over-expression lines corresponding to 634 Transcription factors was generated (Coego et al., 2014) under the TRANSPLANTA consortium. In the context of the TRANSPLANTA programme we screened a subset of the transgenic collection to test the possible involvement of novel transcription factors in plant defence mechanisms against potyviral infections, especially in those using P1b as silencing suppressor.

TRANSPLANTA transgenic plant lines and infectivity validation.

ß-estradiol induction.

It has been reported that different lines in the TRANSPLANTA collection may present notable differences in response to the induction of the same transcription factor, resulting in different expression levels. To assess the response of different transgenic lines to the ß-estradiol induction, preliminary tests were performed with transgenic lines expressing GUS, in the same in vitro conditions to be used during the screening.

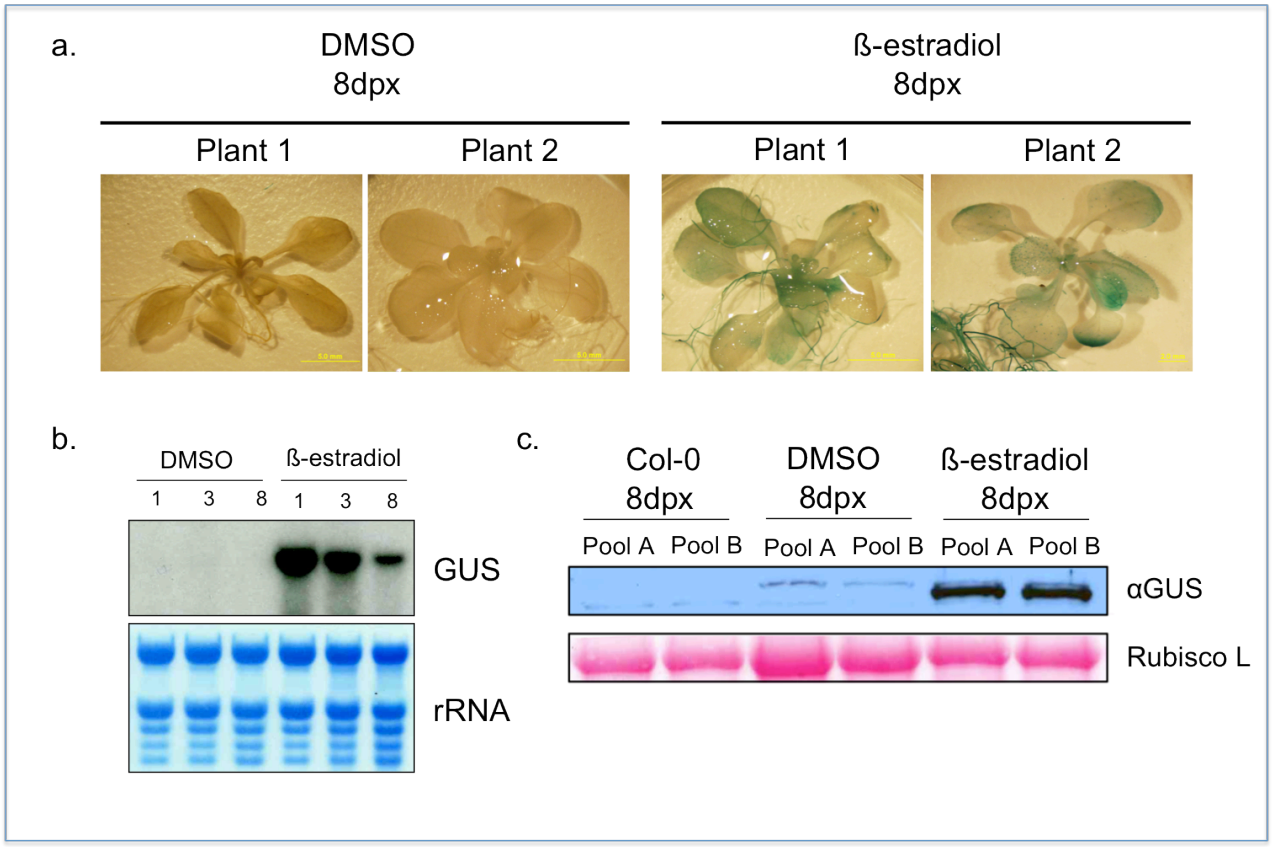

Figure 27. ß-estradiol induction of the control GUS::GFP lines. (a) Plants infiltrated under vacuum with MS media supplemented with 10µM ß-estradiol or DMSO as control. ß-glucuronidase induction was monitored at 8 days post induction (dpx) using GUS stain. Positive ß-glucuronidase shows in the form of a blue precipitate on the tissue. (b) Northern blot analysis of the GUS::GFP expression in plants infiltrated with MS media supplemented with10µM ß-estradiol or DMSO control. Each lane was loaded with 5µg of total RNA from pools of 3 plants taken at 1, 3 and 8 dpx. Detection was performed with a 600bp DNA radio-labelled probe specific to GUS. Methyl blue stained rRNA bands on the membrane are shown as loading control. (c) Western blot analysis of the ß-glucuronidase accumulation in the ß-estradiol and DMSO treated control plants shown in (a). Each lane represents pools of 3 plants. Immunoblot was performed with primary antibody against ß-glucuronidase. Ponceau red is shown as loading control.

Initial tests revealed enhancement of enzyme activity and protein accumulation in response to ß-estradiol even at 8 days post induction (dpx) (Fig. 27. a & c). Although initial published reports showed transgene induction to be rather stable over time (Zuo et al., 2000) a clear decay in the level of ß-estradiol induction was observed along the 8 day kinetic analysis performed, with a maximum transgene expression at 24 hours after induction (Fig. 27. b).

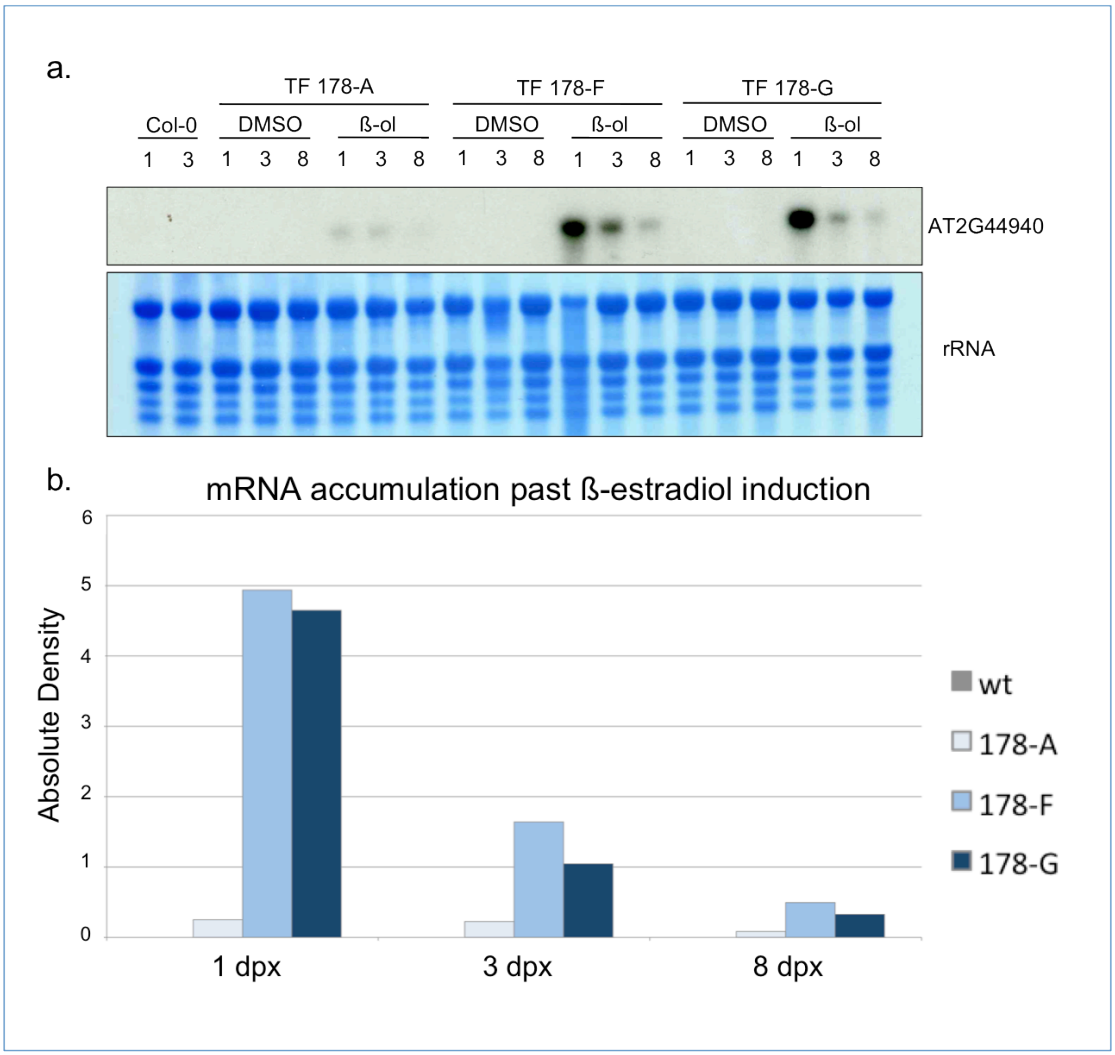

Figure 28. Northern blot analysis of the transcriptional kinetics after induction with ß-estradiol. (a) Three different independent lines for TF178 were infiltrated under vacuum with MS supplemented with 10µm ß-estradiol and grown on MS agar supplemented with 10µm ß-estradiol. DMSO treated plants were used as control. For each line and condition pools of 3 plants were collected at 1, 3, and 8 dpx as indicated. 5µg total RNA was loaded on a denaturing agarose gel and transferred to a nitrocellulose membrane. Methyl blue stained rRNA bands on the membrane are shown as loading control. Detection was performed with a 300bp radio-labelled DNA probe specific to TF178. Col-0, *A. thaliana* Col-0 wild type plants. (b) Densitometry analysis of the samples shown in (a). Absolute densities plotted for each TF line at 1, 3 and 8dpx as indicated.

Having seen that the ß-estradiol induction is not constant despite efforts in maintaining expression levels high by supplementing media with additional ß-

estradiol, interests were focused in assessing whether ß-estradiol induction is homogenous in different transgenic lines resulting in similar expression patterns. The induction of three GUS transgenic lines was tested by Northern blot analysis at different time points post ß-estradiol treatment.

In agreement with results of other TRANSPLANTA partners (Coego et al., 2014), induction kinetics showed significant transcriptional differences in between independent TRANSPLANTA lines for the same transcription factor (Fig. 28). Regardless of the transcription levels gained after induction, decay in mRNA accumulation was observed in the ß-estradiol inducted lines, including the GUS control lines (Fig. 27. b) and expression levels could not be maintained stable regardless of continuously supplementing ß-estradiol in the growth media.

Viral infectivity

To evaluate the effect of over expressing the transcription factors in the the transgenic lines of the TRANSPLANTA collection an initial evaluation on the infection dynamics of the chimeric viruses, PPV-sGFP and PPV-P1b-sGFP was performed.

Infections between the two viruses were seen to differ. PPV-sGFP infects rapidly, spreading quickly to systemic tissue via the vein bundles, avidly colonising systemic tissue at 2 days after first symptoms of infection appears (6 dpi), infecting the plant totally by 8 dpi (Fig. 29. a). PPV-P1b-sGFP, on the other hand, has a slower infection dynamics. Systemic movement of the PPV-P1b-sGFP cannot be clearly observed until 10 dpi, infection time at which GFP fluorescence is observed along the vein bundles of inoculated leaves and some systemic leaves. PPV-P1b-sGFP infected plants at 12 dpi compare, on average, to those infected by PPV-sGFP at 8 dpi, evidencing that there is a four-day lag in infection development between the two viruses for the time span considered.

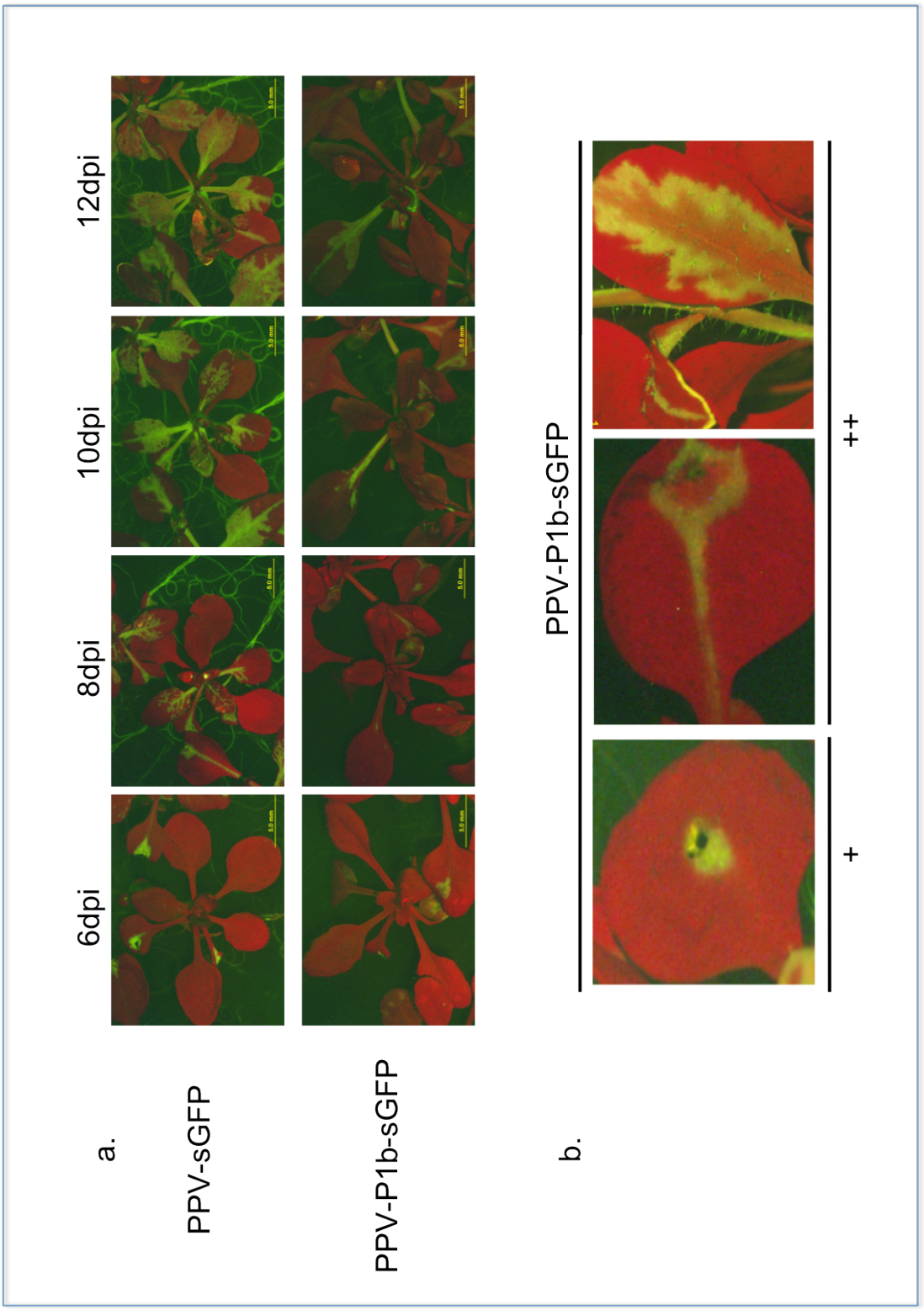

Figure 29. Evaluating viral infections using an *A. thaliana in vitro* model. (a) Infection dynamics at different days post inoculation (dpi) of the two chimerical viruses used in the screening. Three leaves from 10 days-old seedlings grown on MS agar were inoculated with agrobacteria cultures expressing PPV-sGFP or PPV-P1b-sGFP. GFP fluorescence was monitored using an epi-fluorescent stereoscope at 6, 8, 10 and 12 days post inoculation (dpi) as indicated. Scale bars represent 5mm. (b) PPV-P1b-sGFP infections shown in (a) were grouped into two infection categories: +, local infection with no signs of viral movement in the inoculated leaf; ++, signs of viral movement through the inoculated leaf and systemic spread throughout the plant colonising caulinar leaves, stem and influorescences. Pictures taken using an epi-fluorescent stereoscope at different magnitudes.

This accounts to the fact that PPV-P1b-sGFP infection is clearly compromised if compared to PPV-sGFP infections by the substitution of HCPro for P1b. Considering that PPV-P1b-sGFP shows a milder infection with lower viral accumulation, performing the screening with PPV-P1b-sGFP would represent an advantage in detecting transcription factors whose over expression might entrain less drastic, but still significant, effects on the virus. PPV-P1b-sGFP was therefore used in the screening of the TRANSPLANTA collection of *A. thaliana* transgenic lines over-expressing transcription factors after ß-estradiol induction.

Transcription factors affecting PPV infection

Two types of statistical analysis were performed during the first and second TRANSPLANTA screens. Firstly, to determine whether the over-expression of a particular transcription factor could affect infectivity, infections at early infection times (6dpi) and late infection times (10dpi) were divided into bimodal groups and infected versus not infected plants were scrutinised. GFP fluorescence of the infected plants did not show a discrete distribution, making difficult to categorise them. Thus, to assess the effect of the transcription factors tested in the severity of the infection, infected plants were divided into two distinct categories according to the GFP fluorescence observed (Fig. 29. b).

In a first screen, enhancement of PPV-P1b-sGFP infectivity was not observed after ß-estradiol induction in any of the transgenic lines tested. In contrast, the infectivity of PPV-P1b-sGFP appeared reduced, and the ability to cause systemic symptoms altered, in several induced transgenic lines when compared with the rest of lines. A second analysis was performed with these transgenic lines as well as with lines that did not show altered susceptibility to PPV-P1b-sGFP.

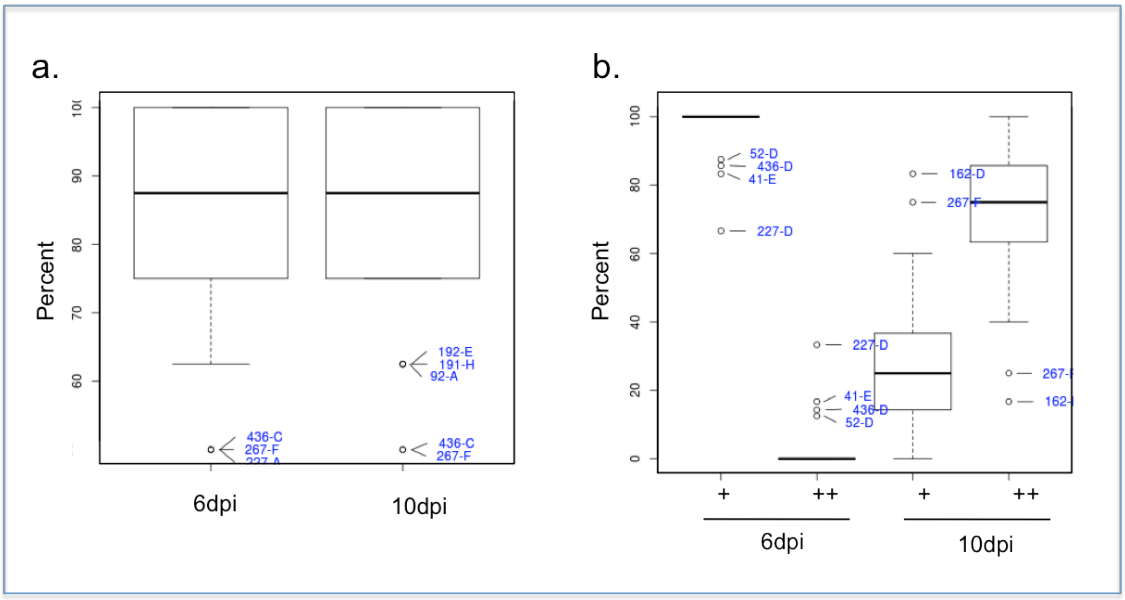

Figure 30. Statistical analysis of PPV-P1b-sGFP-infected ß-estradiol-induced transgenic lines expressing 18 transcription factors selected in a first screen as suspicious of being affected in susceptibility to PPV-P1b-sGFP. Comparison includes the results of the infected GUS control line that was assessed in parallel with the two transgenic lines for each transcription factor. Outliers show Transcription factor lines showing statistically significant differences. (a) Infectivity results at early (6dpi) and late (10dpi) infection times. (b) Systemic symptom results for both infection times analysed. Percent indicate the percentage of infected plants (a) and, among them, the percentage of plants showing systemic symptoms (b).

In this second screen, a total of 6 transcription factor lines showed a significant reduction in virus infectivity, two of which, 436-C and 267-F, showing differences at both early (6dpi) and later (10 dpi) infection times (Fig. 30. a). At 6 dpi, in the control lines and in the majority of transcription factor expressing lines, none of the infected plants showed systemic symptoms (Fig. 30. b). However, some plants from 4 different transcription factor lines showed signs of systemic infection at this early time, suggesting that the systemic movement of the virus may be favoured in this group of lines. In contrast, two lines showed a percentage of plants without systemic symptoms significantly lower than that of the rest of tested lines at 10 dpi, indicating a putative decrease in the systemic spread of the virus in these lines (Fig. 30. b).

To gain further insight into the efficiency of PPV-P1b-GFP infection, a biochemical analysis of the viral CP accumulation was performed for the transcription factor lines tested in the second screening showing differences in response to the virus.

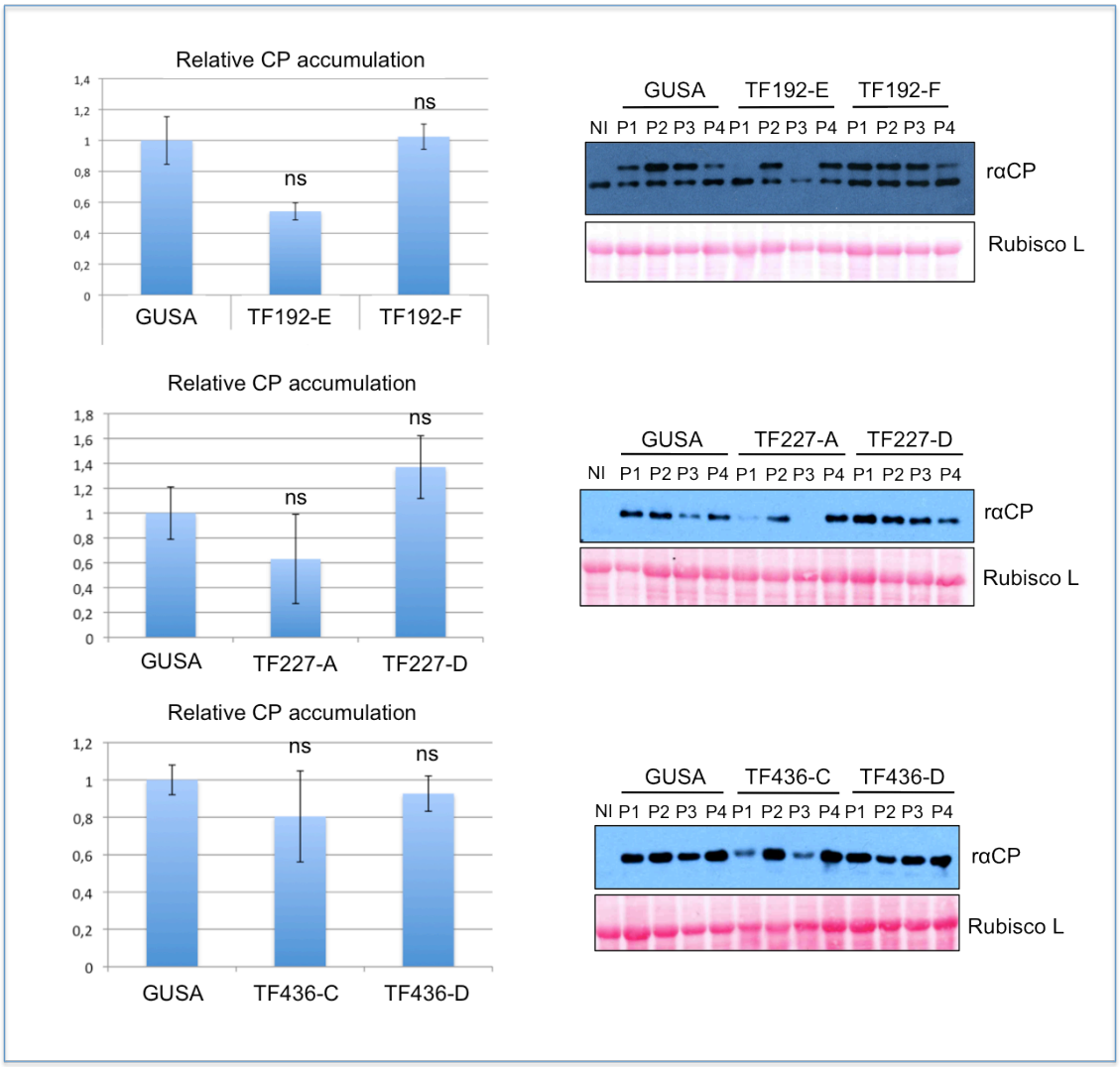

Figure 31. Biochemical analysis of the CP accumulation in the Transcription factor lines that showed infectivity differences. In each case, systemic tissue from the ß-estradiol induced GUSA control line or the TF lines shown inoculated with agrobacteria carrying pBIN-PPV-P1b-SGFP were collected at 10dpi in pools of 2 plants. Right hand side, immunoblots were performed with anti-serum raised against PPV CP protein. Ponceau Red is used as loading control. NI, non-inoculated plant sample. Left hand side, densitometry analysis of each immunoblot samples shown on the right. Mean PPV CP density plots relative to the mean of the GUSA controls. For each condition n=4. ns, no statistical differences between the TF and the GUSA samples using student's t-test. Error bars indicate standard error.

Averages of virus accumulation were lower, although the differences were not statistically significant, in 3 of the 6 outliers (TF lines 192-E, 227-A and 436-C) found during the visual screening if compared to pools of ß-estradiol induced GUS control plants (Fig. 31). From the group of 4 outliers showing an earlier viral movement (Fig. 30 b.), only one transcription factor line showed changes in CP accumulation at 10 dpi (enhanced in TF line 41-E), but also with no statistical significance (Fig. 32). On the other hand, from the group of two outliers showing a delay in viral movement, the biochemical analysis of the CP accumulation confirmed that both TF lines, 162-D and 267-F, accumulate less viral CP than their

corresponding control group of ß-estradiol induced GUS plants, but only one of the TF lines (TF line 162-D) showed a statistical confidence *p*-value of less than 0.05%.

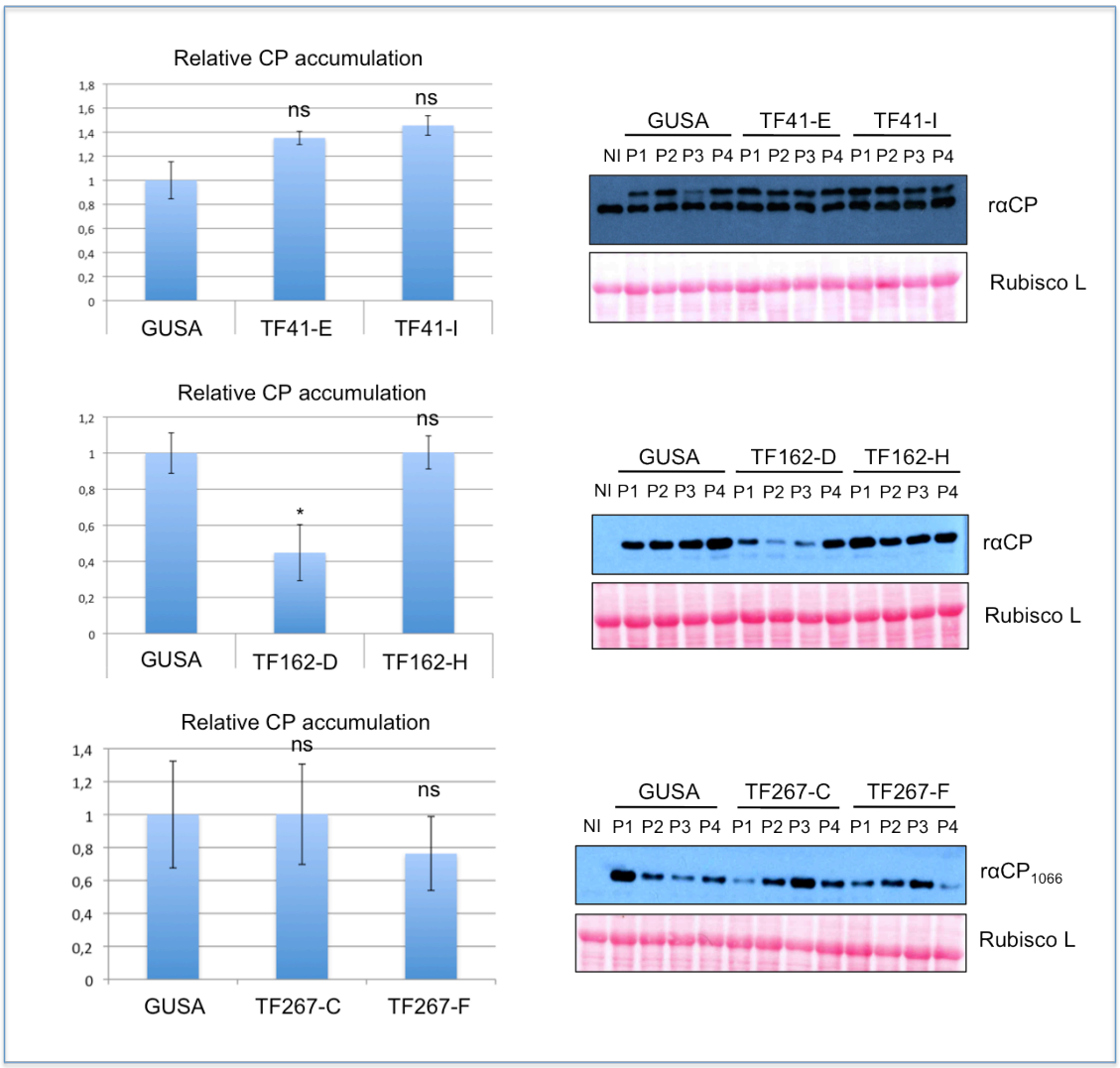

Figure 32. Biochemical analysis of the CP accumulation in the Transcription factor lines that showed differences in the category analysis. In each case, systemic tissue from the ß-estradiol induced GUSA control line or the TF lines shown inoculated with agrobacteria carrying pBIN-PPV-P1b-SGFP were collected at 10dpi in pools of 2 plants. Right hand side, immunoblots were performed with anti-serum raised against PPV CP protein. Ponceau Red is used as loading control. NI, non-inoculated plant sample. Left hand side, densitometry analysis of each immunoblot samples shown on the right. PPV CP density plots relative to the mean of the GUSA controls. For each condition n=4. ns, no statistical differences between the TF and the GUSA samples; * , pval <0.05; using student's t-test. Error bars indicate standard error.

Taken together the results of the different screenings, efficiency of PPV-P1b-GFP infection appears to be reduced in five transcription factor lines, being putatively associated with a decrease in viral infectivity in lines 192-E, 227-A and 436-C, corresponding to transcription factors annotated as BPE (AT1G59640), TBP1 (AT3G13445) and ZFP1 (AT1G80730), and to reduced viral movement in lines 162-D and 267-F, annotated as JUB1 (AT2G43000) and VND7 (AT1G71930). In

contrast efficiency of PPV-P1b-GFP infection might be enhanced for lines TF41, annotated as AGL32 (AT5G23260) as result of increased viral movement.

General comparison of screenings show no clear P1b candidate

The screenings exposed in the previous sections describe two screens searching for physical interactors of CVYV P1b, one screen searching for host proteins differentially accumulating in response to a potyvirus expressing P1b and another additional screen searching for transcription factor with effects on the infection of the P1b-expressing potyvirus. Considering that candidates identified in several independent approaches would likely have more functional relevance, a comparison was made to detect common candidates among the different screens.

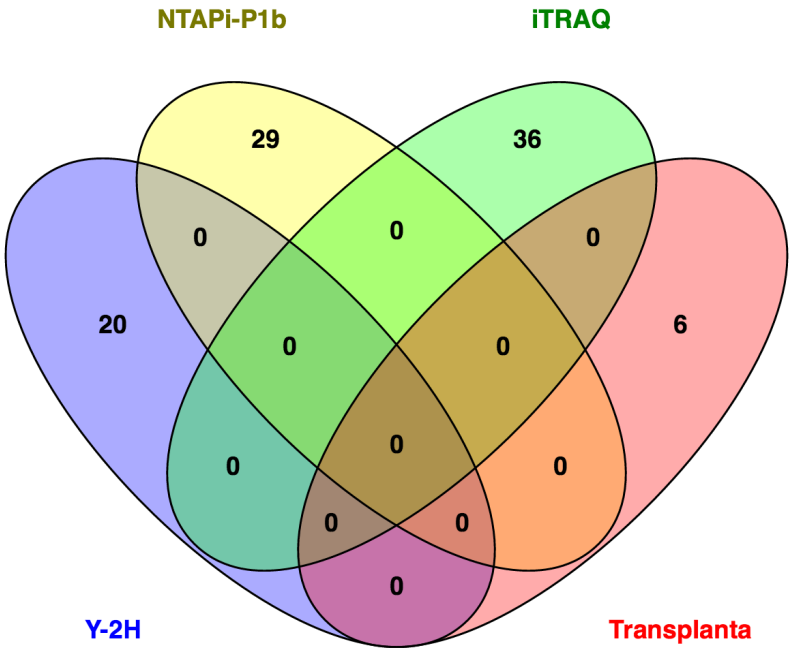

Figure 33. Venn diagram showing the relationship of the different putative P1b host factors found in the four screenings performed. Yeast two hybrid (Y-2H) provided genetic sequences corresponding to 20 genes interacting with P1b, NTAPi co-purified 29 different proteins, 36 different proteins were seen to differentially accumulate in PPV-P1b-sGFP infected samples with respect to PPV-sGFP infection, and 6 Transcription factors showed putative differences in response to PPV-P1b-sGFP infection.

Gene accessions of the 20 genetic sequences confirmed to interact with P1b in yeast, the 29 proteins co-purified with P1b using the TAP strategy from transgenic A. thaliana NTAPi-P1b expressing lines, the 36 differentially accumulating proteins detected using the comparative iTRAQ labelling between a P1b-expressing PPV virus and the wild type not expressing P1b, and the 6 Transcription Factors found to putatively affect the P1b-expressing PPV virus were compared. Regretfully, no common candidate was detected between the different screens performed (Fig. 33).

In planta validation of P1b interactions

Being unable to find any common putative CVYV P1b host partners among the four different screenings performed a group of 11 Yeast two Hybrid interactors were selected based on previous published information involving the putative interactors or similar proteins. On the other hand, the Eukaryotic Translation Initiation Factors (eIF) are among the most widespread reported host factors involved in potyvirus infections. Specifically proteins of the eIF4E/eIF(iso)4E family have been shown to be essential for infection of PPV (Nicaise et al., 2007) and other potyviruses (Lellis et al., 2002; Robaglia & Caranta, 2006). Furthermore eIF4E and eIF(iso)4E are interaction partners of the typical potyviral suppressor HCPro (Ala-Poikela et al., 2011), which can be functionally replaced by CVYV P1b, rising the suspicion if both potyviral RSSs could share the need to interact with this host factor. On the other hand PPV HCPro functionally interacts with its cognate CP protein (Blanc et al., 1997). For this reason eIF4E and eIF(iso)4E, from natural CVYV host *C. melo* and CVYV CP were added to the list of potential P1b interactors selected to be validated in planta. In planta interactions were assessed using Bi-molecular Fluorescence Complementation Assays (BiFC). BiFC technology is widely used to asses protein-protein interactions. It functions by expressing the two candidate proteins fussed to independent fragments (the N-termial residues "YF", and the C-terminal residues "P") of the Yellow Fluorescent Protein (YFP), which do not emit fluorescence if expressed alone (Kerppola, 2006). If interaction is possible, interaction of the candidate proteins, allowing for the sufficient

proximity between the YFP fragments, enables the YFP native tertiary protein-structure to reform, regaining fluorescence. In addition, the intensity of the fluorescence emitted is proportional to the strength of the interaction, with stronger levels of fluorescence indicating close or direct interactions and lower fluorescence levels suggesting weaker or more distant interactions (Morell et al., 2008). Reconstituted fluorescence can be monitored within the cell by using a fluorescent microscope allowing for the subcellular localisation of the interaction to be detected.

In order to have uniform high expression levels, agrobacteria expressing the TBSV P19 silencing suppressor were included in all the infiltration mixtures.

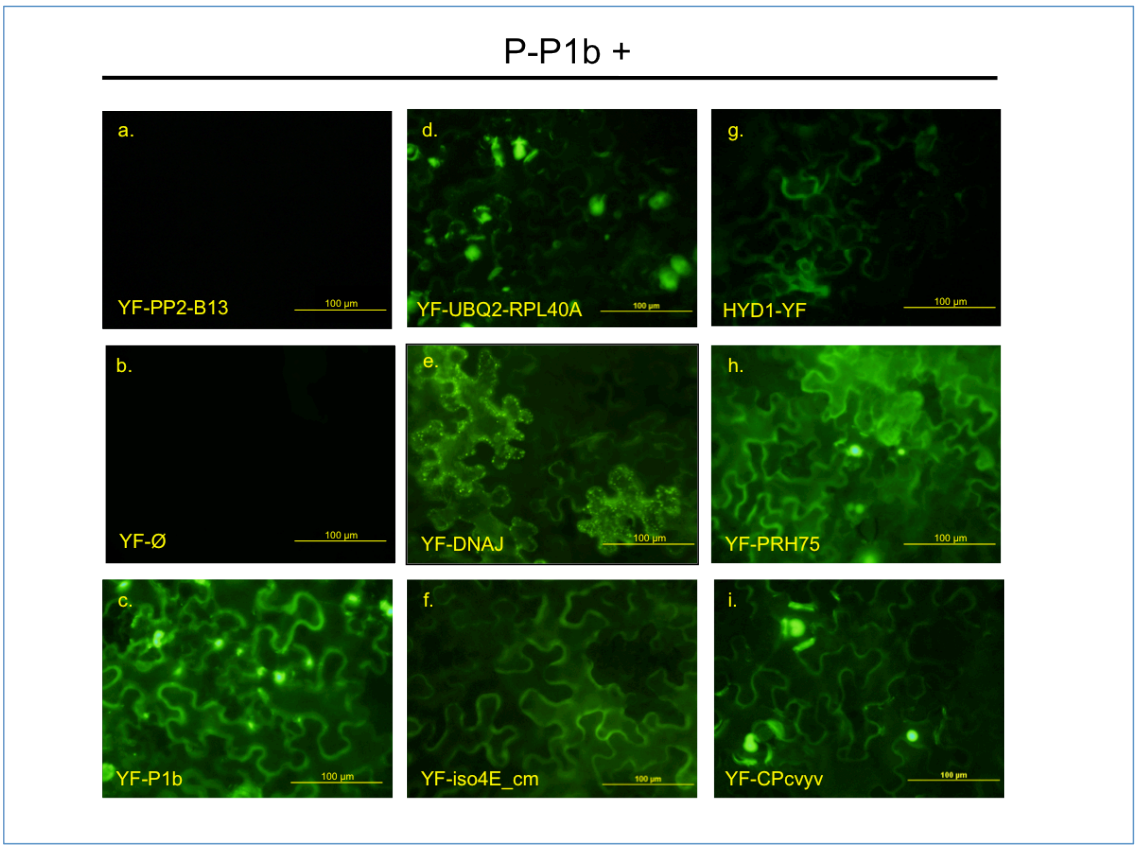

Figure 34. Bi-molecular fluorescent complementation screening in *N. benthamiana* leaves. 12 putative P1b interactors were cloned fused to the N-terminal residues of the YFP ("YF") or the C-terminal residues of the YFP ("P") on the amino or carboxyl end of the protein to be tested. Figure shows only proteins complementing YFP fluorescence using the N-terminal YFP residues fussed to the amino end of the protein. Pictures were taken using an epi-fluorescent microscope at 6 days post-agroinfiltration (dpa). Scale bars represent 100µm. (a) PP2-B13 (AT1G56240) negative control; (b) pBiFP2 empty plasmid; (c) P1b positive interaction as reported in (Valli et al. 2008); (d) UBQ2-RPL40A (AT2G36170); (e) DNAJ Chaperone (AT1G72070); (f) *C. melo* eIF(iso)4E (ICuGI MU5578); (g) HYD1 (AT1G20050); (h) PRH75 (AT5G62190); (i) CVYV Coat Protein (NCBI YP_308886).

Initial *in planta* BiFC screens revealed 5 plant proteins and CVYV CP to interact with P1b. YFP complementation was observed mainly in the cytoplasm, as would be expected from a cytosolic protein, although in certain cases bright fluorescent structures could be observed amidst the cytosolic fluorescence with varying morphologies (Fig. 34). Interaction of P1b with UBQ2-RPL40A would recurrently produce numerous amorphous inclusion-like structures very similar in size to those observed during P1b self-interaction. UBQ2-RPL40A is a fusion of ubiquitin and the ribosomal protein L40, and is used both to build ribosomes and to contribute to the bulk of the free ubiquitin pool (Callis et al., 1990; Catic & Ploegh, 2005). Thus, since UBQ2-RPL40A is tagged on its N-terminus, it would be expected to yield YF-ubiquitin subunit susceptible to be ubiquitination processes. Therefore it is likely that P1b is being ubiquitinated and the fluorescence of the structures observed in cells overexpressing P-P1b and YF-UBQ2-RPL40A results from the complementation of the P- tag of P1b with the YF- tag of ubiquitin residues modifying P1b. PRH75 and CVYV CP also showed cytosolic structures, but different from those observed in UBQ2-RPL40A-expressing cells, as structures were larger in size and perfectly round-shaped resembling nuclei. The cells expressing DNAJ chaperone, on the other hand, showed the most distinct cytosolic speckle-like structures seen occasionally in few groups of cells. None of these cytosolic fluorescent structures could be associated with cell nuclei, as no co-localisation could be seen when cells were stained with DAPI.

Among of the factors that complemented YFP fluorescence in the BiFC assays, three host proteins, PRH75, HYD1 and eIF4E, and the viral CP were chosen to investigate further.

PRH75

RNA helicases are involved in a wide variety of cellular processes within the cell. The RNA helicase gene superfamily is larger and more diverse in plant genomes than in genomes of other organisms (Linder & Owttrim, 2009) In *A. thaliana* it accounts for a total of 113 helicases, with 58 members of the DEAD/DEAH-box

RNA helicase family (Kammel et al., 2013) having diverse and complex biological functions (Lorković et al., 1997; Linder & Lasko, 2006). Although many plant RNA viruses encode RNA helicases in their viral genomes, as in the case of PPV (Laín et al., 1991), host RNA helicases are co-opted during different infection stages to satisfy molecular functions needed for the virus (Kovalev & Nagy, 2014). Since a member of the same DEAD/DEAH-box RNA helicase family was reported to be a host partner of VPg indispensible for PPV and TuMV infection (Huang et al., 2010), biological relevance of the interaction between P1b and PRH75 was further investigated.

PRH75 is part of a distinct group of the DEAD/DEAH-box Helicase family members in *Arabidopsis thaliana*.

PRH75 is a nucleus-localised basic DEAD/H-box helicase containing an N-terminal KDES domain rich in lysine, glutamic acid, aspartic acid, and serine residues, seven highly conserved helicase motifs in the central region, a GUCT domain, and a C-terminal GYR domain harboring a large number of glycine residues interrupted by either arginines or tyrosines, of 685 amino acid residues long and named according to its calculated molecular weight of 75 kDa. Its Nuclear Localisation Signal (NLS) has been mapped empirically along the first 81 amino acid residues, with the most probable motif believed to be KKKKRK (Lorković et al., 1997). PRH75 does not contain a RNA binding domain consensus sequence, instead it has been shown empirically the helicase domain VI (HRIGRTGR) to be a weak RNA binding domain and the C-terminal domain GYR to be a strong RNA binding domain, both responsible for the ATP independent binding of RNA (Lorković et al., 1997). PRH75 was detected in 500 kDa protein fractions (Lorković et al., 1997), suggesting that it is most probably not a monomeric helicase, but instead part of a large protein complex localised in the nucleoli and possibly involved in pre-ribosome assembly (Lorković et al., 1997).

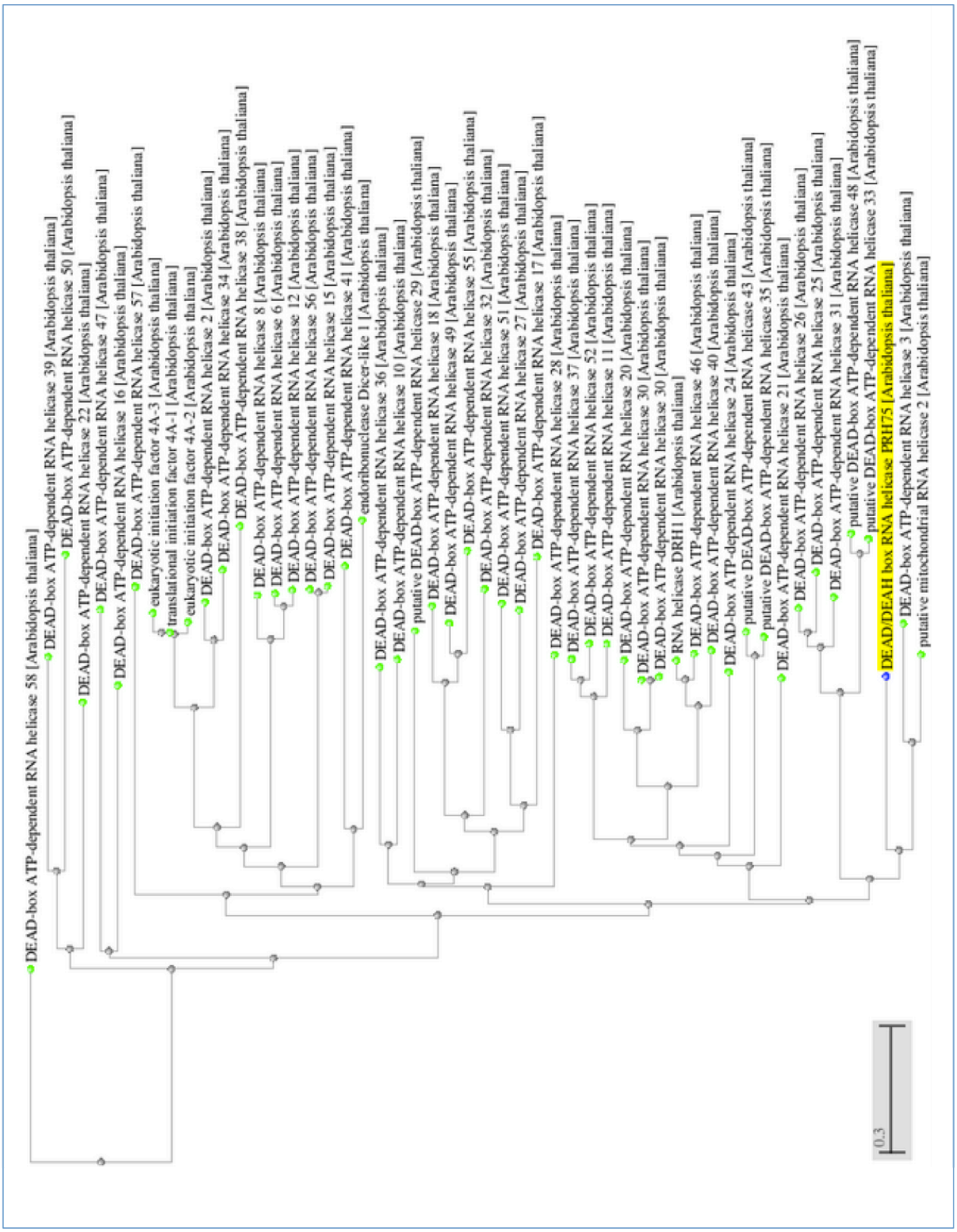

Figure 35. Distance Similarity Tree produced using BLAST pairwise alignment of *A. thaliana* PRH75 (AT5G62190) with DEAD-box helicases encoded in the genome and reported in the NCBI database. Fast minimum evolution algorithm (Desper & Gascuel, 2003) was used to produce a tree from given distances (or dissimilarities) between sequences using the Grishin distance model (Grishin, 1995) and maximum sequence difference of 0.85. PRH75 (AT5G62190) is highlighted in yellow. Scale bar represents the evolutionary distance between two sequences modeled as expected fraction of amino acid substitutions per site given the fraction of mismatched amino acids in the aligned region as calculated in (Grishin, 1995).

Similarity distance analysis shows that DEAD box helicases can be grouped in 8 clusters (Fig. 35). Whereas PRH8 described to be an indispensible PPV host factor in *A. thaliana* (Huang et al., 2010), tends to group in a broad cluster along with eIF4A-related of RNA helicases, PRH75 is situated very distant from PRH8 suggesting different roles or different molecular functions for these two helicases. The two nearest neighbors of PRH75 are PRH3 and Putative mitochondrial RNA Helicase 2 (PMH2/PRH53). These three proteins were previously grouped in a single common clade (Asakura et al., 2012), suggesting they could have redundant or overlapping functions. PRH3 and PMH2 are both believed to function as RNA chaperones in RNA splicing of group II introns (Köhler et al., 2010; Asakura et al., 2012; Gu et al., 2014) and involved in 50S Ribosome subunit assembly (Matthes et al., 2007; Asakura et al., 2012). However, whereas PMH2 has been reported to localise in mitochondria (Matthes et al., 2007; Asakura et al., 2012), PRH3 appears to be targeted to the chloroplast (Baginsky et al., 2007; Asakura et al., 2012; Lee et al., 2013). Thus, PRH3 is believed to be the plastid orthologue of PMH2 (Matthes et al., 2007), raising the question of whether PRH75 could be the nuclear orthologue of both PRH3 and PMH2.

Central C-terminal region of *A. thaliana* PRH75 ($PRH75_{405-614}$) is highly similar to Cucurbit PRH7 and interacts with P1b.

A 209 residue long fragment of PRH75 was found to interact with P1b during the yeast two hybrid mating screens performed. It is located in the C- terminal half of the protein and includes two DEAD-box core domains (V and VI) (Lorković et al., 1997) and a GUCT domain (Asakura et al., 2012) (Fig. 36. a). The complete PRH75 sequence was cloned fused to the sequence coding for the AD domain of GAL4 in the plasmid pGADT7 and the AD-PRH75 fusion protein co-expressed with CVYV P1b fusion fused to the BD domain of GAL4 (BD-P1b). Cell growth in SD-4 media supplemented with 3-AT revealed that P1b interacts with the complete PRH75 protein, although cell proliferation was lower than that of cells expressing the former 209 residue long C-terminal fragment, suggesting a some weaker interaction (Fig. 36. b).

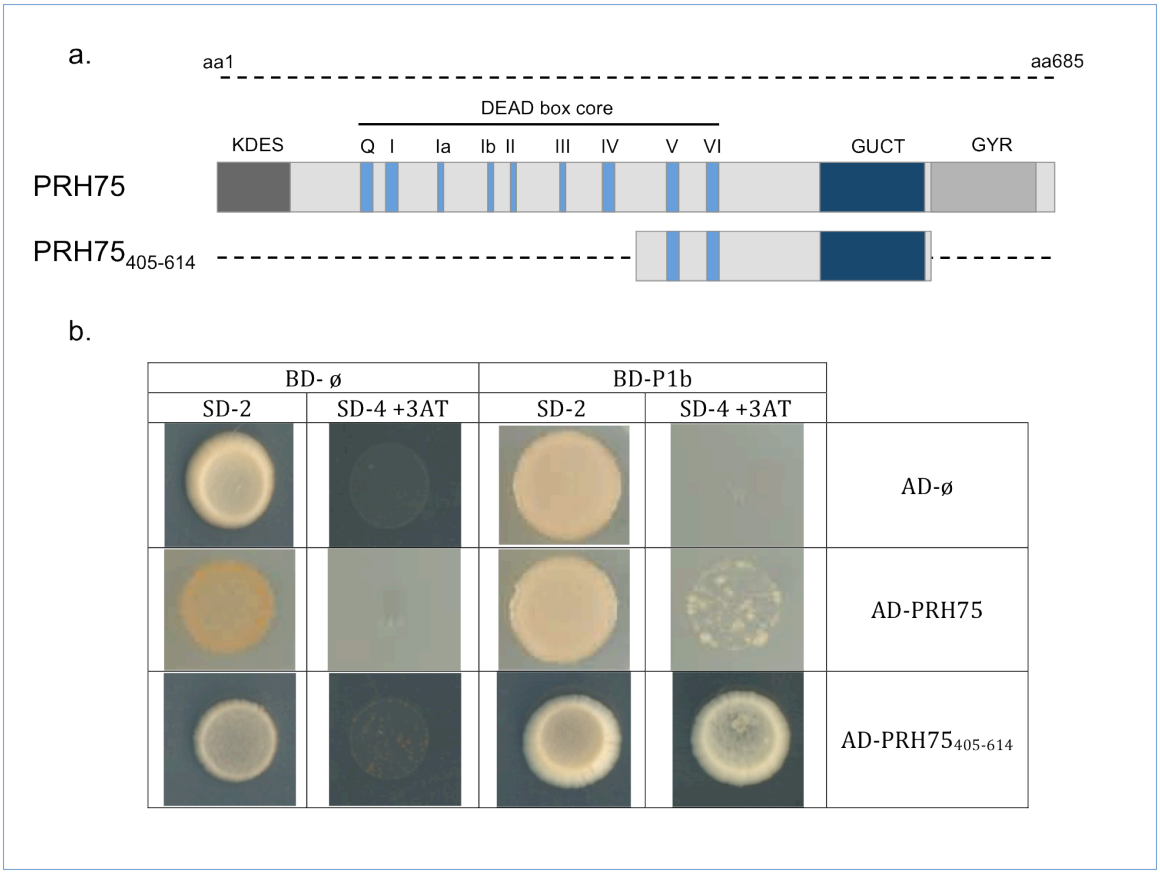

Figure 36. Full length PRH75 and a core fragment of PRH75 interact with P1b in yeast. (a) Diagram of the PRH75 complete protein sequences with the functional domains previously described and the peptide sequence recovered in the mating screen and used in the Y-2H interaction experiments. (b) Y-2H interaction assay of the PRH75$_{405-614}$ fragment and the PRH75 complete protein. Yeast cells activate reporter genes and growth is observed on SD-4 restrictive media supplemented with 3-AT when P1b is co-transformed with the complete PRH75 sequence or the sequence corresponding to the central PRH75 region indicating interaction between both sequences.

The PRH75$_{405-614}$ fragment displays high similarity to the equivalent regions of PRH75 orthologues from other plant species. Curiously the nearest neighbors of the Arabidopsis sequences are from the PRH7 helicases of two *Cucumis* species (Fig. 37), both of them being natural CVYV hosts. Although this is not conclusive evidence that PRH7 proteins from *Cucumis* species are host partners of P1b, it indicates that P1b could encounter a sequence similar to its Y2H interactor in the natural virus infection.

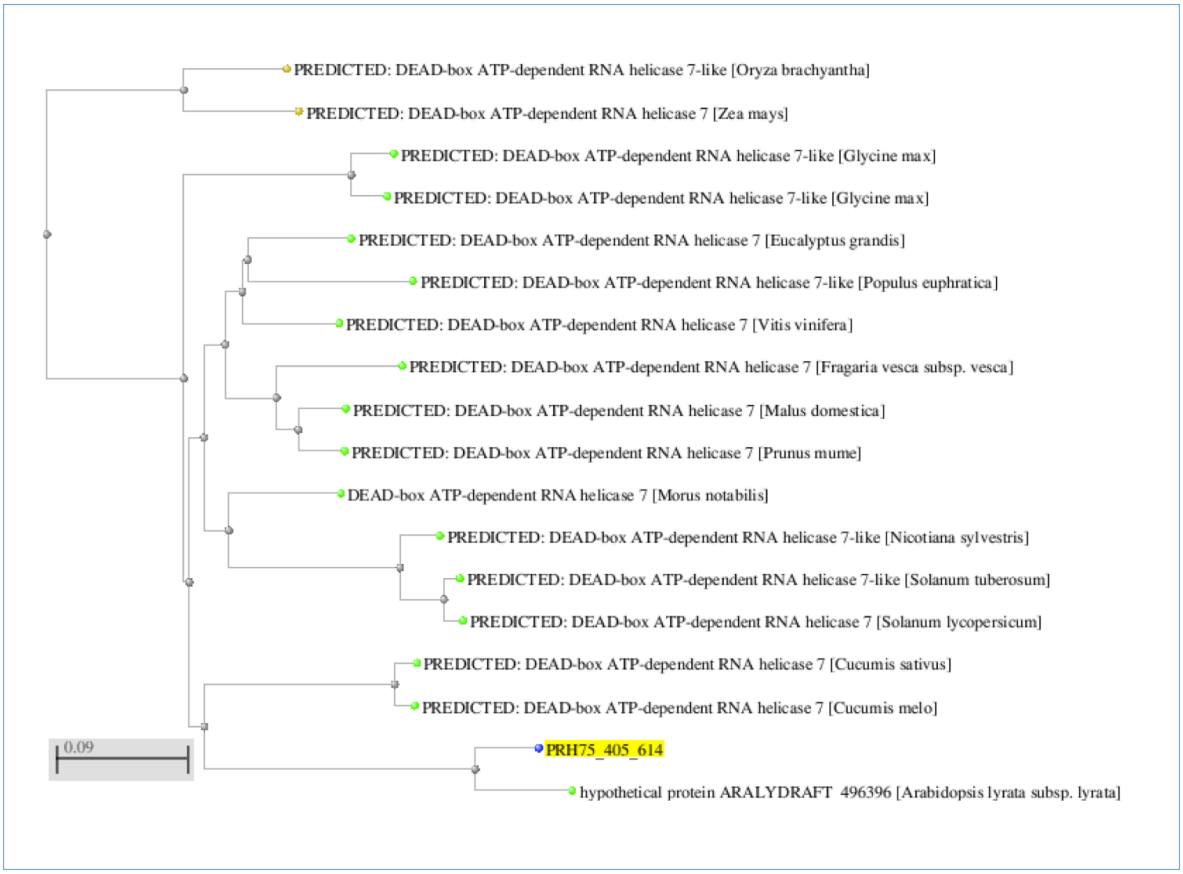

Figure 37. Distance Similarity Tree produced using BLAST pairwise alignment of *A. thaliana* PRH75$_{405-614}$ with PRH75 orthologues from different plant species reported in the databases. Fast minimum evolution algorithm (Desper & Gascuel, 2003) was used to produce a tree from given distances (or dissimilarities) between sequences using the Grishin distance model (Grishin, 1995) and maximum sequence difference of 0.85. PRH75$_{405-614}$ is highlighted in yellow. Scale bar represents the evolutionary distance between two sequences modelled as expected fraction of amino acid substitutions per site given the fraction of mismatched amino acids in the aligned region as calculated in (Grishin, 1995).

N-terminal or C-terminal GFP tags do not affect nuclear localisation of PRH75.

PRH75 has been reported to be a nuclear helicase (Lorković et al., 1997), localising both in the nuclei, including nucleoli, of tobacco leaf protoplasts (Fig. 38. a). Fusion of its N-terminal 81 aa to GUS, where the nuclear localisation signal was empirically located (see above), conferred the same localisation pattern as PRH75 (Fig. 38. a). This same localisation pattern was observed in *N. benthamiana* leaves agroinfiltrated to express a full-length PRH75 fused to two fluorescent protein variants, mCherry or GFP at its C- or N-termini, respectively, under an epi-fluorescence microscope (Fig. 38. b). A more detailed view of the fluorescent structures could be observed using a confocal microscope (Fig. 38. c) showing PRH75-mCherry to localise in the nucleus, including the nucleolus, as can be seen

by counterstaining the nuclei with DAPI, a DNA intercalating fluorophore that does not stain nucleoli. Thus, transient over expression and C- or N- terminal tagging do not seem to affect the sub-cellular localisation of PRH75.

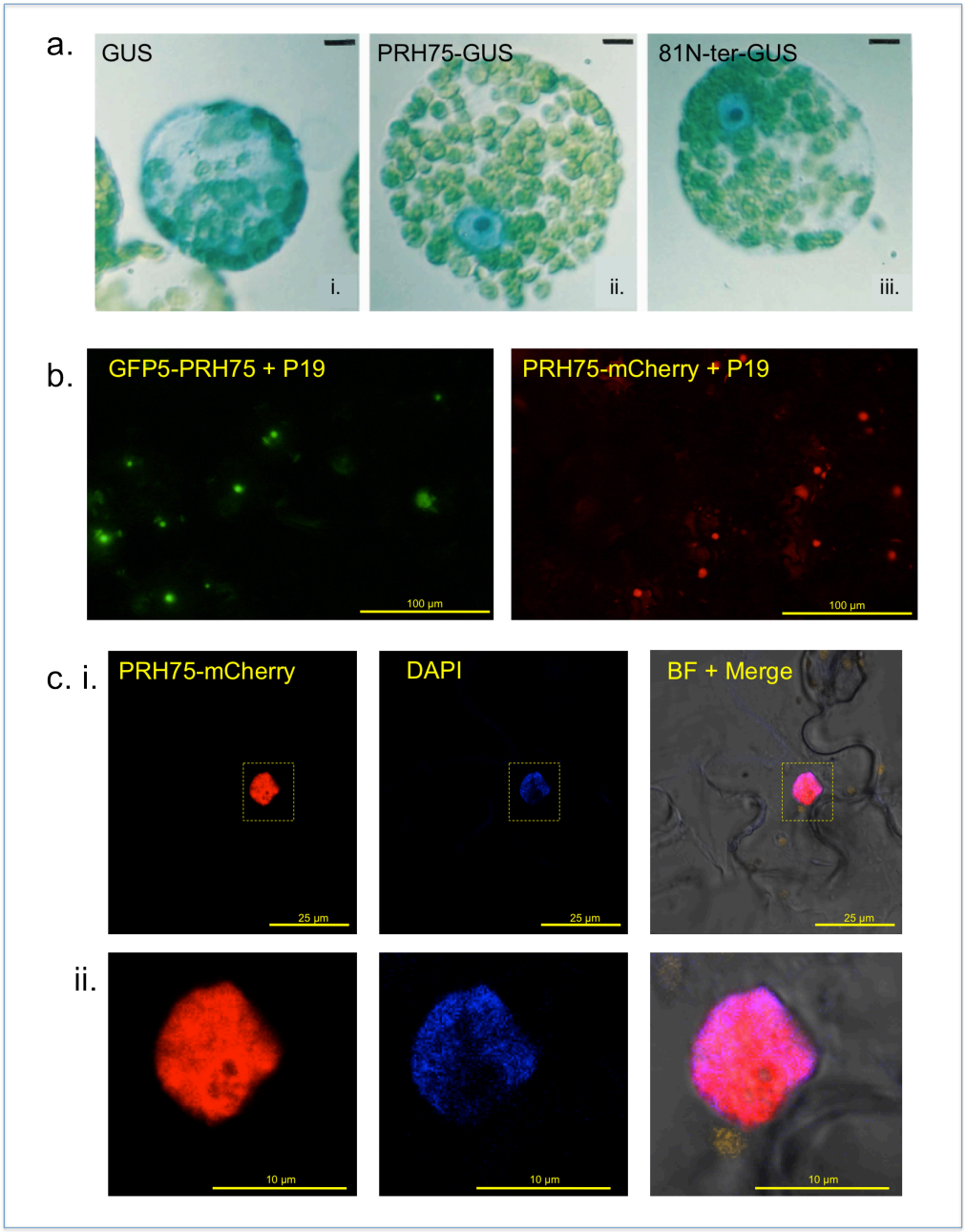

Figure 38. PRH75 localises in the nuclei and nucleoli of plant cells. (a) PRH75 localisation as reported in (Lorković et al., 1997) in Tobacco protoplasts. Images from (Lorković et al., 1997) with modifications. (i), GUS expression. (ii), PRH75-GUS fusion expression localising in the nucleus and nucleolus. (iii), 81 leader residues of PRH75 fused to GUS localising in the nucleus and nucleolus. Bars represent 10µm. (b) Transient expression in *N. benthamiana* leaves of two PRH75 fusion proteins as seen under an epi-fluorescent UV microscope at 6dpa. GFP fusions of PRH75, on the N-terminus (in green) and on the C-terminus (in red) were co-expressed with Tombusvirus RSS P19 to maximise expression levels. Scale bars represent 100µm. (c) Transient expression in *N. benthamiana* leaves C-terminal fusion protein PRH75-mCherry as seen under a confocal microscope (in red), DAPI counterstained nuclei (in blue) and the Bright Field merge of both at a low magnification (i) and at high magnification showing the details in the box (ii). Scale bars represent 25µm in (i), and 10µm in (ii).

PRH75 interacts with P1b in *N. benthamiana* leaves and this interaction causes a dis-localisation of PRH75 from the nucleus.

PRH75 coding sequence was cloned in BiFC plasmids and expressed together with P1b to test for *in planta* interaction between P1b and the complete PRH75 protein. Split portions of the YFP containing the N-terminal residues (YF-) or the C-terminal residues (P-) were fused to the N-terminus or the C-terminus of PRH75 and all four combinations (YF-PRH75, P-PRH75, PRH75-YF, PRH75-P) were tested against P1b fused with split YFP tags at its N-end, already reported to retain RSS activity (Valli et al., 2008). Of the four combinations tested, only YF-PRH75/P-P1b showed YFP fluorescent complementation (Fig. 39. a). The absence of complementation was not due to low expression of P1b, since the levels of this protein were not higher in fluorescent than in non-fluorescent leaves (Fig. 39. b).

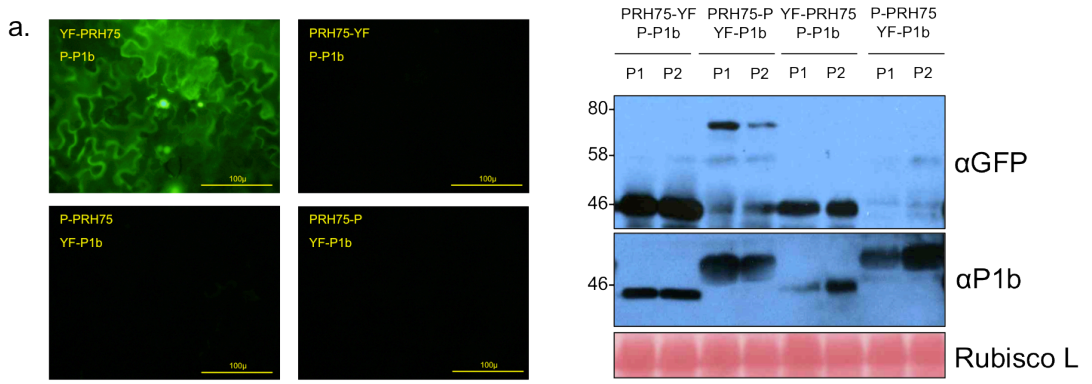

Figure 39. P1b interacts with PRH75 in plant leaves. (a) Bi-molecular fluorescent complementation of the four PRH75 fusion proteins (N-terminal YFP residues "YF" and C-terminal YFP residues "P" used). Pictures taken under a epi-fluorescent microscope 6 dpa and are representative of 2 leaves from 2 plants co-expressing the construct shown together with the RSS TBSV P19 to maximise expression levels. Only YF-PRH75 was seen to complement fluorescent with P-P1b. Scale bars represent 100µm. (b) Western blot analysis of the samples reveal similar P1b protein accumulation levels, but only PRH75-P could be detected, which was used as a negative control. P-PRH75 did not complement fluorescence mainly because no P-PRH75 protein accumulation could be detected. Immunoblot was performed with anti-serum raised against P1b and primary monoclonal antibody against GFP for detecting P-PRH75. Positions of the corresponding pre-stained molecular weight standards (in kDa) running on the same gel are shown on the left. Ponceau Red was used as loading control.

The anti-GFP antibody only recognised efficiently the P-tagged proteins, precluding to soundly assess YF-PRH75 and PRH75-YF accumulation levels. PRH75-P, but not P-PRH75, was detected when expressed together with YF-P1b

(Fig. 39. b), suggesting that the failure to detect fluorescent complementation in the P-PRH75/YF-P1b combination could be caused by inefficient synthesis or enhanced instability of the P-PRH75 fusion product.

Interestingly, despite GFP- or mCherry- tagged PRH75 was only detected in the nucleus when expressed alone (Fig. 38. b) fluorescence derived from the BiFC of YF-PRH75 and P-P1b could be seen mainly in what could seem like cytoplasm (Fig. 39. a), suggesting the interaction with P1b to be delocalising PRH75 from its canonical nuclear localisation to another cell compartment where it plays a virus-related function.

T-DNA insertion in PRH75 could confer partial resistance to PPV-P1b-sGFP

Different T-DNA insertion lines were inoculated with PPV-P1b-sGFP to examine whether loss of function of the PRH75 allele could compromise P1b functions and/or PPV-P1b-sGFP viral accumulation. PRH75 knock out mutants have been reported previously to be embryo-defective (Chen et al., 2010; Nayak et al., 2013) and attempts in obtaining homozygous PRH75 *loss-of-function* lines were unsuccessful. No differences in PPV CP accumulation could be observed in infected plants of different stocks of several T-DNA insertion lines. However, one transgenic line (SAIL_302_D12.v1) with T-DNA inserted in the 5' UTR showed a noticeable reduction in systemic, but not in local, PPV-P1b-sGFP CP accumulation compared to a transgenic control line (Fig. 40). Furthermore, this T-DNA insertion line presented no differences in CP accumulation when infected with the wild type PPV-sGFP virus (Fig. 40), manifesting that the possible effect of PRH75 on PPV infection might be P1b-specific.

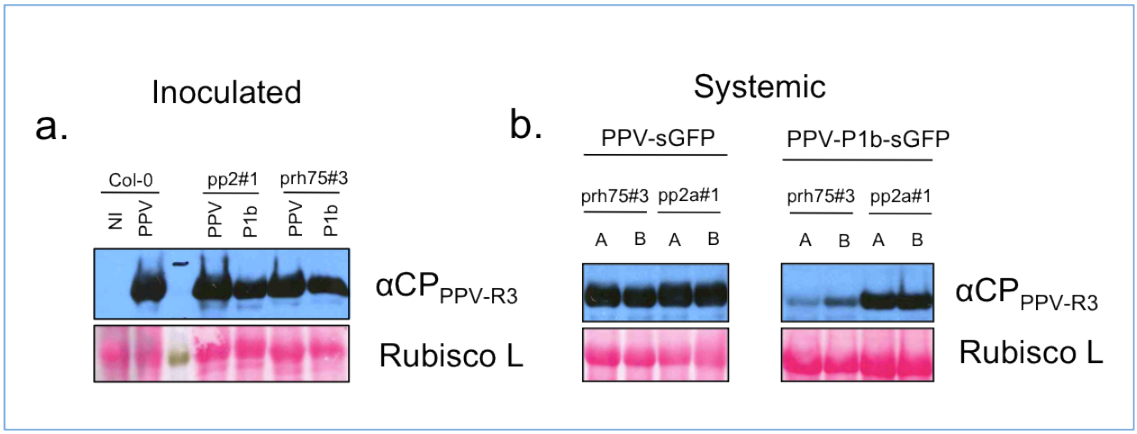

Figure 40. PRH75 mutant plants are partially susceptible to PPV-P1b-sGFP infection. Western blot analysis of the CP accumulation in pools of inoculated leaf tissue (a), and systemic plant tissue (b), of *A thaliana* T-DNA insertion mutant line prh75a#3 (SAIL_302_D12.v1) and pp2a#1 (SALK_144757.54.50.X) control line infected with PPV-sGFP or PPV-P1b-sGFP. Both A and B are pools of four infected plants. NI, refers to Non Inoculated negative control pool. Immunoblots were performed with anti-serum raised against PPV CP. Ponceau Red was used as loading control.

A relative comparison of the CP accumulation between mutant line prh75#3 and the control mutant line pp2a#1 was perfomed, trying to assess the fold-change in accumulation levels. Serial dilutions of pp2a#1 samples were performed in non-infected protein extracts and subjected to electrophoresis and immunoblot detection against PPV CP. The resulting film exposures were used to perform a densitometry analysis of the CP protein present in the samples. From the dilutions tested, only the 1:10 dilution could be used to determine the aproximate change in CP accumulation. Results show that in the PPV-P1b-sGFP infected prh75a#3 mutant plant samples, CP accumulation is at least 10 times less than in the control pp2a#1 plant lines (Fig. 41).

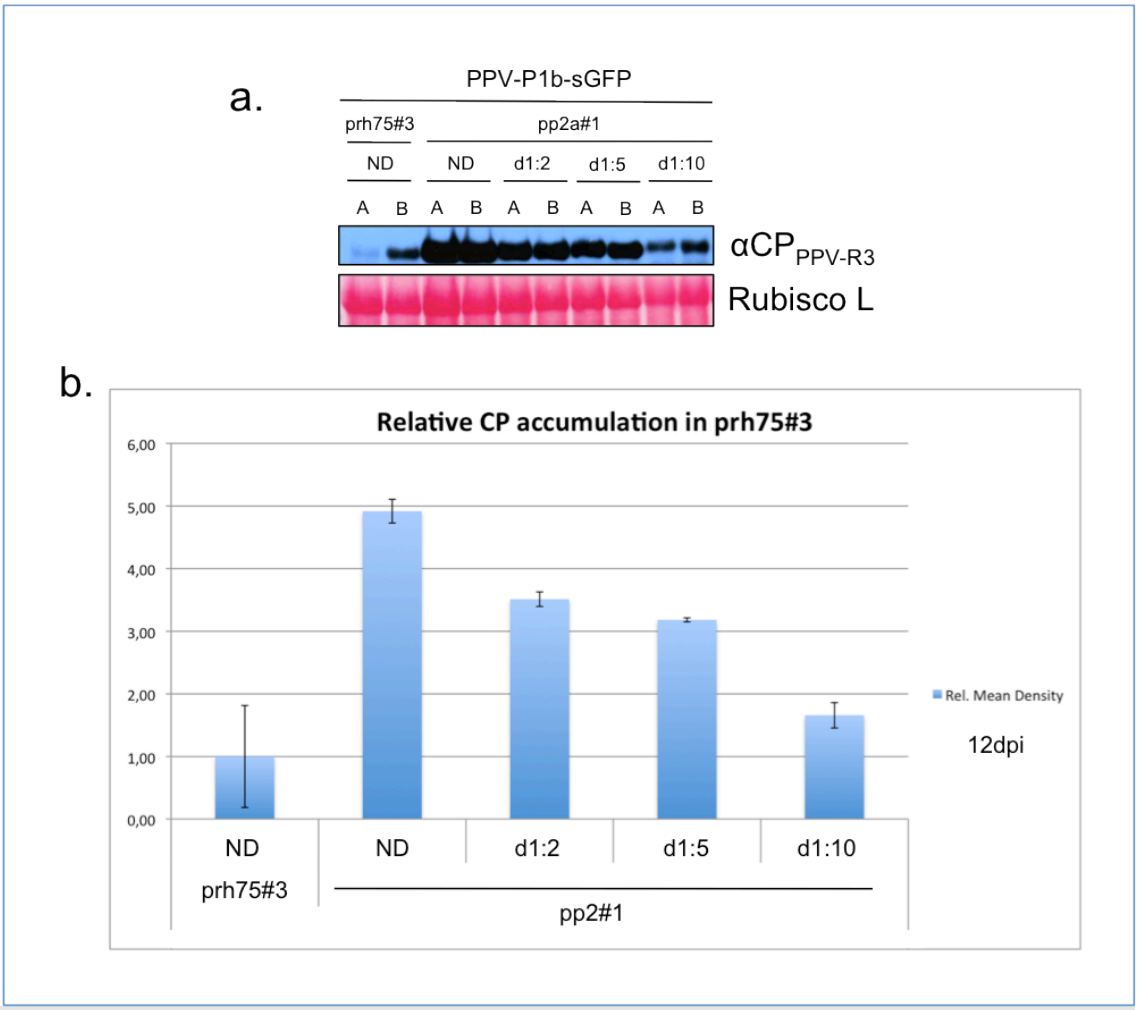

Figure 41. Comparison between the CP accumulation of *A thaliana* T-DNA insertion mutant lines shown in Fig. 34. (a) Immunoblot of prh75a#3 (SAIL_302_D12.v1) and pp2a#1 (SALK_144757.54.50.X) infected with PPV-P1b-sGFP and three serial dilutions of the same pp2a#1 infected samples. ND, not diluted; d1:2, x2 dilution; d1:5, x5 dilution; d1:10, x10 dilution. Samples were diluted in non-infected protein extract and equal volumes loaded. Both A and B are pools of four infected plants collected at 12dpi. Immunoblots were performed with anti-serum raised against PPV CP. Ponceau Red was used as loading control. (b) Densityplots of the CP accumulation shown in (a). Mean densities are shown relative to the mean of the pp75a#3 samples. PPV CP accumulation in prh75#3 mutant line is at least 10 times lower than in the control line pp2#1. Error bars represent standard error.

To determine that the effect observed is not serendipitous and PRH75 protein is indeed involved in the decrease of CP accumulation seen in PPV-P1b-sGFP, a more exhaustive and in depth study of the expression and PRH75 protein accumulation levels is encouraged.

HYD1

HYDRA1 (HYD1), an endoplasmic reticulum and plasma membrane localised (Schrick et al., 2004) C-8 sterol isomerase has been involved in sterols biosynthesis, auxin and ethylene signalling, cell wall and cellulose synthesis, shoot

and root meristem functions, vascular development and stomatal lineage maintenance (Schrick et al., 2002; Souter et al., 2002). HYD1 has also been involved in regulation of the miRNA pathway of RNA silencing (Brodersen et al., 2008) by affecting the membrane bound activation of AGO1 (Brodersen et al., 2012). Mutations in HYD1 greatly affect miRNA accumulation (Brodersen et al., 2012), and mutant phenotypes cannot be restored by exogenous brassinosteroid or sterol supplementation (Schrick et al., 2002), suggesting that other protein function than its catalytic isomerase activity is needed for the correct miRNA-related function. HYD1 was found to interact in initial yeast two hybrid mating screens using P1b as bait. Sequencing of the recovered plasmid revealed an insertion between the AD domain and the beginning of the HYD1 CDS producing a +1 frameshift, which under standard circumstances, would have been regarded as an aberrant interaction. However, umpteen cases demonstrating that frameshifting events corresponding to a -1 and a +1 reading, can occur and are selected for in yeast two-hybrid screens via the production of the frame-shifted fusion proteins have been reported (Giot et al., 2003; Albers et al., 2004). For this reason, and the notorious involvement of HYD1 in miRNA regulation, this putative P1b interactor was chosen to be investigated further.

HYD1 interacts with P1b *in planta.*

To test whether HYD1 could interact with P1b in a plant-based interaction system, HYD1 CDS was cloned in BiFP plasmids However, *in silico* analysis of HYD1 sequence revealed the possibility of HYD1 containing a hydrophobic leader sequence which would be used to correctly anchor HYD1 protein on the Endoplasmic Reticulum (ER) membrane and would be proteolytically processed as has been reported for its *H. sapiens* orthologue. As a result, HYD1 could only accept tags on its C-terminus, for which the -P and -YF regions of the YFP were used. Interaction assay was performed with the wild type P1b and the P1b mutant 6, with the C103A substitution, which affects the Zinc-finger domain of the protein and prevents its proper structural arrangement, and has been previously reported to have lost its self-interaction properties and RSS activity (Valli et al., 2008) as a negative interaction control. HYD1 complemented the YFP fluorescence when

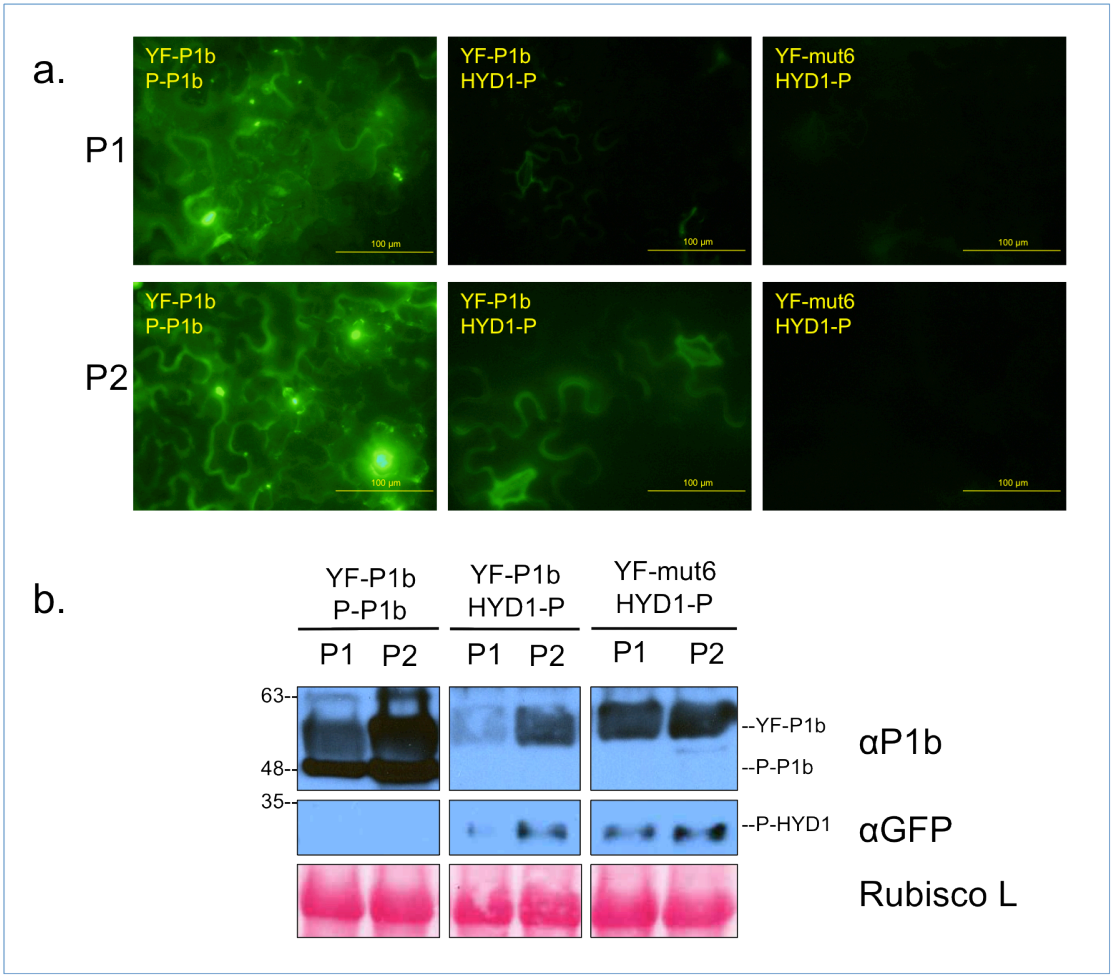

Figure 42. P1b and HYD1 interact in plant leaves. (a) BiFC of HYD1-P with two P1b alleles, a non-functional P1b mutant C103A allele (YF-mut6) and the wild type functional allele (YF-P1b). P1b self-interaction between YF-P1b and P-P1b was used as positive control. Images taken from agroinfiltrated leaves using an epi-fluorescent microscope from two independent plant samples (P1 & P2) at 6dpa. TBSV RSS P19 was co-expressed in all samples to sustain protein accumulation. Scale bars represent 100µm. (b) Western blot analysis showing protein accumulation levels. Each lane represents a pool of two agroinfiltrated leaves from two independent plants (P1 & P2). Immunoblots were performed with anti-serum raised against P1b or primary monoclonal antibody against GFP for detecting "P" tagged proteins. Positions of the corresponding pre-stained molecular weight (in kDa) running on the same gel are shown on the left. Ponceau Red was used as loading control.

Results

tagged with either the N- or C-terminus of YFP and co-expressed with its complementary P1b fusion protein (Fig. 42. a). Thus, HYD1 interacts physically *in planta* with P1b, despite having the putative interactor been initially selected on a frame-shifted fusion protein in yeast two hybrid. No fluorescent complementation could be observed, on the other hand, when co-expression of HYD1 with the non-functional P1b Zinc-finger mutant 6 (P1bmut6) was assessed (Fig. 42. a). Since the protein accumulation levels were similar both in the complementing (wt P1b) and the non-complementing (P1bmut6) samples (Fig. 42. b), it appears that P1b/HYD1 interaction is dependent on a correct folding of P1b. It is interesting to remark that

HYD1 interacted with the P1bmut6 in the Y-2H assay (Fig. 12 & 13), suggesting that the interaction in the natural system might have more stringent requirements than in the heterologous one.

Having confirmed that HYD1 interacts with P1b, and considering the biological relevance of HYD1 in key processes of sterol synthesis and miRNA function, results motivated further research on the functional relevance of the HYD1/P1b interaction in the context of viral infection.

P1b RSS activity is challenged when co-expressed with HYD1.

Initial expression experiment revealed that co-expression of HYD1-P and YF-P1b was a challenge. Over expression of genetic products usually results in the triggering of the RNA silencing machinery and it has become generally accepted that transient expressions are greatly improved by co-expression of RSS proteins. Furthermore, to this date, there are no reports presenting any compound or protein with sufficiently strong antagonic effects against RSS proteins to inhibit RSS activity, making co-expression with RSS proteins a sure bet to achieve gene expression and protein accumulation.

Attempts in co-expressing YF-P1b with HYD1-P all rendered a loss of YF-P1b protein accumulation levels at late expression times (6 dpa) although protein accumulation could be seen at an earlier expression times (3 dpa) with no considerable differences with its controls (Fig. 43. a). This shows that the constructs express their protein products correctly, but YF-P1b is not able to maintain high accumulation levels in the presence of HYD1-P, despite YF-P1b having been reported to entrain efficient RSS activity (Valli et al., 2008). Furthermore, whereas co-expression of the GFP5 reporter gene with YF-P1b sustained high accumulation levels of both proteins, effects on the expression of the same reporter were drastically reduced when co-expression of YF-P1b was accompanied with HYD1-P (Fig. 43. b).

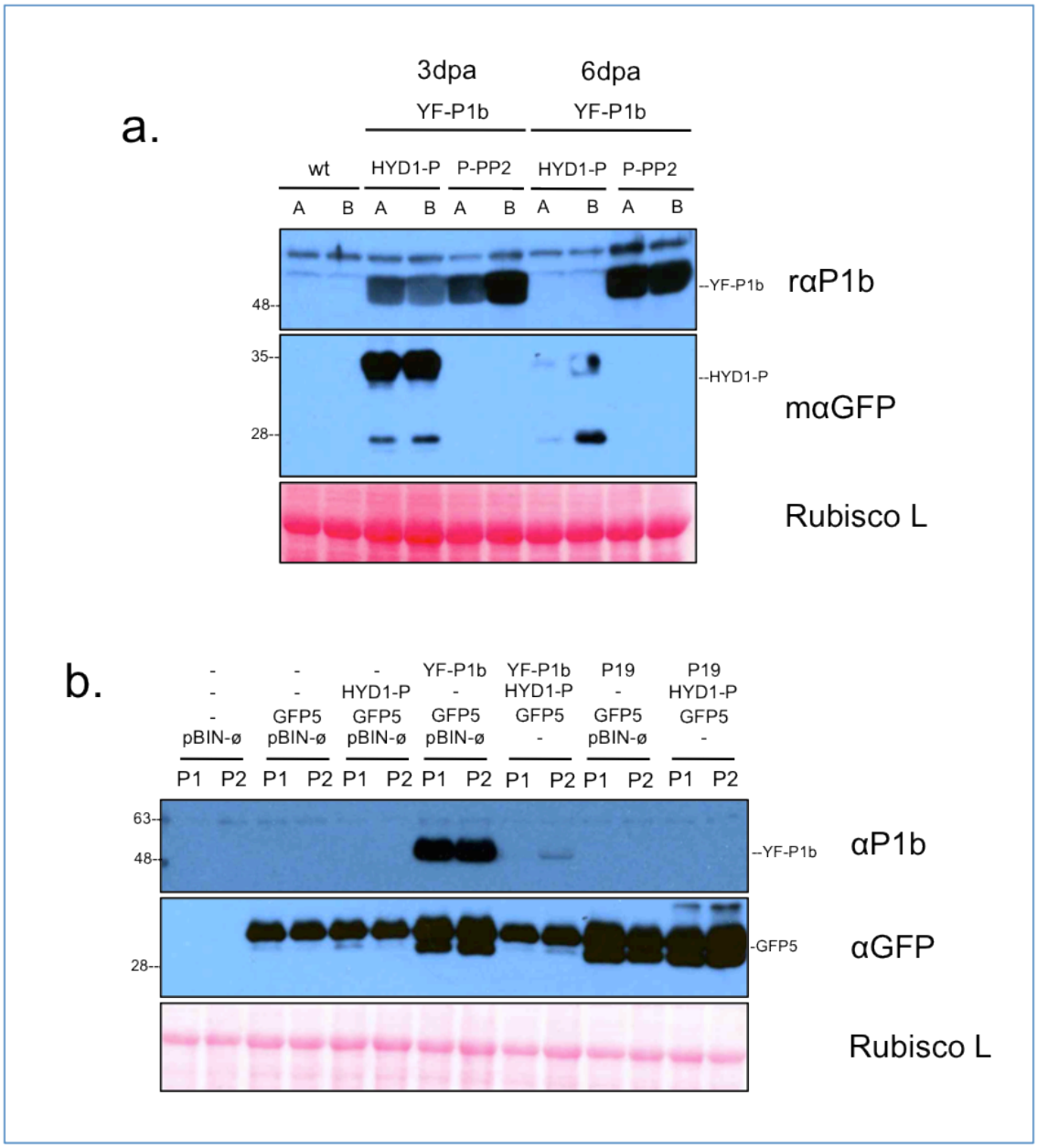

Figure 43. HYD1 affects P1b protein accumulation. Western blot analysis of P1b protein accumulation in co-expression with HYD1. (a) Leaf samples agroinfiltrated with cultures expressing YF-P1b and HYD-1P or P-PP2-B13 constructs taken at 3 and 6 dpa. Each lane (A or B) represents pools of 2 agroinfiltrated leaves from 2 plants. wt are samples not agroinfiltrated. (b) Leaf samples agroinfiltrated with the indicated constructs: GFP5, P19, YF-P1b, HYD1-P and the empty vector pBIN-ø in the combinations shown and collected 6 dpa. Each lane represents pools of 2 agroinfiltrated leaves from individual plants (P1 and P2). Immunoblots were performed with anti-serum raised against P1b or monoclonal antibody against GFP. Positions of the corresponding pre-stained molecular weight standards (in kDa) running on the same gel are shown on the left. Ponceau Red was used as loading control.

In contrast enhancement of GFP accumulation by another silencing suppressor, TBSV P19, was not affected by HYD1-P expression. These initial observations suggested that HYD1 could be stimulating the RNA silencing of the transcripts by challenging the RSS activity of P1b.

To investigate further on the possible effect of HYD1 on the RNA silencing pathway, biochemical analyses on mRNA and small RNA accumulation were performed.

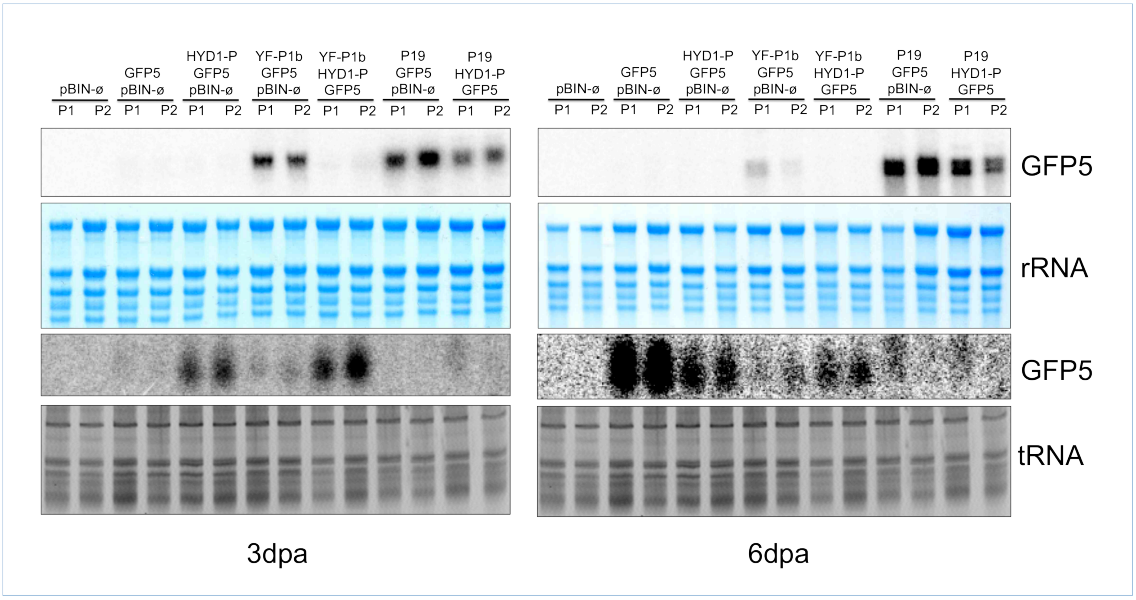

Figure 44. HYD1 expression affects mRNA accumulation. Northern blot analysis of the mRNA and smRNA accumulation extracted from agroinfiltraded leaves with the mixtures indicated above each lane and at early days post agroinfiltration (3dpa) and late days post agroinfiltration (6dpa). Methyl blue and EthBr staining are used as loading controls. Samples at 6dpa correspond to the same samples of Fig. 37. (b). Each lane represents pools of 2 agroinfiltrated leaves from individual plants (P1 and P2). smRNA accumulation is seen when expressing HYD1-P alone or with YF-P1b both at early and late expression times. No smRNA accumulation could be seen when reporter is co-expressed with P19. The GFP5 DNA radio-labelled probe used is specific to GFP5 sequence and does not cross react with YFP tags used.

At 3 dpa GFP mRNA accumulation was not detected in leaves infiltrated without any RSS, suggesting that RNA silencing was already induced at this time. GFP mRNA was detected in samples co-infiltrated with either YF-P1b or TBSV P19, although, it appears to accumulate to some higher levels in the later case. This difference was much more evident at 6 dpa, when the accumulation of mRNA GFP appeared to decline in the presence of YF-P1b, whereas raising with the help of P19. This data suggest that the silencing suppression activity of YF-P1b was weaker than that of the strong RSS P19. HYD-P expression appeared to cause a slight decrease in GFP mRNA accumulation when co-expressed with P19, but this drop was drastic in the presence of YF-P1b (Fig. 44), in agreement with the observed results in protein accumulation (Fig. 43). Small RNA accumulation analysis at 3 dpa showed higher levels of this RNA silencing marker in samples with HYD1-P, either in presence or absence of YF-P1b, supporting a positive effect of HYD1 on RNA silencing induction, which could not be counteracted by the silencing suppression activity of YF-P1b. A similar enhancement of small RNA

accumulation by HYD1-P expression was observed at 6 dpa in samples with YF-P1b. However, absence of YF-P1b, small RNA levels were higher when HYD1-P was also absent, which does not have a straightforward fit with a pro-silencing activity of HYD1. Expression of TBSV P19 prevented noticeable small RNA accumulation regardless the presence of HYD1-P, suggesting that the stimulating effect of HYD1-P on RNA silencing could be efficiently neutralised by the strong activity of this RSS protein.

HYD1 affects the infection of three PPV based chimeras encoding different RSS suppressors.

Initial observations suggested that the effect of HYD1-P expression in RNA silencing could be detected in the presence of YF-P1b but not when P19 was the supplier of RNA silencing suppression activity (Fig. 44). Having different PPV-based virus chimeras available expressing GFP where the endogenous PPV RSS HCPro has been replaced by various heterologous RSS proteins, ipomovirus CVYV encoded P1b and the tombusvirus TBSV encoded P19 (Maliogka et al., 2012), the effect of HYD1-P on potyviral infection supported by different RSS proteins was studied. *N. benthamiana* leaves were inoculated by agroinfiltration, and co-infiltrated either with HYD1-P or with a GUS control. GFP fluorescence monitoring and western blot analysis of viral CP accumulation in the agroinfiltrated tissue revealed that HYD1-P expression greatly inhibited infection of all three RSS chimeric viruses (Fig. 45), both at early infection times (3dpi) and late infection times (6dpi). However, this inhibition did not totally block the virus, as systemic infection could be observed in all plants, due to the virus escaping through cells adjacent to the agroinfiltrated area where HYD1-P is not expressed.

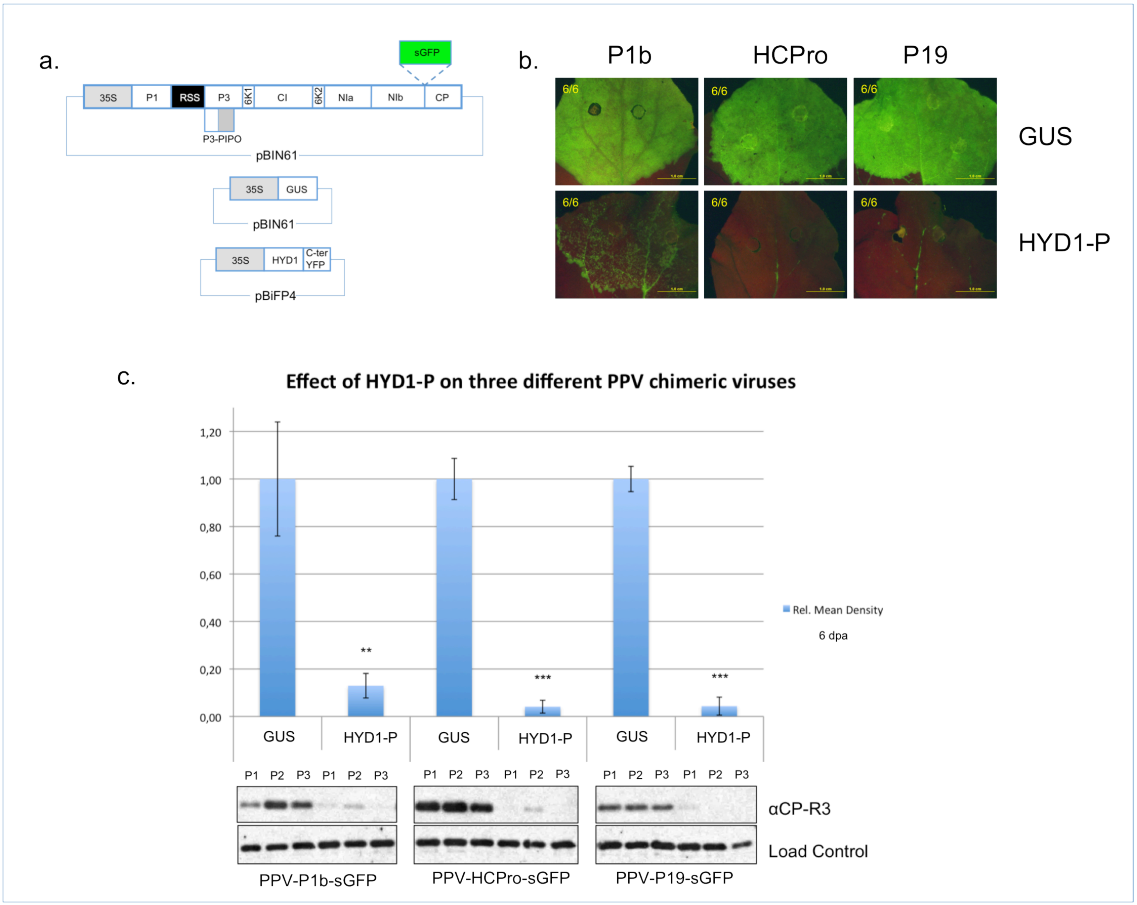

Figure 45. Co-expression of three different chimerical viruses harbouring different RSS proteins with HYD1-P. (a) Schematic diagram of the constructs used. The PPV based chimera harbouring a sGFP reporter gene between NIb and CP was used to substitute HCPro for P1b (CVYV) or P19 (TBSV). (b) Photographs of leaves infected with the viral construct named by the RSS protein encoded; P1b, PPV-P1b-sGFP; HCPro, PPV-sGFP; P19, PPV-P19-sGFP, and co-expressing either HYD1-P or a naive reporter (GUS) as seen under a epifluorescent stereoscope at 6dpa. Numbers on the top right-hand corner refer to the number of leaves representing such phenotype over the total leaves analysed. Scale bars represent 100µm. (c) Quantification of the PPV CP accumulation in tissue infected with the viral constructs shown and co-expressing HYD1-P or a naive reporter (GUS) at 6dpa. Each density plot corresponds to the mean density calculated for the three plant samples shown in the immunoblots below and expressed as relative to the mean values of each GUS control. Statistical significance calculated using t-student test; **, $p<0.01$; ***, $p<0.001$. Error bars refer to the standard error. Immunoblots used in the densitometry analysis of the CP accumulation performed with anti-serum raised against PPV CP protein are shown below the graph. Each lane corresponds to pools of 2 infected leaf samples from one individual plant taken at 6dpa. An unspecific band is shown as loading control.

Effect of HYD1-P on virus inhibition is not fully explained by sequence homology and HYD1 contributes strongly to the inhibition of the RSS activity of P1b.

Since the C-terminal YFP fragment that constitutes the HYD1-P tag is homologous to the reporter sGFP sequence of the reporter encoded in the genome, of the PPV chimeras, it is possible that it contributes to restrict viral infection by enhancing the antiviral RNA silencing response.

To address this possibility, we compared the effect of co-expressing HYD1-P (with identical sequence to the C-end of the reporter gene of the virus) and sGFP (identical sequence to the reporter gene of the virus along its entire length) in PPV-sGFP infected leaves. A considerable reduction in viral accumulation was suggested by monitoring green fluorescence (Fig. 46. a) and confirmed by immunodetection of PPV CP (Fig. 46. b & c) in all plants expressing HYD1-P, whereas PPV-sGFP-infected plants co-expressing free sGFP showed only a small reduction in CP accumulation that was not statistically significant.

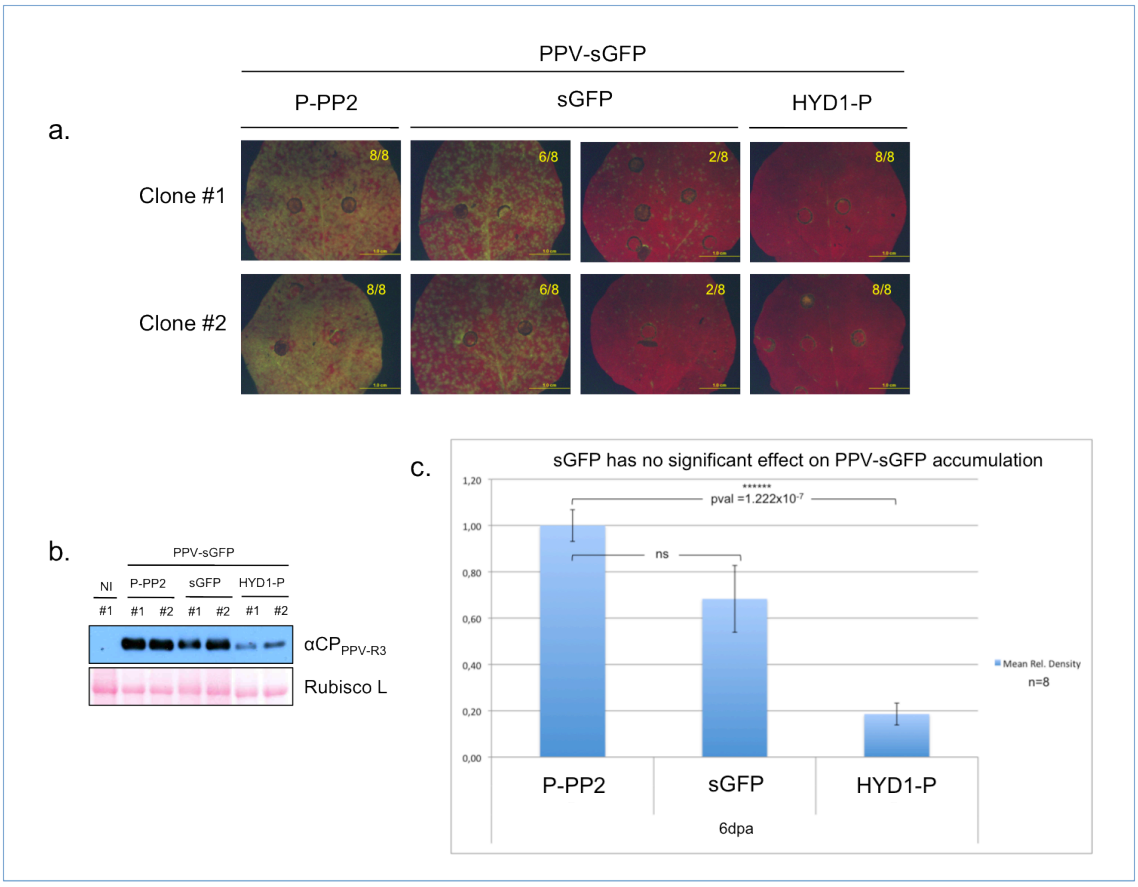

Figure 46. sGFP expression has no considerable effect on the accumulation of PPV-sGFP. (a) Images of infected plants expressing a control (P-PP2), HYD1-P or sGFP as seen under an epifluorescent stereocope at 6dpa. For each mix indicated, two different clones of each construct and 2 leaves per plant for a total of 4 plants were agroinfiltrated. Numbers on the top right corner refer to the number of leaves showing the phenotype presented over the total number of leaves analysed. Scale bar represent 100µm. (b) Biochemical analysis of the agroinfiltrated leaves shown in (a). Each lane represents pools of 8 leaves from 4 different plants, agroinfiltrated with agrobacteria transformed with 2 different clones (Clone #1 & clone #2). No differences can be observed between clones, but differences can be observed between both clones expressing HYD1-P and those expressing P-PP2 or sGFP. Immunoblot was performed with anti-serum raised against PPV CP protein. Ponceau red was used as loading control. (c) Densitometry analysis of PPV CP accumulation in infected plants co-expressing P-PP2, sGFP or HYD1-P, together with PPV-sGFP of the samples shown in (a). Density plots show the mean CP accumulation for each condition in pools of 4 plants of the two different clones used in (a) and relative to the mean value of P-PP2. Statistical significance was calculated using t-student test. ns, no statistical significance; ******, $p<0.000001$. Error bars represent standard error.

Fluorescence monitoring showed that in only one of the four plants infected with each of the two independent viral clones used sGFP co-expression caused a similar phenotype to HYD1-P (Fig. 46. a). This experiment was repeated three times, with similar results obtained in all cases, suggesting that the effect seen by co-expression with sGFP on the virus is sporadic.

To verify that sGFP is being expressed in plants showing high levels of virus accumulation, its coding sequence was amplified by RT-PCRs using primers specific of its CDS flanking regions. Results confirmed that even in heavily infected plants sGFP mRNA accumulated in addition to the sGFP sequence embedded in the genomic viral RNA (data not shown), proving that free GFP and GFP-containing virus sequences co-inhabited without inducing homology-dependent RNA silencing.

Effect of HYD1 against PPV infection is modulated by temperature.

It is known since long that rising temperature uses to attenuate viral infections (Johnson, 1922). More recent reports have shown that antiviral RNA silencing activation at high temperature contributes to this effect (Szittya et al., 2003), although enhancement of virus-induced gene silencing at low temperatures has also been reported (Fu et al., 2006). Since HYD1 has been previously related with AGO1 activation and our initial results suggested that HYD1 could be responsible for RNA silencing activation against PPV, infection experiments were performed under controlled temperatures to determine if temperature has an affect on the activity of HYD1. In these experiments, in addition to P-tagged HYD1 and the GFP-expressing recombinant PPV, we used intact HYD1 and wild type PPV, to avoid possible effects of co-expressing homologous GFP/YFP-derived sequences.

Direct comparison of PPV-GFP and PPV levels at different temperatures showed the expected reduction of virus accumulation when the temperature was raised to 28-30^{o}C (Fig. 47, quantification analysis not shown).

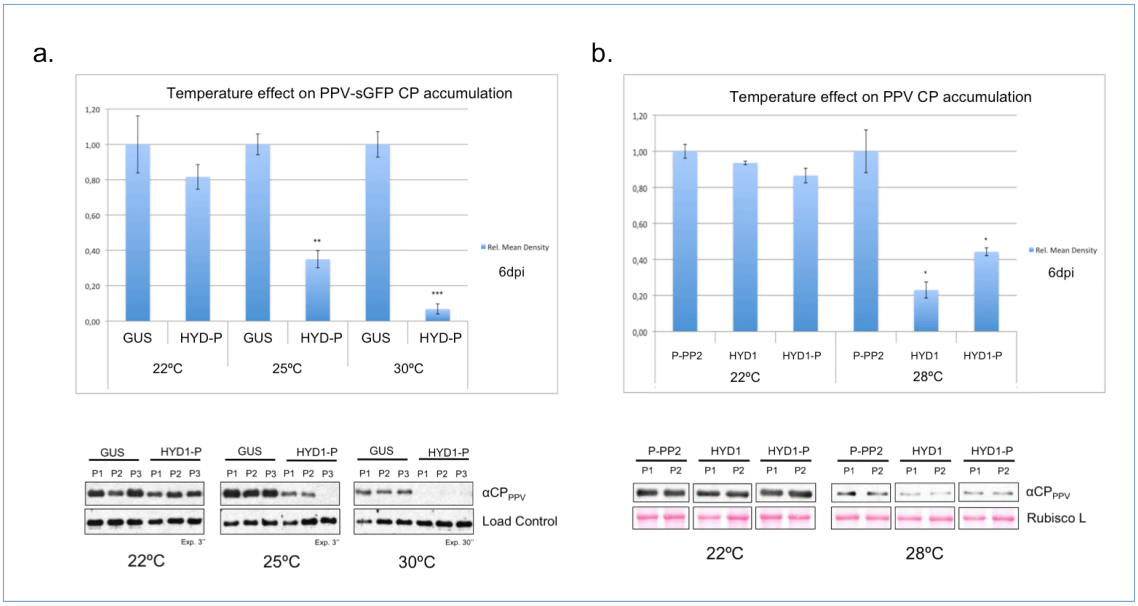

Figure 47. HYD1 affects viral infection and its effect is enhanced by temperature. Densitometry analysis of the CP accumulation of PPV-sGFP (a) and PPV (b). (a) GUS reporter and HYD1-P were co-expressed with PPV-sGFP and infected plants cultured at 22, 25 and 30°C until samples collected at 6dpa. (b) A naive protein, P-PP2, a non tagged HYD1 and HYD1-P were co-expressed with a wild type PPV clone and infected plants cultured at 22 and 28°C before collecting samples at 6dpa. In all cases HYD1 and HYD1-P show lower CP accumulation levels than those of control samples. For each case immunoblots of PPV CP protein accumulation is shown below the graph. Immunoblots were performed with anti-serum raised against PPV CP protein. An unspecific band in (a) or Ponceau Red in (b) was used as loading control. Positions of the corresponding pre-stained molecular weight standards (in kDa) running on the same gel are shown on the left.

HYD1-P caused a decrease of PPV-sGFP accumulation at the three temperatures assayed, but, whereas it was statistically significant at 22ºC, it was notable at 25ºC, and reduction in virus accumulation resulted practically undetectable levels of viral CP at 30ºC (Fig. 47. a). The effect was much lower when GFP/YFP-related sequences were removed. HYD1-P had only a marginal effect on wild type PPV accumulation, which was even lower for non-tagged HYD1, at 22ºC. However, at 28ºC, both HYD1 and HYD1-P caused a statistically significant reduction of wild type PPV accumulation, when compared with co-expression of a control protein (Fig. 47. b).

These results initially point out that sequence similarity, high temperature and HYD1 could have additive effects on enhancing antiviral RNA silencing responses, giving rise to highly efficient PPV restriction, and that HYD1 can disturb wild type PPV infection if aided by high temperatures.

HYD1 appears to be responsible for the effect of HYD1-P on enhancing RNA silencing and disturbing PPV infection

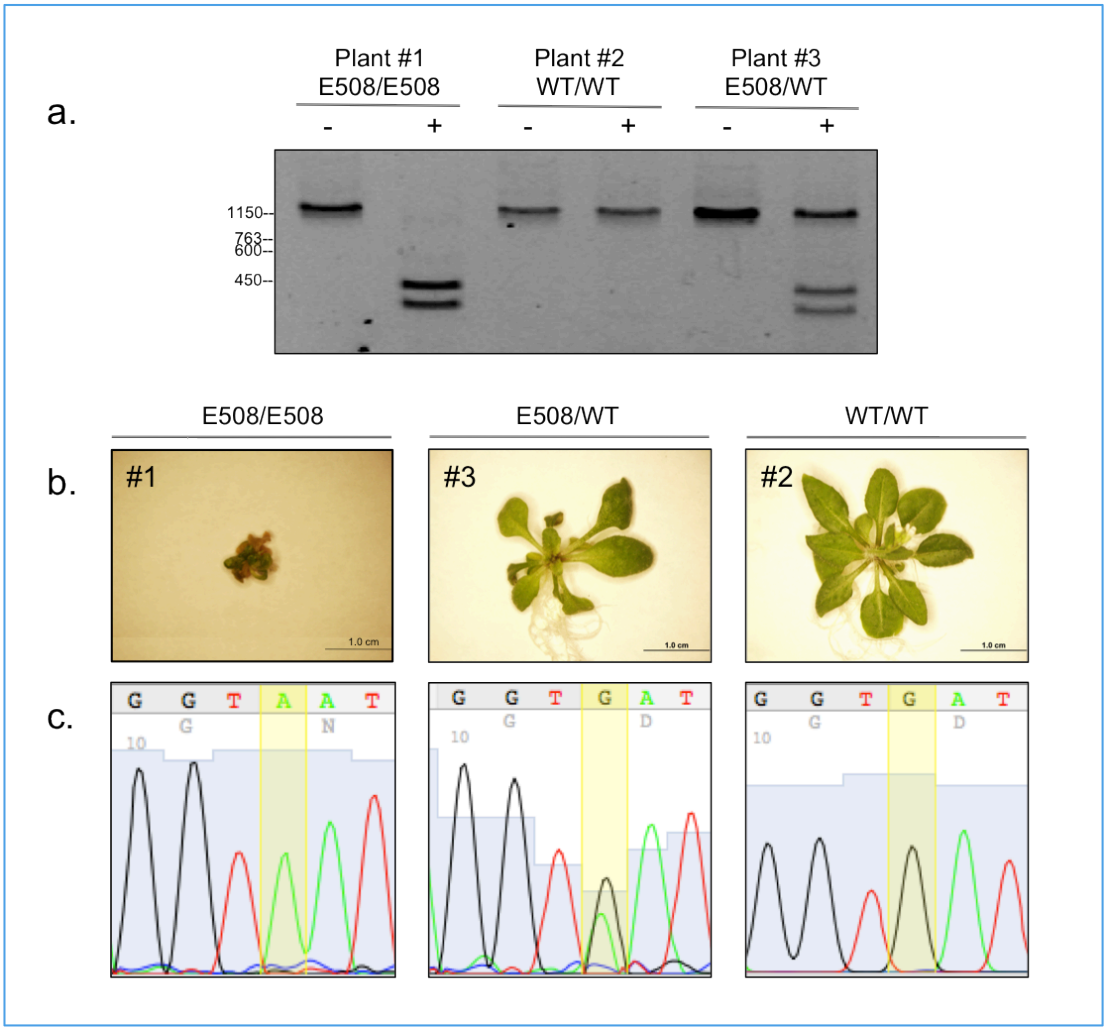

Figure 48. Non-functional mutation on the HYD1 locus produces sever developmental defects and impairs growth in plants. E508 allele as described by (Schrick et al., 2002) harbouring G to A transition causes a D to N residue change affecting the activity of HYD1. (a) genotype can be identified by CAPS. MluCI digestion product of the RT-PCR band produces a double band product of the E508 allele, or no digestion band if WT. -, undigested RT-PCR product; +, MluCI digestion. (b) Phenotype of E508 mutant plants, homozygous E508 mutants are greatly impaired and unviable. Heterozygous E508 mutants and WT plants have similar phenotypes and show no differences in development. Scale bars represent 1.0cm. (c) Sequencing confirmed E508 allele, a single peak can be seen (highlighted) confirming the G to A transition in the homozygous mutant, whereas a double G/A peak can be seen in the heterozygous mutant.

To confirm that HYD1 is to be considered responsible for the effect of HYD1-P on stimulating RNA silencing and disturbing PPV infection, a loss of function mutant allele of HYD1 (E508) (Schrick et al., 2002) was cloned and assayed. E508 homozygotes are generally non viable or considerably underdeveloped with severe morphological and developmental defects (Fig. 48. b. #1). On the contrary,

phenotypes of E508 heterozygotes show no obvious differences to wild type plants. Being E508 homogygotes so severely impaired, transient expression by agroinfiltration or virus inoculation of the plants was not feasible. And when heterozygous E508 plants were inoculated with PPV-P1b-sGFP, no significant differences were observed in viral accumulation, evidencing that if HYD1 activity is important for PPV infection, one single functional allele is sufficient to provide the required activity.

To determine whether HYD1 functionality is required for the effects of HYD1-P on PPV infection, P-tagged HYD1 E508 mutant (E508-P) previously observed to be functionally impaired, was co-agroinfiltrated with PPV-P1b-sGFP in *N. benthamiana* plants. Although both HYD1-P and E508-P caused a notable reduction in virus accumulation compared to the control infected plants, the effect of the E508-P was significantly lower (Fig. 49. a). Similarly, co-expression with HYD1-P and E508-P, even in the presence of TBSV P19, caused a drop in the accumulation of transiently expressed YF-P1b, which was significantly higher in the case of the wild type HYD1-P (Fig. 49. b). HYD1-P and E508-P accumulated to similar levels in agroinfiltrated leaves (Fig. 49. b), evidencing that differences on the expression of both alleles or on the stability of the mutant and the wild type proteins do not account for their different effects on the accumulation of YF-P1b. These results strongly support the assumption that the disturbance effect of HYD1-P on PPV infection is not simply a consequence of sequence similarity between the sGFP reporter encoded in the virus and the tag linked to HYD1, but a consequence of a relevant yet uncharacterized function of HYD1 affecting RNA silencing induction and/or inhibition of RSS activity.

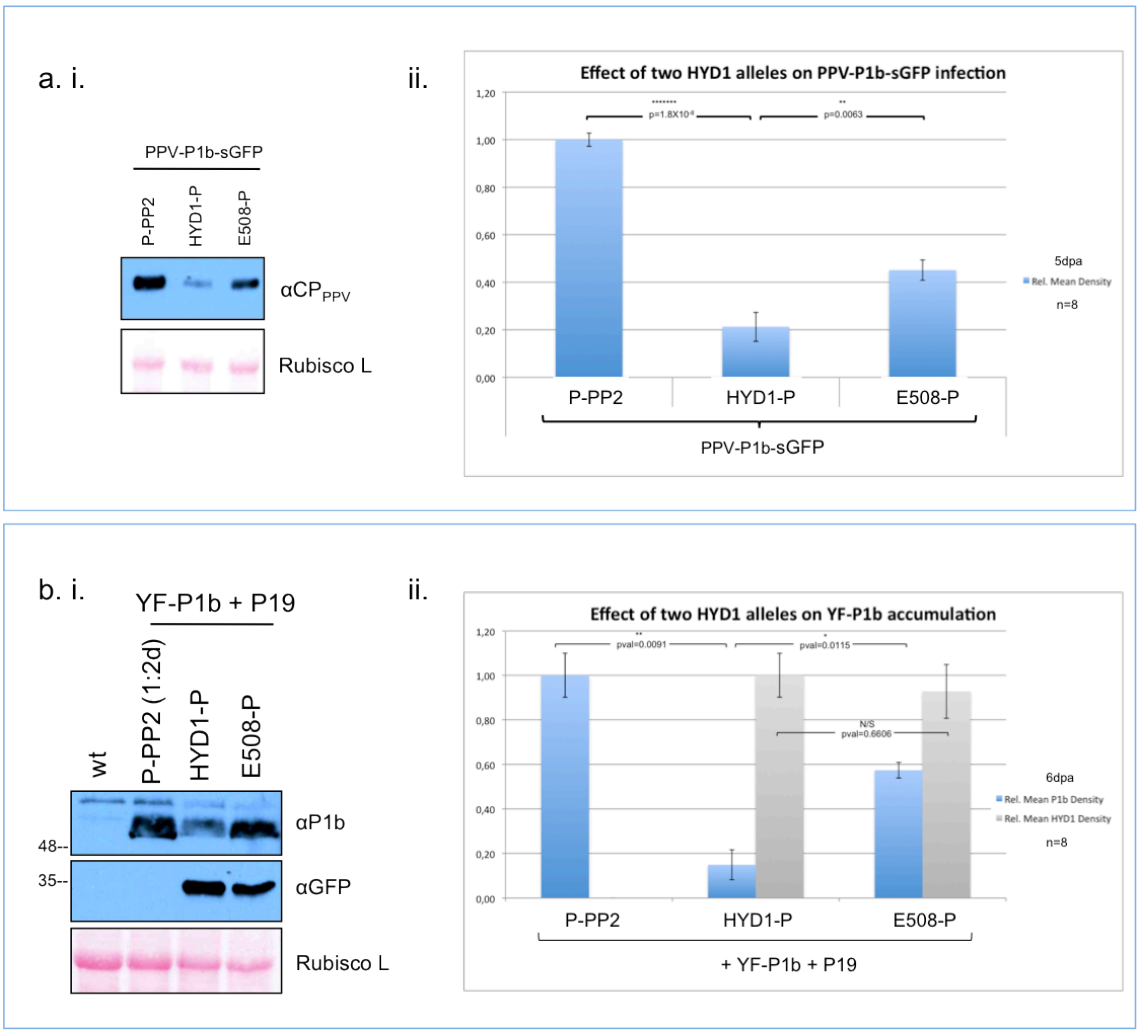

Figure 49. Non-functional HYD1 mutant (E508) partially reconstitutes viral and P1b protein accumulation levels. (a) Viral CP accumulation in infected leaves co-expressing HYD1-P and HYD1 mutant allele E508-P. i., Immunoblots of PPV CP accumulation in the PPV-P1b-sGFP infected plant leaves co-expressing two different HYD1 alleles (HYD1 and E508). A naive protein (P-PP2-B13) was used as control. Pools of 8 plants were used per condition. ii., Density plots of PPV-CP accumulation seen in (a. i) relative to the mean value of P-PP2. Pool of 2 agroinfiltrated and infected leaves from 8 Individual plants were analysed per condition. Statistically Significant differences can be observed between infected plants co-expressing HYD1-P and E508-P. (b) YF-P1b protein accumulation in plant leaves co-expressing HYD1-P and the mutant E508-P allele. A naive protein (P-PP2-B13) is used as negative control. i., Western blot analysis of YF-P1b accumulation in pools of 2 agroinfiltrated leaves belonging to 8 individual plants were used per condition. 1:2d corresponds with a x2 dilution in non-agroinfiltrated protein extract. ii., Density plots of the P1b (in blue) and HYD1 (in grey) protein accumulation and relative to the mean accumulation of P-PP2-B13 and HYD1-P respectively. Pools of 2 agroinfiltraded leaves belonging to 4 individual plants were analysed and quantified per condition. Statistically significant differences could be observed in the accumulation of YF-P1b between HYD1-P and E508-P, but no statistical difference could be seen between the accumulation of HYD1-P and E508-P. For both cases, immunoblots were performed using anti-serum raised against P1b or PPV CP protein, or monoclonal antibody against GFP (to detect HYD1-P). Positions of the corresponding pre-stained molecular weight standards (in kDa) running on the same gel are shown on the left. Ponceau Red was used as loading control.

eIF4E/eIF(iso)4E

Reports describing interactions of the eukariotic translation factors (eIFs) with plant viruses are numerous. Plant eIFs act as key determinants in numerous

Potyviridae viral infections participating in vital host-virus interactions as in the case of the interaction between the viral VPg and eIF4E/eIF(iso)4E from numerous plants systems (Wittmann et al., 1997; Leonard et al., 2000; Schaad et al., 2000; Leonard, 2004; Beauchemin et al., 2007; Charron et al., 2008). In some cases physical interaction of eIF4E/eIF(iso)4E and VPg showed a positive correlation with infectivity (Leonard et al., 2000; Kang et al., 2005; Yeam et al., 2007; German-Retana et al., 2008), but in other case interaction was not consistent with susceptibility to the infection (Gao et al., 2004; Kang et al., 2005; German-Retana et al., 2008). The multifunctional Cilindrical Inclusion protein (CI) (Sorel et al., 2014) is another viral protein that has been shown to be involved in overcoming eIF4E-mediated resistance (Sorel et al., 2014) and to physically interact with eIF4E (Tavert-Roudet et al., 2012), Moreover, PVA, PVX and TEV HCPro have also been described to interact with host eIF4E and eIF(iso)4E, with no involvement in recessive resistance but with important consequences for the virus if the interaction is broken by mutations in its 4E-Binding domain (Ala-Poikela et al., 2011).

P1b interacts specifically with eIF(iso)4E and this interaction does not involve its RSS activity or Serine protease activity.

Since CVYV P1b is able to functionally replace HCPro in a PPV infection, the interaction between eIF4E/eIF(sio)4E and HCPro was tested to determine if it is reproduced with P1b. CVYV P1b, and both eIF4E and eIF(iso)4E from a natural CVYV host, *C. melo*, were cloned in appropriate vectors and BiFC experiments were performed.

P1b specifically interacts with *C. melo* eIF(iso)4E as fluorescent complementation could be observed in all agroinfiltrated leaves expressing theses proteins, which was not observed when P1b was co-expressed with eIF4E even though protein accumulation seemed to be similar (Fig. 50). Interaction of P1b with eIF(iso)4E is not dependant on its RSS activity, as a P1b mutant deficient in binding to small

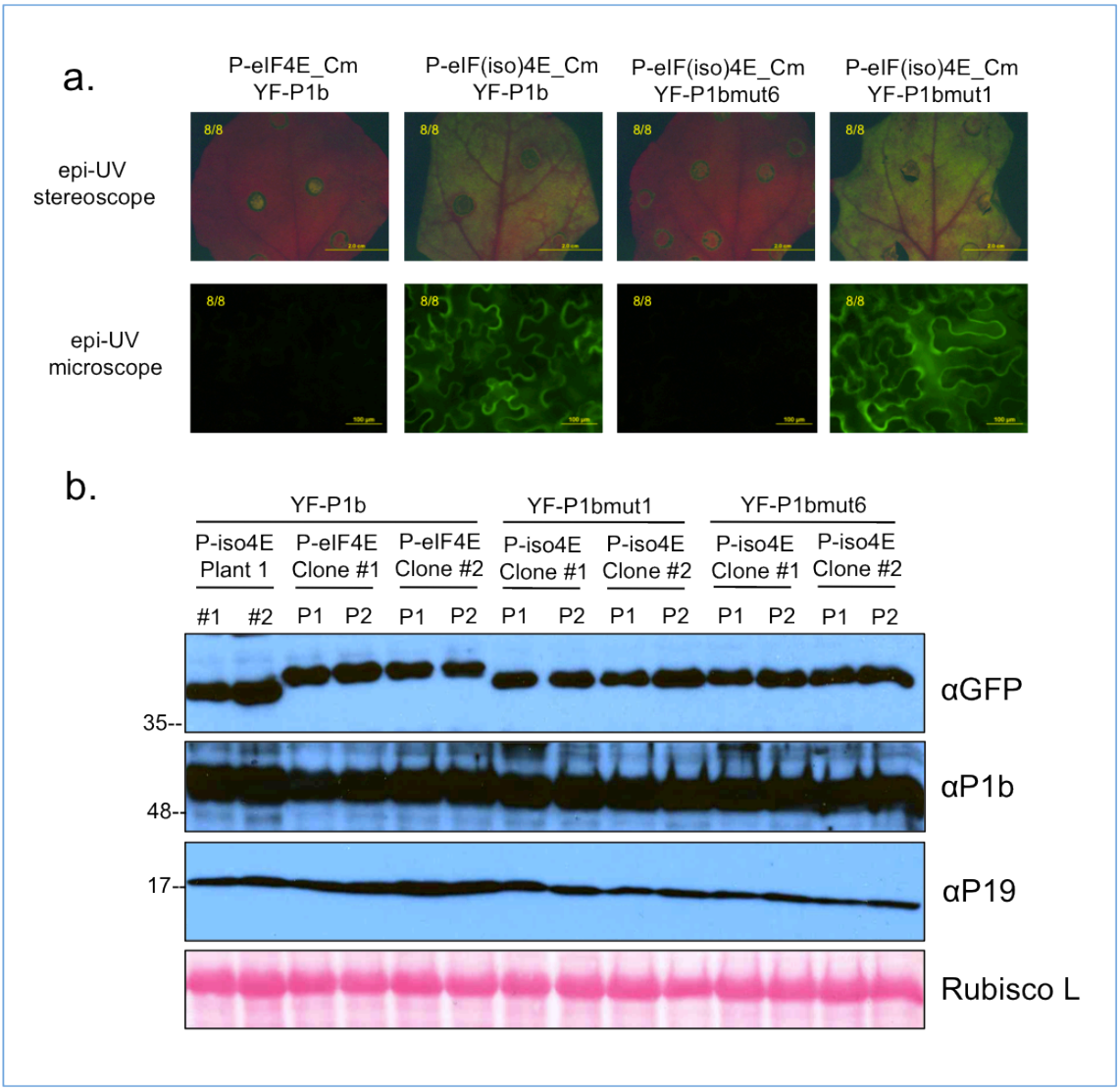

Figure 50. P1b specifically interacts eIF(iso)4E but not eIF4E and this interaction is not dependent on its RSS activity. BiFC interactions of different P1b alleles (P1b, wild type allele; P1bmut1 (RK68,69AA), non-functional RSS activity mutant; P1bmut6 (C103A), non-structural mutant) with *C. melo* eIF4E and eIF(iso)4E. (a) Fluorescent complementation seen using a epi-fluorescent stereoscope (top row) and an epi-fluorescent microscope (bottom row). Numbers in the upper left-hand corner refer to the number of agroinfiltrated leaves showing such phenotype over the total number of agroinfiltrated leaves observed (2 leaves per plant and 2 clones per construct). (b) Immunoblot of the protein accumulation of the samples presented in (a). Each lane represents pools of two agroinfiltrated plant leaves belonging to individual plants. First two lanes on the left represent pools of two leaves belonging from two individual plants agroinfiltrated with two individual clones. Immunoblots were performed using anti-serum raised against P1b or P19 protein, or monoclonal antibody against GFP (to detect "P" tagged fusion proteins). Positions of the corresponding pre-stained molecular weight standards (in kDa) running on the same gel are shown on the left. Ponceau Red was used as loading control.

RNAs unable to suppress silencing P1bmut1 (RK68,69AA) (Valli et al., 2008) was able to complement fluorescence to levels similar to the wild type P1b. In contrast a proper P1b conformation allowing self-interaction seems to be essential for P1b/eIF(iso)4E interaction, since co-expression of eIF(iso)4E with the P1b mutant P1bmut6 (C103A), which is affected in a zinc finger essential for correct folding of

the protein (Valli et al., 2008) did not display fluorescent complementation despite the accumulation levels of the mutant protein being similar to the wild type P1b.

P1b interacts specifically with eIF(iso)4E during a viral infection

To asses whether a functional non-tagged P1b would interact with eIF(iso)4E when expressed during a functional infection, leaves of *N. benthamiana* plants leaves were co-agroinfiltrated with agrobacteria cultures expressing the chimeric PPV-P1b-sGFP viral construct and eIF4E or eIF(iso)4E constructs tagged with four copies of the myc epitope (4xmyc-eIF4E and 4xmyc-eIF(iso)4E). eIF4E/eIF(iso)4E-containing protein complexes were immono-captured with antibodies specific for the myc epitope or CVYV P1b and purified using magnetic Protein A/G dynabeads (Fig. 51). eIF4E and eIF(iso)4E were both found to immunoprecipitate with wild type P1b when co-expressed transiently in *N. benthamiana* leaves. Initially this seamed as a surprise since P1b was not seen to complement fluorescence with eIF4E during BiFC assays, however, regardless of the fluorescent complementation seen, the lack of fluorescence in the BiFC assays should not be interpreted as a lack of interaction between both proteins, as interaction could be present but due to steric constraints, among other explanations, prevent YFP residues from complementing and thus fluorescence not be seen. It is to be noted, however, that under a viral infection using the PPV based chimera, PPV-P1b-sGFP, P1b is preferentially co-purified with eIF(iso)4E which supports the specific interactions previously seen using BiFC. Under a functional viral infection, P1b is selectively interacting with eIF(iso)4E, these results could imply that other viral factors could be involved in determining the specificity of P1b interaction with the host eIF4E proteins.

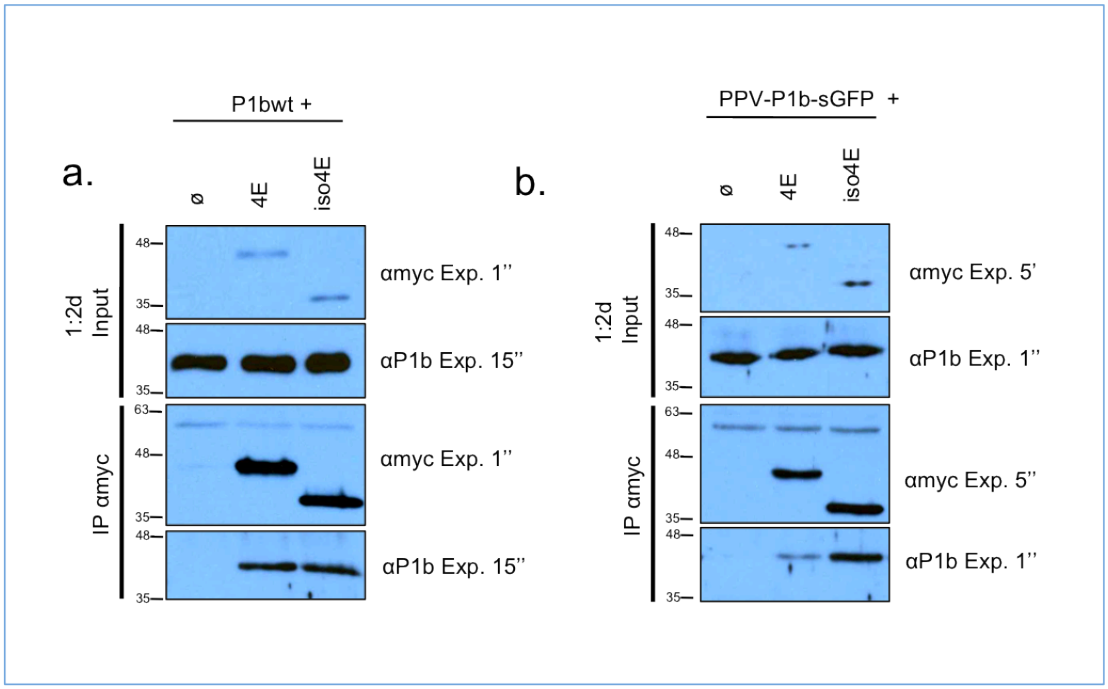

Figure 51. P1b interacts with eIF(iso)4E both during transient expression and during a viral infection. Immunoblots of the immunoprecipitates from plant leaves co-expressing myc tagged eIF4E or eIF(iso)4E with P1b expressed either transiently (a) or within a viral infection (b). Agroinfiltrated leaves expressing impGW718 contructs: ø (expressing only 4xmyc), 4xmyc-eIF4E (expressing N-terminal 4xmyc tagged *C. melo* eIF4E) and 4xmyc-eIF(iso)4E (expressing N-terminal 4xmyc tagged *C. melo* eIF(iso)4E) were immunoprecipitated with Protein A/G coupled magnetic dynabeads after incubation with mouse antibody against the myc epitope. Immunoblots were performed using rabbit polyclonal serum raised against P1b, or monoclonal antibody against myc (to detect myc fusions) and a secondary sheep HRP-conjugated or goat HRP-conjugated antibody for chemiluminescent detection. Positions of the corresponding pre-stained molecular weight standards (in kDa) running on the same gel are shown on the left. 1:2d refers to a 2x dilution performed in protein cracking buffer of samples labelled as input.

CVYV CP

Physical interaction between of the potyviral RNA silencing suppressor HCPro is expected to fulfill its function as helper component in the transmission of virus particles by aphids, an it has been experimentally demonstrated for some potyviruses (Blanc et al., 1997). However, this interaction could not be demonstrated for PPV (Zilian & Maiss, 2011). In contrast, functional relation, probably not directly involved in aphid transmission, has been recently uncovered for PPV CP and HCPro, being HCPro needed for a proper yield and infectivity of virus particles (Valli et al., 2014). Thus, to test whether the ability of the potyviral RSS HCPro to interact with the cognate CP is conserved in a non-related RSS, P1b, from a member of the family *Potyviridae* that is not transmitted by aphids was investigated.

RSS potyviral proteins different from HCPro interact with homologous and heterologous CPs

To test whether the Ipomovirus RSS encoded in CVYV, P1b is able to interact with its cognate CP, their coding sequences were cloned in appropriate plasmids and BiFC experiments where performed. Joint expression of CVYV P1b and CP complemented fluorescence regardless the YFP fragment fused to the N-terminus (Fig 52), indicating that these two proteins are able to interact in plants.

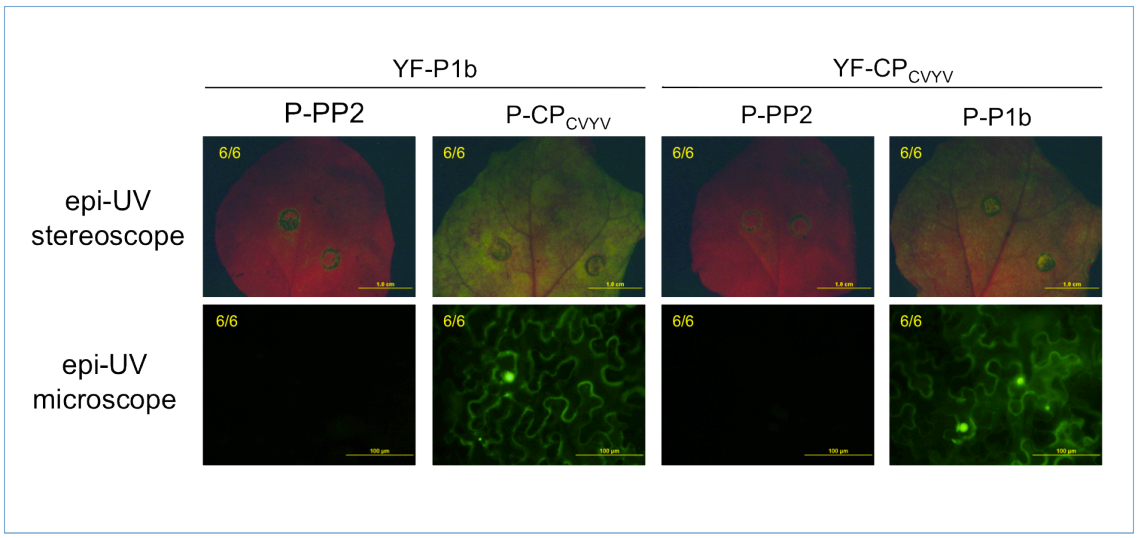

Figure 52. P1b and its canonical CP protein interact in plant leaves. BiFC interactions of P1b with CVYV CP. BiFC fusion construct of P1b, CVYV CP or PP2-B13 tagged with the N-terminal residues (YF-) or C-terminal residues (P-) as indicated, were co-expressed in *N. benthamiana* leaves together with TBSV P19 and visualised under an epi-fluorescent stereoscope (top row) and an epi-fluorescent microscope (bottom row) at 6dpa. Positive interaction is identified by reconstitution of the YFP fluorescence. YFP reconstitution between P1b and CVYV CP is observed as a diffuse cytoplasmic pattern containing big spherical fluorescent structures indistinctly of the YFP residues used. Numbers on the upper left-hand corners refer to the number of agroinfiltrated leaves showing such phenotype over the total number of agroinfiltrated leaves observed (2 leaves per plant and 3 plants per mix). Scale bars in the top rows represent 1.0cm and in the bottom row 100µm.

Whereas CVYV lacks HCPro, tritimoviruses encode for HCPro, but this protein has not been held responsible for the RNA silencing suppression activity needed for the infection, which is instead supplied by the P1 protein (Young et al., 2012). To assess whether the interacation of HCPro with CP in potyviruses could be related with HCPro functions other than RSS and/or with the RSS activity exclusively, the coding sequences of the P1, with active RSS but unrelated to HCPro, HCPro, lacking RSS and CP proteins of the tritimovirus *Brome streak mosaic virus* (BStMV) were cloned in appropriated plasmids and assayed in BiFC experiments. YFP fluorescence was restored when YF-P1, but not YF-HCPro, was co-expressed with

P-CP (Fig. 53. a). This result indicates that the tritimoviral RSS P1 interacts *in planta* with CP, and suggests that an HCPro deprived from RSS activity might not be able to interact with this protein.

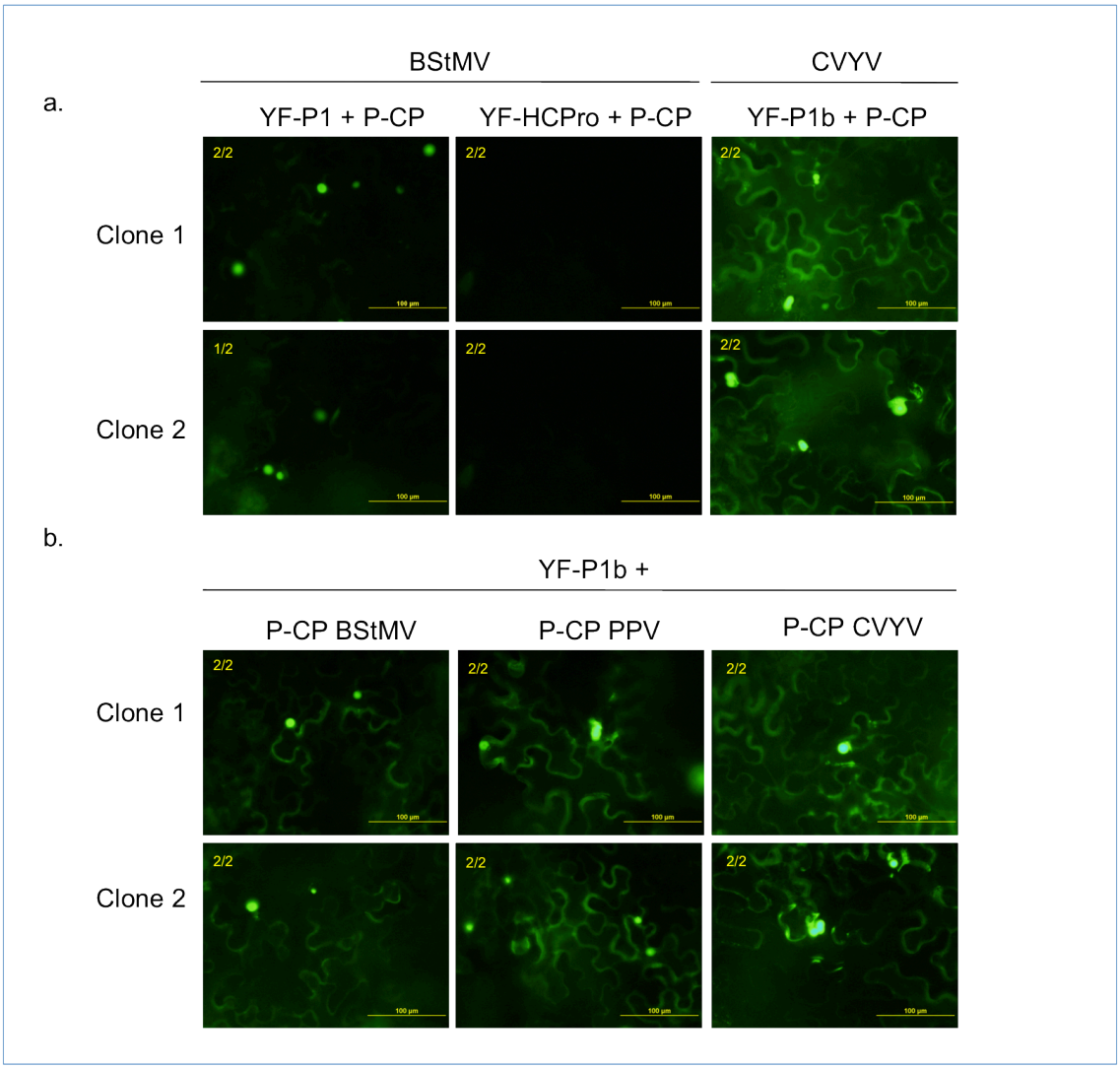

Figure 53. Bimolecular fluorescent complementation assays of proteins belonging to three different viruses: Ipomovirus: Cucumber Vein Yellowing Virus (CVYV); Potyvirus: Plum Pox Virus (PPV); and Poacevirus: Brome Streak Mosaic Virus (BStMV). *N. benthamiana* leaves co-expressing the BIFC constructs fused to the N-terminal (YF-) or C-terminal (P-) of the YFP reporter as indicated, together with TBSV P19 to homogenise expression levels, observed under an epi-fluorescent microscope at 6 dpa. Two independent clones for each construct were used for each expression mix. (a) BStMV P1 but not HCPro interacts with its canonical CP protein. Reconstituted fluorescence portrays a similar fluorescent cytoplasmic pattern with big spherical fluorescent structures as seen previously for P1b and CVYV CP. (b) P1b interacts with CP proteins from different viruses belonging to the *Potyviridae* family. In all cases reconstituted fluorescence is observed as diffuse cytoplasmic pattern containing big spherical fluorescent structures. Numbers on the upper left-hand corners refer to the number of agroinfiltrated plants showing such phenotype over the total number of agroinfiltrated plants observed (2 leaves per plant). Scale bars represent 100µm.

In order to assess the specificity of the interactions between potyvirus RSSs and CPs, YP-P1b was co-expressed with its complementing versions of its cognate or heterlogous CPs from the potyvirus PPV and the tritimovirus BStMV. Strong YFP

fluorescence was observed in all combinations, suggesting CVYV P1b is able to interact with both homologous and heterologous potyvirid CPs (Fig. 53. b).

CP interacts specifically with eIF(iso)4E

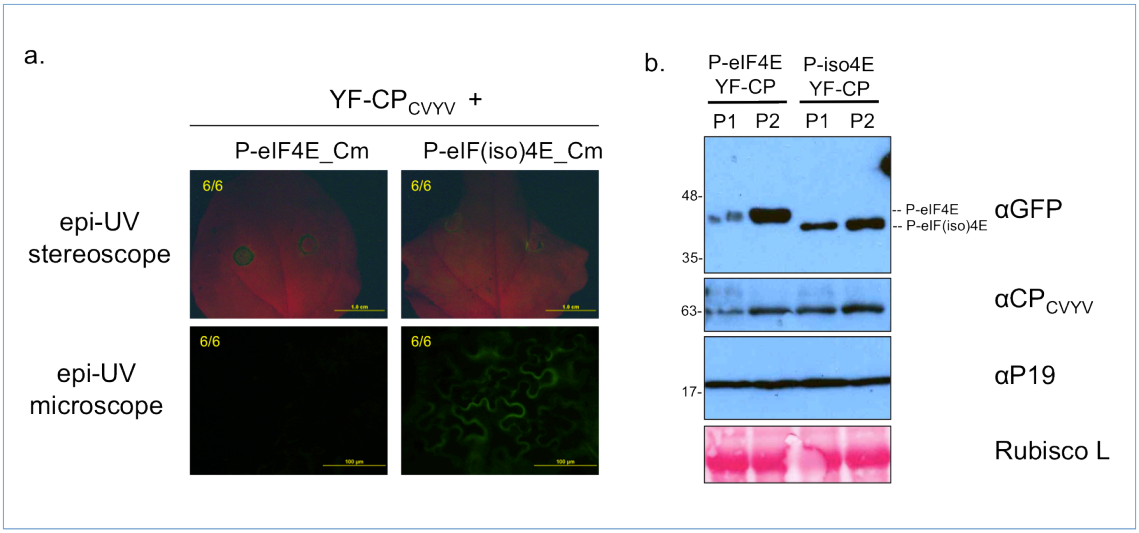

Figure 54. CVYV CP interacts with eIF(iso)4E but not eIF4E from *C. melo*. (a) BiFC interactions of CVYV CP with *C. melo* eukaryotic translation initiation factor eIF4E and eIF(iso)4E. BiFC constructs of CVYV CP and *C. melo* eIF4E or eIF(iso)4E tagged with the N-terminal (YF-) or C-terminal residues (P-) as indicated, were co-expressed in *N. benthamiana* leaves together with TBSV P19 to homogenize expression levels, and visualised under an epi-fluorescent stereoscope (top row) and an epi-fluorescent microscope (bottom row) at 6dpa. Positive interaction is identified by reconstitution of the YFP fluorescence. Numbers on the upper left-hand corners refer to the number of agroinfiltrated leaves showing such phenotype over the total number of agroinfiltrated leaves observed (2 leaves per plant and 3 plants per mix). Scale bars in the top rows represent 1.0cm and in the bottom row 100µm. (b) Western blot analysis showing the protein accumulation levels of samples presented in (a). Each lane represents a pool of two agroinfiltrated leaves from one independent plant expressing the constructs indicated. Immunoblots were performed with anti-serum raised against CVYV CP or primary monoclonal antibody against GFP (to detect "P" tagged fusion proteins). Positions of the corresponding pre-stained molecular weight standards (in kDa) running on the same gel are shown on the left. Ponceau Red was used as loading control.

Inhibitory effects in potyviral RNA translation have been described for viral CP (Hafrén et al., 2010), whereas stimulatory effects have been described with host eIF(iso)4E (Besong-Ndika et al., 2015). Curiously, both proteins have been seen to interact with P1b. To explore the possibility that CP and eIF(sio)4E could be interacting with each other, the coding sequences of CVYV CP, eIF4E and eIF(iso)4E were cloned into appropriate plasmids and interaction asses in BiFC experiments using *N. benthamiana* agroinfiltrated leaves. YFP fluorescence was complemented when YF-CP was co-expressed with P-eIF(iso)4E, but not with P-eIF4E (Fig. 54). This preference of CVYV CP for one of the two eIF4E isoforms was

similar to that seen for P1b, possibly suggesting that specific recruitment of one of the two isoforms might be favoured by CVYV.

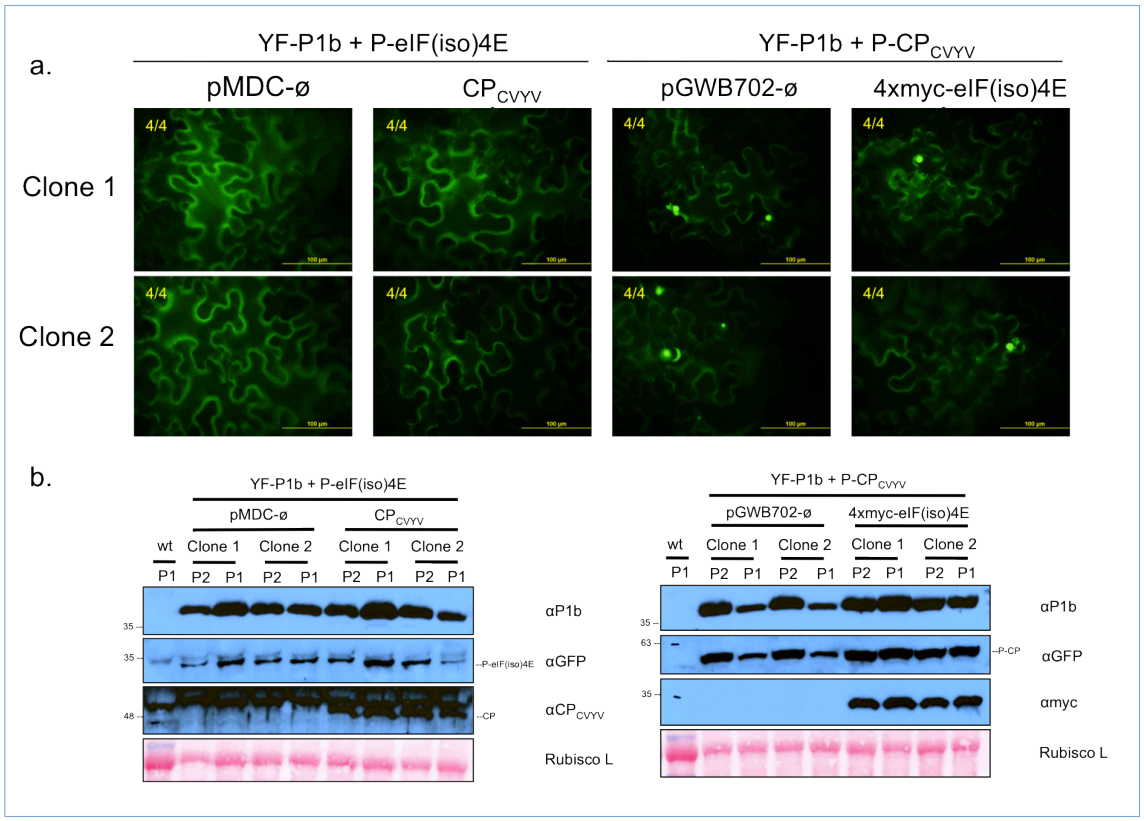

Figure 55. P1b interaction with CVYV CP and *C. melo* eIF(iso)4E are independent. (a) BiFC construct from two independent clones expressing P1b tagged with the N-terminal YFP residues (YF-P1b) and *C. melo* eIF(iso)4E or CVYV CP tagged with the C-terminal YFP residues (P-) were co-expressed in *N. benthamiana* leaves together with constructs expressing CVYV CP or 4xmyc-eIF(iso)4E or their corresponding empty (-ø) control plasmids, as indicated, and TBSV P19 to homogenise expression levels. Co-expressions were visualised under an epi-fluorescent microscope at 6dpa. Numbers on the upper left-hand corners refer to the number of agroinfiltrated leaves showing such phenotype over the total number of agroinfiltrated leaves observed (2 leaves per plant and 2 plants per clone). Scale bars represent 100µm. (b) Western blot analysis showing the protein accumulation levels of samples presented in (a). Each lane represents a pool of two agroinfiltrated leaves from one independent plant expressing the constructs indicated. Immunoblots were performed with anti-serum raised against P1b or CVYV CP, primary monoclonal antibody against GFP and primary monoclonal antibody against myc. Positions of the corresponding pre-stained molecular weight standards (in kDa) running on the same gel are shown on the left. Ponceau Red was used as loading control.

Since CVYV CP and P1b both interact with eIF(iso)4E, both viral proteins could be competing in the recruitment of the same host factor. To test this possibility three-component co-expression experiments were performed where BiFC CVYV/P1b and eIF(iso)4E/P1b interactions were observed in the presence of a third non-tagged eIF(iso)4E or CVYV CP expression. None of the BiFC interactions seemed to be affected by the expression of the third partner (Fig. 55). These results support

thinking that interaction of CVYV CP and P1b with eIF(iso)4E are not mutually exclusive and all three proteins could be recruited in the same protein complex.

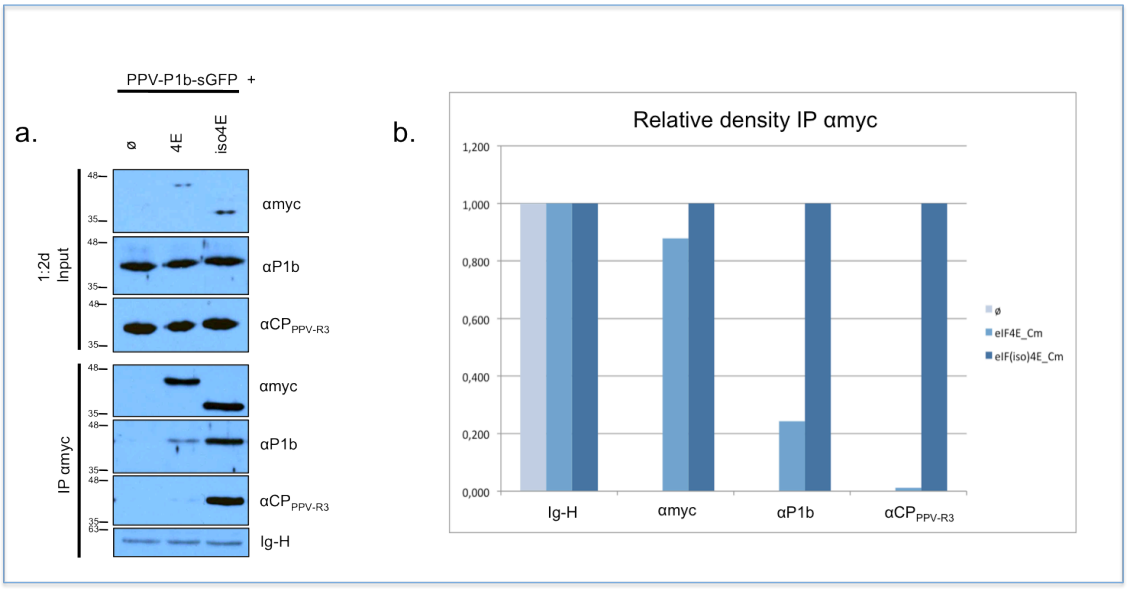

Figure 56. P1b and PPV CP co-immunoprecipitate predominantly with eIF(iso)4E. (a) Immunoblots of the co-immunoprecipitates shown in Fig. 45. b. reveal PPV CP specifically immunoprecipiatates with eIF(iso)4E but not eIF4E. Immunoblots were performed using anti-serum raised against P1b or PPV CP, and primary monoclonal antibody against myc. Positions of the corresponding pre-stained molecular weight standards in kilodaltons (kDA) running on the same gel are shown on the left. 1:2d refers to a 2x dilution performed in protein cracking buffer of samples labelled as input. (b), Relative accumulation of the immunoprecipitates presented in (a). For each lane, protein load was normalised with its corresponding Ig-H density. Bar plots show densities in relation to the eIF(iso)4E immunoprecipitate. Although small differences can be seen between the immunoprecipitated myc tagged proteins, such differences cannot explain the drastic differences seen in P1b or PPV CP.

PPV-P1b-sGFP infected *N. benthamiana* leaves were used to co-immunoprecipitate P1b with 4xmyc-tagged eIF(iso) (Fig. 51). Immunuprecipitates were analysed further and shown to contain PPV CP (Fig. 56. a.). Negligible levels of PPV CP were detected co-immunoprecipitating with 4xmyc-eIF4E, suggesting that not only CVYV CP, but also PPV CP can specifically interacts with eIF(iso)4E and this interaction can take place in the context of a viral infection. However, the possibility that the CP detected in the 4xmyc-eIF(iso)4E immunoprecipitate was captured through an intermediate eIF(iso)4E/P1b interaction can not be discarded, in contrast, the different P1b/CP ratio in both 4xmyc-eIF(iso)4E and 4xmyc-eIF4E immunoprecipitates (Fig. 56. b) suggest that at least part of the co-immunoprecipitated CP comes from a direct eIF(iso)4E/CP interaction

CP interaction with P1b co-localises with SGS3-containing siRNA-bodies

Diffused cytosolic patterns containing discrete large fluorescent structures were observed during the BiFC asseys between P1b and the CPs (Fig. 52 & Fig. 53).

These large fluorescent structures resulting from the interaction of P1b with CPs (P1b/CP-bodies) were not observed to co-localise with nuceli when counter staining with DAPI (not shown). Similar interaction patterns were seen previously describing P1b self-interaction (Valli et al., 2008), UBQ2-RPL40A (Fig. 34), and PRH75 (Fig. 34). In contrast, only a diffuse fluorescence with no dense cytoplasmic structures was observed during the BiFC asseys between P1b and eIF(iso)4E (Fig. 50. a).

BiFC P1b complementation with CVYV CP was co-expressed with different subcellular organelle markers corresponding to plastids (cpsignal-mCherry), vacuole (γ-TIP-mcherry), Golgi apparatus (SM1-mCherry), peroxisomes (mCheery-SKL), mitochondria (cox4ts-mCherry), endoplasmic reticulum (KDEL-mCherry) and plasma membrane (PIP2A-mCherry) (Nelson et al., 2007). However, green fluorescent P1b/CP-bodies did not co-localise with any of the red markers (data not shown) suggesting that P1b/CP-bodies are not associated with these cellular membrane organelles.

Different components of the RNA silencing machinery have been shown to localise in cytoplasmic foci, in particular, siRNA-bodies, which are distinct from P-bodies, where RNA quality control and degradation takes place (Kumakura et al., 2009; Jouannet et al., 2012). Interaction between the potexvirus *Plantago asiatica mosaic virus* (PlAMV) encoded RSS protein TGBp1 and two RNA silencing factors, SGS3 and RDR6, has recently been reported, co-aggregating with siRNA-bodies, to inhibit SGS3/RDR6-dependent dsRNA synthesis (Okano et al., 2014). To assess whether the cytoplasmic P1b-aggregating bodies could be related with these RNA silencing-related siRNA-bodies, YF-P1b and P-CP were co-expressed with either TagRFP-SGS3 (marker for siRNA-bodies) or TagRFP-DCP1 (marker for P-bodies), and fluorescence was monitored under a confocal microscope. The green fluorescence resulting from the interaction of P1b and CP in P1b/CP-bodies co-localised with red TagRFP-SGS3 fluorescence in 15 out of 21 fluorescent foci analyzed (Fig. 57. b), suggesting that P1b and CP could be co-aggregating with siRNA-bodies. It is interesting to remark that whereas green fluorescence showed a rather uniform distribution in P1b/CP-bodies, obscure areas were observed

inside the red TagRFP-SGS3 fluorescent structures (Fig. 57. b. box). The fact that these obscure areas could not be observed in both structures could indicate a distinct distribution of P1b/CP and SGS3 in the siRNA bodies.

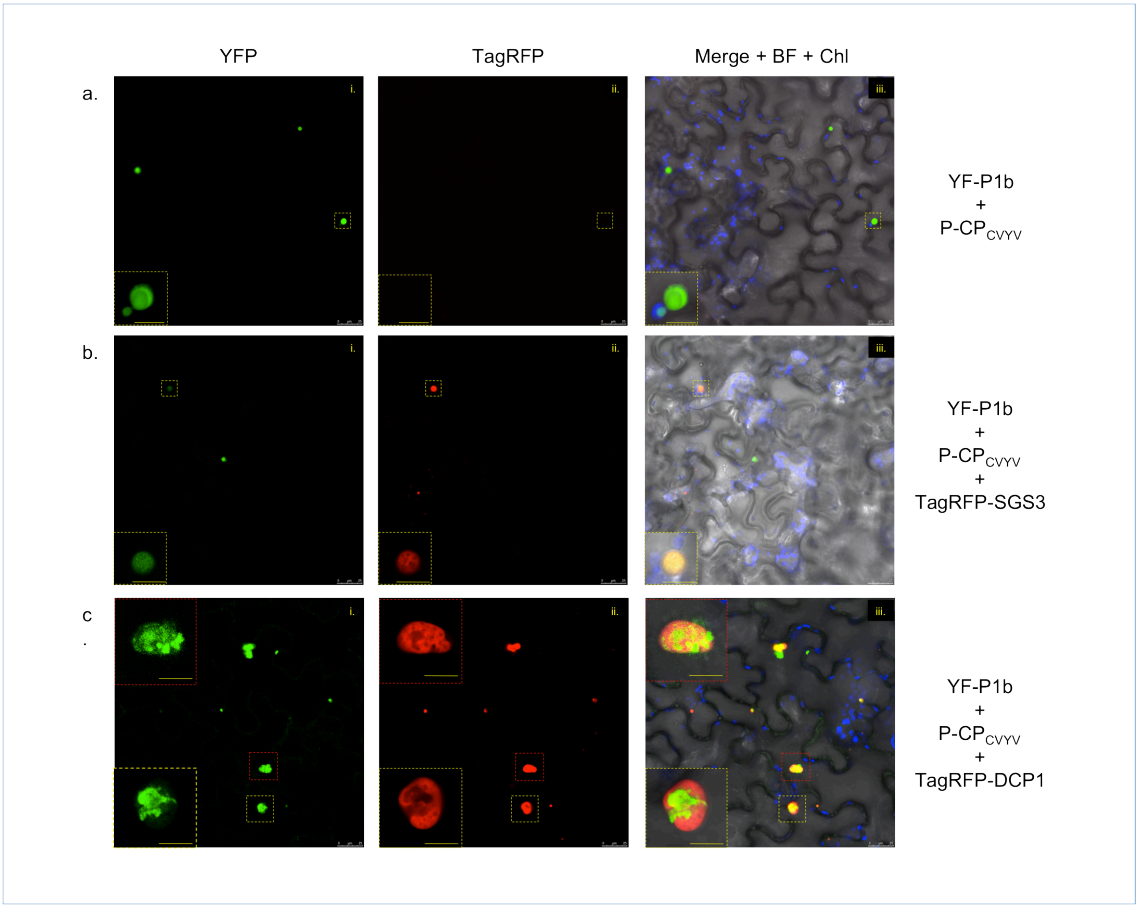

Figure 57. Subcellular localisation of CVYV, decapping and PTGS proteins. Confocal sections of *N. benthamiana* leaves co-expressing BiFC P1b and CVYV CP constructs with the TagRFP fluorescent fusion proteins indicated at 6 dpa. (a) Fluorescent BiFC P1b/CP-bodies seen under a confocal microscope. High magnification close-up of the P1b/CP-body in the box is shown on the lower left-hand corner. (b) P1b/CP-bodies co-localise completely with siRNA-bodies. Co-expression of BiFC P1b/CP-bodies with siRNA-body marker TagRFP-SGS3. High magnification close-up of the P1b/CP-siRNA-body in the box is shown on the lower left-hand corner. (c) P1b/CP-bodies co-localise partially with P-bodies. Co-expression of BiFC P1b/CP-bodies with P-body marker TagRFP-DCP1. High magnification close-up of the two P1b/CP-P-bodies in the red and yellow boxes are shown in the left-hand corners. Images from the first column (marked as i.) represent YFP signal, the second column (marked as ii.) represent RFP signal, and the third column (marked as iii.) represent the merge image of columns i. and ii. together with the Bright Field and the chloroplast autofluorescence (in blue). Scale bars of the low magnification images represent 25µm and in the high magnification images shown in the boxes represent 7.5µm.

Only partial co-localisation was observed between BiFC P1b/CP-bodies showing green fluorescence and the red fluorescence derived from the TagRFP-DCP1 labelled P-bodies. This result further supports the identification of the large fluorescent structures identified during P1b and CP interaction as siRNA-bodies, since P-bodies and siRNA-bodies are usually found juxtaposed forming distorted

clusters (Martinez de Alba et al., 2015). Taken together these results suggest that P1b migth perform its RNA silencing suppression activity, completely or partially, in siRNA-bodies and CP could contribute to this function.

"It is the mark of an educated mind
to be able to entertain a thought without accepting it."

Aristotle.

DISCUSSION

P1b is a RSS protein with cytosolic localisation under a physiological infection.

Previous reports characterising P1b activity all seem to hint a cytosolic localisation. It has been reported previously that P1b forms a homodimer complex with itself assisted by its zinc-finger domain (Valli et al., 2008). This zinc-finger domain plays an important role, not only in the formation of the homodimer P1b complexes, but also in the ability of P1b to suppress RNA silencing. Analysis performed with P1b using BiFC revealed the possible P1b localisation to be other than organellar as BiFC fluorescence could not be observed in any definite organelle structure (Valli et al., 2008). This report shows certain unidentified spherical structures present in samples expressing wild type P1b or two P1b mutants, not affected in RSS activity or homodimer formation (C93A and S264A). Although these structures could not be identified, they were clearly rejected to be nuclear as no co-localisation with DAPI stain could be observed, and were seen to move rapidly through the cytosol (Valli personal communication). Curiously, these spherical structures can not be observed in P1b mutant 1 (RK68,69AA) deprived of RSS activity (Valli et al., 2008) suggesting these structures could be related to RSS functions and probably not to over expression artefacts in the transient expression. In addition, homodimer P1b complexes were reported to bind smRNAs (Valli et al., 2008) and to co-precipitate with endogenous smRNA in agroinfiltrated plant leaves (Valli et al., 2011), authors suggesting P1b RSS activity, HCPro alike, functions by sequestering smRNAs and limiting the smRNAs loading into RISC complexes. As a result, during a viral infection, P1b RSS activity is expected to be localised in the cytosol to efficiently sequester viral-derived smRNA, as viral RNA silencing is triggered in the cytosol during (+)-ssRNA viral infection (Kooter et al., 1999; Martínez de Alba et al., 2013). Although smRNA binding of P1b has only been addressed during transient expression (Valli et al., 2011) rather than in a functional CVYV infection, other similar RSS proteins sequestering smRNAs have been reported to localise in the cytosol. This is the case of P19, a tombusvirus RSS protein, that has been reported to sequester viral smRNAs (Silhavy et al., 2002; Scholthof, 2006). In addition, delocalisation of P19 from the cytosol to the nucleus inhibits P19 RSS activity (Canto et al., 2006) strongly suggesting that P19 is only

functional in the cytosol. Like wise, HCPro from various potyviruses have also been seen decorating mainly the cytosol in different gold immunostain experiments (Riedel et al., 1998), together with the nucleus (Sahana et al., 2014) and chloroplasts (Jin et al., 2007) of infected cells.

Considering P1b is likely a smRNA-sequestering RSS protein, a cytosolic localisation is mostly encouraging. Results from the gold immunostain analysis of CVYV-infected *C. sativus* plants support a cytosolic localisation for P1b. No other subcellular compartment was differentially labelled in spongy mesophyll CVYV-infected cells, suggesting that at least in this particular cell type and at the precise infection time, P1b functions are mainly cytosolic. In addition, the co-localisation of P1b in siRNA-bodies and its partial co-localisation with P-bodies in transient expression experiments (Fig. 57) also supports that at least one pool of P1b is cytosolic. It cannot be excluded, though, that other cell types in different plant organs could present a different P1b localisation profile.

Immunogold labelling against P1b is uniformly distributed through the cytosol, with occasional heavily decorated electrodense globular cytosolic structures that could correspond with the spherical fluorescent bodies previously observed during the BiFC P1b/P1b (Valli et al., 2008), and P1b/CP (this thesis) assays. Despite similarities no experimental evidence supporting this correspondence exists, yet alone any functional relevance for these structures can be suggested. HCPro had been detected in cytosolic inclusions in potyvirus-infected cells, however no function other than simple deposition resulting from the over accumulation of the protein had been proposed (Riedel et al., 1998). Identification of other viral or host factors accompanying P1b or HCPro in these globular cytosolic structures would provide hints on what viral processes if any they could be involved in. It might therefore be interesting to perform co-labelling experiments in CVYV infected *C. sativus* plants to determine if the globular P1b cytosolic structures co-decorate with other viral proteins, like for example, the CP protein.

P1b localisation is altered in a PPV based expression system

P1b suffers a delocalisation when expressed by the PPV recombinant virus PPV-P1b-sGFP. During PPV-P1b-sGFP infection of *N. benthamiana* plants, P1b-specific immunogold labelling can be seen differentially decorating three different subcellular compartments: the cytosol, the nucleoplasm, and the nucleolus. It is commonly observed that passive diffusion of small proteins, like GFP (28 kDA), through the nuclear pore complex (NPC) is possible up to a certain size determined by the size exclusion limit (SEL) of the NPC, commonly around 40 kDA (Merkle, 2003). Proteins above this SEL cannot passively enter the nucleus and their import depends on active mechanisms. P1b is approximately 36 kDA in size (Valli et al., 2008), which makes it just under the NPC SEL to passively diffuse into the nucleus. However, passive diffusion of P1b into the nucleus could not be seen in CVYV infected *C. sativus* cells, indicating either that the NPC SEL in *C. sativus* could be smaller than that of *N. benthamiana*, or that entry of P1b into the nucleus in PPV-P1b-sGFP-infected *N. benthamiana* cells is facilitated by other viral or host proteins that are not available in in the CVYV/cucumber system.

As mentioned above, accumulation of HCPro in the nucleus has been reported for various potyviruses (Riedel et al., 1998; Sahana et al., 2014). HCPro has a calculated molecular size (52 kDA) notably bigger than the NPC SEL. Thus, it is reasonable to think that entrance of HCPro into the nucleus would require mechanisms other than passive diffusion. Localisation of P1, the contiguous cistron in the potyviral genome, from *Tobacco etch virus* has been observed in the nucleus, and nucleoplasmic and nucleolar localisation signals have been identified in this protein (Martínez & Daròs, 2014). These signals could be involved not only in the localisation of P1, but also of the P1-HCPro cleavage intermediate, being the targeting of HCPro to the nucleus regulated by the dynamics of the P1 protease activity. In a similar way, limited proteolysis of the P1-P1b polypeptide could be responsible for the nucleoplasmic and nucleolar localisation of P1b in PPV-P1b-sGFP-infected plants. It is possible to speculate that whereas P1 is driving HCPro to the nucleus where this protein has to perform relevant roles, the same protein is driving P1b fortuitously to the nucleus. In CVYV-infected cucumber cells P1b remains exclusively in the cytoplasm either because CVYV P1a lacks nuclear targeting signals or because of a higher proteolytic cleavage efficiency between

P1a/P1b than P1/P1b in *N. benthamiana*. The RSS activity of HCPro has been reported to be abolished by proteolytic failure in P1, and inefficient RSS activity of P1a-HCPro and P1a-P1b in *N. benthamiana* has been attributed to deficient self cleavage activity of P1a in this host (Pasin et al., 2014). It has been suggested that the lack of RSS activity of P1(P1a)-HCPro(P1b) could be due to very high turnover of the unprocessed protein (Carbonell et al., 2012). However targeting the RSS to the nucleus where it cannot display silencing suppression activity might also be the cause of the inoperativeness of these unprocessed proteins. Supporting this assumption, delocalisation of P19 into the nucleus has been held responsible in the inhibition of P19 RSS activity (Canto et al., 2006). In any case, the fact that PPV-P1b-sGFP systemically infects *N. benthamiana* indicates that, despite P1b being delocalised in the nucleus, it provides enough silencing suppression activity to support PPV infection, probably because there is still enough cytoplasmic P1b to fulfil RSS requirements (Carbonell et al., 2012). In this regard, it is interesting to remark that the donught-shaped phenotype described in local PPV-P1b-sGFP infections (Carbonell et al., 2012) could be revealing a recovery phenomenon due to the fact that delocalisation of P1b into the nucleus compromises its RSS activity.

To summarise, all present evidence point in the direction that P1b is a cytosolic RSS protein forming spherical structures, which, as will be discussed later, could also contain viral CP and be related to siRNA-bodies.

Host proteome signature is altered during viral infection.

Gel-free comparative proteomics analyses provide a fast and relatively simple way of comparing complex proteome samples. Since the initial report describing iTRAQ as a multiplex quantitation strategy for complex protein mixtures (Ross, 2004), advances in mass-spectroscopy technology and iTRAQ reagents have increased precision and detection ranges from complex proteome samples expanded as a universal tool with unlimited possibilities (Jorrin-novo, 2014). iTRAQ strategies have been used to analyse the proteome signatures in different plant conditions like, abiotic stress (Fukao et al., 2011; Liu et al., 2014; Zargar et al., 2015), hormone signalling (Zhao et al., 2010; Alvarez et al., 2011; Alvarez et al., 2013; Li et al., 2014b), light-sensing and development (Quan et al., 2013), plant resistance and

susceptibility to pathogens (Kaffarnik et al., 2009; Lippert et al., 2009), root response to gravitropism (Schenck et al., 2013), and even plant development in Space (Ferl et al., 2015). However, literature on plant proteome profiles during viral infections is scarce. iTRAQ strategies have been used to improve the understanding of aphid-borne *Barley yellow dwarf virus* (BYDV) transmission (Wang et al., 2015a), symptom formation during *Rice stripe virus (RSV)* infection (Wang et al., 2015b), or stress response in salicylic acid (SA) signalling-compromised plants during PPV infection (Pasin et al., 2014). This provides an opportunity in contributing to the knowledge of the proteome changes induced in the host by the viral infection. However, although iTRAQ analysis can provide a general view on the proteome changes inflicted by changes in physiological condition, specific differential accumulations of individual proteins have to be taken carefully as a differential accumulation does not necessarily involve a relevant biological function with consequences for the infection.

PPV infection alters host proteins involved in regulation of redox state and salicylic acid levels.

Previous proteome profiles in different PPV infected prunus species reveal significant changes in the antioxidant system of leaf apoplast relating to the susceptibility of the host to the virus (Diaz-Vivancos et al., 2006). Changes in cellular redox states promoting reactive oxygen species (ROS) in conjunction with other plant signalling molecules like SA and nitric oxide (NO) regulate plant innate immune responses involved in defensive responses towards the viral pathogen (Torres, 2006). Similarly, in another host system, PPV proteome changes affected mainly photosynthesis and carbohydrate metabolism producing imbalanced antioxidant systems with increased generation of ROS believed to result in the appreciable pathogenic symptoms produced by the (Diaz-Vivancos et al., 2008). Results from PPV-sGFP-infected samples show a differential over accumulation of cellular proteins involved in ROS productions. This is the case for Peroxidase 34 (AT3G49120) and the glycolytic metabolic enzymes GAPC1 (AT3G04120) and GAPC2 (AT1G13440), two of seven *A. thaliana* non-phosphorilating GADPH enzymes (Zaffagnini et al., 2013), recently involved in the regulation of ROS production, autophagy and plant immune response (Henry et al., 2015). Hydrogen

peroxide has been reported to inhibit the enzymatic activities of GAPC1 and GAPC2, leading to an enhancement of Phospholipase D activity (Guo et al., 2012). On the other hand, Phospholipase D has been reported recently to be recruited by *Red clover necrotic mosaic virus* (RCNMV) and *Brome mosaic virus* (BMV) replication complexes in *N. benthamiana*, being required for replication of both unrelated viruses (Hyodo et al., 2015). Cellular GAPDH-A has been reported to recruit RCNMV viral movement protein to viral replication sites (Kaido et al., 2014), suggesting that both GAPDH and Phospholipase D play important roles in viral replication, of at least tombusviruses and possibly bromoviruses. Plant GAPCs have been reported to undergo S-nitrosylation and glutationlytation (Zaffagnini et al., 2013), this later post translational modification proposed to serve as protection from over oxidation (Bedhomme et al., 2012). Although the biological relevance of these posttranslational modifications towards the viral replication has not been addressed, it is suggestive that various glutation S-transferases are also differentially over accumulated in PPV-sGFP and PPV-P1b-sGFP infected samples. These changes in redox potential in the cell might be favouring molecular interactions between cytosolic GAPCs and phospholipases modulating potyviral replication. Changes in redox potential could be affecting viral protease activity, and it is well established that NO dramatically inhibits papaine-like cysteine proteases from picorna-like viruses, similar to those encoded in PPV (Saura et al., 1999). The role of these differentially over accumulated proteins involved in cellular redox states towards PPV infection is purely speculative and remains to be addressed experimentally.

Another group of proteins differentially accumulated during both PPV-sGFP and PPV-P1b-sGFP infections are the pathogenesis related proteins (PR). Although these proteins are involved in different host processes, their role towards the viral infection is still widely debated. PR proteins have been reported to be induced in response to virus, bacteria, insect eggs and exogenous application with SA (Hennig et al., 1993; Niki et al., 1998; van Loon et al., 2006). PR-1, PR-2 and PR-5 highly over accumulate during PPV-sGFP virus infection. These proteins have been also reported to be over accumulating in PPV-sGFP mutant infections expressing a deregulated P1 in SA-deprived NahG plants (Pasin et al., 2014). Although no

negative effects have been associated towards the viral amplification levels, PR response is mainly associated to pathogenesis phenotypes. As a result, PR proteins are accepted pathogenesis biotic stress markers. However, there seems to be certain data that could suggests PR-2 protein over accumulation in infected plant tissue could be assisting in promoting the biological fitness of the invertebrate viral vectors (McKenzie et al., 2002), which would ultimately lead to an advantageous virus propagation.

In addition, evidences suggesting involvement of SA in the RNA silencing pathway have also been reported. The transcriptional activation of RDR1 in *N. tabacum* and *A. thaliana* (Alamillo et al., 2006; Hunter et al., 2013) and reduction in PPV-derived smRNA expression in NahG-expressing transgenic *N. tabacum* plants suggest SA to be involved in promoting antiviral RNA silencing (Alamillo et al., 2006; Alazem & Lin, 2015). SA and Abscisic Acid (ABA) are reported to be mutual hormone antagonists (Alazem & Lin, 2015). Although no direct measurements of the SA and ABA levels in PPV-sGFP or PPV-P1b-SGFP infections were performed, the differentially over accumulation of PR-2, PR-1 and under accumulation of an ABA-inducible protein (Fig. 23. b) detected in the iTRAQ experiments could suggest ABA repression due to high SA expression levels.

Increasing SA levels, could serve as a warning from infected tissue preparing distal viral-free tissues for systemic acquired resistance (SAR), but also mediate in the enhancement of local RNA silencing by the mechanisms previously proposed (Alamillo et al., 2006; Hunter et al., 2013). Recent reports have involved abscisic acid, among other plant hormones in regulatory roles of the RNA silencing pathway (Alazem & Lin, 2015), however the relationships between them is still not fully understood. Plant hormones are involved in complicated array of regulatory networks making observations to determine their effects on viral infections, and especially on RNA silencing challenging and conclusions are to be taken carefully. Nevertheless, this field remains largely unexplored and more research is to be encouraged.

On the other hand various members of the Lipid Transfer Proteins are seen to be under accumulated during both PPV-sGFP and PPV-P1b-sGFP infection. This group of proteins have been previously related to plant defence response (Kristensen et al., 2000; Buhot et al., 2001; Girault et al., 2008) and non-vesicular lipid transport (Lev, 2012). Considering the importance of lipid membranes to viral replication, changes in accumulation of these proteins could be indicative of viral processes involving lipid metabolisms, although their relevance towards the infection is unknown.

Comparison between PPV-sGFP and PPV-P1b-sGFP infections revealed proteins differentially accumulating between both viral infections. PR-2, GAPC1 and GAPC2 are the mostly differentially accumulated host proteins in a PPV-sGFP infections harbouring P1b. Although these differences might be initially attributed due to differences in viral accumulation, this seems no to be the case as all viral proteins identified and quantified (with the exception of CP) show no appreciable fold change differences. Instead, these differences could be attributed to the substitution of HCPro for P1b. If this were the case, HCPro would be inducing the accumulation of PR-1, PR-2, GAPC1, and GAPC2, which would explain the higher symptom severity observed in PPV-sGFP infection. HCPro has previously been related to symptom severity during PPV infections (Sáenz et al., 2001), and other potyviruses (Gal-On, 2000; Yambao et al., 2008) independent of viral accumulation, which seem consistent with results presented. On the other hand, only changes in viral CP accumulation could be observed, despite neither viral NIa or NIb accumulation seemed affected. PPV CP stability has been seen to be affected *in vitro* by the absence of HCPro (Valli et al., 2014). This effect could not be reverted by the substitution of HCPro for any other RSS protein like, P1b or P19, indicating that the RSS activity is not involved in the effect on PPV CP stability, which might be due to other HCPro functions. Whether PPV CP stability is a consequence of direct interaction with HCPro, among other host or viral components involved, and the biological relevance towards the infection is to be investigated further.

Transcription Factors affecting plant viral infections

Transcriptional control is crucial in the regulation of all cellular processes involved during the life of eukaryotic organisms and is an important determinant in the activation of complex genetic networks in response to stimuli. It is believed that transcriptional control in plants is by far more important than in other eukaryotes due to the higher percentage of Transcription Factor coding genes (Franco-Zorrilla et al., 2014). As master regulators of gene expression, transcription factors control the activity of numerous plant molecular pathways leading to metabolic and phenotypic changes involved in adaptation to different stresses (Alves et al., 2014). At least six transcription factor families have been described involved in plant defence (Alves et al., 2014): bZIP (Johnson, 2003; Mukhtar et al., 2009; Fu et al., 2012; Alves et al., 2014), WRKY (Pandey & Somssich, 2009; Alves et al., 2014), MYC (Lorenzo et al., 2004), AP2/ERF (Pieterse et al., 2012; Alves et al., 2014; Seo et al., 2015), MYB (Ambawat et al., 2013; Raffaele & Rivas, 2013; Alves et al., 2014) and NAC (NAM/ ATAF /CUC) (Mauch-Mani & Mauch, 2005; Seo et al., 2015). However, few TF have been reported relating directly to viral infections. Members of the NAC transcription factor family have been reported involved in viral infections. This is the case of TCV-Interacting Protein (TIP), specifically interacting with *Turnip crinckle virus* (TCV) CP inducing HR response against TCV in *A. thaliana* (Ren et al., 2000; Donze et al., 2014), and ATAF2, reported to interact with the TMV 126-/183-KDA replicase protein(s) and targeted to degradation by the virus to suppress host basal defence response (Wang et al., 2009). Another member of the NAC transcription factor family, RAV2 involved in ethylene signalling, has been reported to be a host factor required for two unrelated viral RSS proteins, potyviral HCPro and carmovirus P38, being indispensable for their RSS activity (Endres et al., 2010). Alterations in transcriptional regulation of various transcription factors, including RAV2, have also been reported in transgenic HCPro-expressing plant, as well as during TEV and CMV-Y infections (Soitamo et al., 2011). Other transcription factor families have also been related with plant virus infections. Various MYB transcription factors are highly induced during CMV and TMV infection (Yang & Klessig, 1996; Geri et al., 1999) positively regulating PR-1 transcription and SA-mediated SAR during infection. In addition various WRKY transcription factors from different host pathosystems have been shown to

be involved in the defence response against TMV infection (Liu et al., 2004; Chen & Yeh, 2010; Lim et al., 2011) and in suppression of ABA signalling to promote TMV systemic movement (Solovyev & Savenkov, 2014). Moreover, other viruses like carlavirus Chrysanthemum virus B (CVB), have evolved coding for proteins mimicking eukaryotic transcriptional activators. CVB p12, a zinc-finger protein, activates expression of a bHLH transcription factor inducing cell proliferation and hyperplasia, resulting in severe leaf malformation (Lukhovitskaya et al., 2013). Similar strategies are also employed by certain DNA viruses, like geminiviruses, conditioning the control of viral and host processes through interactions with different host transcription factors (Lacatus & Sunter, 2009; Chung & Sunter, 2014; Li et al., 2014a).

Genetic control of gene expression by transcription factors plays a pivotal role in the integration of the diverse stimuli acting as sensors that unchain programmed responses preparing the plant for an environmental change or an imminent pathogen attack. As master regulators in gene expression, the activation or deregulation can stimulate fast transcriptional reorganisation of different and diverse pathways simultaneously with significant biological consequences towards the host and the viral invader. For this reason, the high throughput screening of transcription factors could potentially allow for the isolation of new transcription factors with functional relevance in promoting either viral infections or plant defence responses. The conditional expression technology developed by the TRANSPLANTA consortium enables the opportunity to screen for transcription factors where the constitutive over expression or *loss-of-function* can result in a lethal, aberrant or pleiotropic plant phenotypes. Reports estimate between 1000-3000 transcription factors and regulators are encoded in plant genomes accounting to an average of 5-15% of all protein-encoding genes (Udvardi et al., 2007; Perez-Rodriguez et al., 2010; Jin et al., 2014; Seo et al., 2015). In particular, a number of reports estimate the total of Transcription factors-encoded genes in *A. thaliana* to be at least 1800, representing more than 7% of the total protein coding genes (Riechmann et al., 2000; Guo et al., 2005; Iida et al., 2005; Udvardi et al., 2007; Gabrenaite-Verkhovskaya et al., 2008; Coego et al., 2014), with only one tenth having been characterized genetically (Qu & Zhu, 2006; Udvardi et al., 2007).

At the time of the screen a total of 2839 distinct genes originating from 2191 different loci and belonging to at least 58 different transcription factor families are annotated in the tair10 *A. thaliana* database accounting to an over estimated total of 8% (27,416 protein coding genes annotated in tair10 database using "Transcription" as search word). Of these, a total of 634 TF have been reported to be represented in the TRANSPLANTA collection of which 447 TF were available at the time of this work to use in the screening. The number of TFs available thus accounts to an estimated representation of 20-25% of all anticipated TFs encoded in *A. thaliana*. This relatively low representation and the presumed high occurrence of overlapping functions between TFs together with the technical difficulties in maintaining a high and sustained ß-estradiol induction and the large differences in induced expression between TF transgenic lines (Coego et al., 2014), make the isolation of new uncharacterized TFs involved in viral infection or pathogen response a very challenging endeavour. Nevertheless a small number of initial putative candidates could be selected in our screen to be subjected to further detailed characterization.

Transcription factors putatively involved in PPV-P1b infection

From the total of 447 induced TFs, corresponding to 897 distinct over expressing transgenic lines, a minimum of 11028 PPV inoculations were performed and infections monitored at four different time points producing at least 44112 images using the UV-stereoscope. The large diversity encountered among different plants of the same line and between the two independent lines transformed with the same transgene, highly limitated the analysis. The first limitation was in part derived from intrinsic divergences in the course of viral infections and in the fact that, despite efforts in supplementing culture media with ß-estradiol to maintain expression levels, a constant and durable transgene expression could not be achieved. Differences between sister transgenic lines probably accounted to the tremendous divergences in the ß-estradiol-induction of the transgenes. These differences were observed during the induction procedure used in different TFs lines and in the control GUS::GFP lines as well. In fact, in all screening performed, putative TF candidates only presented differences with the controls in one of the

two transgenic lines expressing them that were analysed. Consistent with these observations other TRANSPLANTA partners also reported discrepancies in the induction levels of different TFs lines expressing the same transgene (Coego et al., 2014).

With these limitations, the vast majority of the infections during the initial screening grouped under the same cluster as the GUS controls. TFs which were found to be highly deregulated under PPV infection in microarray data previously reported (Babu et al., 2008) were shortlisted and analysed first. However, no correlation was observed between these deregulated TFs and those showing differences in GFP fluorescence or CP accumulation during screen. Visual analysis revealed a group of 6 outliers (TFs lines 92-A; 191-H; 192-E; 227-A; 267-F; 436-C) showing significant reduction in viral infectivity. Three of these TF lines (192-E; 227-A; 436-C) presented differences in PPV CP accumulation, when quantified by densitometry. Although none of the differences were statistically significant, the fact that these differences were also observed during the GFP fluorescence analysis, being among the six lines showing reduced infectivity, could suggest they might be functionally relevant.

Similar limiting situations were encountered when analysing the systemic spread of the infection. During the GFP fluorescence analysis, 6 outliers (TF lines 41-E; 52-D; 436-D; 227-D; 162-D; 267-F) presented significant statistical differences when compared to control infections. Lines 41-E, 52-D, 436-D and 227-D all seemed to support faster viral movement, whereas lines 162-D and 267-F showed a reduced movement phenotype. However, only one of the TF lines showing significant statistical differences in the visual analysis reported statistical significant differences in the biochemical analysis. TF line 162-D presented a statistical significant reduction in CP accumulation, which correlated with the visual GFP fluorescence analysis. Moreover, lower CP accumulation in line 267-F and higher CP accumulation in line 227-D, although not statistically significant, positively correlated with the visual GFP fluorescence analysis. TF line 267-F showed both a lower infectivity and a slow movement phenotype, which correlated with lower CP accumulation, suggesting that the TF expressed in this line, JUB1, a member of the

NAC family induced by hydrogen peroxide, could be contributing in antiviral defence.

Interestingly, regardless of expression in the same TF, the behaviour of the two sister lines 227-D and 227-A appears to be contrasting. Line 227-D showed significant lower infectivity whilst line 227-A significant enhancement of viral movement during the visual GFP fluorescence analysis, correlating, although not statistically significantly, with a lower CP accumulation and a higher CP accumulation respectively. Similarly, whereas virus infectivity was significantly reduced in line 436-C, virus spread was significantly faster in its sister line 436-D and differences in CP accumulation were mainly observed in line 436-C (again with no statistical significance), where the reduced viral accumulation observed correlated with the reduced infectivity.

The lack of reproducibility of the infection pattern in lines transformed with the same transgene, especially the cases of those with opposite patterns, question the assignment of a particular phenotype to any specific action of the expected TF expressed in the induced transgenic line. Assessing viral infection of non-induced plants, and comparison of the actual expression levels of lines transformed with the same transgene showing disparate responses to PPV-P1b infection will be required to discriminate between a functional role of the candidate TF and lateral effects of non-specific mutations caused by the transformation procedure.

A systematic bibliography search of these TFs putatively involved in viral infection did not reveal any involvement relating to biotic stress reported previously, with the exception of TF 162 reported to be involved in induction of hydrogen peroxide and oxidative stress which could potentially result in effects on viral infection. However, without confirming that the effects observed are in fact a result of the transgene induction any further comment remains simple unfounded speculation.

P1b has a circus of interacting host proteins involved in multiple host processes.

The yeast two-hybrid system (Fields & Song, 1989) is a widely used powerful genetic tool to identify protein-protein interaction. Y-2H screenings provide high quality binary interaction information (Yu et al., 2008) of physically associating proteins in a simple, sensitive and high-throughput adaptable procedure (Uetz et al., 2000). This method can be successful in detecting even weak or transitive protein interactions, and the interaction strength predicted by Y-2H generally correlates with strengths determined *in vitro,* enabling selection of different interaction affinities (Criekinge & Beyaert, 1999; Causier & Davies, 2002). Numerous contributions in detecting relevant host-viral protein interactions, including HCPro host partners, have been reported (Li et al., 2015; Revers & García, 2015). In addition to Y-2H, column affinity purification followed by mass spectroscopy (AP/MS) could yield different, but complementary high quality data (Yu et al., 2008). Since Y-2H data sets have been reported to contain more false positive interactions than AP/MS data sets (von Mering et al., 2002; Bader et al., 2004; Yu et al., 2008), an AP/MS purifications strategy was performed hoping to identify interactions common to both strategies. Furthermore, since not all physical interactions occur within complexes, and not all proteins in a complex are in physical contact, using Y-2H and AP/MS strategies simultaneously could further widen the involvement of P1b functions at different complexity levels. A total of 20 candidate genes were found to interact with P1b during the Y-2H assay and 29 proteins were identified as putative P1b interactors from the AP/MS experiment using an NTAP-P1b bait expressed in transgenic arabidopsis. However, none of these host factor were found common to both interaction isolation strategies.

Although initially removing frequent protein contaminants in TAP-mediated affinity purifications enabled a curated list, it was agreed to further curate the AP/MS list of putative P1b interactors using other transgenic lines expressing non-functional NTAP-P1b alleles and/or other un-related viral RSS proteins. For this purpose, further transgenic lines were produced, however the long procedure in isolating different independent homogeneous lines limited performing these additional control purifications before presenting this work. Whilst the additional transgenic lines were being produced efforts were focused in validating putative P1b interactions identified during the Y-2H screening. In this sense, the BiFC

system was reported previously to be a convenient method in verifying if interactions isolated in Y-2H screens in yeast can also occur *in planta* (Yu et al., 2008). Because reconstitution of the YFP fluorescence in the BiFC assays does not force any nuclear localisation, as in the transcriptional reconstitution of the Y-2H, proteins can accumulate in distinct subcellular structures, and thereby revealing the subcellular localisation of the interaction, which in turn, could aid in determining a putative function. From 12 selected putative Y-2H P1b interactors only 4 were seen to complement fluorescence, being in agreement with the high false positive rates typically observed in Y-2H screenings (von Mering et al., 2002; Bader et al., 2004; Yu et al., 2008). In parallel, biological assays were performed using PPV-P1b-sGFP to determine if a *loss-of-function* or over expression of the selected candidates from the Y-2H screen could, in some way, affect viral infection. From these viral assays, only two Y-2H P1b putative interactors (PRH75 and HYD1) showed relevant effects on PPV-P1b-sGFP viral infection.

Arabidopsis mutants affected in the PRH75 locus are affected in susceptibility to PPV-P1b-sGFP infection.

The Y-2H screen revealed a cDNA sequence coding for a fragment of the *A. thaliana* RNA helicase PRH75 strongly interacting with P1b in yeast. This fragment consisted of 209 C-terminal amino acids including two core helicase motifs and a GUCT domain reported to be involved in protein-protein interactions (Ohnishi et al., 2009). The interaction with P1b was maintained when the complete PRH75 sequence was expressed in Y-2H system arguing against a casual interaction of P1b with the peptide selected in the initial Y-2H screening. Further validation *in planta* using BiFC also supported the belief that interaction between P1b and PRH75 could be relevant. The fact that reconstituted YFP fluorescence was not observed in the nucleus, were PRH75 has been shown to accumulate in healthy plants, may suggest that the interaction with P1b could be relocalising PRH75 during viral infections. Although we cannot discard possible artefactual consequences of tagging the N-terminus of the protein with the N-terminal moiety of YFP (YF-), the fact that N-terminal and C-terminal GFP tags did not appear to interfere with the nuclear targeting of PRH75 suggests no differences in localisation is to be expected using N-terminal BiFC tags. The delocalisation of PRH75 from the nuclei to the

cytoplasm has previously been observed as a consequence of its interaction with CSP3 under stress to cold (Kim et al., 2013), suggesting PRH75 could have additional cytosolic functions amidst its canonical nuclear ones. Other DEAD box family members, including *A. thaliana* PRH8, a nuclear helicase closely related to eIF4A, have been reported to be indispensable for PPV infection, interacting with PPV VPg in the nucleus (Huang et al., 2010). Although the delocalisation of PRH75 away from the nucleus when interacting with P1b, as observed during the BiFC assays, may hint in favour of a biological role, demonstrating that this delocalisation also occurs in the context of a viral infection (either CVYV or PPV-P1b-sGFP) would be needed to fully support this assumption. Additional efforts were focused in assessing the effects of PRH75 *loss-of-function* on viral infections. PPV-based chimeras were used in limitation of a CVYV cDNA infective clone. Of the different *A. thaliana* T-DNA insertion lines tested against PPV-P1b-sGFP, only one line prh75a#3 (SAIL_302_D12.v1) showed a considerable reduction in CP accumulation suggesting for a partial resistance phenotype. The fact that similar levels of viral accumulation were detected in inoculated leaves between mutant and control plants, suggest a similar response to the agrobacteria inocula, and that systemic spread of the virus is disturbed in prh75a#3 plants, accumulating at least 10 fold less CP protein. The substitution of P1b for HCPro in the PPV-chimera appears to relieve constraints on viral accumulation shown by PPV-P1b-sGFP in prh75a#3 mutant plants. This suggests that either HCPro may not require PRH75 activity as opposed to P1b or that an alternative host factor plays substitutes PRH75 functions in assisting HCPro. Alterantivelly, PRH75 may also be participating in wild type PPV infections but its *loss-of-function* has a less ostensible effect due to the stronger infection exerted by PPV-sGFP in comparison to PPV-P1b-sGFP. In any case, our results suggest PRH75 to be an important P1b host partner with positive effects on viral infection.

PRH75 is a DEAD box RNA helicase with ATP-dependent RNA unwinding activity that is compromised under thermal insult (Nayak et al., 2013), and suggested to be involved in assisting ribosome assembly during translation (Lorković et al., 1997; Lorenzo et al., 2004; Lorkovic et al., 2004; Nayak et al., 2013). Both PRH75 and NIb from various potyviruses undergo sumoylation by interacting with SCE1, an E2

sumo conjugating enzyme (Elrouby & Coupland, 2010; Xiong & Wang, 2013) with important consequences towards TuMV infection when sumoylation is compromised. Whether inhibiting sumoylation of PRH75 can compromise PPV-P1b-sGFP or CVYV infection is not known. Considering the results presented, the interaction between PRH75 and P1b might be involved in altering the host translational machinery in benefit for the virus. These initial results should motivate further research on the molecular functions of this interaction and the relevance in the processes involved.

HYDRA1, a sterol isomerase involved in lipid metabolism and RNA silencing compromises RNA silencing suppression.

HYDRA1 (HYD1) is a transmembrane ER targeted sterol isomerase involved in isoprenoid synthesis. It has been reported to be required for numerous important plant processes including RNA silencing (Schrick et al., 2002; Souter et al., 2002; Souter et al., 2004). HYD1 function is essential for the activation of the membrane bound AGO1 fraction indispensible for miRNA function (Brodersen et al., 2012). Other members of the isoprenoid pathway have also been reported affecting RNA silencing (Brodersen et al., 2008; Brodersen et al., 2012) and viral replication (Sharma et al., 2010). In addition, PVY HCPro has been shown to interact with a component of the chloroplast isoprenoid biosynthesis pathway promoting isoprenoid biosynthesis with important consequences towards hormone metabolism (Li et al., 2015).

HYD1 interacts with P1b. BiFC experiments revealed fluorescent complementation between HYD1-P and YF-P1b but not with the non-functional P1b Zinc finger mutant 6 (C103A) (Fig. 42. a) and, fluorescent complementation appeared to be dependant on protein accumulation levels (Fig. 42. b). Expression of the complete HYD1 sequence might be causing deleterious effects in yeast, allowing for selection only clones with a +1 frameshift at the beginning of the cDNA sequence, probably acting as translational regulation producing lower protein accumulation levels as observed in similar reports (Giot et al., 2003; Albers et al., 2004). YF-P1b was observed to suffer a drastic drop of accumulation at 6 dpa, when it was coexpressed with HYD1-P (Fig. 43), leading to enhanced RNA silencing, as shown

by the very low accumulation of both GFP protein and mRNA and significant production of GFP smRNAs (Fig. 43 & 44). However, it is no clear whether HYD1 expression is enhancing RNA silencing, overwhelming the RSS activity of YF-P1b, or if it is directly disturbing the RSS activity. However, the fact that at 3 dpa HYD1-P expression causes a sharp increase in GFP smRNA accumulation alone (Fig. 44) may argue in favour of the first possibility. Similarly to the effect observed on YF-P1b accumulation in the agroinfiltration system, expression of HYD1-P disturbed PPV-P1b-sGFP infection, but also affecting the infection of PPV-based chimeras expressing HCPro or P19 as silencing suppressors. Although the possibility that HYD1 could also be interacting with HCPro and P19 cannot be totally discarded, it seems more likely that HYD1 mainly interfere with PPV infection directly enhancing antiviral RNA silencing, questioning the relevance of the HYD1/P1b interaction.

Constitutive expression of short viral sequences with sequence similarity to the virus have previously been reported to inhibit viral infections (Guo & García, 1997). However, this phenomenon seems not to be the main cause in the effect observed with HYD1-P on the PPV chimeras expressing the GFP reporter gene. Although the GFP reporter gene encoded in the chimeras shares sequence similarity with the BiFC C-terminal YFP moiety (-P) tag used, control infections expressing transient sGFP could not be seen to cause any significant inhibition of PPV-sGFP (Fig. 46). However, considering HYD1 and HYD1-P seem only to affect wild type PPV at high temperatures, where the efficiency in the viral infection is considerably reduced, slight effects of the co-expression between the BiFC tag (-P) and the viral GFP reporter cannot be discarded. This seems to be in agreement with previous reports relating viral susceptibility to temperature-dependent silencing induction (Chellappan et al., 2005; Dujovny et al., 2009). The facts that the non-functional E508 allele harbouring a single amino acid substitution (D102N) previously characterized (Schrick et al., 2002), had a significantly lower effect on PPV-P1b-sGFP infection and YF-P1b accumulation than that of wild type HYD1, in spite of sharing the same BiFC tag (Fig. 49. a), provides additional evidence that specific HYD1 activity is responsible for disturbing the viral infection. Thus, results suggest that HYD1 potentiate antiviral silencing of PPV

infection, but this effect is only ostensible when other factors, like co-expression of homologous sequences or high temperature contribute to silencing induction.

As it has been already mentioned, HYD1 is suggested to contribute in creating the correct membranous requirements for AGO1 activity (Brodersen et al., 2012). Thus, it is likely that the enhanced antiviral silencing associated with HYD1 observed is the result of a stimulated AGO1 activity. However, the involvement of HYD1 in sterol biosynthesis plays an important role in providing the adequate lipid composition of the diverse cell membranes. Numerous reports describing membrane factors and lipid composition as essential to viral replication have been published (Lee et al., 2001; Lee & Ahlquist, 2003; Sharma et al., 2010; Sharma et al., 2011; Wang et al., 2011a; Zhang et al., 2012a). It is possible that over expression of HYD1 could be causing chemical alterations on the morphology of cellular membranes needed for PPV replication, leading to unsuccessful membrane recruitment compromising viral replication. In this sense, membrane alterations caused as a result of HYD1 over-expression could exert effects on two different fronts sensitive to the viral infection: i. enhancement of RNA silencing on one side, and ii. disturbance of viral replication complexes on the other. Whereas HYD1 *loss-of-function* has been shown to have important deleterious and pleiotropic effects, stable HYD1 over expression has not been yet characterized. It would be interesting to determine the effects on cell membrane structure of HYD1 over-expression in transgenic plants, and how this affects plant physiology and susceptibility to plant viruses.

P1b and CP interact together and with translation initiation factor eIF(iso)4E

Translation is a cellular process crucial for viral infection. The replication machinery of (+) RNA viruses is not encapsidated and are dependent on viral factors that need to be produced by translation of the invading genomic RNA in order for viral replication to commence (Buck, 1996). Upon invasion, virions count with limited viral factors to recruit host translation machinery. In addition to the genomic viral RNA, factors available to recruit translation include the *VPg* protein, linked to the 5' end of the genome (Siaw et al., 1985; Riechmann et al., 1989;

Murphy et al., 1990; Murphy et al., 1991; Grzela et al., 2006; Robaglia & Caranta, 2006; Beauchemin et al., 2007; Khan et al., 2008; Revers & García, 2015), the *CP* protein disposed in a helicoidal structure surrounding the RNA genome with its N and C-terminal domains protruding towards the exterior of the virion (Shukla & Ward, 1989), HCPro and CI proteins, which have been observed in structures at the tip of the viral particles (Manoussopoulos et al., 2000; Torrance et al., 2006; Gabrenaite-Verkhovskaya et al., 2008). Members of the eukaryotic translation initiation factors, including eIF4E and its isoforms, eIF4G and an eIF4A related helicase, atRH8, have been reported to be essential VPg host partners necessary for potyvirus infection (Leonard et al., 2000; Grzela et al., 2006; Michon et al., 2006; Nicaise et al., 2007; Yeam et al., 2007; Charron et al., 2008; Huang et al., 2010). Furthermore, resistance breaking virulent viral strains have been seen to compensate in *loss-of-function A. thaliana* mutant plants for one of the eIF4E or eIF4G isoforms by introducing mutations, mainly in the VPg sequence (Robaglia & Caranta, 2006), but also in CI (Abdul-Razzak et al., 2009; Sorel et al., 2014) or P1 (Nakahara et al., 2012). In the case of PPV, infection of a strain C isolate in *A. thaliana* is aided by mutations in the VPg sequence probably by allowing functional interaction with an eIF4E isoform of this host (Calvo et al., 2014). Vpg has also been reported to inhibit host capped RNA translation while enhancing RNA translation from the virus (Khan et al., 2008; Hafrén et al., 2013) redirecting resources in translation towards the virus. In addition, interaction of eIF4E and isoforms has also been reported with HCPro, with important consequences in viral infectivity if interaction is broken (Ala-Poikela et al., 2011). Although there are no reports demonstrating HCPro is involved in recruiting host translational machinery for viral translation, evidence including HCPro detected at the virion tip with VPg (Torrance et al., 2006) and interactions with VPg (Guo et al., 2001) could suggest a role in assisting VPg in the initial recruitment of eIF4E and isoforms. Viral factors including Vpg, HCPro and NIb, but not CP, have been reported to co-localise with viral induced replication vesicles together with eIF4E and isoforms, the eIF4A related helicase RH8, and eEF1A, a member of the eukaryotic elongation factor family (Schaad et al., 1997; Leonard, 2004; Beauchemin et al., 2007; Thivierge et al., 2008; Cotton et al., 2009; Huang et al., 2010; Ala-Poikela et al., 2011) suggesting a dual role of the eukaryotic translation factors in viral

translation and in assisting VRC during viral replication. Additionally, VPg and the viral replicase NIb were seen to interact with CP, and involvement in viral RNA synthesis in infected cells was suggested, despite no information on subcellular localisation was made available (Hong et al., 1995; Jiang & Laliberté, 2011; Zilian & Maiss, 2011; Elena & Rodrigo, 2012). CP was also proposed to modulate in the sorting of viral RNA between viral translation and viral assembly (Hofius et al., 2007; Hafrén et al., 2010; Besong-Ndika et al., 2015) and highlights the strict control in the early viral multiplication events to bias viral translation and RNA synthesis rather than virus assembly (Revers & García, 2015).

Results in this work show P1b and CPs interact together and with the eukaryotic translation initiation factor from *C. melo,* eIF(iso)4E. BiFC and Co-IP results both show a strong and positive interaction between P1b and eIF(iso)4E. Whereas PVA, PVY and TEV HCPro have been reported to interact with both eIF4E and eIF(iso)4E from two different host species, the interaction was reported to be stronger for PVA HCPro with eIF(iso)4E from both hosts in Y-2H (Ala-Poikela et al., 2011) and for PVA, PVY and TEV HCPro when eIF(iso)4E from *S. tuberosum* is expressed in *N. benthamina* (Ala-Poikela et al., 2011). This seems also to be the case for P1b. P1b specifically interacts with eIF(iso)4E in BiFC assays performed in *N. benthamiana* leaves (Fig. 50. a), but co-immunoprecipitated at similar levels with eIF4E and eIF(iso)4E when expressed deprived of tags by transient expression (Fig. 51. a). This could argue in favour of P1b interacting equally strong with both factors, but structural hindrances impede reconstitution of the YFP fluorescence between P1b and eIF4E when tagged with YFP residues during the BiFC assays. However the fact that eIF(iso)4E co-immunoprecipitates with P1b more efficiently than with eIF4E in PPV-P1b-sGFP-infected samples (Fig. 51. b), suggesting a preference of P1b for the eIF(iso)4E isoform, as observed during the BiFC assay, may hint a functional significance and that other viral proteins, perhaps the CP, can contribute to this specificity.

P1b mutant 1 (RK68,69AA), previously reported to be impaired in smRNA binding, and as a consequence in RSS activity (Valli et al., 2008) interacted with eIF(iso)4E with similar efficiency than wild type P1b (Fig. 50 a.), indicating that P1b

intearction with eIF(iso)4E is not dependent on bind smRNA binding. By contrast, P1b mutant 6 (C103) affected in a zinc finger motif required for correct folding of the protein does not show any interaction with eIF(iso)4E as observed during the BiFC assay, indicating that this interaction is conformation-dependent. Preliminary results not included in this report, revealed that interaction with eIF(iso)4E was greatly impaired in P1b mutant 13 (KR10,11AA) disturbing a basic N-terminal region of the protein previously reported not affecting its RSS activity (Valli et al., 2008).

These findings further separate different P1b activities, resulting eIF(iso)4E binding dispensable for silencing suppression, which would be unnecessary in the early translation events of the virion where RSS activity may not yet be required. Although the established consensus sequence for the eIF4E binding domain (K/R)-X-X-**Y-**D-R-X-F-**L-**(L/M) with tyrosine and leucine residues (indicated in bold face) conserved in all known eIF4E-binding proteins (Lawrence & Abraham, 1997; Rhoads, 2009) could not be found in P1b nor CP, a similar sequence (*KK*R**Y**QTNA**I**D) surrounding the KR10,11AA mutation in P1b mutant 13 was found, highly resembling a previously described eIF(iso)4E binding motif (LKK**Y**RKEE**L**E) of plant lipoxygenase 2 (Freire et al., 2000). This finding further support the appointment of P1b as a eIF(iso)4E-binding protein, and tentatively place its interaction at the N-terminus of the protein.

Results do not permit revealing the RSS-independent functions of P1b involved in the eIF(iso)4E interaction. Abundant previously reported data places eIF4E isoforms and VPg as key stones in assembling the contributions of many viral (P1, CI, HCPro) and host factors (eIF4G, RH8) in important steps involved in potyviral infections. Viral RNA translation can be envisaged as main target of these complex networks of protein interactions, but it likely also contributes to coordinate the production of viral proteins and their use in viral replication. Results presented suggest that P1b can not only substitute RSS functions in replacement of HCPro, but also functions in the eIF(iso)4E-mediated network in which the viral CP could also be involved.

P1b/CP interaction is cytosolic and co-localises with siRNA-bodies.

Interactions of CP proteins with HCPro from various potyviruses have been previously reported, and are necessary for the aphid-borne transmission of virions (Blanc et al., 1997). However, binding between HCPro and CP in non-aphid transmissible viruses has also been reported (Manoussopoulos et al., 2000; Roudet-Tavert et al., 2002) and recent evidence suggesting the interaction between these proteins might play other roles in addition to aphid transmission has been reported (Valli et al., 2014). Interestingly, both HCPro and CP have been shown to enlarge plasmodesmatal SEL, facilitating their transfer through the cell wall along with viral RNA, and suggested to be involved in viral movement (Dolja et al., 1993; Dolja et al., 1995; Rojas et al., 1997). Certainly at the time of these reports the RSS activity of HCPro had not been reported, and distortion in HCPro RSS activity could result in different viral movement restrictions as a result of impairment in genome protection from RNA silencing rather than of viral movement.

Despite functional HCPro/CP interaction has been previously observed though various biochemical approaches (Blanc et al., 1997), attempts in demonstrating PPV HCPro/CP interaction visually using BiFC fail (Zilian & Maiss, 2011), regardless of the fact that functional connection between these proteins has been demonstrated (Valli et al., 2014). To further investigate the broadness in the interactions between RSSs and CPs in family *Potyviridae*, interaction between CVYV P1b and CPs of different potyviruses was assessed using BiFC. CVYV P1b interacted with is cognate CP, but also with PPV CP, contrasting with the inability of P1b to stabilise PPV CP during PPV infection (Valli et al., 2014). Additionally, the CP of the tritimovirus BStMV, found not to interact with its cognate HCPro, interacted both with CVYV P1b, and its BStMV homolog, P1 also exhibiting RSS activity (Young et al., 2012). All these results reveal promiscuous interactions between potyviral RSSs and CPs, whose functional relevance remains still unknown. Round non-nuclear fluorescent intracellular structures were specifically observed when CVYV P1b interacted with potyviral CPs (Fig. 53. b). Similar structures were also observed associated to P1b self interaction (Valli et al., 2008),

but not when P1b was co-expressed with eIF(iso)4E (Fig. 50. a). Interestingly, similar granules were observed in BiFC assays showing interaction between the RSS P1 of the tritimovirus BStMV and its cognate CP protein (Fig. 53. a), suggesting that they could be a general feature of potyviral RSS proteins belonging to the P1b-like family. Whether these structures are shared by HCPro is still unknown, since no data approaching HCPro/CP interactions using BiFC has been made available. Several citoplasmic granules have been reported to be involved in single-stranded RNA turnover in plant cells, processing bodies (P-bodies) and SGS3/RDR6 bodies (siRNA-bodies) among them (Maldonado-Bonilla; Kumakura et al., 2009). Both P-bodies and si-RNA bodies play distinct functions in stress related mRNA degradation. Whereas P-bodies have been related to mRNA decay (Sheth & Parker, 2003) (Sheth & Parker, 2003), siRNA bodies have been involved in RNA silencing amplification as well as ta-siRNA and nat-siRNA production (Jouannet et al., 2012; Moreno et al., 2013). siRNA-bodies are membrane-associated citoplasmic granules (Jouannet et al., 2012), usually found juxtaposed to P-bodies forming distorted clusters (Martinez de Alba et al., 2015). The SGS3 RNA binding protein, which is required for RNA silencing amplification and ta-siRNA synthesis (Mourrain et al., 2000; Béclin et al., 2002; Peragine, 2004; Yoshikawa, 2005; Vaucheret, 2006; Yoshikawa et al., 2013), is a distinctive component of siRNA bodies (Kumakura et al., 2009; Jouannet et al., 2012). Recently, different viral RSS proteins like TYLCV V2 (*Begomovirus*), RSV P2 (*Tenuivirus)*, PlAMV TGBp1 (*Potexvirus*) and PVA VPg (*Potyvirus*) have been described to interact with SGS3 (Glick et al., 2008; Du et al., 2011; Okano et al., 2014; Rajamäki et al., 2014). As a result, speculating whether interaction of the RSS protein P1b with CP could be resulting in SGS3-containing siRNA-bodies was tempting. In order to test this hypothesis, P1b and CVYV CP tagged with complementary BIFC tags where co-expressed either with siRNA- or P-body RFP tagged markers; SGS3 and DCP1. Fluorescent reconstitution derived from P1b/CP interaction largely co-localised with red fluorescence derived from RFP-tagged SG3 in granules exhibiting an average diameter (6.1±0.4µm) similar to the PVA VPg-SGS3 interacting bodies (0.5-6µm) previously described (Rajamäki et al., 2014), suggesting that P1b/CP granules are closely related to siRNA-bodies. These granules were frequently surrounded with larger inclusions labelled with the RFP-tagged P-body marker DCP1, in agreement with the juxtaposition of P-

bodies and siRNA-bodies previously described (Martinez de Alba et al., 2015). SGS3 has been proposed to protect AGO7-mediated cleaved mRNA fragments and other aberrant mRNAs from degradation during ta-siRNA biogenesis, sense RNA silencing and RNA silencing amplification (Yoshikawa et al., 2013; Martinez de Alba et al., 2015). It has been speculated that the viral RSS proteins reported to interact with SGS3 in siRNA-bodies would interfere with this activity, preventing RDR6 amplification and dsRNA synthesis, and thus resulting in repression of siRNA production. The reported P1b RSS activity involves specific binding to double stranded siRNA molecules (Valli et al., 2011), and it is reasonable to think P1b could gain advantage by localising at the precise site where siRNA production occurs. However the hotspot site of siRNA productions is largely debated. Whereas SGS3 and AGO7 have been found co-localising with RDR6 in cytosolic siRNA-bodies (Jouannet et al., 2012), components of siRNA-bodies have also been observed co-localising with DCL4 in the nucleoplasm (Pontes et al., 2013) providing the belief that processing of dsRNA yielding siRNAs appears to occur outside siRNA-bodies (Jouannet et al., 2012). Yet secondary siRNA production has been observed to be mostly dependent on DCL2 activity (Mlotshwa et al., 2008; Parent et al., 2015), localising both in nuclei and cytoplasm (Dorokhov et al., 2006). As a result, P1b functions in siRNA-bodies, requiring the assistance of CP, could be well prior to siRNA sequestering if siRNA production is allochthonous to siRNA-bodies or involved in sequestering siRNA molecules at its production sites. Recent reports show that another viral protein, VPg, also interacts with SGS3 in siRNA bodies (Rajamäki et al., 2014). This interaction appears to be beneficial for the potyvirus PVA. SGS3 has been proposed to be recruited by PVA VPg for viral RNA protection (Rajamäki et al., 2014), and the presence of CP and P1b could be assisting VPg in this function.

Whether P1b/CP association in siRNA-bodies is taking place and has a functional role during CVYV infection is still unknown. Spherical cytosolic electrodense structures were observed highly decorated with anti-P1b antibody in CVYV-infected *C. sativus* leaves in immunogold labelling experiments. It would be interesting to determine if these electrodense cytosolic structure are siRNA-bodies, and if viral CP, together with SGS3 and other factors of the RNA silencing

machinery co-lococalise together with P1b. Until then, results are only initial approximations and conclusions drawn are to be taken carefully.

"Only those who risk going to far, can possibly find out how far one can go."

T. S. Eliot, Preface to Transit of Venus.

CONCLUSIONS

CONCLUSIONS

1. P1b is a viral RSS protein active in three different plants species and localising in the cytosol of CVYV infected cells.

2. Heterologous expression of P1b using a PPV vector based expression system delocalises P1b into the nucleoplasm and nucleoli, however this does not impede the RSS activity of P1b, although it might be affecting other functions required in the viral cycle.

3. Hydra 1, a putative functional interactor of P1b, contributes in RNA silencing induction in the presence of the RSS P1b and limits viral accumulation of several viruses expressing different RSS proteins.

4. P1b and CP both interact with eIF(iso)4E of melon during a viral infection suggesting both protein could share a common role in viral RNA translation.

5. P1b and CVYV CP interact in cytosolic P1b/CP-bodies co-localising with SGS3 in siRNA-bodies which could be important for the RSS function of P1b. The viral CP protein could play a role assisting P1b in siRNA-bodies, and such role could be conserved among the CP proteins of different potyviruses.

CONCLUSIONES

1. P1b es una proteína supresora del silenciamiento viral activa en tres especies vegetales diferentes y con localización citosólica en células de pepino infectadas con CVYV.

2. La expresión heteróloga de P1b por medio de un vector viral basado en el virus de la Sharka, PPV, deslocaliza a P1b hacía el núcleo y nucleolo sin afectar su capacidad supresora del silenciamiento. Sin embargo esta deslocalización pudiera estar afectando otras funciones requeridas en el ciclo viral.

3. De entre los diferentes interactores de P1b encontrados, HYDRA1, contribuye a la inducción del silenciamiento en presencia del RSS P1b y limita la acumulación viral de diversos virus que expresan diferentes proteínas RSS.

4. Tanto P1b como la CP interaccionan con el factor de iniciación a la traducción de melón eIF(iso)4E durante una infección viral. Esta interacción podría estar sugiriendo un rol compartido en procesos de traducción del ARN viral.

5. Las proteínas de CVYV P1b y CP interaccionan en estructuras citosólicas co-localizando con cuerpos de producción de siRNAs pudiendo ser esta localización necesaria para la función de supresión del silenciamiento de P1b. Por otro lado, la proteína CP pudiera tener un rol asistiendo a la proteína P1b en los cuerpos de producción de siRNA, pudiendo estar ese rol conservado entre las diferentes proteínas CP de diversos potyvirus.

"The highest result of education is tolerance."

Hellen Keller, *Optimism*.

BIBLIOGRAPHY

Abdul-Razzak, A., T. Guiraud, M. Peypelut, J. Walter, M. C. Houvenaghel, T. Candresse, O. Le Gall and S. German-Retana (2009) "Involvement of the cylindrical inclusion (CI) protein in the overcoming of an eIF4E-mediated resistance against Lettuce mosaic potyvirus." ***Molecular Plant Pathology*** 10, 109-113. **DOI:** 10.1111/j.1364-3703.2008.00513.x

Adams, M. J., J. F. Antoniw and C. M. Fauquet (2005) "Molecular criteria for genus and species discrimination within the family Potyviridae." ***Arch Virol*** 150, 459-79. **DOI:** 10.1007/s00705-004-0440-6

Agudelo-Romero, P., P. Carbonell, F. de la Iglesia, J. Carrera, G. Rodrigo, A. Jaramillo, M. a. Pérez-Amador and S. F. Elena (2008) "Changes in the gene expression profile of Arabidopsis thaliana after infection with Tobacco etch virus." ***Virology Journal*** 5, 92. **DOI:** 10.1186/1743-422X-5-92

Ahlquist, P. (2002) "RNA-Dependent RNA Polymerases, Viruses, and RNA Silencing." ***Science*** 296, 1270-1273. **DOI:** 10.1126/science.1069132

Ahlquist, P., A. O. Noueiry, W.-M. Lee, D. B. Kushner and B. T. Dye (2003) "Host Factors in Positive-Strand RNA Virus Genome Replication." ***Journal of Virology*** 77, 8181-8186. **DOI:** 10.1128/JVI.77.15.8181-8186.2003

Ala-Poikela, M., E. Goytia, T. Haikonen, M.-L. Rajamaki and J. P. T. Valkonen (2011) "Helper Component Proteinase of the Genus Potyvirus Is an Interaction Partner of Translation Initiation Factors eIF(iso)4E and eIF4E and Contains a 4E Binding Motif." ***Journal of Virology*** 85, 6784-6794. **DOI:** 10.1128/JVI.00485-11

Alamillo, J. M., P. Saénz and J. A. García (2006) "Salicylic acid-mediated and RNA-silencing defense mechanisms cooperate in the restriction of systemic spread of plum pox virus in tobacco." ***The Plant Journal*** 48, 217-227. **DOI:** 10.1111/j.1365-313X.2006.02861.x

Alazem, M. and N.-S. Lin (2015) "Roles of plant hormones in the regulation of host-virus interactions." ***Molecular Plant Pathology*** 16, 529-540. **DOI:** 10.1111/mpp.12204

Albers, M., H. Kranz, I. Kober, C. Kaiser, M. Klink, J. Suckow, R. Kern and M. Koegl (2004) "Automated Yeast Two-hybrid Screening for Nuclear Receptor-interacting Proteins." ***Molecular & Cellular Proteomics*** 4, 205-213. **DOI:** 10.1074/mcp.M400169-MCP200

Alvarez, S., L. M. Hicks and S. Pandey (2011) "ABA-Dependent and -Independent G-Protein Signaling in Arabidopsis Roots Revealed through an iTRAQ Proteomics Approach." ***Journal of Proteome Research*** 10, 3107-3122. **DOI:** 10.1021/pr2001786

Alvarez, S., S. Roy Choudhury, L. M. Hicks and S. Pandey (2013) "Quantitative Proteomics-Based Analysis Supports a Significant Role of GTG Proteins in Regulation of ABA Response in Arabidopsis Roots." ***Journal of Proteome Research*** 12, 1487-1501. **DOI:** 10.1021/pr301159u

Alves, M., S. Dadalto, A. Gonçalves, G. de Souza, V. Barros and L. Fietto (2014) "Transcription Factor Functional Protein-Protein Interactions in Plant Defense Responses." ***Proteomes*** 2, 85-106. **DOI:** 10.3390/proteomes2010085

Amari, K., M. Di Donato, V. V. Dolja and M. Heinlein (2014) "Myosins VIII and XI Play Distinct Roles in Reproduction and Transport of Tobacco Mosaic Virus." ***PLoS Pathogens*** 10, e1004448. **DOI:** 10.1371/journal.ppat.1004448

Ambawat, S., P. Sharma, N. R. Yadav and R. C. Yadav (2013) "MYB transcription factor genes as regulators for plant responses: An overview." ***Physiology and Molecular Biology of Plants*** 19, 307-321. **DOI:** 10.1007/s12298-013-0179-1

Anandalakshmi, R. (2000) "A Calmodulin-Related Protein That Suppresses Posttranscriptional Gene Silencing in Plants." ***Science*** 290, 142-144. **DOI:** 10.1126/science.290.5489.142

Anandalakshmi, R., G. J. Pruss, X. Ge, R. Marathe, A. C. Mallory, T. H. Smith and V. B. Vance (1998) "A viral suppressor of gene silencing in plants." ***Proceedings of the National Academy of Sciences*** 95, 13079-13084. **DOI:** 10.1073/pnas.95.22.13079

Anderson, N. L. (2002) "The Human Plasma Proteome: History, Character, and Diagnostic Prospects." ***Molecular & Cellular Proteomics*** 1, 845-867. **DOI:** 10.1074/mcp.R200007-MCP200

Ansorge, W. (1985) "Fast and sensitive detection of protein and DNA bands by treatment with potassium permanganate." ***Journal of Biochemical and Biophysical Methods*** 11, 13-20. **DOI:** 10.1016/0165-022X(85)90037-5

Aravin, A. and T. Tuschl (2005) "Identification and characterization of small RNAs involved in RNA silencing." ***FEBS Letters*** 579, 5830-5840. **DOI:** 10.1016/j.febslet.2005.08.009

Asakura, Y., E. Galarneau, K. P. Watkins, A. Barkan and K. J. van Wijk (2012) "Chloroplast RH3 DEAD Box RNA Helicases in Maize and Arabidopsis Function in Splicing of Specific Group II Introns and Affect Chloroplast Ribosome Biogenesis." ***PLANT PHYSIOLOGY*** 159, 961-974. **DOI:** 10.1104/pp.112.197525

Atreya, C. D., P. L. Atreya, D. W. Thornbury and T. P. Pirone (1992) "Site-directed mutations in the potyvirus HC-Pro gene affect helper component activity, virus accumulation, and symptom expression in infected tobacco plants." ***Virology*** 191, 106-11. **DOI:** 10.1016/0042-6822(92)90171-K

Atreya, C. D. and T. P. Pirone (1993). "Mutational analysis of the helper component-proteinase gene of a potyvirus: effects of amino acid substitutions, deletions, and gene replacement on virulence and aphid transmissibility." **Proc Natl Acad Sci U S A** 90(24): 11919-23.

Azevedo, J., D. Garcia, D. Pontier, S. Ohnesorge, A. Yu, et al. (2010) "Argonaute quenching and global changes in Dicer homeostasis caused by a pathogen-encoded GW repeat protein." ***Genes & Development*** 24, 904-915. **DOI:** 10.1101/gad.1908710

Babu, M., J. S. Griffiths, T.-S. Huang and A. Wang (2008) "Altered gene expression changes in Arabidopsis leaf tissues and protoplasts in response to Plum pox virus infection." ***BMC Genomics*** 9, 325. **DOI:** 10.1186/1471-2164-9-325

Bader, J. S., A. Chaudhuri, J. M. Rothberg and J. Chant (2004) "Gaining confidence in high-throughput protein interaction networks." ***Nature Biotechnology*** 22, 78-85. **DOI:** 10.1038/nbt924

Baginsky, S., J. Grossmann and W. Gruissem (2007) "Proteome Analysis of Chloroplast mRNA Processing and Degradation." ***Journal of Proteome Research*** 6, 809-820. **DOI:** 10.1021/pr060473q

Ballut, L. (2005) "HcPro, a multifunctional protein encoded by a plant RNA virus, targets the 20S proteasome and affects its enzymic activities." ***Journal of General Virology*** 86, 2595-2603. **DOI:** 10.1099/vir.0.81107-0

Ballut, L., F. Petit, S. Mouzeyar, O. Le Gall, T. Candresse, P. Schmid, P. Nicolas and S. Badaoui (2003) "Biochemical identification of proteasome-associated endonuclease activity in sunflower." ***Biochimica et Biophysica Acta (BBA) - Proteins and Proteomics*** 1645, 30-39. **DOI:** 10.1016/S1570-9639(02)00500-9

Bantscheff, M., M. Schirle, G. Sweetman, J. Rick and B. Kuster (2007) "Quantitative mass spectrometry in proteomics: a critical review." ***Analytical and Bioanalytical Chemistry*** 389, 1017-1031. **DOI:** 10.1007/s00216-007-1486-6

Barajas, D., Y. Jiang and P. D. Nagy (2009) "A Unique Role for the Host ESCRT Proteins in Replication of Tomato bushy stunt virus." ***PLoS Pathogens*** 5, e1000705. **DOI:** 10.1371/journal.ppat.1000705

Barajas, D., K. Xu, I. F. de Castro Martín, Z. Sasvari, F. Brandizzi, C. Risco and P. D. Nagy (2014) "Co-opted Oxysterol-Binding ORP and VAP Proteins Channel Sterols to RNA Virus Replication Sites via Membrane Contact Sites." ***PLoS Pathogens*** 10, e1004388. **DOI:** 10.1371/journal.ppat.1004388

Bartel, D. P. (2004) "MicroRNAs: Genomics, Biogenesis, Mechanism, and Function." ***Cell*** 116, 281-297. **DOI:** 10.1016/S0092-8674(04)00045-5

Baulcombe, D. (2004) "RNA silencing in plants." ***Nature*** 431, 356-363. **DOI:** 10.1038/nature02874

Bayne, E. H., D. V. Rakitina, S. Y. Morozov and D. C. Baulcombe (2005) "Cell-to-cell movement of Potato Potexvirus X is dependent on suppression of RNA silencing." ***The Plant Journal*** 44, 471-482. **DOI:** 10.1111/j.1365-313X.2005.02539.x

Beauchemin, C., N. Boutet and J.-F. Laliberte (2007) "Visualization of the Interaction between the Precursors of VPg, the Viral Protein Linked to the Genome of Turnip Mosaic Virus, and the Translation Eukaryotic Initiation Factor iso 4E In Planta." ***Journal of Virology*** 81, 775-782. **DOI:** 10.1128/JVI.01277-06

Beauchemin, C. and J.-F. Laliberte (2007) "The Poly(A) Binding Protein Is Internalized in Virus-Induced Vesicles or Redistributed to the Nucleolus during Turnip Mosaic Virus Infection." ***Journal of Virology*** 81, 10905-10913. **DOI:** 10.1128/JVI.01243-07

Beck, D. L., C. J. Van Dolleweerd, T. J. Lough, E. Balmori, D. M. Voot, M. T. Andersen, I. E. O'Brien and R. L. Forster (1994) "Disruption of virus movement confers broad-spectrum resistance against systemic infection by plant viruses with a triple gene block." ***Proceedings of the National Academy of Sciences*** 91, 10310-10314. **DOI:** 10.1073/pnas.91.22.10310

Beckham, C. J., H. R. Light, T. Amar Nissan, P. Ahlquist, R. Parker and A. Noueiry (2007) "Interactions between Brome Mosaic Virus RNAs and Cytoplasmic Processing Bodies." ***Journal of Virology*** 81, 9759-9768. **DOI:** 10.1128/JVI.00844-07

Beclin, C., R. Berthome, J. C. Palauqui, M. Tepfer and H. Vaucheret (1998) "Infection of tobacco or Arabidopsis plants by CMV counteracts systemic post-transcriptional silencing of nonviral (trans)genes." ***Virology*** 252, 313-7. **DOI:** 10.1006/viro.1998.9457

Béclin, C., S. Boutet, P. Waterhouse and H. Vaucheret (2002) "A Branched Pathway for Transgene-Induced RNA Silencing in Plants." ***Current Biology*** 12, 684-688. **DOI:** 10.1016/S0960-9822(02)00792-3

Bedhomme, M., M. Adamo, C. H. Marchand, J. Couturier, N. Rouhier, S. D. Lemaire, M. Zaffagnini and P. Trost (2012) "Glutathionylation of cytosolic glyceraldehyde-3-phosphate dehydrogenase from the model plant Arabidopsis thaliana is reversed by both glutaredoxins and thioredoxins in vitro." ***Biochemical Journal*** 445, 337-347. **DOI:** 10.1042/BJ20120505

Bernard, P. and M. Couturier (1992) "Cell killing by the F plasmid CcdB protein involves poisoning of DNA-topoisomerase II complexes." ***Journal of Molecular Biology*** 226, 735-745. **DOI:** 10.1016/0022-2836(92)90629-X

Besong-Ndika, J., K. I. Ivanov, A. Hafrèn, T. Michon and K. Mäkinen (2015) "Cotranslational Coat Protein-Mediated Inhibition of Potyviral RNA Translation." ***Journal of Virology*** 89, 4237-4248. **DOI:** 10.1128/JVI.02915-14

Blanc, S., J.-J. López-Moya, R. Wang, S. García-Lampasona, D. W. Thornbury and T. P. Pirone (1997) "A Specific Interaction between Coat Protein and Helper Component Correlates with Aphid Transmission of a Potyvirus." ***Virology*** 231, 141-147. **DOI:** 10.1006/viro.1997.8521

Blevins, T. (2010) "Northern Blotting Techniques for Small RNAs." ***Methods in molecular biology (Clifton, N.J.)*** 631, 87-107. **DOI:** 10.1007/978-1-60761-646-7_9

Blevins, T., R. Rajeswaran, P. V. Shivaprasad, D. Beknazariants, A. Si-Ammour, et al. (2006) "Four plant Dicers mediate viral small RNA biogenesis and DNA virus induced silencing." ***Nucleic Acids Research*** 34, 6233-6246. **DOI:** 10.1093/nar/gkl886

Bouché, N., D. Lauressergues, V. Gasciolli and H. Vaucheret (2006) "An antagonistic function for Arabidopsis DCL2 in development and a new function for DCL4 in generating viral siRNAs." ***The EMBO Journal*** 25, 3347-3356. **DOI:** 10.1038/sj.emboj.7601217

Brigneti, G. (1998) "Viral pathogenicity determinants are suppressors of transgene silencing in Nicotiana benthamiana." ***The EMBO Journal*** 17, 6739-6746. **DOI:** 10.1093/emboj/17.22.6739

Brodersen, P., L. Sakvarelidze-Achard, M. Bruun-Rasmussen, P. Dunoyer, Y. Y. Yamamoto, L. Sieburth and O. Voinnet (2008) "Widespread Translational Inhibition by Plant miRNAs and siRNAs." ***Science*** 320, 1185-1190. **DOI:** 10.1126/science.1159151

Brodersen, P., L. Sakvarelidze-Achard, H. Schaller, M. Khafif, G. Schott, A. Bendahmane and O. Voinnet (2012) "Isoprenoid biosynthesis is required for miRNA function and affects membrane association of ARGONAUTE 1 in Arabidopsis." ***Proceedings of the National Academy of Sciences*** 109, 1778-1783. **DOI:** 10.1073/pnas.1112500109

Brosius, J. (2003) "The contribution of RNAs and retroposition to evolutionary novelties." ***Genetica*** 118, 99-116. **DOI:** 10.1023/A:1024141306559

Brosseau, C. and P. Moffett (2015) "Functional and Genetic Analysis Identify a Role for Arabidopsis ARGONAUTE5 in Antiviral RNA Silencing." ***The Plant Cell*** 27, 1742-1754. **DOI:** 10.1105/tpc.15.00264

Bruenn, J. a. (1991). "Relationships among the positive strand and double-strand RNA viruses as viewed through their RNA-dependent RNA polymerases." **Nucleic acids research** 19: 217-226.

Buck, K. W. (1996) "Comparison of The Replication of Positive-Stranded Rna Viruses of Plants and Animals." Volume 47, 159-251. **DOI:** 10.1016/S0065-3527(08)60736-8

Buhot, N., J.-P. Douliez, A. Jacquemard, D. Marion, V. Tran, et al. (2001) "A lipid transfer protein binds to a receptor involved in the control of plant defence responses." ***FEBS Letters*** 509, 27-30. **DOI:** 10.1016/S0014-5793(01)03116-7

Callis, J., J. A. Raasch and R. D. Vierstra (1990). "Ubiquitin extension proteins of Arabidopsis thaliana. Structure, localization, and expression of their promoters in transgenic tobacco." **Journal of Biological Chemistry** 265: 12486-12493.

Calvo, M., S. Martínez-Turiño and J. A. García (2014) "Resistance to Plum pox virus Strain C in Arabidopsis thaliana and Chenopodium foetidum Involves Genome-Linked Viral Protein and Other Viral Determinants and Might Depend on Compatibility With Host Translation Initiation Factors." ***Molecular Plant-Microbe Interactions*** 27, 1291-1301. **DOI:** 10.1094/MPMI-05-14-0130-R

Cambra, M., N. Capote, A. Myrta and G. Llácer (2006) "Plum pox virus and the estimated costs associated with sharka disease." ***EPPO Bulletin*** 36, 202-204. **DOI:** 10.1111/j.1365-2338.2006.01027.x

Canto, T., J. F. Uhrig, M. Swanson, K. M. Wright and S. a. MacFarlane (2006) "Translocation of Tomato Bushy Stunt Virus P19 Protein into the Nucleus by ALY Proteins Compromises Its Silencing Suppressor Activity." ***Journal of Virology*** 80, 9064-9072. **DOI:** 10.1128/JVI.00953-06

Carbonell, A., G. Dujovny, J. A. García and A. Valli (2012) "The Cucumber vein yellowing virus Silencing Suppressor P1b Can Functionally Replace HCPro in Plum pox virus Infection in a Host-Specific Manner." ***Molecular Plant-Microbe Interactions*** 25, 151-164. **DOI:** 10.1094/MPMI-08-11-0216

Carette, J. E., K. Guhl, J. Wellink and A. Van Kammen (2002) "Coalescence of the Sites of Cowpea Mosaic Virus RNA Replication into a Cytopathic Structure." ***Journal of Virology*** 76, 6235-6243. **DOI:** 10.1128/JVI.76.12.6235-6243.2002

Carette, J. E., M. Stuiver, J. Van Lent, J. Wellink and A. Van Kammen (2000) "Cowpea Mosaic Virus Infection Induces a Massive Proliferation of Endoplasmic Reticulum but Not Golgi Membranes and Is Dependent on De Novo Membrane Synthesis." ***Journal of Virology*** 74, 6556-6563. **DOI:** 10.1128/JVI.74.14.6556-6563.2000

Carrington, J. C., D. D. Freed and T. C. Sanders (1989). "Autocatalytic processing of the potyvirus helper component proteinase in Escherichia coli and in vitro." **Journal of virology** 63: 4459-4463.

Carrington, J. C., K. D. Kasschau and L. K. Johansen (2001) "Activation and Suppression of RNA Silencing by Plant Viruses." ***Virology*** 281, 1-5. **DOI:** 10.1006/viro.2000.0812

Carroll, M. W., D. a. Matthews, J. a. Hiscox, M. J. Elmore, G. Pollakis, et al. (2015) "Temporal and spatial analysis of the 2014–2015 Ebola virus outbreak in West Africa." ***Nature*** 524, 97-101. **DOI:** 10.1038/nature14594

Casadaban, M. J. and S. N. Cohen (1980) "Analysis of gene control signals by DNA fusion and cloning in Escherichia coli." ***Journal of Molecular Biology*** 138, 179-207. **DOI:** 10.1016/0022-2836(80)90283-1

Caspar, D. and K. Namba (1990) "Switching in the self-assembly of tobacco mosaic virus." ***Advances in Biophysics*** 26, 157-185. **DOI:** 10.1016/0065-227X(90)90011-H

Catic, A. and H. L. Ploegh (2005) "Ubiquitin – conserved protein or selfish gene?" ***Trends in Biochemical Sciences*** 30, 600-604. **DOI:** 10.1016/j.tibs.2005.09.002

Causier, B. and B. Davies (2002) "Analysing protein-protein interactions with the yeast two-hybrid system." ***Plant Molecular Biology*** 50, 855-870. **DOI:** 10.1023/A:1021214007897

Charron, C., M. Nicolaï, J.-L. Gallois, C. Robaglia, B. Moury, A. Palloix and C. Caranta (2008) "Natural variation and functional analyses provide evidence for co-evolution between plant eIF4E and potyviral VPg." ***The Plant Journal*** 54, 56-68. **DOI:** 10.1111/j.1365-313X.2008.03407.x

Chellappan, P., R. Vanitharani, F. Ogbe and C. M. Fauquet (2005) "Effect of Temperature on Geminivirus-Induced RNA Silencing in Plants." ***PLANT PHYSIOLOGY*** 138, 1828-1841. **DOI:** 10.1104/pp.105.066563

Chen, C.-e. and H.-h. Yeh (2010). "Plant Defense-related Transcription Factor WRKY6 Plays Both Supportive and Inhibitory Roles in Tobacco mosaic virus Infection." **Plant Pathology Bulletin**: 31-40.

Chen, T., N. Nayak, S. M. Majee, J. Lowenson, K. R. Schafermeyer, et al. (2010) "Substrates of the Arabidopsis thaliana Protein Isoaspartyl Methyltransferase 1 Identified Using Phage Display and Biopanning." ***Journal of Biological Chemistry*** 285, 37281-37292. **DOI:** 10.1074/jbc.M110.157008

Chen, X. (2004) "A MicroRNA as a Translational Repressor of APETALA2 in Arabidopsis Flower Development." ***Science*** 303, 2022-2025. **DOI:** 10.1126/science.1088060

Cheng, Y. Q., Z. M. Liu, J. Xu, T. Zhou, M. Wang, Y. T. Chen, H. F. Li and Z. F. Fan (2008) "HC-Pro protein of sugar cane mosaic virus interacts specifically with maize ferredoxin-5 in vitro and in planta." ***Journal of General Virology*** 89, 2046-2054. **DOI:** 10.1099/vir.0.2008/001271-0

Chien, C. T., P. L. Bartel, R. Sternglanz and S. Fields (1991) "The two-hybrid system: a method to identify and clone genes for proteins that interact with a protein of interest." ***Proceedings of the National Academy of Sciences*** 88, 9578-9582. **DOI:** 10.1073/pnas.88.21.9578

Chisholm, S. T., M. A. Parra, R. J. Anderberg and J. C. Carrington (2001) "Arabidopsis RTM1 and RTM2 Genes Function in Phloem to Restrict Long-Distance Movement of Tobacco Etch Virus." ***PLANT PHYSIOLOGY*** 127, 1667-1675. **DOI:** 10.1104/pp.010479

Chung, B. Y., W. A. Miller, J. F. Atkins and A. E. Firth (2008) "An overlapping essential gene in the Potyviridae." ***Proc Natl Acad Sci U S A*** 105, 5897-902. **DOI:** 10.1073/pnas.0800468105

Chung, H. Y. and G. Sunter (2014) "Interaction between the transcription factor AtTIFY4B and begomovirus AL2 protein impacts pathogenicity." ***Plant Molecular Biology*** 86, 185-200. **DOI:** 10.1007/s11103-014-0222-9

Cillo, F., I. M. Roberts and P. Palukaitis (2002) "In Situ Localization and Tissue Distribution of the Replication-Associated Proteins of Cucumber Mosaic Virus in Tobacco and Cucumber." ***Journal of Virology*** 76, 10654-10664. **DOI:** 10.1128/JVI.76.21.10654-10664.2002

Coego, A., E. Brizuela, P. Castillejo, S. Ruíz, C. Koncz, et al. (2014) "The TRANSPLANTA collection of Arabidopsis lines: a resource for functional analysis of transcription factors based on their conditional overexpression." ***The Plant Journal*** 77, 944-953. **DOI:** 10.1111/tpj.12443

Cotton, S., R. Grangeon, K. Thivierge, I. Mathieu, C. Ide, T. Wei, A. Wang and J.-F. Laliberte (2009) "Turnip Mosaic Virus RNA Replication Complex Vesicles Are Mobile, Align with Microfilaments, and Are Each Derived from a Single Viral Genome." ***Journal of Virology*** 83, 10460-10471. **DOI:** 10.1128/JVI.00819-09

Covey, S. N., N. S. Al-Kaff, A. Lángara and D. S. Turner (1997) "Plants combat infection by gene silencing." ***Nature*** 385, 781-782. **DOI:** 10.1038/385781a0

Criekinge, W. and R. Beyaert (1999) "Yeast two-hybrid: State of the art." ***Biological Procedures Online*** 2, 1-38. **DOI:** 10.1251/bpo16

Csorba, T., L. Kontra and J. Burgyán (2015) "viral silencing suppressors: Tools forged to fine-tune host-pathogen coexistence." ***Virology*** 479-480, 85-103. **DOI:** 10.1016/j.virol.2015.02.028

Culver, J. N. (2002) "Tobacco mosaic virus assembly and disassembly: determinants in pathogenicity and resistance." ***Annual review of phytopathology*** 40, 287-308. **DOI:** 10.1146/annurev.phyto.40.120301.102400

Culver, J. N., W. O. Dawson, K. Plonk and G. Stubbs (1995) "Site-directed mutagenesis confirms the involvement of carboxylate groups in the disassembly of tobacco mosaic virus." ***Virology*** 206, 724-730. **DOI:** 10.1016/S0042-6822(95)80096-4

Curtis, M. D. and U. Grossniklaus (2003) "A Gateway cloning vector set for high-hhroughput hunctional hnalysis of henes in planta." ***Breakthrough technologies*** 133, 462-469. **DOI:** 10.1104/pp.103.027979.specific

Dalmay, T., A. Hamilton, S. Rudd, S. Angell and D. Baulcombe (2000) "An RNA-dependent RNA polymerase gene in Arabidopsis is required for posttranscriptional gene silencing mediated by a transgene but not by a virus." ***Cell*** 101, 543-553. **DOI:** S0092-8674(00)80864-8 [pii]

Dangl, J. L. and J. D. G. Jones (2001) "Plant pathogens and integrated defence responses to infection." ***Nature*** 411, 826-833. **DOI:** 10.1038/35081161

Deblaere, R., B. Bytebier, H. De Greve, F. Deboeck, J. Schell, M. Van Montagu and J. Leemans (1985) "Efficient octopine Ti plasmid-derived vectors for Agrobacterium -mediated gene transfer to plants." ***Nucleic Acids Research*** 13, 4777-4788. **DOI:** 10.1093/nar/13.13.4777

Dekker, E. L., a. F. L. M. Derks, C. J. Asjes, M. E. C. Lemmers, J. F. Boll and S. a. Langeveld (1993) "Characterization of potyviruses from tulip and lily which cause flower-breaking." ***Journal of General Virology*** 74, 881-887. **DOI:** 10.1099/0022-1317-74-5-881

Deleris, A., J. Gallego-Bartolome, J. Bao, K. D. Kasschau, J. C. Carrington and O. Voinnet (2006) "Hierarchical Action and Inhibition of Plant Dicer-Like Proteins in Antiviral Defense." ***Science*** 313, 68-71. **DOI:** 10.1126/science.1128214

den Boon, J. A., A. Diaz and P. Ahlquist (2010) "Cytoplasmic Viral Replication Complexes." ***Cell Host & Microbe*** 8, 77-85. **DOI:** 10.1016/j.chom.2010.06.010

DeSouza, L. V., A. D. Romaschin, T. J. Colgan and K. W. M. Siu (2009) "Absolute Quantification of Potential Cancer Markers in Clinical Tissue Homogenates Using Multiple Reaction Monitoring on a Hybrid Triple Quadrupole/Linear Ion Trap Tandem Mass Spectrometer." ***Analytical Chemistry*** 81, 3462-3470. **DOI:** 10.1021/ac802726a

Desper, R. and O. Gascuel (2003) "Theoretical Foundation of the Balanced Minimum Evolution Method of Phylogenetic Inference and Its Relationship to Weighted Least-Squares Tree Fitting." ***Molecular Biology and Evolution*** 21, 587-598. **DOI:** 10.1093/molbev/msh049

Desprez, T., M. Juraniec, E. F. Crowell, H. Jouy, Z. Pochylova, F. Parcy, H. Höfte, M. Gonneau and S. Vernhettes (2007) "Organization of cellulose synthase complexes involved in primary cell wall synthesis in Arabidopsis thaliana." ***Proceedings of the National Academy of Sciences of the United States of America*** 104, 15572-7. **DOI:** 10.1073/pnas.0706569104

Diaz, A., X. Wang and P. Ahlquist (2010) "Membrane-shaping host reticulon proteins play crucial roles in viral RNA replication compartment formation and function." ***Proceedings of the National Academy of Sciences*** 107, 16291-16296. **DOI:** 10.1073/pnas.1011105107

Diaz-Vivancos, P., M. J. Clemente-Moreno, M. Rubio, E. Olmos, J. A. Garcia, P. Martinez-Gomez and J. A. Hernandez (2008) "Alteration in the chloroplastic metabolism leads to ROS accumulation in pea plants in response to plum pox virus." ***Journal of Experimental Botany*** 59, 2147-2160. **DOI:** 10.1093/jxb/ern082

Diaz-Vivancos, P., M. Rubio, V. Mesonero, P. Periago, A. Ros Barcelo, P. Martinez-Gomez and J. Hernandez (2006) "The apoplastic antioxidant system in Prunus: response to long-term plum pox virus infection." ***Journal of Experimental Botany*** 57, 3813-3824. **DOI:** 10.1093/jxb/erl138

Dielen, A.-S., S. Badaoui, T. Candresse and S. German-Retama (2010) "The ubiquitin/26S proteasome system in plant-pathogen interactions: a never-ending hide-and-seek game." ***Molecular Plant Pathology*** 11, 293-308. **DOI:** 10.1111/j.1364-3703.2009.00596.x

Dielen, A.-S., F. T. Sassaki, J. Walter, T. Michon, G. Ménard, et al. (2011) "The 20S proteasome α5 subunit of Arabidopsis thaliana carries an RNase activity and interacts in planta with the Lettuce mosaic potyvirus HcPro protein." ***Molecular Plant Pathology*** 12, 137-150. **DOI:** 10.1111/j.1364-3703.2010.00654.x

Diez, J., M. Ishikawa, M. Kaido and P. Ahlquist (2000) "Identification and characterization of a host protein required for efficient template selection in viral RNA replication." ***Proceedings of the National Academy of Sciences*** 97, 3913-3918. **DOI:** 10.1073/pnas.080072997

Ding, S.-W. and O. Voinnet (2007) "Antiviral Immunity Directed by Small RNAs." ***Cell*** 130, 413-426. **DOI:** 10.1016/j.cell.2007.07.039

Dolja, V. V., R. Haldeman-Cahill, A. E. Montgomery, K. A. Vandenbosch and J. C. Carrington (1995) "Capsid protein determinants involved in cell-to-cell and long distance movement of tobacco etch potyvirus." ***Virology*** 206, 1007-1016. **DOI:** 10.1006/viro.1995.1023

Dolja, V. V., K. L. Herndon, T. P. Pirone and J. C. Carrington (1993). "Spontaneous mutagenesis of a plant potyvirus genome after insertion of a foreign gene." **Journal of virology** 67: 5968-5975.

Domingo, E. (1997). "Rapid evolution of viral RNA genomes." **The Journal of nutrition** 127: 958S-961S.

Donaire, L., D. Barajas, B. Martinez-Garcia, L. Martinez-Priego, I. Pagan and C. Llave (2008) "Structural and Genetic Requirements for the Biogenesis of Tobacco Rattle Virus-Derived Small Interfering RNAs." ***Journal of Virology*** 82, 5167-5177. **DOI:** 10.1128/JVI.00272-08

Donze, T., F. Qu, P. Twigg and T. J. Morris (2014) "Turnip crinkle virus coat protein inhibits the basal immune response to virus invasion in Arabidopsis by binding to the NAC transcription factor TIP." ***Virology*** 449, 207-214. **DOI:** 10.1016/j.virol.2013.11.018

Dorokhov, Y. L., O. Y. Frolova, E. V. Skurat, P. A. Ivanov, T. V. Gasanova, et al. (2006) "A novel function for a ubiquitous plant enzyme pectin methylesterase: the enhancer of RNA silencing." ***FEBS Lett*** 580, 3872-8. **DOI:** 10.1016/j.febslet.2006.06.013

Du, Q.-S., C.-G. Duan, Z.-H. Zhang, Y.-Y. Fang, R.-X. Fang, Q. Xie and H.-S. Guo (2007) "DCL4 targets Cucumber mosaic virus satellite RNA at novel secondary structures." ***Journal of virology*** 81, 9142-9151. **DOI:** 10.1128/JVI.02885-06

Du, Z., D. Xiao, J. Wu, D. jia, Z. Yuan, et al. (2011) "p2 of Rice stripe virus (RSV) interacts with OsSGS3 and is a silencing suppressor." ***Molecular Plant Pathology*** 12, 808-814. **DOI:** 10.1111/j.1364-3703.2011.00716.x

Dufresne, P. J., E. Ubalijoro, M. G. Fortin and J.-F. Laliberte (2008) "Arabidopsis thaliana class II poly(A)-binding proteins are required for efficient multiplication of turnip mosaic virus." ***Journal of General Virology*** 89, 2339-2348. **DOI:** 10.1099/vir.0.2008/002139-0

Duharcourt, S., G. Lepère and E. Meyer (2009) "Developmental genome rearrangements in ciliates: a natural genomic subtraction mediated by non-coding transcripts." ***Trends in Genetics*** 25, 344-350. **DOI:** 10.1016/j.tig.2009.05.007

Dujovny, G., A. Valli, M. Calvo and J. A. García (2009) "A temperature-controlled amplicon system derived from Plum pox potyvirus." ***Plant Biotechnology Journal*** 7, 49-58. **DOI:** 10.1111/j.1467-7652.2008.00373.x

Dunoyer, P., C.-H. Lecellier, E. A. Parizotto, C. Himber and O. Voinnet (2004) "RETRACTED: Probing the MicroRNA and Small Interfering RNA Pathways with Virus-Encoded Suppressors of RNA Silencing." ***The Plant Cell*** 16, 1235-1250. **DOI:** 10.1105/tpc.020719

Dunoyer, P., C. Ritzenthaler, O. Hemmer, P. Michler and C. Fritsch (2002) "Intracellular Localization of the Peanut Clump Virus Replication Complex in Tobacco BY-2 Protoplasts Containing Green Fluorescent Protein-Labeled Endoplasmic Reticulum or Golgi Apparatus." ***Journal of Virology*** 76, 865-874. **DOI:** 10.1128/JVI.76.2.865-874.2002

Dunoyer, P. and O. Voinnet (2005) "The complex interplay between plant viruses and host RNA-silencing pathways." ***Current Opinion in Plant Biology*** 8, 415-423. **DOI:** 10.1016/j.pbi.2005.05.012

Duprat, A., C. Caranta, F. Revers, B. Menand, K. S. Browning and C. Robaglia (2002) "The Arabidopsis eukaryotic initiation factor (iso)4E is dispensable

for plant growth but required for susceptibility to potyviruses." ***The Plant Journal*** 32, 927-934. **DOI:** 10.1046/j.1365-313X.2002.01481.x

Durfee, T., R. Nelson, S. Baldwin, G. Plunkett, V. Burland, et al. (2008) "The Complete Genome Sequence of Escherichia coli DH10B: Insights into the Biology of a Laboratory Workhorse." ***Journal of Bacteriology*** 190, 2597-2606. **DOI:** 10.1128/JB.01695-07

Eagles, R. M., E. Balmori-Melian, D. L. Beck, R. C. Gardner and R. L. S. Forster (1994) "Characterization of NTPase, RNA-binding and RNA-helicase Activities of the Cytoplasmic Inclusion Protein of Tamarillo Mosaic Potyvirus." ***European Journal of Biochemistry*** 224, 677-684. **DOI:** 10.1111/j.1432-1033.1994.t01-1-00677.x

Eigen, M. and P. Schuster (1977) "A principle of natural self-organization." ***Naturwissenschaften*** 64, 541-565. **DOI:** 10.1007/BF00450633

Elena, S. F. and G. Rodrigo (2012) "Towards an integrated molecular model of plant–virus interactions." ***Current Opinion in Virology*** 2, 719-724. **DOI:** 10.1016/j.coviro.2012.09.004

Ellis, R. J. (1979) "The most abundant protein in the world." ***Trends in Biochemical Sciences*** 4, 241-244. **DOI:** 10.1016/0968-0004(79)90212-3

Elrouby, N. and G. Coupland (2010) "Proteome-wide screens for small ubiquitin-like modifier (SUMO) substrates identify Arabidopsis proteins implicated in diverse biological processes." ***Proceedings of the National Academy of Sciences*** 107, 17415-17420. **DOI:** 10.1073/pnas.1005452107

Endres, M. W., B. D. Gregory, Z. Gao, A. W. Foreman, S. Mlotshwa, et al. (2010) "Two Plant Viral Suppressors of Silencing Require the Ethylene-Inducible Host Transcription Factor RAV2 to Block RNA Silencing." ***PLoS Pathogens*** 6, e1000729. **DOI:** 10.1371/journal.ppat.1000729

Enquist, L. W. (2009) "Virology in the 21st Century." ***Journal of Virology*** 83, 5296-5308. **DOI:** 10.1128/JVI.00151-09

Erhardt, M., P. Dunoyer, H. Guilley, K. Richards, G. Jonard and S. Bouzoubaa (2001). "Beet Necrotic Yellow Vein Virus Particles Localize to Mitochondria during Infection." **Virology** 286: 256-262.

Esquela-Kerscher, A. and F. J. Slack (2006) "Oncomirs — microRNAs with a role in cancer." ***Nature Reviews Cancer*** 6, 259-269. **DOI:** 10.1038/nrc1840

Falk, B. W., T. J. Morris and J. E. Duffus (1979). "Unstable infectivity and sedimentable ds-RNA associated with lettuce speckles mottle virus." **Virology** 96(1): 239-48.

Fang, Y. and D. L. Spector (2007) "Identification of Nuclear Dicing Bodies Containing Proteins for MicroRNA Biogenesis in Living Arabidopsis Plants." ***Current Biology*** 17, 818-823. **DOI:** 10.1016/j.cub.2007.04.005

Ferl, R. J., J. Koh, F. Denison and A.-L. Paul (2015) "Spaceflight Induces Specific Alterations in the Proteomes of Arabidopsis." ***Astrobiology*** 15, 32-56. **DOI:** 10.1089/ast.2014.1210

Fernández-Fernández, M. R., M. Mouriño, J. Rivera, F. Rodríguez, J. Plana-Durán and J. A. García (2001) "Protection of rabbits against rabbit hemorrhagic disease virus by immunization with the VP60 protein expressed in plants with a potyvirus-based vector." ***Virology*** 280, 283-291. **DOI:** 10.1006/viro.2000.0762

Fields, S. and O.-k. Song (1989) "A novel genetic system to detect protein-protein interactions." ***Nature*** 340, 245-246. **DOI:** 10.1038/340245a0

Fire, A., S. Xu, M. K. Montgomery, S. A. Kostas, S. E. Driver and C. C. Mello (1998) "Potent and specific genetic interference by double-stranded RNA in Caenorhabditis elegans." ***Nature*** 391, 806-11. **DOI:** 10.1038/35888

Forler, D., T. Köcher, M. Rode, M. Gentzel, E. Izaurralde and M. Wilm (2002) "An efficient protein complex purification method for functional proteomics in higher eukaryotes." ***Nature Biotechnology*** 21, 89-92. **DOI:** 10.1038/nbt773

Forterre, P. (2006) "The origin of viruses and their possible roles in major evolutionary transitions." ***Virus Research*** 117, 5-16. **DOI:** 10.1016/j.virusres.2006.01.010

Forterre, P. (2011) "Manipulation of cellular syntheses and the nature of viruses: The virocell concept." ***Comptes Rendus Chimie*** 14, 392-399. **DOI:** 10.1016/j.crci.2010.06.007

Forterre, P. (2013) "The virocell concept and environmental microbiology." ***The ISME Journal*** 7, 233-236. **DOI:** 10.1038/ismej.2012.110

Forterre, P. and D. Prangishvili (2009) "The Great Billion-year War between Ribosome- and Capsid-encoding Organisms (Cells and Viruses) as the Major Source of Evolutionary Novelties." ***Annals of the New York Academy of Sciences*** 1178, 65-77. **DOI:** 10.1111/j.1749-6632.2009.04993.x

Francia, S., F. Michelini, A. Saxena, D. Tang, M. de Hoon, V. Anelli, M. Mione, P. Carninci and F. d'Adda di Fagagna (2012) "Site-specific DICER and DROSHA RNA products control the DNA-damage response." ***Nature*** 488, 231-235. **DOI:** 10.1038/nature11179

Franco-Zorrilla, J. M., I. López-Vidriero, J. L. Carrasco, M. Godoy, P. Vera and R. Solano (2014) "DNA-binding specificities of plant transcription factors and their potential to define target genes." ***Proceedings of the National Academy of Sciences of the United States of America*** 111, 2367-72. **DOI:** 10.1073/pnas.1316278111

Freire, M. A., C. Tourneur, F. Granier, J. Camonis, A. El Amrani, K. S. Browning and C. Robaglia (2000) "Plant lipoxygenase 2 is a translation initiation factor-4E-binding protein." ***Plant Mol Biol*** 44, 129-40. **DOI:** 10.1023/A:1006494628892

Fu, D. Q., B. Z. Zhu, H. L. Zhu, H. X. Zhang, Y. H. Xie, W. B. Jiang, X. D. Zhao and Y. B. Luo (2006) "Enhancement of virus-induced gene silencing in tomato by low temperature and low humidity." ***Molecules and Cells*** 21, 153-160. **DOI:** 10.1016/j.engstruct.2005.08.006

Fu, Z. Q., S. Yan, A. Saleh, W. Wang, J. Ruble, et al. (2012) "NPR3 and NPR4 are receptors for the immune signal salicylic acid in plants." ***Nature***, 6-11. **DOI:** 10.1038/nature11162

Fukao, Y., A. Ferjani, R. Tomioka, N. Nagasaki, R. Kurata, Y. Nishimori, M. Fujiwara and M. Maeshima (2011) "iTRAQ Analysis Reveals Mechanisms of Growth Defects Due to Excess Zinc in Arabidopsis." ***PLANT PHYSIOLOGY*** 155, 1893-1907. **DOI:** 10.1104/pp.110.169730

Fusaro, A. F., L. Matthew, N. A. Smith, S. J. Curtin, J. Dedic-Hagan, et al. (2006) "RNA interference-inducing hairpin RNAs in plants act through the viral defence pathway." ***EMBO reports*** 7, 1168-1175. **DOI:** 10.1038/sj.embor.7400837

Gabrenaite-Verkhovskaya, R., I. a. Andreev, N. O. Kalinina, L. Torrance, M. E. Taliansky and K. Makinen (2008) "Cylindrical inclusion protein of potato

virus A is associated with a subpopulation of particles isolated from infected plants." ***Journal of General Virology*** 89, 829-838. **DOI:** 10.1099/vir.0.83406-0

Gal-On, A. (2000) "A Point Mutation in the FRNK Motif of the Potyvirus Helper Component-Protease Gene Alters Symptom Expression in Cucurbits and Elicits Protection Against the Severe Homologous Virus." ***Phytopathology*** 90, 467-473. **DOI:** 10.1094/PHYTO.2000.90.5.467

Gale, P., A. Brouwer, V. Ramnial, L. Kelly, R. Kosmider, A. R. Fooks and E. L. Snary (2010) "Assessing the impact of climate change on vector-borne viruses in the EU through the elicitation of expert opinion." ***Epidemiology and infection*** 138, 214-225. **DOI:** 10.1017/S0950268809990367

Gallie, D. R. (2001) "Cap-Independent Translation Conferred by the 5' Leader of Tobacco Etch Virus Is Eukaryotic Initiation Factor 4G Dependent." ***Journal of Virology*** 75, 12141-12152. **DOI:** 10.1128/JVI.75.24.12141-12152.2001

Gallois, J.-L., C. Charron, F. Sanchez, G. Pagny, M.-C. Houvenaghel, et al. (2010) "Single amino acid changes in the turnip mosaic virus viral genome-linked protein (VPg) confer virulence towards Arabidopsis thaliana mutants knocked out for eukaryotic initiation factors eIF(iso)4E and eIF(iso)4G." ***Journal of General Virology*** 91, 288-293. **DOI:** 10.1099/vir.0.015321-0

Gao, Z., E. Johansen, S. Eyers, C. L. Thomas, T. H. Noel Ellis and A. J. Maule (2004) "The potyvirus recessive resistance gene, sbm1, identifies a novel role for translation initiation factor eIF4E in cell-to-cell trafficking." ***The Plant Journal*** 40, 376-385. **DOI:** 10.1111/j.1365-313X.2004.02215.x

García, J. A., M. Glasa, M. Cambra and T. Candresse (2014) "Plum pox virus and sharka: a model potyvirus and a major disease." ***Molecular Plant Pathology*** 15, 226-241. **DOI:** 10.1111/mpp.12083

Garcia, J. A., J. L. Riechmann, M. T. Martín and S. Laín (1989) "Proteolytic activity of the plum pox potyvirus NIa-protein on excess of natural and artificial substrates in Escherichia coli." ***FEBS Letters*** 257, 269-273. **DOI:** 10.1016/0014-5793(89)81550-9

Garcia-Ruiz, H., A. Takeda, E. J. Chapman, C. M. Sullivan, N. Fahlgren, K. J. Brempelis and J. C. Carrington (2010) "Arabidopsis RNA-Dependent RNA Polymerases and Dicer-Like Proteins in Antiviral Defense and Small Interfering RNA Biogenesis during Turnip Mosaic Virus Infection." ***The Plant Cell*** 22, 481-496. **DOI:** 10.1105/tpc.109.073056

Gasciolli, V., A. C. Mallory, D. P. Bartel and H. Vaucheret (2005) "Partially Redundant Functions of Arabidopsis DICER-like Enzymes and a Role for DCL4 in Producing trans-Acting siRNAs." ***Current Biology*** 15, 1494-1500. **DOI:** 10.1016/j.cub.2005.07.024

Geddes, A. M. (2006) "The history of smallpox." ***Clinics in Dermatology*** 24, 152-157. **DOI:** 10.1016/j.clindermatol.2005.11.009

Geng, C., Q.-Q. Cong, X.-D. Li, A.-L. Mou, R. Gao, J.-L. Liu and Y.-P. Tian (2015) "DEVELOPMENTALLY REGULATED PLASMA MEMBRANE PROTEIN of Nicotiana benthamiana Contributes to Potyvirus Movement and Transports to Plasmodesmata via the Early Secretory Pathway and the Actomyosin System." ***Plant Physiology*** 167, 394-410. **DOI:** 10.1104/pp.114.252734

Geri, C., E. Cecchini, M. E. Giannakou, S. N. Covey and J. J. Milner (1999) "Altered Patterns of Gene Expression in Arabidopsis Elicited by Cauliflower Mosaic Virus (CaMV) Infection and by a CaMV Gene VI Transgene."

Molecular Plant-Microbe Interactions 12, 377-384. **DOI:** 10.1094/MPMI.1999.12.5.377

German-Retana, S., J. Walter, B. Doublet, G. Roudet-Tavert, V. Nicaise, et al. (2008) "Mutational analysis of plant cap-binding protein eIF4E reveals key amino acids involved in biochemical functions and potyvirus infection." ***Journal of virology*** 82, 7601-7612. **DOI:** 10.1128/JVI.00209-08

Getts, D. R., E. M. L. Chastain, R. L. Terry and S. D. Miller (2013). "Virus infection, antiviral immunity, and autoimmunity." **Immunological Reviews** 255: 197-209.

Gibbs, A. J., K. Ohshima, M. J. Phillips and M. J. Gibbs (2008) "The Prehistory of Potyviruses: Their Initial Radiation Was during the Dawn of Agriculture." ***PLoS ONE*** 3, e2523. **DOI:** 10.1371/journal.pone.0002523

Giner, A., L. Lakatos, M. García-Chapa, J. J. López-Moya and J. Burgyán (2010) "Viral Protein Inhibits RISC Activity by Argonaute Binding through Conserved WG/GW Motifs." ***PLoS Pathogens*** 6, e1000996. **DOI:** 10.1371/journal.ppat.1000996

Giot, L., J. S. Bader, C. Brouwer, A. Chaudhuri, B. Kuang, et al. (2003) "A protein interaction map of Drosophila melanogaster." ***Science*** 302, 1727-1736. **DOI:** 10.1126/science.1090289

Girault, T., J. François, H. Rogniaux, S. Pascal, S. Delrot, P. Coutos-Thévenot and E. Gomès (2008) "Exogenous application of a lipid transfer protein-jasmonic acid complex induces protection of grapevine towards infection by Botrytis cinerea." ***Plant Physiology and Biochemistry*** 46, 140-149. **DOI:** 10.1016/j.plaphy.2007.10.005

Glick, E., A. Zrachya, Y. Levy, A. Mett, D. Gidoni, E. Belausov, V. Citovsky and Y. Gafni (2008) "Interaction with host SGS3 is required for suppression of RNA silencing by tomato yellow leaf curl virus V2 protein." ***Proceedings of the National Academy of Sciences of the United States of America*** 105, 157-161. **DOI:** 10.1073/pnas.0709036105

Grangeon, R., M. Agbeci, J. Chen, G. Grondin, H. Zheng and J.-F. Laliberte (2012) "Impact on the Endoplasmic Reticulum and Golgi Apparatus of Turnip Mosaic Virus Infection." ***Journal of Virology*** 86, 9255-9265. **DOI:** 10.1128/JVI.01146-12

Gregory, B. D., R. C. O'Malley, R. Lister, M. a. Urich, J. Tonti-Filippini, H. Chen, a. H. Millar and J. R. Ecker (2008) "A Link between RNA Metabolism and Silencing Affecting Arabidopsis Development." ***Developmental Cell*** 14, 854-866. **DOI:** 10.1016/j.devcel.2008.04.005

Griffiths, G. (1993) "Fine Structure Immunocytochemistry." ***Trends in Cell Biology*** 4, 30. **DOI:** 10.1007/978-3-642-77095-1

Grishin, N. V. (1995) "Estimation of the number of amino acid substitutions per site when the substitution rate varies among sites." ***Journal of molecular evolution*** 41, 675-679. **DOI:** 10.1007/BF00175885

Grishok, A. (2005) "RNAi mechanisms in Caenorhabditis elegans." ***FEBS Letters*** 579, 5932-5939. **DOI:** 10.1016/j.febslet.2005.08.001

Grzela, R., L. Strokovska, J.-P. Andrieu, B. Dublet, W. Zagorski and J. Chroboczek (2006) "Potyvirus terminal protein VPg, effector of host eukaryotic initiation factor eIF4E." ***Biochimie*** 88, 887-896. **DOI:** 10.1016/j.biochi.2006.02.012

Gu, L., T. Xu, K. Lee, K. H. Lee and H. Kang (2014) "A chloroplast-localized DEAD-box RNA helicaseAtRH3 is essential for intron splicing and plays an important role in the growth and stress response in Arabidopsis thaliana." ***Plant Physiology and Biochemistry*** 82, 309-318. **DOI:** 10.1016/j.plaphy.2014.07.006

Gully, D., D. Moinier, L. Loiseau and E. Bouveret (2003) "New partners of acyl carrier protein detected in Escherichia coli by tandem affinity purification." ***FEBS Letters*** 548, 90-96. **DOI:** 10.1016/S0014-5793(03)00746-4

Guo, A., K. He, D. Liu, S. Bai, X. Gu, L. Wei and J. Luo (2005) "DATF: a database of Arabidopsis transcription factors." ***Bioinformatics*** 21, 2568-2569. **DOI:** 10.1093/bioinformatics/bti334

Guo, D., M. L. Rajamäki, M. Saarma and J. P. T. Valkonen (2001). "Towards a protein interaction map of potyviruses: Protein interaction matrixes of two potyviruses based on the yeast two-hybrid system." **Journal of General Virology** 82: 935-939.

Guo, H. S. and J. A. García (1997) "Delayed Resistance to Plum Pox Potyvirus Mediated by a Mutated RNA Replicase Gene: Involvement of a Gene-Silencing Mechanism." ***Molecular Plant-Microbe Interactions*** 10, 160-170. **DOI:** 10.1094/MPMI.1997.10.2.160

Guo, L., S. P. Devaiah, R. Narasimhan, X. Pan, Y. Zhang, W. Zhang and X. Wang (2012) "Cytosolic Glyceraldehyde-3-Phosphate Dehydrogenases Interact with Phospholipase D to Transduce Hydrogen Peroxide Signals in the Arabidopsis Response to Stress." ***The Plant Cell*** 24, 2200-2212. **DOI:** 10.1105/tpc.111.094946

Guo, L., F. Ma, F. Wei, B. Fanella, D. K. Allen and X. Wang (2014) "Cytosolic Phosphorylating Glyceraldehyde-3-Phosphate Dehydrogenases Affect Arabidopsis Cellular Metabolism and Promote Seed Oil Accumulation." ***The Plant Cell*** 26, 3023-3035. **DOI:** 10.1105/tpc.114.126946

Hafrén, A., K. Eskelin and K. Mäkinen (2013) "Ribosomal protein P0 promotes Potato virus A infection and functions in viral translation together with VPg and eIF(iso)4E." ***Journal of virology*** 87, 4302-12. **DOI:** 10.1128/JVI.03198-12

Hafrén, A., D. Hofius, G. Rönnholm, U. Sonnewald and K. Mäkinen (2010) "HSP70 and its cochaperone CPIP promote potyvirus infection in Nicotiana benthamiana by regulating viral coat protein functions." ***The Plant cell*** 22, 523-535. **DOI:** 10.1105/tpc.109.072413

Haikonen, T., M.-L. Rajamäki and J. P. T. Valkonen (2013) "Interaction of the Microtubule-Associated Host Protein HIP2 with Viral Helper Component Proteinase Is Important in Infection with Potato virus A." ***Molecular Plant-Microbe Interactions*** 26, 734-744. **DOI:** 10.1094/MPMI-01-13-0023-R

Hall, D. B. and K. Struhl (2002) "The VP16 Activation Domain Interacts with Multiple Transcriptional Components as Determined by Protein-Protein Cross-linking in Vivo." ***Journal of Biological Chemistry*** 277, 46043-46050. **DOI:** 10.1074/jbc.M208911200

Hamilton, A. J. and D. C. Baulcombe (1999) "A Species of Small Antisense RNA in Posttranscriptional Gene Silencing in Plants." ***Science*** 286, 950-952. **DOI:** 10.1126/science.286.5441.950

Han, M.-H., S. Goud, L. Song and N. Fedoroff (2004) "The Arabidopsis double-stranded RNA-binding protein HYL1 plays a role in microRNA-mediated

gene regulation." ***Proceedings of the National Academy of Sciences of the United States of America*** 101, 1093-1098. **DOI:** 10.1073/pnas.0307969100

Hannon, G. J. (2002) "RNA interference." ***Nature*** 418, 244-251. **DOI:** 10.1038/418244a

Harrison, B. D. and I. M. Roberts (1968) "Association of tobacco rattle virus with mitochondria." ***Journal of General Virology*** 3, 121-124. **DOI:** 10.1099/0022-1317-3-1-121

Harvey, J. J. W., M. G. Lewsey, K. Patel, J. Westwood, S. Heimstädt, J. P. Carr and D. C. Baulcombe (2011) "An antiviral defense role of AGO2 in plants." ***PLoS ONE*** 6, e14639. **DOI:** 10.1371/journal.pone.0014639

Hatta, T., S. Bullivant and R. E. Matthews (1973). "Fine structure of vesicles induced in chloroplasts of Chinese cabbage leaves by infection with turnip yellow mosaic virus." **J Gen Virol** 20(1): 37-50.

Hatta, T. and R. I. Francki (1981). "Identification of small polyhedral virus particles in thin sections of plant cells by an enzyme cytochemical technique." **J Ultrastruct Res** 74(1): 116-29.

Hatta, T., T. Nakamoto, Y. Tagaki and R. Ushiyama (1971). "Cytological abnormalities of mitochondria induced by infection with cucumber green mottle mosaic virus." **Virology** 45(1): 292-7.

Heinlein, M. (2015) "Plant virus replication and movement." ***Virology*** 479-480, 657-671. **DOI:** 10.1016/j.virol.2015.01.025

Heinlein, M., H. S. Padgett, J. S. Gens, B. G. Pickard, S. J. Casper, B. L. Epel and R. N. Beachy (1998) "Changing patterns of localization of the tobacco mosaic virus movement protein and replicase to the endoplasmic reticulum and microtubules during infection." ***The Plant cell*** 10, 1107-1120. **DOI:** 10.1105/tpc.10.7.1107

Hennig, J., R. E. Dewey, J. R. Cutt and D. F. Klessig (1993) "Pathogen, salicylic acid and developmental dependent expression of a beta-1,3-glucanase/GUS gene fusion in transgenic tobacco plants." ***The Plant Journal*** 4, 481-493. **DOI:** 10.1046/j.1365-313X.1993.04030481.x

Henry, E., N. Fung, J. Liu, G. Drakakaki and G. Coaker (2015) "Beyond Glycolysis: GAPDHs Are Multi-functional Enzymes Involved in Regulation of ROS, Autophagy, and Plant Immune Responses." ***PLOS Genetics*** 11, e1005199. **DOI:** 10.1371/journal.pgen.1005199

Hernandez-Pinzon, I., N. E. Yelina, F. Schwach, D. J. Studholme, D. Baulcombe and T. Dalmay (2007) "SDE5, the putative homologue of a human mRNA export factor, is required for transgene silencing and accumulation of trans-acting endogenous siRNA." ***The Plant Journal*** 50, 140-148. **DOI:** 10.1111/j.1365-313X.2007.03043.x

Hiraguri, A., R. Itoh, N. Kondo, Y. Nomura, D. Aizawa, et al. (2005) "Specific interactions between Dicer-like proteins and HYL1/DRB- family dsRNA-binding proteins in Arabidopsis thaliana." ***Plant Molecular Biology*** 57, 173-188. **DOI:** 10.1007/s11103-004-6853-5

Hofius, D., A. T. Maier, C. Dietrich, I. Jungkunz, F. Bornke, E. Maiss and U. Sonnewald (2007) "Capsid Protein-Mediated Recruitment of Host DnaJ-Like Proteins Is Required for Potato Virus Y Infection in Tobacco Plants." ***Journal of Virology*** 81, 11870-11880. **DOI:** 10.1128/JVI.01525-07

Hong, Y. and A. G. Hunt (1996) "RNA Polymerase Activity Catalyzed by a Potyvirus-Encoded RNA-Dependent RNA Polymerase." ***Virology*** 226, 146-151. **DOI:** 10.1006/viro.1996.0639

Hong, Y., K. Levay, J. F. Murphy, P. G. KLEIN, J. G. Shaw and A. G. Hunt (1995) "A Potyvirus Polymerase Interacts with the Viral Coat Protein and VPg in Yeast Cells." ***Virology*** 214, 159-166. **DOI:** 10.1006/viro.1995.9944

Howard, C. R. and N. F. Fletcher (2012) "Emerging virus diseases: can we ever expect the unexpected?" ***Emerging microbes & infections*** 1, e46. **DOI:** 10.1038/emi.2012.47

Huang, T.-S. and P. D. Nagy (2011) "Direct Inhibition of Tombusvirus Plus-Strand RNA Synthesis by a Dominant Negative Mutant of a Host Metabolic Enzyme, Glyceraldehyde-3-Phosphate Dehydrogenase, in Yeast and Plants." ***Journal of Virology*** 85, 9090-9102. **DOI:** 10.1128/JVI.00666-11

Huang, T.-S., T. Wei, J.-F. Laliberte and A. Wang (2010) "A Host RNA Helicase-Like Protein, AtRH8, Interacts with the Potyviral Genome-Linked Protein, VPg, Associates with the Virus Accumulation Complex, and Is Essential for Infection." ***PLANT PHYSIOLOGY*** 152, 255-266. **DOI:** 10.1104/pp.109.147983

Hunter, L. J. R., J. H. Westwood, G. Heath, K. Macaulay, A. G. Smith, S. a. MacFarlane, P. Palukaitis and J. P. Carr (2013) "Regulation of RNA-Dependent RNA Polymerase 1 and Isochorismate Synthase Gene Expression in Arabidopsis." ***PLoS ONE*** 8, e66530. **DOI:** 10.1371/journal.pone.0066530

Hwang, J., J. Li, W.-Y. Liu, S.-J. An, H. Cho, N. H. Her, I. Yeam, D. Kim and B.-C. Kang (2009) "Double mutations in eIF4E and eIFiso4E confer recessive resistance to Chilli veinal mottle virus in pepper." ***Molecules and Cells*** 27, 329-336. **DOI:** 10.1007/s10059-009-0042-y

Hyodo, K., A. Mine, T. Taniguchi, M. Kaido, K. Mise, H. Taniguchi and T. Okuno (2013) "ADP Ribosylation Factor 1 Plays an Essential Role in the Replication of a Plant RNA Virus." ***Journal of Virology*** 87, 163-176. **DOI:** 10.1128/JVI.02383-12

Hyodo, K., T. Taniguchi, Y. Manabe, M. Kaido, K. Mise, T. Sugawara, H. Taniguchi and T. Okuno (2015) "Phosphatidic Acid Produced by Phospholipase D Promotes RNA Replication of a Plant RNA Virus." ***PLOS Pathogens*** 11, e1004909. **DOI:** 10.1371/journal.ppat.1004909

Ibrahim, A., H. M. Hutchens, R. Howard Berg and L. Sue Loesch-Fries (2012) "Alfalfa mosaic virus replicase proteins, P1 and P2, localize to the tonoplast in the presence of virus RNA." ***Virology*** 433, 449-461. **DOI:** 10.1016/j.virol.2012.08.018

Iida, K., M. Seki, T. Sakurai, M. Satou, K. Akiyama, T. Toyoda, A. Konagaya and K. Shinozaki (2005) "RARTF: Database and Tools for Complete Sets of Arabidopsis Transcription Factors." ***DNA Research*** 12, 247-256. **DOI:** 10.1093/dnares/dsi011

Iki, T., M. Yoshikawa, M. Nishikiori, M. C. Jaudal, E. Matsumoto-Yokoyama, I. Mitsuhara, T. Meshi and M. Ishikawa (2010) "In Vitro Assembly of Plant RNA-Induced Silencing Complexes Facilitated by Molecular Chaperone HSP90." ***Molecular Cell*** 39, 282-291. **DOI:** 10.1016/j.molcel.2010.05.014

Incarbone, M. and P. Dunoyer (2013) "RNA silencing and its suppression: novel insights from< i> in planta</i> analyses." ***Trends in plant science*** 18. **DOI:** doi.org/10.1016/j.tplants.2013.04.001

Ivanov, K. I., K. Eskelin, A. Lohmus and K. Makinen (2014) "Molecular and cellular mechanisms underlying potyvirus infection." ***Journal of General Virology*** 95, 1415-1429. **DOI:** 10.1099/vir.0.064220-0

James, P., J. Halladay and E. a. Craig (1996). "Genomic libraries and a host strain designed for highly efficient two-hybrid selection in yeast." **Genetics** 144: 1425-1436.

Jamous, R. M., K. Boonrod, M. W. Fuellgrabe, M. S. Ali-Shtayeh, G. Krczal and M. Wassenegger (2011) "The helper component-proteinase of the Zucchini yellow mosaic virus inhibits the Hua Enhancer 1 methyltransferase activity in vitro." ***Journal of General Virology*** 92, 2222-2226. **DOI:** 10.1099/vir.0.031534-0

Janssen, D., G. Martin, L. Velasco, P. Gomez, E. Segundo, L. Ruiz and I. M. Cuadrado (2005) "Absence of a coding region for the helper component-proteinase in the genome of cucumber vein yellowing virus, a whitefly-transmitted member of the Potyviridae." ***Arch Virol*** 150, 1439-47. **DOI:** 10.1007/s00705-005-0515-z

Jauvion, V., T. Elmayan and H. Vaucheret (2010) "The Conserved RNA Trafficking Proteins HPR1 and TEX1 Are Involved in the Production of Endogenous and Exogenous Small Interfering RNA in Arabidopsis." ***The Plant Cell*** 22, 2697-2709. **DOI:** 10.1105/tpc.110.076638

Jay, F., Y. Wang, A. Yu, L. Taconnat, S. Pelletier, V. Colot, J.-P. Renou and O. Voinnet (2011) "Misregulation of AUXIN RESPONSE FACTOR 8 Underlies the Developmental Abnormalities Caused by Three Distinct Viral Silencing Suppressors in Arabidopsis." ***PLoS Pathogens*** 7, e1002035. **DOI:** 10.1371/journal.ppat.1002035

Jiang, J. and J.-F. Laliberté (2011) "The genome-linked protein VPg of plant viruses—a protein with many partners." ***Current Opinion in Virology*** 1, 347-354. **DOI:** 10.1016/j.coviro.2011.09.010

Jin, J., H. Zhang, L. Kong, G. Gao and J. Luo (2014) "PlantTFDB 3.0: a portal for the functional and evolutionary study of plant transcription factors." ***Nucleic Acids Research*** 42, D1182-D1187. **DOI:** 10.1093/nar/gkt1016

Jin, Y., D. Ma, J. Dong, D. Li, C. Deng, J. Jin and T. Wang (2007) "The HC-Pro Protein of Potato Virus Y Interacts with NtMinD of Tobacco." ***Molecular Plant-Microbe Interactions*** 20, 1505-1511. **DOI:** 10.1094/MPMI-20-12-1505

Johnson, C. (2003) "Salicylic Acid and NPR1 Induce the Recruitment of trans-Activating TGA Factors to a Defense Gene Promoter in Arabidopsis." ***THE PLANT CELL ONLINE*** 15, 1846-1858. **DOI:** 10.1105/tpc.012211

Johnson, J. (1922). "The Relation of Air Temperature to the Mosaic Disease of Potatoes and Other Plants»." **Phytopathology** 12: 438-440.

Jones, J. D. G. and J. L. Dangl (2006) "The plant immune system." ***Nature*** 444, 323-329. **DOI:** 10.1038/nature05286

Jones-Rhoades, M. W., D. P. Bartel and B. Bartel (2006) "MicroRNAs AND THEIR REGULATORY ROLES IN PLANTS." ***Annual Review of Plant Biology*** 57, 19-53. **DOI:** 10.1146/annurev.arplant.57.032905.105218

Jorrin-novo, J. V. (2014). **Plant Proteomics**. Totowa, NJ, Humana Press.

Jouannet, V., A. B. Moreno, T. Elmayan, H. Vaucheret, M. D. Crespi and A. Maizel (2012) "Cytoplasmic Arabidopsis AGO7 accumulates in membrane-

associated siRNA bodies and is required for ta-siRNA biogenesis." ***The EMBO Journal*** 31, 1704-1713. **DOI:** 10.1038/emboj.2012.20

Kachroo, A. and G. P. Robin (2013) "Systemic signaling during plant defense." ***Current Opinion in Plant Biology*** 16, 527-533. **DOI:** 10.1016/j.pbi.2013.06.019

Kaffarnik, F. a. R., A. M. E. Jones, J. P. Rathjen and S. C. Peck (2009) "Effector Proteins of the Bacterial Pathogen Pseudomonas syringae Alter the Extracellular Proteome of the Host Plant, Arabidopsis thaliana." ***Molecular & Cellular Proteomics*** 8, 145-156. **DOI:** 10.1074/mcp.M800043-MCP200

Kaido, M., K. Abe, A. Mine, K. Hyodo, T. Taniguchi, H. Taniguchi, K. Mise and T. Okuno (2014) "GAPDH-A Recruits a Plant Virus Movement Protein to Cortical Virus Replication Complexes to Facilitate Viral Cell-to-Cell Movement." ***PLoS Pathogens*** 10, e1004505. **DOI:** 10.1371/journal.ppat.1004505

Kammel, C., M. Thomaier, B. B. Sørensen, T. Schubert, G. Längst, M. Grasser and K. D. Grasser (2013) "Arabidopsis DEAD-Box RNA Helicase UAP56 Interacts with Both RNA and DNA as well as with mRNA Export Factors." ***PLoS ONE*** 8, e60644. **DOI:** 10.1371/journal.pone.0060644

Kang, B.-C., I. Yeam, J. D. Frantz, J. F. Murphy and M. M. Jahn (2005) "The pvr1 locus in Capsicum encodes a translation initiation factor eIF4E that interacts with Tobacco etch virus VPg." ***The Plant Journal*** 42, 392-405. **DOI:** 10.1111/j.1365-313X.2005.02381.x

Karp, N. a., W. Huber, P. G. Sadowski, P. D. Charles, S. V. Hester and K. S. Lilley (2010) "Addressing Accuracy and Precision Issues in iTRAQ Quantitation." ***Molecular & Cellular Proteomics*** 9, 1885-1897. **DOI:** 10.1074/mcp.M900628-MCP200

Kasschau, K. D. and J. C. Carrington (1998) "A Counterdefensive Strategy of Plant Viruses." ***Cell*** 95, 461-470. **DOI:** 10.1016/S0092-8674(00)81614-1

Kasschau, K. D., Z. Xie, E. Allen, C. Llave, E. J. Chapman, K. a. Krizan and J. C. Carrington (2003) "P1/HC-Pro, a Viral Suppressor of RNA Silencing, Interferes with Arabidopsis Development and miRNA Function." ***Developmental Cell*** 4, 205-217. **DOI:** 10.1016/S1534-5807(03)00025-X

Kavi, H. H., H. R. Fernandez, W. Xie and J. a. Birchler (2005) "RNA silencing in Drosophila." ***FEBS Letters*** 579, 5940-5949. **DOI:** 10.1016/j.febslet.2005.08.069

Kawakami, S., Y. Watanabe and R. N. Beachy (2004) "Tobacco mosaic virus infection spreads cell to cell as intact replication complexes." ***Proceedings of the National Academy of Sciences*** 101, 6291-6296. **DOI:** 10.1073/pnas.0401221101

Kekarainen, T. (2002) "Functional Genomics on Potato Virus A: Virus Genome-Wide Map of Sites Essential for Virus Propagation." ***Genome Research*** 12, 584-594. **DOI:** 10.1101/gr.220702

Kerppola, T. K. (2006) "Design and implementation of bimolecular fluorescence complementation (BiFC) assays for the visualization of protein interactions in living cells." ***Nature Protocols*** 1, 1278-1286. **DOI:** 10.1038/nprot.2006.201

Khan, M. a., H. Miyoshi, D. R. Gallie and D. J. Goss (2008) "Potyvirus Genome-linked Protein, VPg, Directly Affects Wheat Germ in Vitro Translation: Interactions with translation initiation factors eIF4F and eIF(iso)4F."

Journal of Biological Chemistry 283, 1340-1349. **DOI:** 10.1074/jbc.M703356200

Kim, M.-H., Y. Sonoda, K. Sasaki, H. Kaminaka and R. Imai (2013) "Interactome analysis reveals versatile functions of Arabidopsis COLD SHOCK DOMAIN PROTEIN 3 in RNA processing within the nucleus and cytoplasm." ***Cell Stress and Chaperones*** 18, 517-525. **DOI:** 10.1007/s12192-012-0398-3

Kim, S., J.-Y. Yang, J. Xu, I.-C. Jang, M. J. Prigge and N.-H. Chua (2008) "Two Cap-Binding Proteins CBP20 and CBP80 are Involved in Processing Primary MicroRNAs." ***Plant and Cell Physiology*** 49, 1634-1644. **DOI:** 10.1093/pcp/pcn146

Klein, P. G., R. R. Klein, E. Rodriguez-Cerezo, A. G. Hunt and J. G. Shaw (1994) "Mutational Analysis of the Tobacco Vein Mottling Virus Genome." ***Virology*** 204, 759-769. **DOI:** 10.1006/viro.1994.1591

Knuesel, M. (2003) "Identification of Novel Protein-Protein Interactions Using A Versatile Mammalian Tandem Affinity Purification Expression System." ***Molecular & Cellular Proteomics*** 2, 1225-1233. **DOI:** 10.1074/mcp.T300007-MCP200

Köhler, D., S. Schmidt-Gattung and S. Binder (2010) "The DEAD-box protein PMH2 is required for efficient group II intron splicing in mitochondria of Arabidopsis thaliana." ***Plant Molecular Biology*** 72, 459-467. **DOI:** 10.1007/s11103-009-9584-9

Kong, L.-J. and L. Hanley-Bowdoin (2002) "A Geminivirus Replication Protein Interacts with a Protein Kinase and a Motor Protein That Display Different Expression Patterns during Plant Development and Infection." ***The Plant Cell*** 14, 1817-1832. **DOI:** 10.1105/tpc.003681

Kooter, J., M. A. Matzke and P. Meyer (1999) "Listening to the silent genes: transgene silencing, gene regulation and pathogen control." ***Trends in Plant Science*** 4, 340-347. **DOI:** 10.1016/S1360-1385(99)01467-3

Kovalev, N., D. Barajas and P. D. Nagy (2012a) "Similar roles for yeast Dbp2 and Arabidopsis RH20 DEAD-box RNA helicases to Ded1 helicase in tombusvirus plus-strand synthesis." ***Virology*** 432, 470-484. **DOI:** 10.1016/j.virol.2012.06.030

Kovalev, N. and P. D. Nagy (2014) "The Expanding Functions of Cellular Helicases: The Tombusvirus RNA Replication Enhancer Co-opts the Plant eIF4AIII-Like AtRH2 and the DDX5-Like AtRH5 DEAD-Box RNA Helicases to Promote Viral Asymmetric RNA Replication." ***PLoS Pathogens*** 10, e1004051. **DOI:** 10.1371/journal.ppat.1004051

Kovalev, N., J. Pogany and P. D. Nagy (2012b) "A Co-Opted DEAD-Box RNA Helicase Enhances Tombusvirus Plus-Strand Synthesis." ***PLoS Pathogens*** 8, e1002537. **DOI:** 10.1371/journal.ppat.1002537

Kristensen, A. K., J. Brunstedt, K. K. Nielsen, P. Roepstorff and J. D. Mikkelsen (2000) "Characterization of a new antifungal non-specific lipid transfer protein (nsLTP) from sugar beet leaves." ***Plant Science*** 155, 31-40. **DOI:** 10.1016/S0168-9452(00)00190-4

Kumakura, N., A. Takeda, Y. Fujioka, H. Motose, R. Takano and Y. Watanabe (2009) "SGS3 and RDR6 interact and colocalize in cytoplasmic SGS3/RDR6-bodies." ***FEBS Letters*** 583, 1261-1266. **DOI:** 10.1016/j.febslet.2009.03.055

Lacatus, G. and G. Sunter (2009) "The Arabidopsis PEAPOD2 transcription factor interacts with geminivirus AL2 protein and the coat protein promoter." ***Virology*** 392, 196-202. **DOI:** 10.1016/j.virol.2009.07.004

Lagrimini, L. M., W. Burkhart, M. Moyer and S. Rothstein (1987) "Molecular cloning of complementary DNA encoding the lignin-forming peroxidase from tobacco: Molecular analysis and tissue-specific expression." ***Proceedings of the National Academy of Sciences of the United States of America*** 84, 7542-7546. **DOI:** 10.1073/pnas.84.21.7542

Laín, S., M. T. Martín, J. L. Riechmann and J. A. García (1991). "Novel catalytic activity associated with positive-strand RNA virus infection: nucleic acid-stimulated ATPase activity of the plum pox potyvirus helicaselike protein." **Journal of virology** 65: 1-6.

Lain, S., J. L. Riechmann and J. A. Garciá (1990) "RNA helicase: a novel activity associated with a protein encoded by a positive strand RNA virus." ***Nucleic Acids Research*** 18, 7003-7006. **DOI:** 10.1093/nar/18.23.7003

Lakatos, L., T. Csorba, V. Pantaleo, E. J. Chapman, J. C. Carrington, et al. (2006) "Small RNA binding is a common strategy to suppress RNA silencing by several viral suppressors." ***The EMBO Journal*** 25, 2768-2780. **DOI:** 10.1038/sj.emboj.7601164

Laubinger, S., T. Sachsenberg, G. Zeller, W. Busch, J. U. Lohmann, G. Ratsch and D. Weigel (2008) "Dual roles of the nuclear cap-binding complex and SERRATE in pre-mRNA splicing and microRNA processing in Arabidopsis thaliana." ***Proceedings of the National Academy of Sciences*** 105, 8795-8800. **DOI:** 10.1073/pnas.0802493105

Lawrence, J. C., Jr. and R. T. Abraham (1997) "PHAS/4E-BPs as regulators of mRNA translation and cell proliferation." ***Trends Biochem Sci*** 22, 345-9. **DOI:** 10.1016/S0968-0004(97)01101-8

Lecoq, H., S. Cohen, B. Delécolle, A. Mansour and C. Desbiez (2000) "Cytological and molecular evidence that the whitefly-transmitted Cucumber vein yellowing virus is a tentative member of the family Potyviridae." ***Journal of General Virology*** 81, 2289-2293. **DOI:** 10.1099/0022-1317-81-9-2289

Lee, H.-C., S.-S. Chang, S. Choudhary, A. P. Aalto, M. Maiti, D. H. Bamford and Y. Liu (2009) "qiRNA is a new type of small interfering RNA induced by DNA damage." ***Nature*** 459, 274-277. **DOI:** 10.1038/nature08041

Lee, K.-H., J. Park, D. S. Williams, Y. Xiong, I. Hwang and B.-H. Kang (2013) "Defective chloroplast development inhibits maintenance of normal levels of abscisic acid in a mutant of the Arabidopsis RH3 DEAD-box protein during early post-germination growth." ***The Plant Journal*** 73, 720-732. **DOI:** 10.1111/tpj.12055

Lee, W.-M. and P. Ahlquist (2003) "Membrane Synthesis, Specific Lipid Requirements, and Localized Lipid Composition Changes Associated with a Positive-Strand RNA Virus RNA Replication Protein." ***Journal of Virology*** 77, 12819-12828. **DOI:** 10.1128/JVI.77.23.12819-12828.2003

Lee, W.-M., M. Ishikawa and P. Ahlquist (2001) "Mutation of Host 9 Fatty Acid Desaturase Inhibits Brome Mosaic Virus RNA Replication between Template Recognition and RNA Synthesis." ***Journal of Virology*** 75, 2097-2106. **DOI:** 10.1128/JVI.75.5.2097-2106.2001

Lellis, A. D., K. D. Kasschau, S. A. Whitham and J. C. Carrington (2002) "Loss-of-Susceptibility Mutants of Arabidopsis thaliana Reveal an Essential Role for

eIF(iso)4E during Potyvirus Infection." ***Current Biology*** 12, 1046-1051. **DOI:** 10.1016/S0960-9822(02)00898-9

Leonard, S. (2004) "Interaction of VPg-Pro of Turnip mosaic virus with the translation initiation factor 4E and the poly(A)-binding protein in planta." ***Journal of General Virology*** 85, 1055-1063. **DOI:** 10.1099/vir.0.19706-0

Leonard, S., D. Plante, S. Wittmann, N. Daigneault, M. G. Fortin and J.-F. Laliberte (2000) "Complex Formation between Potyvirus VPg and Translation Eukaryotic Initiation Factor 4E Correlates with Virus Infectivity." ***Journal of Virology*** 74, 7730-7737. **DOI:** 10.1128/JVI.74.17.7730-7737.2000

Lev, S. (2012) "Nonvesicular Lipid Transfer from the Endoplasmic Reticulum." ***Cold Spring Harbor Perspectives in Biology*** 4, a013300-a013300. **DOI:** 10.1101/cshperspect.a013300

Li, H., D. Ma, Y. Jin, Y. Tu, L. Liu, C. Leng, J. Dong and T. Wang (2015) "Helper component-proteinase enhances the activity of 1-deoxy- D -xylulose-5-phosphate synthase and promotes the biosynthesis of plastidic isoprenoids in Potato virus Y-infected tobacco." ***Plant, Cell & Environment*** 38, 2023-2034. **DOI:** 10.1111/pce.12526

Li, R., B. T. Weldegergis, J. Li, C. Jung, J. Qu, et al. (2014a) "Virulence factors of geminivirus interact with MYC2 to subvert plant resistance and promote vector performance." ***The Plant cell*** 26, 4991-5008. **DOI:** 10.1105/tpc.114.133181

Li, Z., D. Barajas, T. Panavas, D. a. Herbst and P. D. Nagy (2008) "Cdc34p Ubiquitin-Conjugating Enzyme Is a Component of the Tombusvirus Replicase Complex and Ubiquitinates p33 Replication Protein." ***Journal of Virology*** 82, 6911-6926. **DOI:** 10.1128/JVI.00702-08

Li, Z., O. Czarnecki, K. Chourey, J. Yang, G. a. Tuskan, G. B. Hurst, C. Pan and J.-G. Chen (2014b) "Strigolactone-Regulated Proteins Revealed by iTRAQ-Based Quantitative Proteomics in Arabidopsis." ***Journal of Proteome Research*** 13, 1359-1372. **DOI:** 10.1021/pr400925t

Li, Z., J. Pogany, T. Panavas, K. Xu, A. M. Esposito, T. G. Kinzy and P. D. Nagy (2009) "Translation elongation factor 1A is a component of the tombusvirus replicase complex and affects the stability of the p33 replication co-factor." ***Virology*** 385, 245-260. **DOI:** 10.1016/j.virol.2008.11.041

Li, Z., J. Pogany, S. Tupman, A. M. Esposito, T. G. Kinzy and P. D. Nagy (2010) "Translation Elongation Factor 1A Facilitates the Assembly of the Tombusvirus Replicase and Stimulates Minus-Strand Synthesis." ***PLoS Pathogens*** 6, e1001175. **DOI:** 10.1371/journal.ppat.1001175

Lim, J. H., C.-J. Park, S. U. Huh, L. M. Choi, G. J. Lee, Y. J. Kim and K.-H. Paek (2011) "Capsicum annuum WRKYb transcription factor that binds to the CaPR-10 promoter functions as a positive regulator in innate immunity upon TMV infection." ***Biochemical and Biophysical Research Communications*** 411, 613-619. **DOI:** 10.1016/j.bbrc.2011.07.002

Linder, P. and P. Lasko (2006) "Bent out of Shape: RNA Unwinding by the DEAD-Box Helicase Vasa." ***Cell*** 125, 219-221. **DOI:** 10.1016/j.cell.2006.03.030

Linder, P. and G. W. Owttrim (2009) "Plant RNA helicases: linking aberrant and silencing RNA." ***Trends in Plant Science*** 14, 344-352. **DOI:** 10.1016/j.tplants.2009.03.007

Lippert, D. N., S. G. Ralph, M. Phillips, R. White, D. Smith, et al. (2009) "Quantitative iTRAQ proteome and comparative transcriptome analysis of elicitor-induced Norway spruce (Picea abies) cells reveals elements of calcium signaling in the early conifer defense response." ***PROTEOMICS*** 9, 350-367. **DOI:** 10.1002/pmic.200800252

Liu, G.-T., L. Ma, W. Duan, B.-C. Wang, J.-H. Li, et al. (2014) "Differential proteomic analysis of grapevine leaves by iTRAQ reveals responses to heat stress and subsequent recovery." ***BMC Plant Biology*** 14, 110. **DOI:** 10.1186/1471-2229-14-110

Liu, H., X. Wang, H. Zhang, Y. Yang, X. Ge and F. Song (2008) "A rice serine carboxypeptidase-like gene OsBISCPL1 is involved in regulation of defense responses against biotic and oxidative stress." ***Gene*** 420, 57-65. **DOI:** 10.1016/j.gene.2008.05.006

Liu, J.-Z. (2005) "The Tobacco Mosaic Virus 126-Kilodalton Protein, a Constituent of the Virus Replication Complex, Alone or within the Complex Aligns with and Traffics along Microfilaments." ***PLANT PHYSIOLOGY*** 138, 1853-1865. **DOI:** 10.1104/pp.105.065722

Liu, Q., L. Shi and Y. Fang (2012) "Dicing Bodies." ***PLANT PHYSIOLOGY*** 158, 61-66. **DOI:** 10.1104/pp.111.186734

Liu, Y., M. Schiff and S. P. Dinesh-Kumar (2004) "Involvement of MEK1 MAPKK, NTF6 MAPK, WRKY/MYB transcription factors, COI1 and CTR1 in N -mediated resistance to tobacco mosaic virus." ***The Plant Journal*** 38, 800-809. **DOI:** 10.1111/j.1365-313X.2004.02085.x

Lobbes, D., G. Rallapalli, D. D. Schmidt, C. Martin and J. Clarke (2006) "SERRATE: a new player on the plant microRNA scene." ***EMBO reports*** 7, 1052-1058. **DOI:** 10.1038/sj.embor.7400806

Loebenstein, G. (2009) "Local Lesions and Induced Resistance." ***Advances in virus research*** 75, 73-117. **DOI:** 10.1016/S0065-3527(09)07503-4

Lopez-Bueno, A., J. Tamames, D. Velazquez, A. Moya, A. Quesada and A. Alcami (2009) "High Diversity of the Viral Community from an Antarctic Lake." ***Science*** 326, 858-861. **DOI:** 10.1126/science.1179287

López-Moya, J. J. and J. A. García (2000) "Construction of a stable and highly infectious intron-containing cDNA clone of plum pox potyvirus and its use to infect plants by particle bombardment." ***Virus Research*** 68, 99-107. **DOI:** 10.1016/S0168-1702(00)00161-1

Lorenzo, O., J. M. Chico, J. J. Sánchez-Serrano and R. Solano (2004) "JASMONATE-INSENSITIVE1 encodes a MYC transcription factor essential to discriminate between different jasmonate-regulated defense responses in Arabidopsis." ***The Plant cell*** 16, 1938-1950. **DOI:** 10.1105/tpc.022319

Lorković, Z. J., R. G. Herrmann and R. Oelmüller (1997) "PRH75, a new nucleus-localized member of the DEAD-box protein family from higher plants." ***Molecular and cellular biology*** 17, 2257-2265. **DOI:**

Lorkovic, Z. J., H. N. Higgs and K. J. Peterson (2004) "Use of Fluorescent Protein Tags to Study Nuclear Organization of the Spliceosomal Machinery in Transiently Transformed Living Plant Cells." ***Molecular Biology of the Cell*** 15, 3233-3243. **DOI:** 10.1091/mbc.E04-01-0055

Lu, M., Q. Zhang, M. Deng, J. Miao, Y. Guo, W. Gao and Q. Cui (2008) "An Analysis of Human MicroRNA and Disease Associations." ***PLoS ONE*** 3, e3420. **DOI:** 10.1371/journal.pone.0003420

Lukhovitskaya, N. I., A. D. Solovieva, S. K. Boddeti, S. Thaduri, A. G. Solovyev and E. I. Savenkov (2013) "An RNA Virus-Encoded Zinc-Finger Protein Acts as a Plant Transcription Factor and Induces a Regulator of Cell Size and Proliferation in Two Tobacco Species." ***The Plant Cell*** 25, 960-973. **DOI:** 10.1105/tpc.112.106476

MacDiarmid, R. (2005) "RNA silencing in productive virus infections." ***Annual review of phytopathology*** 43, 523-544. **DOI:** 10.1146/annurev.phyto.43.040204.140204

Maia, I. G. and F. Bernardi (1996) "Nucleic acid-binding properties of a bacterially expressed potato virus Y helper component-proteinase." ***Journal of General Virology*** 77, 869-877. **DOI:** 10.1099/0022-1317-77-5-869

Maldonado, A. M., P. Doerner, R. A. Dixon, C. J. Lamb and R. K. Cameron (2002) "A putative lipid transfer protein involved in systemic resistance signalling in Arabidopsis." ***Nature*** 419, 399-403. **DOI:** 10.1038/nature00962

Maldonado-Bonilla, L. D. "Composition and function of P bodies in Arabidopsis thaliana." ***Front Plant Sci*** 5, 201. **DOI:** 10.3389/fpls.2014.00201

Maliogka, V. I., M. Calvo, A. Carbonell, J. A. Garcia and A. Valli (2012) "Heterologous RNA-silencing suppressors from both plant- and animal-infecting viruses support plum pox virus infection." ***Journal of General Virology*** 93, 1601-1611. **DOI:** 10.1099/vir.0.042168-0

Mandadi, K. K. and K.-B. G. Scholthof (2013) "Plant Immune Responses Against Viruses: How Does a Virus Cause Disease?" ***The Plant Cell*** 25, 1489-1505. **DOI:** 10.1105/tpc.113.111658

Manley, R., M. Boots and L. Wilfert (2015) "REVIEW: Emerging viral disease risk to pollinating insects: ecological, evolutionary and anthropogenic factors." ***Journal of Applied Ecology*** 52, 331-340. **DOI:** 10.1111/1365-2664.12385

Manoussopoulos, I. N., M. Tsagris and E. Maiss (2000) "Native electrophoresis and Western blot analysis (NEWeB): a method for characterization of different forms of potyvirus particles and similar nucleoprotein complexes in extracts of infected plant tissues." ***Journal of General Virology*** 81, 2295-2298. **DOI:** 10.1099/0022-1317-81-9-2295

Marston, H. D., G. K. Folkers, D. M. Morens and A. S. Fauci (2014) "Emerging Viral Diseases: Confronting Threats with New Technologies." ***Science Translational Medicine*** 6, 253ps10-253ps10. **DOI:** 10.1126/scitranslmed.3009872

Martin, G. B., A. J. Bogdanove and G. Sessa (2003) "Understanding the Functions of Plant Disease Resistance Proteins." ***Annual Review of Plant Biology*** 54, 23-61. **DOI:** 10.1146/annurev.arplant.54.031902.135035

Martin, M. T., M. T. Cervera and J. A. Garcia (1995) "Properties of the active plum pox potyvirus RNA polymerase complex in defined glycerol gradient fractions." ***Virus Research*** 37, 127-137. **DOI:** 10.1016/0168-1702(95)00028-O

Martin, M. T. and B. Gélie (1997) "Non-structural plum pox potyvirus proteins detected by immunogold labelling." ***European Journal of Plant Pathology*** 103, 427-431. **DOI:** 10.1023/A:1008653000005

Martínez de Alba, A. E., E. Elvira-Matelot and H. Vaucheret (2013) "Gene silencing in plants: A diversity of pathways." ***Biochimica et Biophysica Acta (BBA) - Gene Regulatory Mechanisms*** 1829, 1300-1308. **DOI:** 10.1016/j.bbagrm.2013.10.005

Martinez de Alba, A. E., A. B. Moreno, M. Gabriel, A. C. Mallory, A. Christ, et al. (2015) "In plants, decapping prevents RDR6-dependent production of small interfering RNAs from endogenous mRNAs." ***Nucleic Acids Research*** 43, 2902-2913. **DOI:** 10.1093/nar/gkv119

Martínez, F. and J.-A. Daròs (2014) "Tobacco etch virus P1 protein traffics to the nucleolus and associates with the host 60S ribosomal subunits during infection." ***Journal of virology*** 88, 1-15. **DOI:** 10.1128/JVI.00928-14

Martínez-García, B., C. F. Marco, E. Goytia, D. López-abella, M. T. Serra, M. A. Aranda and J. J. López-moya (2004) "Development and use of detection methods specific for Cucumber vein yellowing virus (CVYV)." ***European Journal of Plant Pathology*** 110, 811-821. **DOI:** 10.1007/s10658-004-2491-7

Martínez-Turiño, S. and C. Hernández (2012). "Analysis of the subcellular targeting of the smaller replicase protein of Pelargonium flower break virus." **Virus Research** 163: 580-591.

Mas, A., I. Alves-Rodrigues, A. Noueiry, P. Ahlquist and J. Diez (2006) "Host Deadenylation-Dependent mRNA Decapping Factors Are Required for a Key Step in Brome Mosaic Virus RNA Replication." ***Journal of Virology*** 80, 246-251. **DOI:** 10.1128/JVI.80.1.246-251.2006

Matsuda, D., S. Yoshinari and T. W. Dreher (2004) "eEF1A binding to aminoacylated viral RNA represses minus strand synthesis by TYMV RNA-dependent RNA polymerase." ***Virology*** 321, 47-56. **DOI:** 10.1016/j.virol.2003.10.028

Matthes, A., S. Schmidt-Gattung, D. Kohler, J. Forner, S. Wildum, M. Raabe, H. Urlaub and S. Binder (2007) "Two DEAD-Box Proteins May Be Part of RNA-Dependent High-Molecular-Mass Protein Complexes in Arabidopsis Mitochondria." ***PLANT PHYSIOLOGY*** 145, 1637-1646. **DOI:** 10.1104/pp.107.108076

Matzke, M., W. Aufsatz, T. Kanno, L. Daxinger, I. Papp, M. F. Mette and A. J. M. Matzke (2004) "Genetic analysis of RNA-mediated transcriptional gene silencing." ***Biochimica et Biophysica Acta (BBA) - Gene Structure and Expression*** 1677, 129-141. **DOI:** 10.1016/j.bbaexp.2003.10.015

Matzke, M. A. and J. A. Birchler (2005) "RNAi-mediated pathways in the nucleus." ***Nature Reviews Genetics*** 6, 24-35. **DOI:** 10.1038/nrg1500

Mauch-Mani, B. and F. Mauch (2005) "The role of abscisic acid in plant–pathogen interactions." ***Current Opinion in Plant Biology*** 8, 409-414. **DOI:** 10.1016/j.pbi.2005.05.015

Mayhew, T. M. (2011) "Quantifying immunogold localization on electron microscopic thin sections: a compendium of new approaches for plant cell biologists." ***Journal of Experimental Botany*** 62, 4101-4113. **DOI:** 10.1093/jxb/err176

Mayhew, T. M., J. M. Lucocq and G. Griffiths (2002) "Relative labelling index: a novel stereological approach to test for non-random immunogold labelling of organelles and membranes on transmission electron microscopy thin sections." ***Journal of Microscopy*** 205, 153-164. **DOI:** 10.1046/j.0022-2720.2001.00977.x

McCartney, A. W., J. S. Greenwood, M. R. Fabian, K. A. White and R. T. Mullen (2005) "Localization of the tomato bushy stunt virus replication protein

p33 reveals a peroxisome-to-endoplasmic reticulum sorting pathway." ***The Plant cell*** 17, 3513-3531. **DOI:** 10.1105/tpc.105.036350

McKenzie, C. L., R. G. Shatters, H. Doostdar, S. D. Lee, M. Inbar and R. T. Mayer (2002) "Effect of geminivirus infection andBemisia infestation on accumulation of pathogenesis-related proteins in tomato." ***Archives of Insect Biochemistry and Physiology*** 49, 203-214. **DOI:** 10.1002/arch.10020

Meins, F., A. Si-Ammour and T. Blevins (2005) "RNA Silencing systems and their relevance to Plant development." ***Annual Review of Cell and Developmental Biology*** 21, 297-318. **DOI:** 10.1146/annurev.cellbio.21.122303.114706

Merai, Z., Z. Kerenyi, S. Kertesz, M. Magna, L. Lakatos and D. Silhavy (2006) "Double-Stranded RNA Binding May Be a General Plant RNA Viral Strategy To Suppress RNA Silencing." ***Journal of Virology*** 80, 5747-5756. **DOI:** 10.1128/JVI.01963-05

Merits, A., M. L. Rajamäki, P. Lindholm, P. Runeberg-Roos, T. Kekarainen, P. Puustinen, K. Mäkeläinen, J. P. T. Valkonen and M. Saarma (2002) "Proteolytic processing of potyviral proteins and polyprotein processing intermediates in insect and plant cells." ***Journal of General Virology*** 83, 1211-1221. **DOI:** 10.1099/0022-1317-83-5-1211

Merkle, T. (2003) "Nucleo-cytoplasmic partitioning of proteins in plants: implications for the regulation of environmental and developmental signalling." ***Current Genetics*** 44, 231-260. **DOI:** 10.1007/s00294-003-0444-x

Meselson, M. and R. Yuan (1968) "DNA restriction enzyme from E. coli." ***Nature*** 217, 1110-1114. **DOI:** 10.1038/2171110a0

Michalik, K. M., R. Bottcher and K. Forstemann (2012) "A small RNA response at DNA ends in Drosophila." ***Nucleic Acids Research*** 40, 9596-9603. **DOI:** 10.1093/nar/gks711

Michon, T., Y. Estevez, J. Walter, S. German-Retana and O. Gall (2006) "The potyviral virus genome-linked protein VPg forms a ternary complex with the eukaryotic initiation factors eIF4E and eIF4G and reduces eIF4E affinity for a mRNA cap analogue." ***FEBS Journal*** 273, 1312-1322. **DOI:** 10.1111/j.1742-4658.2006.05156.x

Miernyk, J. a. and J. J. Thelen (2008) "Biochemical approaches for discovering protein-protein interactions." ***The Plant Journal*** 53, 597-609. **DOI:** 10.1111/j.1365-313X.2007.03316.x

Miki, T., J. Ae Park, K. Nagao, N. Murayama and T. Horiuchi (1992) "Control of segregation of chromosomal DNA by sex factor F in Escherichia coli." ***Journal of Molecular Biology*** 225, 39-52. **DOI:** 10.1016/0022-2836(92)91024-J

Miller, S. and J. Krijnse-Locker (2008) "Modification of intracellular membrane structures for virus replication." ***Nature Reviews Microbiology*** 6, 363-374. **DOI:** 10.1038/nrmicro1890

Mlotshwa, S. (2005) "Ectopic DICER-LIKE1 Expression in P1/HC-Pro Arabidopsis Rescues Phenotypic Anomalies but Not Defects in MicroRNA and Silencing Pathways." ***THE PLANT CELL ONLINE*** 17, 2873-2885. **DOI:** 10.1105/tpc.105.036608

Mlotshwa, S., G. J. Pruss and V. Vance (2008) "Small RNAs in viral infection and host defense." ***Trends in Plant Science*** 13, 375-382. **DOI:** 10.1016/j.tplants.2008.04.009

Mochizuki, T., K. Hirai, A. Kanda, J. Ohnishi, T. Ohki and S. Tsuda (2009). "Induction of necrosis via mitochondrial targeting of Melon necrotic spot virus replication protein p29 by its second transmembrane domain." **Virology** 390: 239-249.

Moissiard, G., E. A. Parizotto, C. Himber and O. Voinnet (2007) "Transitivity in Arabidopsis can be primed, requires the redundant action of the antiviral Dicer-like 4 and Dicer-like 2, and is compromised by viral-encoded suppressor proteins." ***RNA*** 13, 1268-1278. **DOI:** 10.1261/rna.541307

Moissiard, G. and O. Voinnet (2006) "RETRACTED: RNA silencing of host transcripts by cauliflower mosaic virus requires coordinated action of the four Arabidopsis Dicer-like proteins." ***Proceedings of the National Academy of Sciences*** 103, 19593-19598. **DOI:** 10.1073/pnas.0604627103

Molina, A. and F. Garcia-Olmedo (1993) "Developmental and pathogen-induced expression of three barley genes encoding lipid transfer proteins." ***The Plant Journal*** 4, 983-991. **DOI:** 10.1046/j.1365-313X.1993.04060983.x

Moran, P. J. and G. A. Thompson (2001) "Molecular Responses to Aphid Feeding in Arabidopsis in Relation to Plant Defense Pathways." ***PLANT PHYSIOLOGY*** 125, 1074-1085. **DOI:** 10.1104/pp.125.2.1074

Morel, J. B., C. Godon, P. Mourrain, C. Beclin, S. Boutet, F. Feuerbach, F. Proux and H. Vaucheret (2002) "Fertile hypomorphic ARGONAUTE (ago1) mutants impaired in post-transcriptional gene silencing and virus resistance." ***Plant Cell*** 14, 629-39. **DOI:** 10.1105/tpc.010358

Morell, M., A. Espargaro, F. X. Aviles and S. Ventura (2008) "Study and selection of in vivo protein interactions by coupling bimolecular fluorescence complementation and flow cytometry." ***Nature Protocols*** 3, 22-33. **DOI:** 10.1038/nprot.2007.496

Moreno, A. B., A. E. Martinez de Alba, F. Bardou, M. D. Crespi, H. Vaucheret, A. Maizel and A. C. Mallory (2013) "Cytoplasmic and nuclear quality control and turnover of single-stranded RNA modulate post-transcriptional gene silencing in plants." ***Nucleic Acids Research*** 41, 4699-4708. **DOI:** 10.1093/nar/gkt152

Morris, J., E. Steel, P. Smith, N. Boonham, N. Spence and I. Barker (2006) "Host Range Studies for Tomato chlorosis virus, and Cucumber vein yellowing virus Transmitted by Bemisia tabaci (Gennadius)." ***European Journal of Plant Pathology*** 114, 265-273. **DOI:** 10.1007/s10658-005-5767-7

Mourrain, P., C. Béclin, T. Elmayan, F. Feuerbach, C. Godon, et al. (2000) "Arabidopsis SGS2 and SGS3 Genes Are Required for Posttranscriptional Gene Silencing and Natural Virus Resistance." ***Cell*** 101, 533-542. **DOI:** 10.1016/S0092-8674(00)80863-6

Mukhtar, M. S., M. T. Nishimura and J. Dangl (2009) "NPR1 in Plant Defense: It's Not over 'til It's Turned over." ***Cell*** 137, 804-806. **DOI:** 10.1016/j.cell.2009.05.010

Mundry, K. W., P. a. C. Watkins, T. Ashfield, K. a. Plaskitt, S. Eisele-Walter and T. M. a. Wilson (1991) "Complete uncoating of the 5' leader sequence of tobacco mosaic virus RNA occurs rapidly and is required to initiate

cotranslational virus disassembly in vitro." ***Journal of General Virology*** 72, 769-777. **DOI:** 10.1099/0022-1317-72-4-769

Murphy, J. F., R. E. Rhoads, A. G. Hunt and J. G. Shaw (1990). "The VPg of tobacco etch virus RNA is the 49-kDa proteinase or the N-terminal 24-kDa part of the proteinase." **Virology** 178: 285-288.

Murphy, J. F., W. Rychlik, R. E. Rhoads, a. G. Hunt and J. G. Shaw (1991). "A tyrosine residue in the small nuclear inclusion protein of tobacco vein mottling virus links the VPg to the viral RNA." **Journal of virology** 65: 511-513.

Murray, G. G. R., S. L. Kosakovsky Pond and D. J. Obbard (2013) "Suppressors of RNAi from plant viruses are subject to episodic positive selection." ***Proceedings of the Royal Society B: Biological Sciences*** 280, 20130965-20130965. **DOI:** 10.1098/rspb.2013.0965

Nakagawa, T., T. Suzuki, S. Murata, S. Nakamura, T. Hino, et al. (2007) "Improved Gateway binary vectors: high-performance vectors for creation of fusion constructs in transgenic analysis of plants." ***Bioscience, Biotechnology, and Biochemistry*** 71, 2095-2100. **DOI:** 10.1271/bbb.70216

Nakahara, K. S., C. Masuta, S. Yamada, H. Shimura, Y. Kashihara, et al. (2012) "Tobacco calmodulin-like protein provides secondary defense by binding to and directing degradation of virus RNA silencing suppressors." ***Proceedings of the National Academy of Sciences*** 109, 10113-10118. **DOI:** 10.1073/pnas.1201628109

Nakayashiki, H. (2005) "RNA silencing in fungi: Mechanisms and applications." ***FEBS Letters*** 579, 5950-5957. **DOI:** 10.1016/j.febslet.2005.08.016

Nasir, A., F.-J. Sun, K. M. Kim and G. Caetano-Anollés (2015) "Untangling the origin of viruses and their impact on cellular evolution." ***Annals of the New York Academy of Sciences*** 1341, 61-74. **DOI:** 10.1111/nyas.12735

Nayak, N. R., A. a. Putnam, B. Addepalli, J. D. Lowenson, T. Chen, et al. (2013) "An Arabidopsis ATP-Dependent, DEAD-Box RNA Helicase Loses Activity upon IsoAsp Formation but Is Restored by PROTEIN ISOASPARTYL METHYLTRANSFERASE." ***The Plant Cell*** 25, 2573-2586. **DOI:** 10.1105/tpc.113.113456

Nelson, B. K., X. Cai and A. Nebenführ (2007) "A multicolored set of in vivo organelle markers for co-localization studies in Arabidopsis and other plants." ***The Plant Journal*** 51, 1126-1136. **DOI:** 10.1111/j.1365-313X.2007.03212.x

Nicaise, V. (2003) "The Eukaryotic Translation Initiation Factor 4E Controls Lettuce Susceptibility to the Potyvirus Lettuce mosaic virus." ***PLANT PHYSIOLOGY*** 132, 1272-1282. **DOI:** 10.1104/pp.102.017855

Nicaise, V. (2014) "Crop immunity against viruses: outcomes and future challenges." ***Frontiers in Plant Science*** 5, 1-18. **DOI:** 10.3389/fpls.2014.00660

Nicaise, V., J.-L. Gallois, F. Chafiai, L. M. Allen, V. Schurdi-Levraud, et al. (2007) "Coordinated and selective recruitment of eIF4E and eIF4G factors for potyvirus infection in Arabidopsis thaliana." ***FEBS Letters*** 581, 1041-1046. **DOI:** 10.1016/j.febslet.2007.02.007

Niki, T., I. Mitsuhara, S. Seo, N. Ohtsubo and Y. Ohashi (1998) "Antagonistic Effect of Salicylic Acid and Jasmonic Acid on the Expression of

Pathogenesis-Related (PR) Protein Genes in Wounded Mature Tobacco Leaves." ***Plant and Cell Physiology*** 39, 500-507. **DOI:** 10.1093/oxfordjournals.pcp.a029397

Nishikiori, M., K. Dohi, M. Mori, T. Meshi, S. Naito and M. Ishikawa (2006) "Membrane-Bound Tomato Mosaic Virus Replication Proteins Participate in RNA Synthesis and Are Associated with Host Proteins in a Pattern Distinct from Those That Are Not Membrane Bound." ***Journal of Virology*** 80, 8459-8468. **DOI:** 10.1128/JVI.00545-06

Nishikiori, M., M. Mori, K. Dohi, H. Okamura, E. Katoh, S. Naito, T. Meshi and M. Ishikawa (2011) "A Host Small GTP-binding Protein ARL8 Plays Crucial Roles in Tobamovirus RNA Replication." ***PLoS Pathogens*** 7, e1002409. **DOI:** 10.1371/journal.ppat.1002409

Nobrega, F. L., A. R. Costa, L. D. Kluskens and J. Azeredo (2015) "Revisiting phage therapy: new applications for old resources." ***Trends in Microbiology*** 23, 185-191. **DOI:** 10.1016/j.tim.2015.01.006

Obbard, D. J., K. H. J. Gordon, A. H. Buck and F. M. Jiggins (2009) "The evolution of RNAi as a defence against viruses and transposable elements." ***Philosophical Transactions of the Royal Society B: Biological Sciences*** 364, 99-115. **DOI:** 10.1098/rstb.2008.0168

Ohnishi, S., K. Pääkkönen, S. Koshiba, N. Tochio, M. Sato, et al. (2009) "Solution structure of the GUCT domain from human RNA helicase II/Gu β reveals the RRM fold, but implausible RNA interactions." ***Proteins: Structure, Function, and Bioinformatics*** 74, 133-144. **DOI:** 10.1002/prot.22138

Okano, Y., H. Senshu, M. Hashimoto, Y. Neriya, O. Netsu, et al. (2014) "In Planta Recognition of a Double-Stranded RNA Synthesis Protein Complex by a Potexviral RNA Silencing Suppressor." ***The Plant Cell*** 26, 2168-2183. **DOI:** 10.1105/tpc.113.120535

Olspert, A., B. Y.-w. Chung, J. F. Atkins, J. P. Carr and A. E. Firth (2015) "Transcriptional slippage in the positive-sense RNA virus family Potyviridae." ***EMBO reports*** 16, 995-1004. **DOI:** 10.15252/embr.201540509

Omarov, R., K. Sparks, L. Smith, J. Zindovic and H. B. Scholthof (2006) "Biological Relevance of a Stable Biochemical Interaction between the Tombusvirus-Encoded P19 and Short Interfering RNAs." ***Journal of Virology*** 80, 3000-3008. **DOI:** 10.1128/JVI.80.6.3000-3008.2006

Panavas, T., E. Serviene, J. Brasher and P. D. Nagy (2005) "Yeast genome-wide screen reveals dissimilar sets of host genes affecting replication of RNA viruses." ***Proceedings of the National Academy of Sciences of the United States of America*** 102, 7326-7331. **DOI:** 10.1073/pnas.0502604102

Pandey, S. P. and I. E. Somssich (2009) "The Role of WRKY Transcription Factors in Plant Immunity." ***PLANT PHYSIOLOGY*** 150, 1648-1655. **DOI:** 10.1104/pp.109.138990

Parent, J. S., N. Bouteiller, T. Elmayan and H. Vaucheret (2015) "Respective contributions of Arabidopsis DCL2 and DCL4 to RNA silencing." ***Plant J*** 81, 223-32. **DOI:** 10.1111/tpj.12720

Pasin, F., C. Simón-Mateo and J. A. García (2014) "The Hypervariable Amino-Terminus of P1 Protease Modulates Potyviral Replication and Host Defense Responses." ***PLoS Pathogens*** 10, e1003985. **DOI:** 10.1371/journal.ppat.1003985

Pathak, K. B., Z. Sasvari and P. D. Nagy (2008) "The host Pex19p plays a role in peroxisomal localization of tombusvirus replication proteins." ***Virology*** 379, 294-305. **DOI:** 10.1016/j.virol.2008.06.044

Paul, D. and R. Bartenschlager (2013) "Architecture and biogenesis of plus-strand RNA virus replication factories." ***World journal of virology*** 2, 32-48. **DOI:** 10.5501/wjv.v2.i2.32

Peiro, A., A. C. Izquierdo-Garcia, J. A. Sanchez-Navarro, V. Pallas, J. M. Mulet and F. Aparicio (2014) "Patellins 3 and 6, two members of the Plant Patellin family, interact with the movement protein of A lfalfa mosaic virus and interfere with viral movement." ***Molecular Plant Pathology*** 15, n/a-n/a. **DOI:** 10.1111/mpp.12146

Peragine, A. (2004) "SGS3 and SGS2/SDE1/RDR6 are required for juvenile development and the production of trans-acting siRNAs in Arabidopsis." ***Genes & Development*** 18, 2368-2379. **DOI:** 10.1101/gad.1231804

Perez-Rodriguez, P., D. M. Riano-Pachon, L. G. G. Correa, S. a. Rensing, B. Kersten and B. Mueller-Roeber (2010) "PlnTFDB: updated content and new features of the plant transcription factor database." ***Nucleic Acids Research*** 38, D822-D827. **DOI:** 10.1093/nar/gkp805

Pieterse, C. M. J., D. Van der Does, C. Zamioudis, A. Leon-Reyes and S. C. M. Van Wees (2012) "Hormonal Modulation of Plant Immunity." ***Annual Review of Cell and Developmental Biology*** 28, 489-521. **DOI:** 10.1146/annurev-cellbio-092910-154055

Plasterk, R. H. a. (2002) "RNA Silencing: The Genome's Immune System." ***Science*** 296, 1263-1265. **DOI:** 10.1126/science.1072148

Poulsen, C., H. Vaucheret and P. Brodersen (2013) "Lessons on RNA Silencing Mechanisms in Plants from Eukaryotic Argonaute Structures." ***The Plant Cell*** 25, 22-37. **DOI:** 10.1105/tpc.112.105643

Prasanth, K. R., Y.-W. Huang, M.-R. Liou, R. Y.-L. Wang, C.-C. Hu, C.-H. Tsai, M. Meng, N.-S. Lin and Y.-H. Hsu (2011) "Glyceraldehyde 3-Phosphate Dehydrogenase Negatively Regulates the Replication of Bamboo Mosaic Virus and Its Associated Satellite RNA." ***Journal of Virology*** 85, 8829-8840. **DOI:** 10.1128/JVI.00556-11

Pugliese, A., T. Beltramo and D. Torre (2007) "Emerging and re-emerging viral infections in Europe." ***Cell biochemistry and function*** 25, 1-13. **DOI:** 10.1002/cbf.1342

Pumplin, N. and O. Voinnet (2013) "RNA silencing suppression by plant pathogens: defence, counter-defence and counter-counter-defence." ***Nature Reviews Microbiology*** 11, 745-760. **DOI:** 10.1038/nrmicro3120

Pyee, J., H. S. Yu and P. E. Kolattukudy (1994) "Identification of a Lipid Transfer Protein as the Major Protein in the Surface Wax of Broccoli (Brassica oleracea) Leaves." ***Archives of Biochemistry and Biophysics*** 311, 460-468. **DOI:** 10.1006/abbi.1994.1263

Pyott, D. E. and A. Molnar (2015) "Going mobile: Non-cell-autonomous small RNAs shape the genetic landscape of plants." ***Plant Biotechnology Journal*** 13, 306-318. **DOI:** 10.1111/pbi.12353

Qu, F., X. Ye and T. J. Morris (2008) "Arabidopsis DRB4, AGO1, AGO7, and RDR6 participate in a DCL4-initiated antiviral RNA silencing pathway negatively regulated by DCL1." ***Proceedings of the National Academy of Sciences*** 105, 14732-14737. **DOI:** 10.1073/pnas.0805760105

Qu, L.-J. and Y.-X. Zhu (2006) "Transcription factor families in Arabidopsis: major progress and outstanding issues for future research." ***Current Opinion in Plant Biology*** 9, 544-549. **DOI:** 10.1016/j.pbi.2006.07.005

Quadt, R., C. C. Kao, K. S. Browning, R. P. Hershberger and P. Ahlquist (1993) "Characterization of a host protein associated with brome mosaic virus RNA-dependent RNA polymerase." ***Proceedings of the National Academy of Sciences*** 90, 1498-1502. **DOI:** 10.1073/pnas.90.4.1498

Quan, S., P. Yang, G. Cassin-Ross, N. Kaur, R. Switzenberg, K. Aung, J. Li and J. Hu (2013) "Proteome analysis of peroxisomes from etiolated Arabidopsis seedlings identifies a peroxisomal protease involved in β-oxidation and development." ***Plant physiology*** 163, 1518-38. **DOI:** 10.1104/pp.113.223453

Raffaele, S. and S. Rivas (2013) "Regulate and be regulated: integration of defense and other signals by the AtMYB30 transcription factor." ***Frontiers in Plant Science*** 4, 98. **DOI:** 10.3389/fpls.2013.00098

Rajamäki, M.-L., J. Streng and J. P. T. Valkonen (2014) "Silencing Suppressor Protein VPg of a Potyvirus Interacts With the Plant Silencing-Related Protein SGS3." ***Molecular Plant-Microbe Interactions*** 27, 1199-1210. **DOI:** 10.1094/MPMI-04-14-0109-R

Raoult, D. and P. Forterre (2008) "Redefining viruses: lessons from Mimivirus." ***Nature Reviews Microbiology*** 6, 315-319. **DOI:** 10.1038/nrmicro1858

Ratcliff, F. (1997) "A Similarity Between Viral Defense and Gene Silencing in Plants." ***Science*** 276, 1558-1560. **DOI:** 10.1126/science.276.5318.1558

Ravelonandro, M., O. Peyruchaud, L. Garrigue, G. de Marcillac and J. Dunez (1993) "Immunodetection of the plum pox virus helper component in infected plants and expression of its gene in transgenic plants." ***Archives of Virology*** 130, 251-268. **DOI:** 10.1007/BF01309658

Ren, G., M. Xie, Y. Dou, S. Zhang, C. Zhang and B. Yu (2012) "Regulation of miRNA abundance by RNA binding protein TOUGH in Arabidopsis." ***Proceedings of the National Academy of Sciences*** 109, 12817-12821. **DOI:** 10.1073/pnas.1204915109

Ren, T., F. Qu and T. J. Morris (2000) "HRT gene function requires interaction between a NAC protein and viral capsid protein to confer resistance to turnip crinkle virus." ***The Plant cell*** 12, 1917-1926. **DOI:** 10.1105/tpc.12.10.1917

Restrepo-Hartwig, M. a. and P. Ahlquist (1996). "Brome mosaic virus helicase- and polymerase-like proteins colocalize on the endoplasmic reticulum at sites of viral RNA synthesis." **Journal of virology** 70: 8908-8916.

Restrepo-Hartwig, M. a. and J. C. Carrington (1994). "The tobacco etch potyvirus 6-kilodalton protein is membrane associated and involved in viral replication." **Journal of virology** 68: 2388-2397.

Revers, F. and J. A. García (2015) "Chapter Three - Molecular Biology of Potyviruses." ***Advances in Virus Research*** Volume 92, 101-199. **DOI:** 10.1016/bs.aivir.2014.11.006

Rhoades, M. W., B. J. Reinhart, L. P. Lim, C. B. Burge, B. Bartel and D. P. Bartel (2002) "Prediction of Plant MicroRNA Targets." ***Cell*** 110, 513-520. **DOI:** 10.1016/S0092-8674(02)00863-2

Rhoads, R. E. (2009) "eIF4E: new family members, new binding partners, new roles." ***J Biol Chem*** 284, 16711-5. **DOI:** 10.1074/jbc.R900002200

Riechmann, J. L., J. Heard, G. Martin, L. Reuber, C. -Z., et al. (2000) "Arabidopsis Transcription Factors: Genome-Wide Comparative Analysis Among Eukaryotes." ***Science*** 290, 2105-2110. **DOI:** 10.1126/science.290.5499.2105

Riechmann, J. L., S. Lain and J. A. Garcia (1989) "The Genome-linked Protein and 5' End RNA Sequence of Plum Pox Potyvirus." ***Journal of General Virology*** 70, 2785-2789. **DOI:** 10.1099/0022-1317-70-10-2785

Riechmann, J. L., S. Lain and J. A. Garcia (1992) "Highlights and prospects of potyvirus molecular biology." ***Journal of General Virology*** 73, 1-16. **DOI:** 10.1099/0022-1317-73-1-1

Riedel, D., D. E. Lesemann and E. Maiß (1998) "Ultrastructural localization of nonstructural and coat proteins of 19 potyviruses using antisera to bacterially expressed proteins of plum pox potyvirus." ***Archives of Virology*** 143, 2133-2158. **DOI:** 10.1007/s007050050448

Rigaut, G., A. Shevchenko, B. Rutz, M. Wilm, M. Mann and B. Séraphin (1999) "A generic protein purification method for protein complex characterization and proteome exploration." ***Nature biotechnology*** 17, 1030-1032. **DOI:** 10.1038/13732

Ritzenthaler, C., C. Laporte, F. Gaire, C. Schmitt, S. Duval, a. Pie, a. M. Loudes, O. Rohfritsch and P. Pfeiffer (2002) "Grapevine Fanleaf Virus Replication Occurs on Endoplasmic Reticulum-Derived Membranes." ***Journal of Virology*** 76, 8808-8819. **DOI:** 10.1128/JVI.76.17.8808

Robaglia, C. and C. Caranta (2006) "Translation initiation factors: a weak link in plant RNA virus infection." ***Trends in Plant Science*** 11, 40-45. **DOI:** 10.1016/j.tplants.2005.11.004

Robatzek, S. and I. E. Somssich (2002) "Targets of AtWRKY6 regulation during plant senescence and pathogen defense." ***Genes & Development*** 16, 1139-1149. **DOI:** 10.1101/gad.222702

Rocha, P. S. C. F. (2005) "The Arabidopsis HOMOLOGY-DEPENDENT GENE SILENCING1 Gene Codes for an S-Adenosyl-L-Homocysteine Hydrolase Required for DNA Methylation-Dependent Gene Silencing." ***THE PLANT CELL ONLINE*** 17, 404-417. **DOI:** 10.1105/tpc.104.028332

Rohila, J. S., M. Chen, R. Cerny and M. E. Fromm (2004) "Improved tandem affinity purification tag and methods for isolation of protein heterocomplexes from plants." ***The Plant Journal*** 38, 172-181. **DOI:** 10.1111/j.1365-313X.2004.02031.x

Rojas, M. R., F. M. Zerbini, R. F. Allison, R. L. Gilbertson and W. J. Lucas (1997) "Capsid Protein and Helper Component-Proteinase Function as Potyvirus Cell-to-Cell Movement Proteins." ***Virology*** 237, 283-295. **DOI:** 10.1006/viro.1997.8777

Ross, P. L. (2004) "Multiplexed Protein Quantitation in Saccharomyces cerevisiae Using Amine-reactive Isobaric Tagging Reagents." ***Molecular & Cellular Proteomics*** 3, 1154-1169. **DOI:** 10.1074/mcp.M400129-MCP200

Roudet-Tavert, G., S. German-Retana, T. Delaunay, B. Delécolle, T. Candresse and O. Le Gall (2002). "Interaction between potyvirus helper component-proteinase and capsid protein in infected plants." **Journal of General Virology** 83: 1765-1770.

Rubino, L., B. Navarro and M. Russo (2007) "Cymbidium ringspot virus defective interfering RNA replication in yeast cells occurs on endoplasmic reticulum-

derived membranes in the absence of peroxisomes." ***Journal of General Virology*** 88, 1634-1642. **DOI:** 10.1099/vir.0.82729-0

Rubio, V., Y. Shen, Y. Saijo, Y. Liu, G. Gusmaroli, S. P. Dinesh-Kumar and X. W. Deng (2005) "An alternative tandem affinity purification strategy applied to Arabidopsis protein complex isolation." ***The Plant Journal*** 41, 767-778. **DOI:** 10.1111/j.1365-313X.2004.02328.x

Ryna, F. P. (2006) "Genomic creativity and natural selection: a modern synthesis." ***Biological Journal of the Linnean Society*** 88, 655-672. **DOI:** 10.1111/j.1095-8312.2006.00650.x

Sáenz, P., L. Quiot, J.-B. Quiot, T. Candresse and J. A. García (2001) "Pathogenicity Determinants in the Complex Virus Population of a Plum pox virus Isolate." ***Molecular Plant-Microbe Interactions*** 14, 278-287. **DOI:** 10.1094/MPMI.2001.14.3.278

Sahana, N., H. Kaur, Basavaraj, F. Tena, R. K. Jain, P. Palukaitis, T. Canto and S. Praveen (2012) "Inhibition of the Host Proteasome Facilitates Papaya Ringspot Virus Accumulation and Proteosomal Catalytic Activity Is Modulated by Viral Factor HcPro." ***PLoS ONE*** 7, e52546. **DOI:** 10.1371/journal.pone.0052546

Sahana, N., H. Kaur, R. K. Jain, P. Palukaitis, T. Canto and S. Praveen (2014) "The asparagine residue in the FRNK box of potyviral helper-component protease is critical for its small RNA binding and subcellular localization." ***Journal of General Virology*** 95, 1167-1177. **DOI:** 10.1099/vir.0.060269-0

Sambrook, J., E. F. Fritsch and T. Maniatis (1989). **Molecular Cloning: A Laboratory Manual**, Cold Spring Harbor Laboratory Press.

Sasvari, Z., L. Izotova, T. G. Kinzy and P. D. Nagy (2011) "Synergistic Roles of Eukaryotic Translation Elongation Factors 1Bγ and 1A in Stimulation of Tombusvirus Minus-Strand Synthesis." ***PLoS Pathogens*** 7, e1002438. **DOI:** 10.1371/journal.ppat.1002438

Sasvari, Z. and P. D. Nagy (2010) "Making of Viral Replication Organelles by Remodeling Interior Membranes." ***Viruses*** 2, 2436-2442. **DOI:** 10.3390/v2112436

Sato, M., K. Nakahara, M. Yoshii, M. Ishikawa and I. Uyeda (2005) "Selective involvement of members of the eukaryotic initiation factor 4E family in the infection of Arabidopsis thaliana by potyviruses." ***FEBS Letters*** 579, 1167-1171. **DOI:** 10.1016/j.febslet.2004.12.086

Saunders, K., I. D. Bedford, T. Yahara and J. Stanley (2003) "Aetiology: The earliest recorded plant virus disease." ***Nature*** 422, 831-831. **DOI:** 10.1038/422831a

Saura, M., C. Zaragoza, A. McMillan, R. a. Quick, C. Hohenadl, J. M. Lowenstein and C. J. Lowenstein (1999) "An Antiviral Mechanism of Nitric Oxide." ***Immunity*** 10, 21-28. **DOI:** 10.1016/S1074-7613(00)80003-5

Schaad, M. C., R. J. Anderberg and J. C. Carrington (2000) "Strain-Specific Interaction of the Tobacco Etch Virus NIa Protein with the Translation Initiation Factor eIF4E in the Yeast Two-Hybrid System." ***Virology*** 273, 300-306. **DOI:** 10.1006/viro.2000.0416

Schaad, M. C., P. E. Jensen and J. C. Carrington (1997) "Formation of plant RNA virus replication complexes on membranes: role of an endoplasmic reticulum-targeted viral protein." ***The EMBO Journal*** 16, 4049-4059. **DOI:** 10.1093/emboj/16.13.4049

Schenck, C. a., V. Nadella, S. L. Clay, J. Lindner, Z. Abrams and S. E. Wyatt (2013) "A proteomics approach identifies novel proteins involved in gravitropic signal transduction." ***American Journal of Botany*** 100, 194-202. **DOI:** 10.3732/ajb.1200339

Schneider, C. a., W. S. Rasband and K. W. Eliceiri (2012) "NIH Image to ImageJ: 25 years of image analysis." ***Nature Methods*** 9, 671-675. **DOI:** 10.1038/nmeth.2089

Scholthof, H. B. (2006) "The Tombusvirus-encoded P19: from irrelevance to elegance." ***Nature Reviews Microbiology*** 4, 405-411. **DOI:** 10.1038/nrmicro1395

Schrick, K., S. Fujioka, S. Takatsuto, Y.-D. Stierhof, H. Stransky, S. Yoshida and G. Jürgens (2004) "A link between sterol biosynthesis, the cell wall, and cellulose in Arabidopsis." ***The Plant Journal*** 38, 227-243. **DOI:** 10.1111/j.1365-313X.2004.02039.x

Schrick, K., U. Mayer, G. Martin, C. Bellini, C. Kuhnt, J. Schmidt and G. Jürgens (2002) "Interactions between sterol biosynthesis genes in embryonic development of Arabidopsis." ***The Plant Journal*** 31, 61-73. **DOI:** 10.1046/j.1365-313X.2002.01333.x

Schultz, D. E., C. C. Hardin and S. M. Lemon (1996) "Specific interaction of glyceraldehyde 3-phosphate dehydrogenase with the 5′ -nontranslated RNA of hepatitis a virus." ***Journal of Biological Chemistry*** 271, 14134-14142. **DOI:** 10.1074/jbc.271.24.14134

Schwach, F., F. E. Vaistij, L. Jones and D. C. Baulcombe (2005) "An RNA-Dependent RNA Polymerase Prevents Meristem Invasion by Potato Virus X and Is Required for the Activity But Not the Production of a Systemic Silencing Signal." ***PLANT PHYSIOLOGY*** 138, 1842-1852. **DOI:** 10.1104/pp.105.063537

Schwartz, M., J. Chen, M. Janda, M. Sullivan, J. den Boon and P. Ahlquist (2002) "A Positive-Strand RNA Virus Replication Complex Parallels Form and Function of Retrovirus Capsids." ***Molecular Cell*** 9, 505-514. **DOI:** 10.1016/S1097-2765(02)00474-4

Seo, E., D. Choi and Choi (2015) "Functional studies of transcription factors involved in plant defenses in the genomics era." ***Briefings in Functional Genomics***, 1-8. **DOI:** 10.1093/bfgp/elv011

Shabalina, S. and E. Koonin (2008) "Origins and evolution of eukaryotic RNA interference." ***Trends in Ecology & Evolution*** 23, 578-587. **DOI:** 10.1016/j.tree.2008.06.005

Sharma, M., Z. Sasvari and P. D. Nagy (2010) "Inhibition of Sterol Biosynthesis Reduces Tombusvirus Replication in Yeast and Plants." ***Journal of Virology*** 84, 2270-2281. **DOI:** 10.1128/JVI.02003-09

Sharma, M., Z. Sasvari and P. D. Nagy (2011) "Inhibition of phospholipid biosynthesis decreases the activity of the tombusvirus replicase and alters the subcellular localization of replication proteins." ***Virology*** 415, 141-152. **DOI:** 10.1016/j.virol.2011.04.008

Shaw, J. G. (1999) "Tobacco mosaic virus and the study of early events in virus infections." ***Philosophical Transactions of the Royal Society B: Biological Sciences*** 354, 603-611. **DOI:** 10.1098/rstb.1999.0412

Shaw, J. G., K. A. Plaskitt and T. M. A. Wilson (1986) "Evidence that tobacco mosaic virus particles disassemble contranslationally in vivo." ***Virology*** 148, 326-336. **DOI:** 10.1016/0042-6822(86)90329-6

Sheth, U. and R. Parker (2003) "Decapping and decay of messenger RNA occur in cytoplasmic processing bodies." ***Science*** 300, 805-8. **DOI:** 10.1126/science.1082320

Shukla, D. D. and C. W. Ward (1989) "Structure of Potyvirus Coat Proteins and its Application in the Taxonomy of the Potyvirus Group." ***Advances in virus research*** 36, 273-314. **DOI:** 10.1016/S0065-3527(08)60588-6

Siaw, M. F. E., M. Shahabuddin, S. Ballard, J. G. Shaw and R. E. Rhoads (1985) "Identification of a protein covalently linked to the 5′ terminus of tobacco vein mottling virus RNA." ***Virology*** 142, 134-143. **DOI:** 10.1016/0042-6822(85)90428-3

Sijen, T. and R. H. A. Plasterk (2003) "Transposon silencing in the Caenorhabditis elegans germ line by natural RNAi." ***Nature*** 426, 310-314. **DOI:** 10.1038/nature02107

Silhavy, D., A. Molnár, A. Lucioli, G. Szittya, C. Hornyik, M. Tavazza and J. Burgyán (2002) "A viral protein suppresses RNA silencing and binds silencing-generated, 21- to 25-nucleotide double-stranded RNAs." ***EMBO Journal*** 21, 3070-3080. **DOI:** 10.1093/emboj/cdf312

Simon-Buela, L., H. S. Guo and J. A. Garcia (1997) "Cap-independent leaky scanning as the mechanism of translation initiation of a plant viral genomic RNA." ***Journal of General Virology*** 78, 2691-2699. **DOI:** 10.1099/0022-1317-78-10-2691

Simón-Mateo, C. and J. A. García (2006) "MicroRNA-Guided Processing Impairs Plum Pox Virus Replication, but the Virus Readily Evolves To Escape This Silencing Mechanism." ***Journal of Virology*** 80, 2429-2436. **DOI:** 10.1128/JVI.80.5.2429-2436.2006

Sirover, M. a. (2011) "On the functional diversity of glyceraldehyde-3-phosphate dehydrogenase: biochemical mechanisms and regulatory control." ***Biochimica et biophysica acta*** 1810, 741-751. **DOI:** 10.1016/j.bbagen.2011.05.010

Soitamo, A. J., B. Jada and K. Lehto (2011) "HC-Pro silencing suppressor significantly alters the gene expression profile in tobacco leaves and flowers." ***BMC plant biology*** 11, 68. **DOI:** 10.1186/1471-2229-11-68

Sokal, R. R. and F. J. Rohlf (2012). **Biometry. The principles and Practice of Statistics in Biological Research**. New York, W.H. Freeman and Company.

Solovyev, A. G. and E. I. Savenkov (2014) "Factors involved in the systemic transport of plant RNA viruses: the emerging role of the nucleus." ***Journal of Experimental Botany*** 65, 1689-1697. **DOI:** 10.1093/jxb/ert449

Soosaar, J. L. M., T. M. Burch-Smith and S. P. Dinesh-Kumar (2005) "Mechanisms of plant resistance to viruses." ***Nature Reviews Microbiology*** 3, 789-798. **DOI:** 10.1038/nrmicro1239

Sorel, M., L. Svanella-Dumas, T. Candresse, G. Acelin, A. Pitarch, M. C. Houvenaghel and S. German-Retana (2014) "Key Mutations in the Cylindrical Inclusion Involved in Lettuce mosaic virus Adaptation to eIF4E-Mediated Resistance in Lettuce." ***Molecular Plant-Microbe Interactions*** 27, 1014-1024. **DOI:** 10.1094/MPMI-04-14-0111-R

Souter, M., M. Pullen, J. Topping, X. Zhang and K. Lindsey (2004) "Rescue of defective auxin-mediated gene expression and root meristem function by inhibition of ethylene signalling in sterol biosynthesis mutants of Arabidopsis." ***Planta*** 219, 773-783. **DOI:** 10.1007/s00425-004-1280-z

Souter, M., J. Topping, M. Pullen, J. Friml, K. Palme, R. Hackett, D. Grierson and K. Lindsey (2002) "hydra Mutants of Arabidopsis Are Defective in Sterol Profiles and Auxin and Ethylene Signaling." ***THE PLANT CELL ONLINE*** 14, 1017-1031. **DOI:** 10.1105/tpc.001248

Szittya, G., D. Silhavy, A. Molnár, Z. Havelda, Á. Lovas, L. Lakatos, Z. Bánfalvi and J. Burgyán (2003) "Low temperature inhibits RNA silencing-mediated defence by the control of siRNA generation." ***The EMBO Journal*** 22, 633-640. **DOI:** 10.1093/emboj/cdg74

Takeda, A., S. Iwasaki, T. Watanabe, M. Utsumi and Y. Watanabe (2008) "The Mechanism Selecting the Guide Strand from Small RNA Duplexes is Different Among Argonaute Proteins." ***Plant and Cell Physiology*** 49, 493-500. **DOI:** 10.1093/pcp/pcn043

Tanaka, Y., S. Nakamura, M. Kawamukai, N. Koizumi and T. Nakagawa (2011) "Development of a Series of Gateway Binary Vectors Possessing a Tunicamycin Resistance Gene as a Marker for the Transformation of Arabidopsis thaliana." ***Bioscience, Biotechnology and Biochemistry*** 75, 804-807. **DOI:** 10.1271/bbb.110063

Tavert-Roudet, G., A. Abdul-Razzak, B. Doublet, J. Walter, T. Delaunay, S. German-Retana, T. Michon, O. Le Gall and T. Candresse (2012) "The C terminus of lettuce mosaic potyvirus cylindrical inclusion helicase interacts with the viral VPg and with lettuce translation eukaryotic initiation factor 4E." ***Journal of General Virology*** 93, 184-193. **DOI:** 10.1099/vir.0.035881-0

Thivierge, K., S. Cotton, P. J. Dufresne, I. Mathieu, C. Beauchemin, C. Ide, M. G. Fortin and J.-F. Laliberté (2008) "Eukaryotic elongation factor 1A interacts with Turnip mosaic virus RNA-dependent RNA polymerase and VPg-Pro in virus-induced vesicles." ***Virology*** 377, 216-225. **DOI:** 10.1016/j.virol.2008.04.015

Tijsterman, M., R. F. Ketting and R. H. a. Plasterk (2002) "The Genetics of RNA Silencing." ***Annual Review of Genetics*** 36, 489-519. **DOI:** 10.1146/annurev.genet.36.043002.091619

Torrance, L., I. a. Andreev, R. Gabrenaite-Verhovskaya, G. Cowan, K. Mäkinen and M. E. Taliansky (2006) "An Unusual Structure at One End of Potato Potyvirus Particles." ***Journal of Molecular Biology*** 357, 1-8. **DOI:** 10.1016/j.jmb.2005.12.021

Torres, M. A. (2006) "Reactive Oxygen Species Signaling in Response to Pathogens." ***PLANT PHYSIOLOGY*** 141, 373-378. **DOI:** 10.1104/pp.106.079467

Tristan, C., N. Shahani, T. W. Sedlak and A. Sawa (2011) "The diverse functions of GAPDH: Views from different subcellular compartments." ***Cellular Signalling*** 23, 317-323. **DOI:** 10.1016/j.cellsig.2010.08.003

Tsuboi, S., T. Osafune, R. Tsugeki, M. Nishimura and M. Yamada (1992). "Nonspecific lipid transfer protein in castor bean cotyledon cells: subcellular localization and a possible role in lipid metabolism." **Journal of biochemistry** 111: 500-508.

Udvardi, M. K., K. Kakar, M. Wandrey, O. Montanari, J. Murray, et al. (2007) "Legume Transcription Factors: Global Regulators of Plant Development and Response to the Environment." ***PLANT PHYSIOLOGY*** 144, 538-549. **DOI:** 10.1104/pp.107.098061

Uetz, P., L. Giot, G. Cagney, T. a. Mansfield, R. S. Judson, et al. (2000) "A comprehensive analysis of protein-protein interactions in Saccharomyces cerevisiae." ***Nature*** 403, 623-627. **DOI:** 10.1038/35001009

Urcuqui-Inchima, S., A.-L. Haenni and F. Bernardi (2001) "Potyvirus proteins: a wealth of functions." ***Virus Research*** 74, 157-175. **DOI:** 10.1016/S0168-1702(01)00220-9

Valli, A., G. Dujovny and J. A. Garcia (2008) "Protease Activity, Self Interaction, and Small Interfering RNA Binding of the Silencing Suppressor P1b from Cucumber Vein Yellowing Ipomovirus." ***Journal of Virology*** 82, 974-986. **DOI:** 10.1128/JVI.01664-07

Valli, A., A. Gallo, M. Calvo, J. D. J. Perez and J. A. Garcia (2014) "A Novel Role of the Potyviral Helper Component Proteinase Contributes To Enhance the Yield of Viral Particles." ***Journal of Virology*** 88, 9808-9818. **DOI:** 10.1128/JVI.01010-14

Valli, A., J. J. Lopez-Moya and J. A. Garcia (2007) "Recombination and gene duplication in the evolutionary diversification of P1 proteins in the family Potyviridae." ***Journal of General Virology*** 88, 1016-1028. **DOI:** 10.1099/vir.0.82402-0

Valli, A., J. J. López-Moya and J. A. García (2009). RNA Silencing and its Suppressors in the Plant-virus Interplay. **Encyclopedia of Life Sciences**. Chichester, UK, John Wiley & Sons, Ltd**:** 1-29.

Valli, A., A. M. Martin-Hernandez, J. J. Lopez-Moya and J. A. Garcia (2006) "RNA Silencing Suppression by a Second Copy of the P1 Serine Protease of Cucumber Vein Yellowing Ipomovirus, a Member of the Family Potyviridae That Lacks the Cysteine Protease HCPro." ***Journal of Virology*** 80, 10055-10063. **DOI:** 10.1128/JVI.00985-06

Valli, A., J. C. Oliveros, A. Molnar, D. Baulcombe and J. A. Garcia (2011) "The specific binding to 21-nt double-stranded RNAs is crucial for the anti-silencing activity of Cucumber vein yellowing virus P1b and perturbs endogenous small RNA populations." ***RNA*** 17, 1148-1158. **DOI:** 10.1261/rna.2510611

Van Der Heijden, M. W., J. E. Carette, P. J. Reinhoud, A. Haegi and J. F. Bol (2001) "Alfalfa mosaic virus replicase proteins P1 and P2 interact and colocalize at the vacuolar membrane." ***J Virol*** 75, 1879-87. **DOI:** 10.1128/JVI.75.4.1879-1887.2001

Van Leene, J., H. Stals, D. Eeckhout, G. Persiau, E. Van De Slijke, et al. (2007) "A tandem affinity purification-based technology platform to study the cell cycle interactome in Arabidopsis thaliana." ***Molecular & cellular proteomics : MCP*** 6, 1226-1238. **DOI:** 10.1074/mcp.M700078-MCP200

Van Leene, J., E. Witters, D. Inzé and G. De Jaeger (2008) "Boosting tandem affinity purification of plant protein complexes." ***Trends in Plant Science*** 13, 517-520. **DOI:** 10.1016/j.tplants.2008.08.002

van Loon, L. C., M. Rep and C. M. J. Pieterse (2006) "Significance of Inducible Defense-related Proteins in Infected Plants." ***Annual Review of***

Phytopathology 44, 135-162. **DOI:** 10.1146/annurev.phyto.44.070505.143425

Vance, V. (2001) "RNA Silencing in Plants--Defense and Counterdefense." ***Science*** 292, 2277-2280. **DOI:** 10.1126/science.1061334

Vargason, J. M., G. Szittya, J. Burgyán and T. M. T. Hall (2003) "Size Selective Recognition of siRNA by an RNA Silencing Suppressor." ***Cell*** 115, 799-811. **DOI:** 10.1016/S0092-8674(03)00984-X

Vaucheret, H. (2006) "Post-transcriptional small RNA pathways in plants: mechanisms and regulations." ***Genes & Development*** 20, 759-771. **DOI:** 10.1101/gad.1410506

Vaucheret, H. (2008) "Plant ARGONAUTES." ***Trends in Plant Science*** 13, 350-358. **DOI:** 10.1016/j.tplants.2008.04.007

Vazquez, F. (2004) "The Nuclear dsRNA Binding Protein HYL1 Is Required for MicroRNA Accumulation and Plant Development, but Not Posttranscriptional Transgene Silencing." ***Current Biology*** 14, 346-351. **DOI:** 10.1016/S0960-9822(04)00047-8

Verchot, J. and J. C. Carrington (1995). "Evidence that the potyvirus P1 proteinase functions in trans as an accessory factor for genome amplification." **Journal of virology** 69: 3668-3674.

Vijayapalani, P., M. Maeshima, N. Nagasaki-Takekuchi and W. A. Miller (2012) "Interaction of the Trans-Frame Potyvirus Protein P3N-PIPO with Host Protein PCaP1 Facilitates Potyvirus Movement." ***PLoS Pathogens*** 8, e1002639. **DOI:** 10.1371/journal.ppat.1002639

Voinnet, O. (2001) "RNA silencing as a plant immune system against viruses." ***Trends in Genetics*** 17, 449-459. **DOI:** 10.1016/S0168-9525(01)02367-8

Voinnet, O. (2009) "Origin, Biogenesis, and Activity of Plant MicroRNAs." ***Cell*** 136, 669-687. **DOI:** 10.1016/j.cell.2009.01.046

Voinnet, O., C. Lederer and D. C. Baulcombe (2000) "A viral movement protein prevents spread of the gene silencing signal in Nicotiana benthamiana." ***Cell*** 103, 157-167. **DOI:** 10.1016/S0092-8674(00)00095-7

Voinnet, O., S. Rivas, P. Mestre and D. Baulcombe (2003) "An enhanced transient expression system in plants based on suppression of gene silencing by the p19 protein of tomato bushy stunt virus." ***Plant Journal*** 33, 949-956. **DOI:** 10.1046/j.1365-313X.2003.01676.x

von Mering, C., R. Krause, B. Snel, M. Cornell, S. G. Oliver, S. Fields and P. Bork (2002) "Comparative assessment of large-scale data sets of protein–protein interactions." ***Nature*** 417, 399-403. **DOI:** 10.1038/nature750

Walsh, D. and I. Mohr (2011) "Viral subversion of the host protein synthesis machinery." ***Nature Reviews Microbiology*** 9, 860-875. **DOI:** 10.1038/nrmicro2655

Wang, B., J.-U.-D. Hajano, Y. Ren, C. Lu and X. Wang (2015a) "iTRAQ-based quantitative proteomics analysis of rice leaves infected by Rice stripe virus reveals several proteins involved in symptom formation." ***Virology Journal*** 12, 99. **DOI:** 10.1186/s12985-015-0328-y

Wang, H., K. Wu, Y. Liu, Y. Wu and X. Wang (2015b) "Integrative proteomics to understand the transmission mechanism of Barley yellow dwarf virus-GPV by its insect vector Rhopalosiphum padi." ***Scientific Reports*** 5, 10971. **DOI:** 10.1038/srep10971

Wang, R. Y.-L. and P. D. Nagy (2008) "Tomato bushy stunt virus Co-Opts the RNA-Binding Function of a Host Metabolic Enzyme for Viral Genomic RNA Synthesis." ***Cell Host & Microbe*** 3, 178-187. **DOI:** 10.1016/j.chom.2008.02.005

Wang, X., A. Diaz, L. Hao, B. Gancarz, J. a. den Boon and P. Ahlquist (2011a) "Intersection of the Multivesicular Body Pathway and Lipid Homeostasis in RNA Replication by a Positive-Strand RNA Virus." ***Journal of Virology*** 85, 5494-5503. **DOI:** 10.1128/JVI.02031-10

Wang, X., S. P. Goregaoker and J. N. Culver (2009) "Interaction of the Tobacco mosaic virus replicase protein with a NAC domain transcription factor is associated with the suppression of systemic host defenses." ***Journal of virology*** 83, 9720-9730. **DOI:** 10.1128/JVI.00941-09

Wang, X., S. E. Kohalmi, A. Svircev, A. Wang, H. Sanfaçon and L. Tian (2013) "Silencing of the Host Factor eIF(iso)4E Gene Confers Plum Pox Virus Resistance in Plum." ***PLoS ONE*** 8, e50627. **DOI:** 10.1371/journal.pone.0050627

Wang, X., Z. Ullah and R. Grumet (2000) "Interaction between Zucchini Yellow Mosaic Potyvirus RNA-Dependent RNA Polymerase and Host Poly-(A) Binding Protein." ***Virology*** 275, 433-443. **DOI:** 10.1006/viro.2000.0509

Wang, X.-B., J. Jovel, P. Udomporn, Y. Wang, Q. Wu, W.-X. Li, V. Gasciolli, H. Vaucheret and S.-W. Ding (2011b) "The 21-Nucleotide, but Not 22-Nucleotide, Viral Secondary Small Interfering RNAs Direct Potent Antiviral Defense by Two Cooperative Argonautes in Arabidopsis thaliana." ***The Plant Cell*** 23, 1625-1638. **DOI:** 10.1105/tpc.110.082305

Wang, X.-B., Q. Wu, T. Ito, F. Cillo, W.-X. Li, X. Chen, J.-L. Yu and S.-W. Ding (2010) "RNAi-mediated viral immunity requires amplification of virus-derived siRNAs in Arabidopsis thaliana." ***Proceedings of the National Academy of Sciences of the United States of America*** 107, 484-489. **DOI:** 10.1073/pnas.0904086107

Waterhouse, P. M., M. W. Graham and M.-B. Wang (1998) "Virus resistance and gene silencing in plants can be induced by simultaneous expression of sense and antisense RNA." ***Proceedings of the National Academy of Sciences*** 95, 13959-13964. **DOI:** 10.1073/pnas.95.23.13959

Wei, T., T.-S. Huang, J. McNeil, J.-F. Laliberte, J. Hong, R. S. Nelson and A. Wang (2010) "Sequential Recruitment of the Endoplasmic Reticulum and Chloroplasts for Plant Potyvirus Replication." ***Journal of Virology*** 84, 799-809. **DOI:** 10.1128/JVI.01824-09

Wei, T., C. Zhang, X. Hou, H. Sanfaçon and A. Wang (2013) "The SNARE Protein Syp71 Is Essential for Turnip Mosaic Virus Infection by Mediating Fusion of Virus-Induced Vesicles with Chloroplasts." ***PLoS Pathogens*** 9, e1003378. **DOI:** 10.1371/journal.ppat.1003378

Wei, W., Z. Ba, M. Gao, Y. Wu, Y. Ma, et al. (2012) "A Role for Small RNAs in DNA Double-Strand Break Repair." ***Cell*** 149, 101-112. **DOI:** 10.1016/j.cell.2012.03.002

Weigel, D. and J. Glazebrook (2002). **Arabidopsis: A Laboratory Manual**, Cold Spring Harbor Laboratory Press.

Wellink, J. and A. van Kammen (1988) "Proteases involved in the processing of viral polyproteins." ***Archives of Virology*** 98, 1-26. **DOI:** 10.1007/BF01321002

Whitham, S. a., R. J. Anderberg, S. T. Chisholm and J. C. Carrington (2000) "Arabidopsis RTM2 Gene Is Necessary for Specific Restriction of Tobacco Etch Virus and Encodes an Unusual Small Heat Shock-Like Protein." ***The Plant Cell*** 12, 569. **DOI:** 10.2307/3871070

Willmann, M. R., M. W. Endres, R. T. Cook and B. D. Gregory (2011) "The Functions of RNA-Dependent RNA Polymerases in Arabidopsis." ***The Arabidopsis Book*** 9, e0146. **DOI:** 10.1199/tab.0146

Wilson, R. C. and J. a. Doudna (2013) "Molecular mechanisms of RNA interference." ***Annual review of biophysics*** 42, 217-39. **DOI:** 10.1146/annurev-biophys-083012-130404

Wittmann, S., H. Chatel, M. G. Fortin and J.-F. Laliberté (1997) "Interaction of the Viral Protein Genome Linked of Turnip Mosaic Potyvirus with the Translational Eukaryotic Initiation Factor (iso) 4E ofArabidopsis thalianaUsing the Yeast Two-Hybrid System." ***Virology*** 234, 84-92. **DOI:** 10.1006/viro.1997.8634

Wu, X. and J. G. Shaw (1997) "Evidence That a Viral Replicase Protein Is Involved in the Disassembly of Tobacco Mosaic Virus Particlesin Vivo." ***Virology*** 239, 426-434. **DOI:** 10.1006/viro.1997.8870

Wu, X., Y. Shi, J. Li, L. Xu, Y. Fang, X. Li and Y. Qi (2013) "A role for the RNA-binding protein MOS2 in microRNA maturation in Arabidopsis." ***Cell Research*** 23, 645-657. **DOI:** 10.1038/cr.2013.23

Wu, X., Z. Xu and J. G. Shaw (1994) "Uncoating of Tobacco Mosaic Virus RNA in Protoplasts." ***Virology*** 200, 256-262. **DOI:** 10.1006/viro.1994.1183

Xiong, R. and A. Wang (2013) "SCE1, the SUMO-Conjugating Enzyme in Plants That Interacts with NIb, the RNA-Dependent RNA Polymerase of Turnip Mosaic Virus, Is Required for Viral Infection." ***Journal of Virology*** 87, 4704-4715. **DOI:** 10.1128/JVI.02828-12

Yamaji, Y., T. Kobayashi, K. Hamada, K. Sakurai, A. Yoshii, M. Suzuki, S. Namba and T. Hibi (2006) "In vivo interaction between Tobacco mosaic virus RNA-dependent RNA polymerase and host translation elongation factor 1A." ***Virology*** 347, 100-108. **DOI:** 10.1016/j.virol.2005.11.031

Yamanaka, T., T. Imai, R. Satoh, A. Kawashima, M. Takahashi, et al. (2002) "Complete Inhibition of Tobamovirus Multiplication by Simultaneous Mutations in Two Homologous Host Genes." ***Journal of Virology*** 76, 2491-2497. **DOI:** 10.1128/jvi.76.5.2491-2497.2002

Yambao, M. L. M., H. Yagihashi, H. Sekiguchi, T. Sekiguchi, T. Sasaki, et al. (2008) "Point mutations in helper component protease of clover yellow vein virus are associated with the attenuation of RNA-silencing suppression activity and symptom expression in broad bean." ***Archives of Virology*** 153, 105-115. **DOI:** 10.1007/s00705-007-1073-3

Yang, L., Z. Liu, F. Lu, A. Dong and H. Huang (2006) "SERRATE is a novel nuclear regulator in primary microRNA processing in Arabidopsis." ***The Plant Journal*** 47, 841-850. **DOI:** 10.1111/j.1365-313X.2006.02835.x

Yang, Y. and D. F. Klessig (1996) "Isolation and characterization of a tobacco mosaic virus-inducible myb oncogene homolog from tobacco." ***Proceedings of the National Academy of Sciences of the United States of America*** 93, 14972-14977. **DOI:** 10.1073/pnas.93.25.14972

Yeam, I., J. R. Cavatorta, D. R. Ripoll, B.-C. Kang and M. M. Jahn (2007) "Functional dissection of naturally occurring amino acid substitutions in

eIF4E that confers recessive potyvirus resistance in plants." ***The Plant cell*** 19, 2913-2928. **DOI:** 10.1105/tpc.107.050997

Yoshii, M., M. Nishikiori, K. Tomita, N. Yoshioka, R. Kozuka, S. Naito and M. Ishikawa (2004) "The Arabidopsis Cucumovirus Multiplication 1 and 2 Loci Encode Translation Initiation Factors 4E and 4G." ***Journal of Virology*** 78, 6102-6111. **DOI:** 10.1128/JVI.78.12.6102-6111.2004

Yoshikawa, M. (2005) "A pathway for the biogenesis of trans-acting siRNAs in Arabidopsis." ***Genes & Development*** 19, 2164-2175. **DOI:** 10.1101/gad.1352605

Yoshikawa, M., T. Iki, Y. Tsutsui, K. Miyashita, R. S. Poethig, Y. Habu and M. Ishikawa (2013) "3' fragment of miR173-programmed RISC-cleaved RNA is protected from degradation in a complex with RISC and SGS3." ***Proceedings of the National Academy of Sciences*** 110, 4117-4122. **DOI:** 10.1073/pnas.1217050110

Young, B. a., D. C. Stenger, F. Qu, T. J. Morris, S. Tatineni and R. French (2012) "Tritimovirus P1 functions as a suppressor of RNA silencing and an enhancer of disease symptoms." ***Virus Research*** 163, 672-677. **DOI:** 10.1016/j.virusres.2011.12.019

Yu, B., L. Bi, B. Zheng, L. Ji, D. Chevalier, et al. (2008) "The FHA domain proteins DAWDLE in Arabidopsis and SNIP1 in humans act in small RNA biogenesis." ***Proceedings of the National Academy of Sciences*** 105, 10073-10078. **DOI:** 10.1073/pnas.0804218105

Yu, B., Z. Yang, J. Li, S. Minakhina, M. Yang, R. W. Padgett, R. Steward and X. Chen (2005) "Methylation as a crucial step in plant microRNA biogenesis." ***Science (New York, N.Y.)*** 307, 932-935. **DOI:** 10.1126/science.1107130

Zaffagnini, M., S. Fermani, A. Costa, S. D. Lemaire and P. Trost (2013) "Plant cytoplasmic GAPDH: redox post-translational modifications and moonlighting properties." ***Frontiers in Plant Science*** 4, 450. **DOI:** 10.3389/fpls.2013.00450

Zargar, S. M., R. Kurata, S. Inaba, A. Oikawa, R. Fukui, Y. Ogata, G. K. Agrawal, R. Rakwal and Y. Fukao (2015) "Quantitative proteomics of Arabidopsis shoot microsomal proteins reveals a cross-talk between excess zinc and iron deficiency." ***Proteomics*** 15, 1196-1201. **DOI:** 10.1002/pmic.201400467

Zeenko, V. and D. R. Gallie (2005) "Cap-independent Translation of Tobacco Etch Virus Is Conferred by an RNA Pseudoknot in the 5'-Leader." ***Journal of Biological Chemistry*** 280, 26813-26824. **DOI:** 10.1074/jbc.M503576200

Zhang, J., A. Diaz, L. Mao, P. Ahlquist and X. Wang (2012a) "Host Acyl Coenzyme A Binding Protein Regulates Replication Complex Assembly and Activity of a Positive-Strand RNA Virus." ***Journal of Virology*** 86, 5110-5121. **DOI:** 10.1128/JVI.06701-11

Zhang, X., P. Du, L. Lu, Q. Xiao, W. Wang, X. Cao, B. Ren, C. Wei and Y. Li (2008) "Contrasting effects of HC-Pro and 2b viral suppressors from Sugarcane mosaic virus and Tomato aspermy cucumovirus on the accumulation of siRNAs." ***Virology*** 374, 351-360. **DOI:** 10.1016/j.virol.2007.12.045

Zhang, X., R. Henriques, S.-S. Lin, Q.-W. Niu and N.-H. Chua (2006) "Agrobacterium-mediated transformation of Arabidopsis thaliana using the floral dip method." ***Nature Protocols*** 1, 641-646. **DOI:** 10.1038/nprot.2006.97

Zhang, X., X. Zhang, J. Singh, D. Li and F. Qu (2012b) "Temperature-Dependent Survival of Turnip Crinkle Virus-Infected Arabidopsis Plants Relies on an RNA Silencing-Based Defense That Requires DCL2, AGO2, and HEN1." ***Journal of Virology*** 86, 6847-6854. **DOI:** 10.1128/JVI.00497-12

Zhao, Z., B. a. Stanley, W. Zhang and S. M. Assmann (2010) "ABA-Regulated G Protein Signaling in Arabidopsis Guard Cells: A Proteomic Perspective." ***Journal of Proteome Research*** 9, 1637-1647. **DOI:** 10.1021/pr901011h

Zilian, E. and E. Maiss (2011) "Detection of plum pox potyviral protein-protein interactions in planta using an optimized mRFP-based bimolecular fluorescence complementation system." ***Journal of General Virology*** 92, 2711-2723. **DOI:** 10.1099/vir.0.033811-0

Zuo, J., Q.-W. Niu and N.-H. Chua (2000) "An estrogen receptor-based transactivator XVE mediates highly inducible gene expression in transgenic plants." ***The Plant Journal*** 24, 265-273. **DOI:** 10.1046/j.1365-313x.2000.00868.x

Advances in molecular biology have shed new understandings in important cellular processes during the virus-host crosstalk. Among them, RNA silencing is an important mechanism in the control of gene expression regulating many physiological processes during the host ontogenetic development, adaptation to stress, genetic stability maintenance and defence against invading nucleic acids, like viruses.

This ancestral antiviral function of the RNA silencing system enables cells to detect and target invading foreign replicative genetic elements for degradation in a precise and sequence specific mechanism producing small interfering RNA (siRNA) molecules. These siRNA molecules carriers of the digital information to detect the invading sequences will spread guarding neighbouring cells from infection and immunising distal plant tissues.

However, viruses have acquired abilities to suppress the RNA silencing system by incorporating RNA silencing suppressor (RSS) functions in their proteins to highjack and stall RNA silencing with diverse and complementing strategies. The multifunctional requirements of viral proteins as a result of size restrictions in viral genomes obligate viral proteins to deploy functions whilst participating in the recruitment of host factors assisting in fundamental and accessory viral processes. Interactions of viral RSS proteins with host factors have related RSS in diverse and different cellular and molecular processes. The study of interactions between viral RSS proteins and host factors can provide a further understanding of the mechanisms in RSS, but also new functions imprinted in viral RSS proteins yet to discover.

CNB
CENTRO NACIONAL DE BIOTECNOLOGIA

EXCELENCIA
SEVERO
OCHOA

CSIC